Quiescence induces epigenetic changes in bovine fibroblasts and improves their reprogramming into cloned embryos

A thesis submitted in fulfillment

of the requirements for the degree of

Doctor of Philosophy

in

Biological Sciences

at

The University of Waikato

by

Prasanna Kumar Kallingappa

THE UNIVERSITY OF
WAIKATO
Te Whare Wānanga o Waikato

2013

Dedicated

To

My Wonderful Late Father,

Mr. Kallingappa Basappa

and Loving Mother,

Mrs. Rudramma B.S.

Abstract

Cloning by somatic cell nuclear transfer (SCNT) forces cells to lose their lineage-specific epigenetic marks and become totipotent again. This reprogramming process often results in epigenetic and transcriptional aberrations that compromise development. Development rates after SCNT can thus serve as a functional assay for genome-wide epigenetic reprogramming. Dolly the sheep, the first mammalian SCNT clone, was derived from a donor cell that was induced into quiescence by serum starvation. We hypothesized that quiescence alters the epigenetic status of donor cells and elevates their reprogrammability. In order to test this idea, we compared chromatin composition and cloning efficiency of serum-starved, quiescent (G_0), bovine fibroblasts vs non-starved, diploid G_1 controls. Mechanically synchronized G_1 cells were generated by mitotic shake-off and harvested within 3 h post-mitosis. Based on morphological assessment and EdU incorporation during continuous labeling, >93% of cells were captured in G_1.

Using quantitative confocal immunofluorescence microscopy and fluorometric ELISA, we show that G_0 fibroblasts were significantly hypomethylated at lysines (K) of histone 3 (H3), specifically H3K4me3, H3K9me2, H3K9me3 and H3K27me3, but not H3K9me1. Histone acetylation was reduced at H3K9 and H4K5, increased at H3K12 and remained unchanged at H3K16. G_0 cells also significantly reduced DNAme. In addition, they significantly down-regulated the nuclear abundance of RNA polymerase II, histone variant H2A.Z, as well as Polycomb group (PcG) proteins EED, SUZ12, PHC1 and RING2. Histone variant H3.3, PcG proteins EZH2 and histone deacetylase HDAC1 did not change compared to the G_1 controls. Following NT into metaphase-arrested oocytes, G_0 DNA condensed slower than that of G_1 cells, indicating a more relaxed chromatin configuration. After seven days of in vitro culture, H3K9me3, but not H3K4me3, H3K27me3, SUZ12 and RING2, remained hypomethylated in G_0- vs G_1-derived NT blastocysts, both in the inner cell mass and trophectoderm. Furthermore, G_0 donors significantly improved development into cloned blastocysts. In conclusion, quiescence induced long-term epigenetic changes, specifically H3K9me3 hypomethylation, that correlated with increased donor cell reprogrammability.

Acknowledgements

This study was carried out at the Department of Biological Sciences, University of Waikato and the Reproductive Technology Group, AgResearch (Ruakura), Hamilton, New Zealand during the years 2007-2012.

There are plenty more who should be mentioned, but there is not enough room to mention them all. Therefore, I would like to thank all the people who are not named below for their great co-operation in creating this thesis. Without their contribution, this work, and the time that I have spent in research and writing, would have been inferior. I owe them a great deal.

First and foremost, I would like to express my deepest gratitude to my supervisor, Dr. Björn Oback (AgResearch, NZ), for the opportunity to conduct my PhD studies in his research laboratory, providing mentoring and critical feedback. Without his guidance, my brain would probably have operated in a different mode. His perpetual energy and enthusiasm in research has always motivated me. He has contributed enormously to this PhD, in terms of intellectual input, support and encouragement. I feel deeply grateful and privileged to have been his student, not only because of his breadth of knowledge, but also because he always sees positive outcomes from every experiment, even the failed ones. This PhD work has been more than just learning the scientific facts, collecting the scientific findings and the presenting them into the thesis. It has been a wonderful journey throughout, mainly because of Björn. I cannot thank him enough to express my sincere gratitude for all the help he has provided in the last five years of my study.

I am thankful and my appreciation must go to my university supervisors Drs. David Musgrave and Nicholas Ling for their guidance and support in my research. I owe you both a great deal of gratitude and respect for your valuable guidance to achieve this goal.

I would like to thank Dr. David Wells for all his help with the NT experiments, as this would never have been possible without him. I really admire Dave and the work he has been doing. I would like to convey my sincere thanks to Pavla Turner, Fleur Oback, Jan Oliver, Andria Green and Jaime Oswald for all the help they have offered to me in the day-to-day lab work, with special thanks to Pavla, who has shared a lot of work

with me, and Fleur, who always offered me assistance, both professionally and personally.

I would also like to thank the other group members and friends, namely Drs. Md Anower Jabed, Sandeep Gupta, Tanushree Gupta, Ben Huang, Jingwei Wei and Vinod Verma for their constant encouragement and valuable suggestions.

Special thanks to Drs. Goetz Liable and Jisha Antony for gladly sharing the antibodies, without which, I cannot assume how I could have finished my work.

I would like to thank Dr. Vish Vishwanath, who has supported my work since the beginning and has been a great help. I also would like to convey my sincere thanks to Corrine Hanna, Science Administrator, Animal Biosciences, who was always ready to help me with a smile and Ljiljana Popovic for all the cordial support she offered.

The most important part of my life is my family. I am at a loss to express my gratitude to my parents. I am blessed to have such parents who not only believed in me, but also supported me in all aspects of life. The only, but the biggest sorrow of my entire PhD study, is losing my father on the way. He would have been a very proud man today for all the motivation, encouragement and sacrifices he had made to support me. My deepest gratitude goes to my brothers, Niranjana Kallingappa (Appi), Raju Patel, Prakash Nijalingappa, sister, Usha Kallingappa and brother-in-law, Maheshwarappa Bangali. I would have never been able to achieve my goals without their support; they were always there when I needed them. A very special thank you to my wife, Kavitha Halavarthi Gowdara. I will never be able to express my gratitude, but without Kavitha, I would never have made it. I thank her for all her help and sacrifice. I am thankful to our only daughter Sinchana Prasanna Kumar, as she brought joy into my life giving me strength, motivation and love. Because of her, all the challenges in life never looked long.

I am sincerely thankful to Dr. Thomas Jenuwein, Max Planck Institute, Freiberg, Germany, for generously providing histone methylation antibodies and Dr. David Tremethick, ANU College of Medicine, Canberra ACT, Australia, for generously providing H2A.Z antibody. The New Zealand Foundation of Research, Science and Technology, AgResearch Ltd and the University of Waikato generously supported my PhD study.

Finally, I want to thank the unknown source of that perpetual Energy, most know by the name of almighty God, for being with me in my happiness, supporting me when in sorrow and showing me the way out of difficulties.

List of Publications and Conference Contributions

Studies completed during candidature and some of which are reported in this thesis have been presented in the following conference presentations:

I. **Prasanna Kumar Kallingappa,** Pavla Turner, David Wells and Björn Oback. 2012. *Quiescence induces epigenetic changes in fibroblasts and improves their reprogramming into cloned animals*. (Manuscript in preparation).

II. **Prasanna Kumar Kallingappa** and Björn Oback. *Serum starvation-induced epigenetic changes in donor cells correlate with increased nuclear transfer cloning efficiency*. 2010. Abstract. 2nd PhD Student Conference, Waikato University, NZ.

III. **Prasanna Kumar Kallingappa,** Pavla Turner, David Wells and Björn Oback. *Quiescence induces epigenetic changes in fibroblasts and improves their reprogramming into cloned animals*. 2011. Abstract. Mammalian Gametogenesis and Embryogenesis, GRC, Waterville Valley, NH. USA.

IV. **Prasanna Kumar Kallingappa,** Pavla Turner, Andria, Green, Jan Oliver, Fleur Oback, Michael Eichenlaub, Alice Chibnall, David Wells and Björn Oback. *Quiescence induces long-term epigenetic changes in bovine fibroblasts that improve their reprogramming into cloned animals.* 2013. Abstract. 39th IETS Annual Conference, Hannover, Germany. (Accepted).

Abbreviations

Abbreviation	Description
µM	Micromolar
1° Ab	Primary antibody
2° Ab	Secondary antibody
5-aza-dC	5-aza-2′-deoxycytidine
5hmC	5-hydroxymethylcytosine
5mC	5-methylcytosine
Ac	Acetylation
AdoMet	*S*-adenosyl methionine
AMP	Adenosine triphosphate
AMPK	AMP-activated protein kinase
BSA	Bovine serum albumin
COC	Cumulus-oocyte complex
CGI	CpG islands
ChIP	Chromatin immunoprecipitation
CI	Cell index
CIFM	Confocal immunofluorescence microscopy
COL3A1	Collagen-3A1
COMPASS	Complex proteins associated with SET1
CTCF	CCCTC binding factor
DIC	Differential interference contrast
DMEM	Dulbecco's Modified Eagle's medium
DNA	Deoxyribonucleic acid
DNAme	DNA methylation
DNMTs	DNA methyl transferases
DTT	Dithiothreitol
ECM	Extra cellular matrix
ECNT	Embryonic cell nuclear transfer
EDTA	Disodium ethylenediaminetetra acetate
EdU	5-ethynyl-2-deoxyuridine
EED	Embryonic ectoderm development
ELISA	Enzyme-linked immunosorbent assay
ES	Embryonic stem
ESC	Embryonic stem cell
ESCC	ESC-specific cell cycle regulating
ESOF	Early synthetic oviduct fluid
EZH2	Enhancer of zeste homolog 2

FCS	Fetal calf serum
FHAPI	Frame with highest average pixel intensity
G_2	Gap2
G_0	Quiescence
G_1	Gap1
GCNT	Germ cell nuclear transfer
GV	Germinal vesicle
h	Hour
H3	Histone 3
H4	Histone 4
H33342	Hoechst 33342
HAPI	Highest average pixel intensity
HAT	Histone acetyl transferase
HCL	Hydrochloric acid
HCNE	Highly conserved noncoding elements
HDAC	Histone deacetylase
HDACi	HDAC inhibitors
HKMT	Histone lysine methyl transferase
HP	Heterochromatin protein
HSOF	HEPES buffered synthetic oviduct fluid
ICM	Inner cell mass
ICR	Imprinting control region
iPSC	Induced pluripotent stem cell
IVC	*In vitro* culture
IVF	*In vitro* fertilisation
IVM	*In vitro* maturation
K	Lysine
KDM	Lysine demethylase
Kme1	Monomethyl lysine
Kme2	Dimethyl lysine
Kme3	Trimethyl lysine
KMT	Lysine methyl transferase
LAMC1	Laminin-C1
LSD	Least significant difference
LSD1	Lysine-specific demethylase
LSOF	Late synthetic oviduct fluid
M	Molar
MBT	Malignant brain tumour
me1	Monomethylation
me2	Dimethylation

me3	Trimethylation
MII	Metaphase second
min	Minutes
miRNA	microRNA
MLL1	Mixed-lineage leukemia 1
mM	Millimolar
M-phase	Metaphase
NaB	Sodium butyrate
NT	Nuclear transfer
PBS	Phosphate buffered saline
PBST	PBS containing 0.05% Tween® 20
PcG	Polycomb group
PFA	Paraformaldehyde
PGC	Primordial germ cell
PHC	Polyhomeotic
PHD	Plant homeodomain
Pol II	RNA polymerase II
post-TX	4% PFA fixation followed by permeabilisation with Triton® x-100
PRC	Polycomb repressive complex
pre-TX	Pre-permeabilisation with Triton® x-100
PTM	Post-translational modification
PVA	Polyvinyl alcohol
RD	Replication-dependent
RI	Replication-independent
RING2	Really interesting new gene 2
RNA	Ribonucleic acid
ROI	Region of interest
RT	Room temperature
SCNT	Somatic cell nuclear transfer
sec	Seconds
sim-MeOH	Methanol fixation/permeabilisation
sim-TX_PFA	Simultaneous permeabilisation with Triton® x-100 and fixation with 3.7% PFA
SOF	Synthetic oviduct fluid
S-phase	DNA synthesis-phase
SuVAR	Suppressor variegation
SUZ12	Suppressor of zeste 12
TDG	Thymine-DNA-glycosylase
TE	Trophectoderm
TET	Ten eleven translocation

TNC	Tenascin C
TRX	Trithorax
TS	Trophoblast stem
TSA	Trichostatin A
TSS	Transcription start site
V	Volt
v/v	Volume per volume
VPA	Valproic acid
w/v	Weight per volume
XCI	X-chromosome inactivation
X_i	Inactivated X-chromosome

Table of Contents

List of Figures

List of Tables

Chapter One: Review of literature

1.1 Introduction

Reproduction is the key for continuation of life as no multicellular organism can live forever. The fertilised egg or zygote is the starting point for such a continuation in mammals. Following the union of egg and sperm, the zygote cleaves further to form early embryos. Zygote and cleavage-stage blastomeres, the constituents of each embryo, are the only totipotent cells, i.e. they are able to give rise to all embryonic and extra-embryonic lineages (Kelly 1977). The inner cell mass (ICM) of an early preimplantation embryo ('blastocyst') can give rise to all embryonic, but not extra-embryonic lineages and is thus pluripotent. As the blastocyst develops further, cells get progressively committed to forming particular lineages, ultimately leading to terminally differentiated cells in adult animals.

Even though almost all cells within an individual animal are genetically identical, the cells acquire different gene expression patterns (Morgan, Santos *et al*. 2005). These changes in gene activity without changes in DNA sequence are referred to as epigenetic (Probst, Dunleavy *et al*. 2009). Epigenetic changes impose heritable cellular memories to guide differentiation of pluripotent cells into different cell types, progressively acquiring distinct epigenetic modifications (Hemberger, Dean *et al*. 2009). During development, germ cells are set aside in the early gastrulating embryo.

'Epigenetic reprogramming', i.e. the dynamic changes to epigenetic marks, happens twice during normal mammalian development. These two reprogramming periods are gametogenesis and early embryogenesis (Reik, Dean *et al*. 2001). Extensive genome-wide DNA demethylation first occurs in primordial germ cells (PGCs), erasing epigenetic marks at most

imprinted and non-imprinted genes (Morgan, Santos *et al*. 2005). Before fertilization, sex-specific methylation at imprinted loci is re-established in both male and female gametes (Delaval & Feil 2004). Another wave of genome-wide reprogramming follows between fertilization and blastocyst formation. This second wave resolves the early parental asymmetry in histone modifications (Santos, Peters *et al.* 2005, van der Heijden, Dieker *et al.* 2005, Torres-Padilla, Parfitt *et al.* 2007), DNA methylation (DNAme) (Dean, Santos *et al*. 2001) and polycomb group (PcG) proteins (Puschendorf, Terranova *et al*. 2008) that exists up to the eight-cell stage. It generates methylation marks in both DNA and histones that correlate with the first differentiation event during preimplantation development, namely the specification of an embryonic and extraembryonic lineage (Torres-Padilla, Parfitt *et al*. 2007). These lineages later diversify into hundreds of different cell types of a multicellular organism.

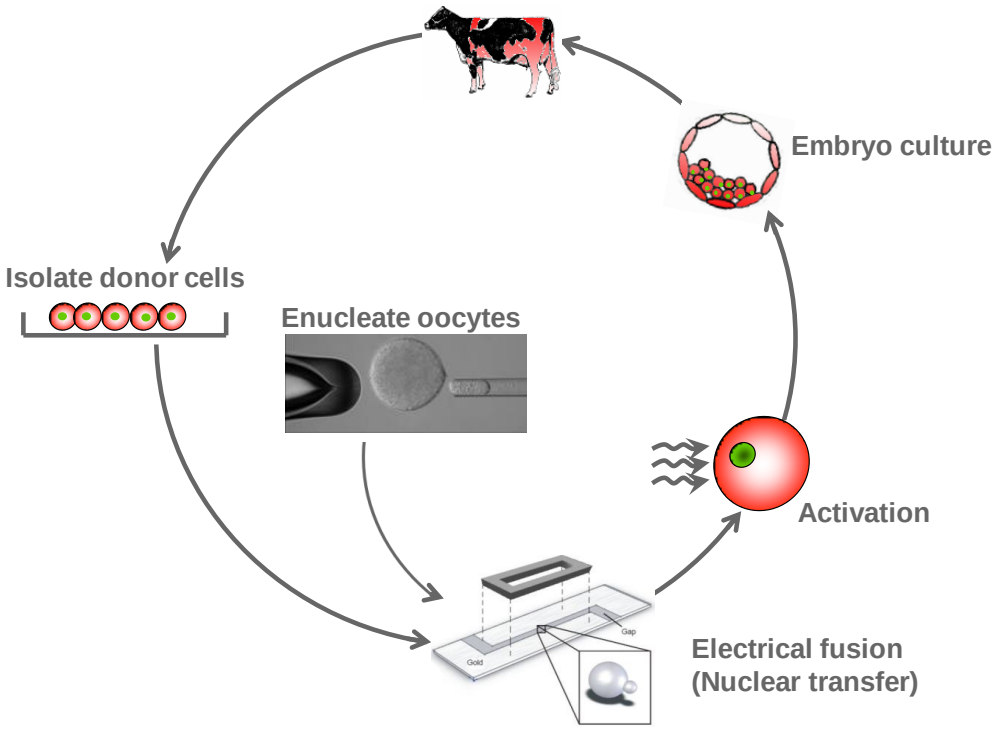

Figure 1: Process of nuclear transfer (Adapted from Oback & Wells, 2003).

Epigenetic reprogramming can also be induced by experimental manipulations, such as nuclear transfer (NT) cloning (Figure 1) or induced pluripotent stem cell (iPSC) -derivation. During NT, a somatic cell nucleus is transplanted into an enucleated oocyte where its epigenetic marks must be cleared to regain totipotency. This technique is used to either produce animals whose genome is identical to that of the donor cell or to generate pluripotent embryonic stem (ES) cells for regenerative medicine (Campbell, Fisher *et al*. 2007).

NT is also the preferred method of generating genetically modified animals in species where ES cell are not available. The ES cells generated from NT and fertilized blastocysts are transcriptionally, post-transcriptionally and functionally very similar (Brambrink, Hochedlinger *et al.* 2006, Ding, Guo *et al.* 2009). However, epigenetic differences in imprinted regions are apparent after long-term culture (Chang, Liu *et al*. 2009). Lack of proper imprinting in NT- derived ES cells is attributed to inefficient reprogramming by metaphase (M) II-arrested enucleated oocyte (cytoplast). The inefficient reprogramming is also a major cause of low cloning efficiency (Wakayama 2007). Cloning efficiency, defined as the number of viable animals surviving into adulthood as a proportion of cloned embryos transferred into surrogate mothers, ranges from 0-10% in most mammalian species (Oback 2009).

1.2 Factors affecting the efficiency of cloning

Reprogramming efficiency after NT critically depends on two processes: 1) the ability of the oocyte to carry out the reprogramming reactions and 2) the ability of the nuclear donor cell to be fully reprogrammed. It is currently unclear which process is more important for reprogramming success. Here, we will focus on the influence of the donor cell.

1.2.1 Donors

1.2.1.1 Cell type

Several cell types have been successfully used for cloning. They generally fall into three categories: embryonic, germ or somatic cells. The cloning techniques are thus called embryonic cell nuclear transfer (ECNT), germ cell nuclear transfer (GCNT) or somatic cell nuclear transfer (SCNT), respectively (Oback & Wells 2007). Early success in cattle cloning was realised through use of blastomeres from early embryos (Prather, Barnes *et al*. 1987). After the first SCNT success using cumulus and oviduct epithelial cells (Kato, Tani *et al*. 1998), several other somatic cells were successfully used in cattle SCNT. This includes cells derived from the follicle (Wells, Misica *et al*. 1999), adult and fetal skin (Hill, Winger *et al*. 2000), mammary gland epithelium (Kishi, Itagaki *et al*. 2000), uterus, ear, liver (Kato, Tani *et al*. 2000), lung and muscle (Powell, Talbot *et al*. 2004). Whilst there is still no consensus on the ideal somatic donor type, fetal fibroblasts are the most commonly used donor cells in domestic species. For ECNT, early totipotent blastomeres can achieve better cloning efficiency than late-stage blastomeres (Cheong, Takahashi *et al.* 1993, Hiiragi & Solter 2005). In cattle, cloning efficiency progressively decreases with developmental stage of donor cells, from morula to fetal fibroblast to adult fibroblast (Heyman, Chavatte-Palmer *et al*. 2002). Similarly, mouse cloning efficiency from particular pluripotent ES cell lines was better than commonly used cumulus (Rideout, Wakayama *et al*. 2000), fibroblast (Eggan, Akutsu *et al*. 2001) and mature Sertoli cells (Wakayama & Yanagimachi 1999). For the reasons not clearly known, exceptional high cloning efficiency of mouse ES cells is only associated with F1 hybrid of the 129 genotype. In direct comparison, there was no difference in cloning efficiency between ES cells and adult neural stem cells. In summary, cloning efficiency progressively decreases with each blastomere could not be confirmed for several cell types and cell lineages across the somatic differentiation continuum (Oback 2010). However, the hypothesis

postulated that somatic differentiation status is inversely proportional to cloning efficiency (Jaenisch, Eggan *et al.* 2002, Oback & Wells 2002).

1.2.1.2 Passage number

The age of the donor cell in a dividing population, which is proportional to the number of doublings or passages in cell culture, could also potentially influence cloning efficiency (Kasinathan, Knott *et al.* 2001a). Some reports suggested that lower passage numbers were better nuclear donors (Roh, Shim *et al.* 2000, Gao, Chung *et al.* 2003), but others found no significant difference between them (Hill, Winger *et al*. 2001). Some reports even claimed that later donor passages developed better into NT embryos than earlier ones (Kubota, Yamakuchi *et al.* 2000, Arat, Rzucidlo *et al.* 2001). Despite this, lower passage numbers are generally preferred as they are presumed to have more epigenetic plasticity and thus get better reprogrammed by oocytes. Successful cloning of animals from donor cells derived from 13 and 17 years old animals suggests that age of animal from which donor cells are derived does not matter (Kubota, Yamakuchi *et al.* 2000, Enright, Taneja *et al.* 2002). This was further substantiated by the fact that there was no difference in embryonic development rate, when fetal and adult cells of the same genotypes were used as NT donors (Hill, Winger *et al*. 2000).

1.3 Epigenetic modifications

Differences in cellular phenotype and function are due to different characteristic gene expression profiles that are set by an epigenetic program early in the development of that organism (Eilertsen, Power *et al*. 2007). These expression profiles are achieved by chemical modification to DNA and its associated histone proteins, but without modifying DNA sequence (Probst, Dunleavy *et al*. 2009). These heritable epigenetic modifications are crucial for development and survival of an organism, but

can be reversible and reprogrammable (Wilmut, Schnieke *et al.* 1997, Takahashi & Yamanaka 2006).

1.3.1 DNA methylation

The epigenetic reprogramming associated with DNA itself involves removal and resetting of DNAme patterns. DNAme is established at 5′ cytosine by a set of enzymes called DNA methyl transferases (DNMTs). These enzymes catalyse transfer of a methyl group from *S*-Adenosyl methionine (AdoMet) to cytosine (Chen & Riggs 2011). There are three well-known types of DNMTs: DNMT1, DNMT3a and DNMT3b (Bestor 2000). DNMT1 preferentially methylates hemimethylated CpG sites (Pradhan, Bacolla *et al*. 1999) and is required for maintaining the 5-methylcytosine (5mC) patterns on newly synthesised DNA strands (Chen & Li 2004) and on imprinted genes in the developing embryo (Li, Beard *et al*. 1993). DNMT3a and -3b are involved in de novo methylation (Okano, Bell *et al.* 1999, Gowher & Jeltsch 2001). DNMT3b methylates pericentric satellite repeats (Okano, Bell *et al*. 1999), while DNMT3a methylates most loci of germ cells (Kaneda, Okano *et al.* 2004, Sasaki & Matsui 2008), which is essential for spermatogenesis (Hata, Okano *et al*. 2002). DNMT3a is also essential for establishing the maternal and paternal imprinting (Kaneda, Okano *et al*. 2004) and for later development (Gowher & Jeltsch 2001).

In vertebrates, DNAme mainly occurs as 5mC, predominantly at the symmetrical CpG dinucleotides (Bird & Wolffe 1999). The genomic regions with high frequency of these CpG dinucleotides are known as CpG islands (CGI) and most CpGs in CGIs are methylated. In plants and animals, DNAme is also found at CpNpG and CpNpN, where N represents either nucleotide C, T or A (Clark, Harrison *et al*. 1995). Normally, high levels of DNAme at the promoter region are associated with gene silencing (Bird 2002). In mammals, tissue- and cell type-specific methylation is present in a small fraction of 5′ CpG Island promoters, while a far bigger fraction

emerges across gene bodies (5' UTRs, coding exons, introns and 3' UTRs), which can act as regulator of intragenic alternative promoters (Maunakea, Nagarajan *et al*. 2010). Genome-wide single base resolution maps of methylated cytosines in human ES cells found non-CpG methylations, associated with gene bodies, which positively correlated with gene expression, rather than with promoters. In human lung fetal fibroblasts, this non-CpG methylation is absent (Lister, Pelizzola *et al*. 2009). The DNAme repression mechanism works both directly, by interfering with transcription factor binding, and indirectly, by recruiting proteins with a methyl binding domain (MBD), such as MeCP2 (Fuks, Hurd *et al*. 2003), MBD1 (Ng, Jeppesen *et al*. 2000) and MBD2 (Jiang, Jin *et al*. 2004), which subsequently recruit histone deacetylases (HDACs) that silence the gene.

DNAme also occurs in the form of 5-hydroxymethylcytosine (5hmC), now referred to as the sixth base (Penn, Suwalski *et al*. 1972). It is found in brain of human, rat, mouse and frog (Penn, Suwalski *et al.* 1972, Kriaucionis & Heintz 2009, Maunakea, Nagarajan *et al.* 2010), heart of mouse and human (Kinney, Chin *et al*. 2011) and liver of rat (Penn, Suwalski *et al*. 1972). It is also present in human and mouse ES cells (Tahiliani, Koh *et al.* 2009, Stroud, Feng *et al.* 2011, Wu, D'Alessio *et al.* 2011). 5hmC is generally associated with gene bodies of actively transcribed genes (Stroud, Feng *et al.* 2011, Wu, D'Alessio *et al.* 2011), but its presence on extended promoter regions of polycomb-repressed developmental regulators may indicate some tissue- and site-specific dual regulation (Wu, D'Alessio *et al*. 2011).

DNA demethylation is a complex process. In mammals, ten eleven translocation (TET) 1 converts 5mC to 5hmC by oxidation (Tahiliani, Koh *et al.* 2009, Guo, Su *et al.* 2011). All TET proteins (TET 1, TET 2 and TET 3) generate 5-formylcytosine (5fC) and 5-carboxylcytosine (5caC) from 5hmC (Ito, Shen *et al*. 2011). Base excision of 5caC by thymine-DNA-

glycosylase (TDG) results in unmodified cytosine and thus achieves complete DNA demethylation from 5mC nucleotides (He, Li *et al*. 2011).

1.3.2 Histone modifications

Histones were long thought to be the basic nucleosomal proteins around which the DNA is wound to form the chromatin. This view of histones as mere helpers to form higher-order chromatin structure and neutralize DNA turned out to be incorrect. Advancements over the past years have linked histones in gene regulation (Jenuwein & Allis 2001, Campos & Reinberg 2009). Gene regulation is achieved through a set of modifications on the amino terminal tail of histones by several chromatin modifiers. The set of the histone modifications (Figure 2) governing gene silencing and activation is referred to as “histone code” (Jenuwein & Allis 2001). It has been proposed that this code is recognised by a variety of chromatin-modifying agents and leads to distinct functional readouts of chromosomal DNA in accordance with the code (Lachner, Sengupta *et al.* 2004, Campos & Reinberg 2009). Covalent post-translational modifications (PTMs) of histones alter the inherent characters of a nucleosome on which it is present and influence the binding of chromatin-modifying complexes and the higher-order folding of the chromatin itself. The core of chromatin is the nucleosome formed by 147 base pairs of DNA wound around the histone octamer comprising two histone H3-H4 dimers linked together as tetramer and flanked by two H2A-H2B dimers. These nucleosomes interact through hydrophobic globular domains, referred to as histone fold domains (Luger, Mader *et al.* 1997, Davey, Sargent *et al.* 2002). Individual nucleosomes are linked by a linker histone H1 that protects the internucleosomal linker DNA. Crystal structures of the nucleosome core revealed NH2-terminals (N-terminal) of the histone tails protruding outside the core. These tails are amenable for PTMs, such as acetylation, methylation, phosphorylation, ubiquitinisation, sumoylation and ADP-ribosylation (Van Holde 1988). Overall these modifications modulate gene

expression in cis or trans by binding to chromatin-modifying complexes (Kubicek, Schotta *et al.* 2006a). There is also a possible internucleosomal crosstalk. Methylated residues are bound by chromo-like domains (chromo, malignant brain tumour (MBT) and Tudor), plant homeodomain (PHD) and ankyrin repeats, while acetylated residues are bound by bromodomains and phosphorylated residues are bound by 14-3-3 proteins (Izzo & Schneider 2010).

1.3.2.1 Histone methylation

Histone methylation is implicated in heterochromatin formation, PcG-mediated gene silencing, X-chromosome inactivation (XCI) and life-span regulation (Schotta, Lachner *et al.* 2004a, Martin & Zhang 2005, Peters & Schubeler 2005, Han & Brunet 2012). Histone methylation can occur mostly on H3 and H4 at various basic amino acids, lysine (K), arginine (R) and histidine (H), along various positions. Lysines could be mono- (Kme1), di- (Kme2) or tri- (Kme3) (Figure 3) methylated (Bannister, Schneider *et al*. 2002). In contrast to acetylation and phosphorylation, histone charge is unaltered by histone methylation.

1.3.2.1.1 Histone lysine methylation

Histone lysine methylations are catalysed by lysine methyl transferases (KMTs). H3K9-targeting SUV39h1 (KMT1A) was identified as the first histone KMT (HKMT) (Rea, Eisenhaber *et al*. 2000). Later several other HKMTs that mostly methylate the N-terminal regions have been identified. All HKMTs use cofactor AdoMet as a donor to transfer methyl groups to ε-amino group of lysine (Figure 3). All HKMTs that methylate N-terminal tale lysines comprise of catalytically active Su(var)3-9 and enhancer of zeste (SET) domain, with the exception of DOT1, which methylates H3K79, the lysine within the globular histone structure (Bannister & Kouzarides 2011).

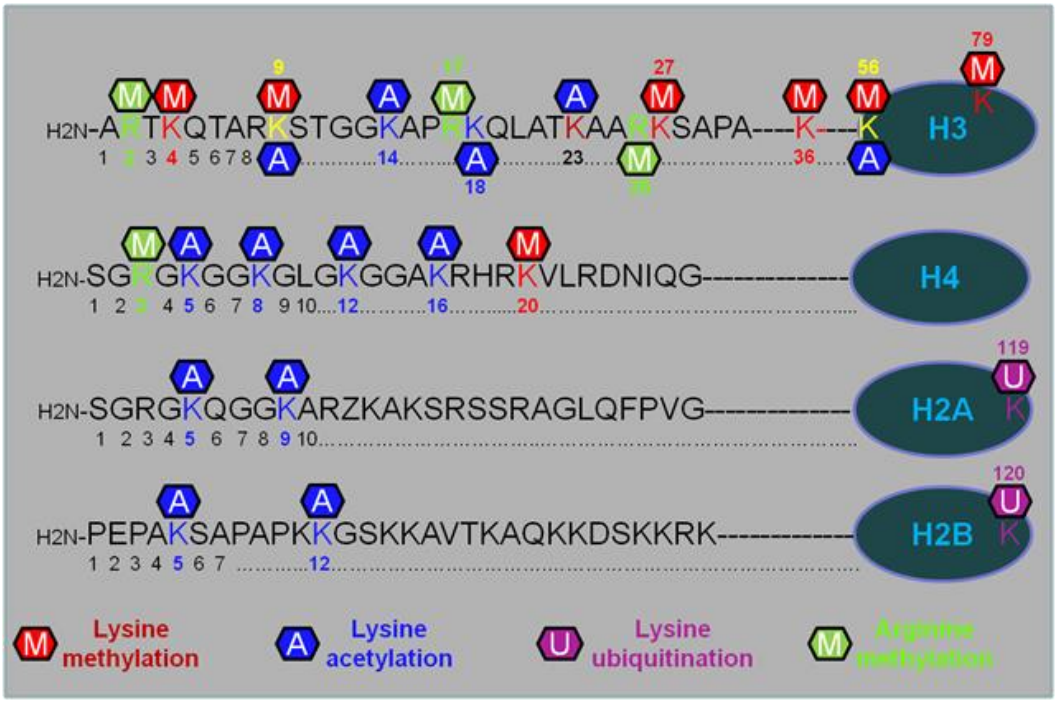

Figure 2: Histone (H3, H4, H2A and H2B) modifications overview. Oval structures representing the globular structure and the amino tail terminal is represented by individual amino acids. Numbers represent the position of the amino acids. Hexagons represent the modifications. While most known PTMs of histones occur on the amino terminal tail, some occur on globular structures. (Modified from Zhang & Reinberg, 2001).

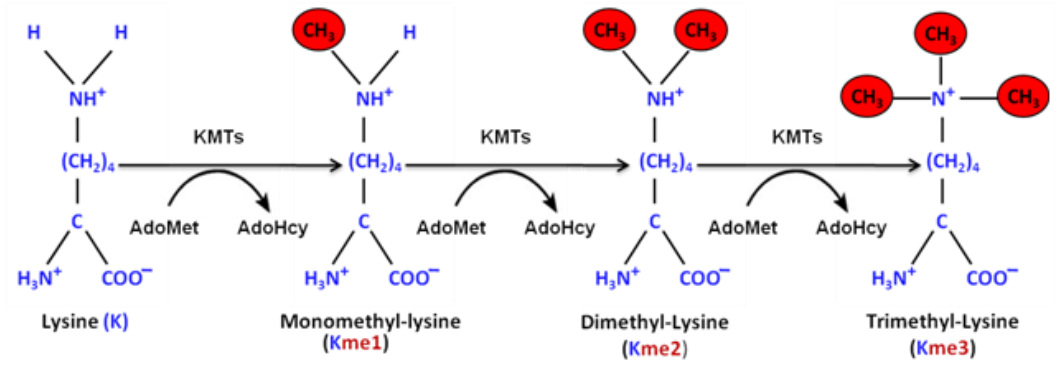

Figure 3: Different histone lysine methylation states. Illustrated is the enzymatic conversion of lysine by KMTs to different states of lysine methylations using AdoMet as the methyl donor. State of lysine methylation depends on the type of KMT. (Modified from Zhang & Reinberg, 2001).

Extensive work on the epigenetic marks has led to the understanding that, generally, transcriptionally active genes are methylated at H3K4 (Santos-Rosa, Schneider *et al.* 2002, Schubeler, MacAlpine *et al.* 2004), H3K79 (Schubeler, MacAlpine *et al*. 2004) and H3K36 (Krogan, Kim *et al*. 2003), while transcriptionally repressed genes carry H3K9 (Nielsen, Schneider *et al.* 2001, Ait-Si-Ali, Guasconi *et al.* 2004), H3K27 (Cao & Zhang 2004a), H3K64 (Daujat, Weiss *et al*. 2009) and H4K20 (Lachner, Sengupta *et al.* 2004, Schotta, Lachner *et al.* 2004b). However, there are some reports that implicate some of these modifications in contradicting functions at regions of the genome. Hence it is possible that function of these marks depends on genomic location, degree of methylation and presence of other cis/trans acting cross-talking histone marks (Campos & Reinberg 2009, Izzo & Schneider 2010, Bannister & Kouzarides 2011)

Histone methylation was long thought to be a permanent mark (Lachner, Sengupta *et al*. 2004) as its ε-amino group is refractory to direct cleavage. It was therefore, considered a potential mark that can steadily perpetuate through many cell divisions (Kubicek & Jenuwein 2004, Lachner, Sengupta *et al.* 2004). This notion of irreversible methylation was supported by the experimental evidence that the half-life of the histone mark is nearly equal to that of histone itself (Byvoet, Shepherd *et al.* 1972, Thomas, Lange *et al.* 1972). At last, a lysine-specific demethylase (LSD1 or KDM1A), an amine oxidase, that could remove mono- and di-, but not tri- methylation of H3K4 was demonstrated in human (Shi, Lan *et al*. 2004). From then on several lysine demethylases (KDMs) were identified. These can demethylate most of the known histone methylations (Bannister & Kouzarides 2011).

Both demethylating and methylating enzymes occur in macromolecular complexes harboring HDACs, SWItch/Sucrose NonFermentable (SWI/SNF) remodelling factors, along with PHD and chromodomain-

containing proteins (Mosammaparast & Shi 2010), indicating that they all act together to modulate gene activity through histone PTMs.

1.3.2.1.1.1 H3K4 methylation

Methylation on H3K4 can occur as mono-, di- and tri-methylation (H3K4me1, -me2 and -me3, respectively) and H3K4me1 or -me2 is required to acquire H3K4me3 (Shilatifard 2006). In mammals, H3K4 is largely methylated by trithorax (TRX) group proteins, a group of SET domain-containing proteins (Schuettengruber, Martinez *et al*. 2011). The first H3K4 KMTase to be discovered was SET1 in yeast (Briggs, Bryk *et al*. 2001). It is a crucial component of the H3K4 methylating complex, complex proteins associated with SET1 (COMPASS) (Miller, Krogan *et al*. 2001) that can generate all three H3K4 methylation states (Wang, Lin *et al*. 2009). Mammalian homologues of SET1, mixed-lineage leukemia (MLL) 1 - MLL4 (KMT2A-D), human SET1A and SET1B (KMT2F and KMT2G) are associated with COMPASS-like complexes (Wang, Lin *et al*. 2009) and are commonly known as KMT2 family proteins. The diverse KMT2 family members have non-overlapping functions, probably governing site-specific methylation (Ruthenburg, Allis *et al*. 2007).

It is postulated that H3K4 and H3K36 methylation are involved in early events of transcription and elongation, respectively (Peters & Schubeler 2005). H3K4me3 might be playing a supportive role in elongation. It was found in humans that it was bound by CHD1, which bridges spliceosomal components, to facilitate the maturation of pre-mRNA (Sims, Millhouse *et al*. 2007). Several KDMs responsible for removal of H3K4 methylations have been found (Table 1).

Table 1: Enzymes involved in different states of H3K4 methylation and demethylation

H3K4 modification	K4 KMTs	K4 KMDs
me1	KMT2A (MLL1) (Patel, Dharmarajan *et al*. 2009) KMT2E (MLL5) (Fujiki, Chikanishi *et al*. 2009) KMT7 (SET7/9) (Nishioka, Chuikov *et al.* 2002)	KDM1A (LSD1) (Shi, Lan *et al*. 2004) KDM1B (LSD2) (Fang, Barbera *et al*. 2010)
me2	NSD2 (MMSET) (Kang, Choi *et al*. 2009) NSD3 (Kim, Kee *et al*. 2006) KMT2E (MLL5) (Fujiki, Chikanishi *et al*. 2009)	KDM1A (LSD1) (Shi, Lan *et al*. 2004) KDM1B (LSD2) (Fang, Barbera *et al*. 2010) KDM5B (JARID1B) (Christensen, Agger *et al*. 2007) KDM5D (JARID1D) (Iwase, Lan *et al*. 2007)
me3	KMT2E (MLL5) (Dou, Milne *et al*. 2005) KMT2B (MLL2) (Demers, Chaturvedi *et al*. 2007) KMT2C (MLL3) (Goo, Sohn *et al*. 2003) KMT2D (MLL4) (Lee, Lee *et al*. 2006) KMT2F (SET1A) (Wu, Wang *et al*. 2008) KMT2G (SET1B) (Wu, Wang *et al*. 2008) KMT3E (SMYD) (Hamamoto, Furukawa *et al.* 2004) PRDM9 (Hayashi, Yoshida *et al*. 2005)	KDM2B (JHDM1B) (Frescas, Guardavaccaro *et al*. 2007) KDM5A (JARID1A) (Christensen, Agger *et al*. 2007) KDM5B (JARID1B) (Yamane, Tateishi *et al*. 2007) KDM5C-D (JARID1C-D) (Iwase, Lan *et al*. 2007) NO66 (Sinha, Yasuda *et al*. 2010)

Function

H3K4me3 is enriched in promoters of most eukaryotes from yeast (Pokholok, Harbison *et al*. 2005) to mammals (Bernstein, Kamal *et al.* 2005, Heintzman, Stuart *et al.* 2007). While H3K4me3 enriched at the transcription start sites, H3K4me1 and -me2 progressively spread along the gene body (Pokholok, Harbison *et al.* 2005, Heintzman, Stuart *et al.* 2007). High-resolution genome-wide mapping in human CD4+ T cells shows H3K4me3 to be more localised at -300 and +100 from either side of the transcription start site (TSS), followed by H3K4me2 at -500 and +700 and H3K4me1 at -900 and +1000. All three forms correlate with gene activation (Barski, Cuddapah *et al*. 2007). Enhancers of various cell types enrich for H3K4me1 but not -me3 (Heintzman, Stuart *et al*. 2007). H3K4 methylation is also found in active genes of the Homeobox (Hox) cluster, probably driving their expression (Bernstein, Kamal *et al*. 2005). All three states of H3K4 methylations found at the CCCTC binding factor (CTCF) binding insulators may function as barrier for heterochromatin spreading (Barski, Cuddapah *et al*. 2007).

1.3.2.1.1.2 H3K9 methylation

H3K9 methylation can also occur in the form of H3K9me1, -me2 or -me3. Doubling of H3K9me3 amount after replication is evidence of faithful inheritance of this mark through several replication cycles (McManus, Biron *et al*. 2006). SET domain-containing KMT1A was the first mammalian KMTase to be identified (Rea, Eisenhaber *et al*. 2000), followed by SUV39h2 (KMT1B) (O'Carroll, Scherthan *et al*. 2000). There are several KMTs and KDMs that regulate the dynamics of H3K9me3 in the cell (Table 2) Both KMT1A and -B are responsible for pericentric H3K9me3. This defines a region adjacent to the centromeric heterochromatin consisting of major satellite repeats. The KMT1A is also involved in suppression of a set of retinoblastoma protein target genes

(Nielsen, Schneider *et al*. 2001), particularly S phase genes. It targets these genes in differentiating, but not in cycling cells (Ait-Si-Ali, Guasconi *et al*. 2004), indicating that this suppression is required for permanent, but not for transient silencing. There is also evidence for DNAme requiring hierarchal deposition of H3K9me3 (Tamaru & Selker 2001, Jackson, Lindroth *et al.* 2002, Lehnertz, Ueda *et al.* 2003). In mammals, this seems to be site-dependent, as only pericentric repeats depend on SUV39 KMTase-mediated methylation, while centromeric repeats do not (Lehnertz, Ueda *et al*. 2003).

SET domain and ankyrin repeat domain-containing G9a (KMT1C) and GLP (KMT1D) KMTases are responsible for H3K9me1 and -me2 (Tachibana, Sugimoto *et al.* 2001, Tachibana, Ueda *et al.* 2005). KMT1C can also guide DNAme by binding to DNMT3a/b DNA methylases through its ankyrin domain (Epsztejn-Litman, Feldman *et al*. 2008). Both KMT1C and KMT1D silence E2F1-5, myc and brachyury-responsive genes in quiescent cells, by forming a complex with E2F6, heterochromatin protein (HP) 1γ and PcG proteins (Ogawa, Ishiguro *et al*. 2002). KMT1A-B/HP1, guided by retinoblastoma, silences the genes involved in S-phase progression in differentiating cells (Nielsen, Schneider *et al.* 2001, Ait-Si-Ali, Guasconi *et al.* 2004), again implying that KMT1A/B-mediated silencing may be involved in long term effects.

Table 2: Enzymes involved in different states of H3K9 methylation and demethylation

H3K9 modification	K9 KMTs	K9 KDMs
me1	KMT1C (EHMT2) (Tachibana, Sugimoto *et al*. 2001) KMT1D (EHMT1) (Tachibana, Ueda *et al*. 2005) KMT1E (SETDB1) (Loyola, Tagami *et al*. 2009).	PHF2 (JHDM1E) (Wen, Li *et al*. 2010) PHF8 (JHDM1F) (Liu, Tanasa *et al*. 2010) KDM3A-B (JMJD1A-B , JHDM2A-B) (Yamane, Toumazou *et al*. 2006) KDM7 (JHDM1D) (Tsukada, Ishitani *et al*. 2010) KDM1A (LSD1) (Metzger, Wissmann *et al*. 2005)
me2	KMT1C (EHMT2) (Tachibana, Sugimoto *et al*. 2001) KMT1D (EHMT1) (Tachibana, Ueda *et al*. 2005) KMT8 (PRDM2) (Kim, Geng *et al*. 2003) KMT1A (SUV39H1) (Murayama, Ohmori *et al*. 2008)	KDM3A-B (JMJD1A-B, JHDM2A-B) (Yamane, Toumazou *et al*. 2006) KDM7 (JHDM1D) (Tsukada, Ishitani *et al*. 2010) KDM4C-D (JMJD2C-D, JHDM3C-D) (Whetstine, Nottke *et al*. 2006) PHF8 (JHDM1F) (Zhu, Wang *et al*. 2010) KDM1A (LSD1) (Metzger, Wissmann *et al*. 2005) PHF2 (JHDM1E) (Baba, Ohtake *et al*. 2011)
me3	KMT1A (SUV39H1) (Rea, Eisenhaber *et al*. 2000) KMT1B (SUV39H2) (O'Carroll, Scherthan *et al*. 2000) KMT1E (SETDB1) (Wang, An *et al*. 2003) KMT1F (SETDB2) (Falandry, Fourel *et al*. 2010).	KDM4A-D (JMJD2A-D, JHDM3A-D) (Whetstine, Nottke *et al*. 2006)

Function

A high-resolution genome-wide histone methylation profiling shows H3K9me3 and H3K9me2 in higher concentration around silent than active genes across 10 kb of the TSS. High levels of H3K9me1 near the 5′ end of active promoters and enhancer regions correlate well with gene expression (Barski, Cuddapah *et al*. 2007), contradicting an earlier report of H3K9me1 association with silent chromatin (Sims, Houston *et al*. 2006). H3K9me3 was also present at some of active promoters (Squazzo, O'Geen *et al*. 2006), as well as in transcribed regions (Vakoc, Mandat *et al.* 2005, Brinkman, Roelofsen *et al.* 2006). Barski *et al*. found highly localised peaks of H3K9me3 in active genes, such as STAT1 and STAT4. These reports hints at the gene-specific action of the H3K9me3 mark (Barski, Cuddapah *et al*. 2007).

Despite this, H3K9me3 is still generally regarded as a proven mark of pericentric heterochromatin and well implicated in gene repression (Bannister, Zegerman *et al.* 2001, Lehnertz, Ueda *et al.* 2003, Su, Brown *et al.* 2004). H3K9me3 at pericentric heterochromatin recruits HP1 isoforms HP1α and HP1β (Lehnertz, Ueda *et al*. 2003). HP1 facilitates heterochromatin formation by compacting individual chromatin fibres (Fan, Rangasamy *et al*. 2004) through its ability to oligomerise (Thiru, Nietlispach *et al*. 2004). This compaction of chromatin is believed to be non-permissive for transcription (Nakayama, Rice *et al*. 2001). Dimers of HP1, in turn, can spread pericentric methylation of H3K9me3, H4K20me3 and 5mC by recruiting the respective enzyme machinery (Campos & Reinberg 2009). H3K9me2 is one of the major repressive marks (Barski, Cuddapah *et al.* 2007, Wang, Zang *et al.* 2008), that maintain imprinting independently of DNAme (Lewis, Mitsuya *et al.* 2004, Umlauf, Goto *et al.* 2004) and is also associated with the inactivated X-chromosome (X_i) in females (Heard 2004). Demethylation of H3K9me2 and acetylation of H3K9 determines the re-expression of *OCT4* and *NANOG* during

reprogramming of HEK 293T cells (Freberg, Dahl *et al*. 2007). H3K9me2 methylation and H3 deacetylation determines the repression of rDNA loci during energy deprived state (Murayama, Ohmori *et al*. 2008).

Cells lacking both KMT1A and -B fail to localise HP1α and –β. Instead of H3K9me3, they enrich H3K9me and H3K27me3 marks at pericentric heterochromatin. They also fail to segregate centromeres properly during mitosis, resulting in increase of ploidy and genomic instability (Peters, O'Carroll *et al*. 2001). The loss of KMT1A/B-mediated H3K9me3 also leads to altered DNAme (Lehnertz, Ueda *et al*. 2003) and loss of H4K20me3 at pericentric heterochromatin (Schotta, Lachner *et al.* 2004b). Knock-out mice for KMT1C and -D show reduced H3K9me1 and -me2 at euchromatic regions in ES cells, resulting in retarded growth and early embryo lethality (Tachibana, Sugimoto *et al.* 2002, Tachibana, Ueda *et al.* 2005). KMT1C or -D deficient mouse ES cells also show reduction in DNAme (Dong, Maksakova *et al.* 2008, Epsztejn-Litman, Feldman *et al.* 2008, Tachibana, Matsumura *et al.* 2008).

1.3.2.1.1.3 H3K27 methylation

In mammals, enhancer of zeste homolog 2 (EZH2) is a major H3K27 methylase. Although EZH1 and other enzymes are capable of methylating H3K27, this is not substantial (Kim, Kee *et al.* 2006, Margueron, Li *et al.* 2008, Shen, Liu *et al.* 2008, Wu & Rice 2011). EZH1 and EZH2 are part of the polycomb repressive complexes (PRCs). These PRC proteins are discussed later in this chapter (section 1.5.1). Enzymes that can demethylate H3K27 methylation have been identified recently (Table 3).

Table 3: Enzymes involved in different states of H3K27 methylation and demethylation

H3K27 modification	K27 KMTs	K27 KDMs
me1	KMT1C (EHMT2) (Wu, Chen *et al*. 2011) KMT1D (EHMT1) (Wu, Chen *et al*. 2011) KMT6A (EZH2) (Margueron, Li *et al*. 2008) KMT6B (EZH1) (Margueron, Li *et al*. 2008)	KDM7 (JHDM1D) (Tsukada, Ishitani *et al*. 2010)
me2	NSD3 (Kim, Kee *et al*. 2006) KMT6A (EZH2) (Margueron, Li *et al*. 2008) KMT6B (EZH1) (Margueron, Li *et al*. 2008)	KDM6A (UTX) (Lan, Bayliss *et al*. 2007) KDM6B (JMJD3) (Agger, Cloos *et al*. 2007) KDM7 (JHDM1D) (Tsukada, Ishitani *et al*. 2010) PHF8 (Liu, Tanasa *et al*. 2010)
me3	KMT6A (EZH2) (Cao & Zhang 2004) KMT6B (EZH1) (Margueron, Li *et al*. 2008) NSD3 (Kim, Kee *et al*. 2006)	KDM6A (UTX) (Agger, Cloos *et al*. 2007) KDM6B (JMJD3) (Agger, Cloos *et al*. 2007)

H3K27me1 was shown to be enriching at heterochromatin regions in mammalian cells (Peters, Kubicek *et al*. 2003). A high-resolution genome-wide study of histone modifications shows H3K27me2 and -me3 at high levels in silent promoters and at reduced levels in promoters and transcribed regions of genes that expressed at low levels. The same study also describes H3K27me1 peaking at the 5′ region and evenly distributing throughout the transcribed region of active genes, which correlates with gene expression (Barski, Cuddapah *et al*. 2007). Most of the TSS with transposon exclusion zones, domains with little or no identifiable transposon derived sequence, have H3K27me3 (Bernstein, Mikkelsen *et al*. 2006). In Hela cells, H3K27me3 is predominantly found in places where

H3 is unmethylated at K36 (Yuan, Xu *et al*. 2011). In certain region of chromatin, it can co-occur with the active mark H3K4me1 (Rada-Iglesias, Bajpai *et al*. 2011) or -me3 (Bernstein, Mikkelsen *et al*. 2006). Such regions are termed 'bivalent' domains. In ES cells, bivalent domains would contain H3K27me3 along with either H3K4me3 in highly conserved noncoding elements (HCNE) rich loci (Bernstein, Mikkelsen *et al*. 2006) or H3K4me1 in enhancer regions (Rada-Iglesias, Bajpai *et al*. 2011). HCNEs cluster within regions that harbour genes for transcription factors involved in development. About 50% of the identified bivalent domains are binding sites of pluripotency-associated transcription factors NANOG, SOX2 and OCT4 (Bernstein, Mikkelsen *et al*. 2006). Trimethyl H3K4 and -K27 bivalent domains are also reported in human T cells (Roh, Cuddapah *et al.* 2006, Barski, Cuddapah *et al.* 2007). The bivalent domains are implicated in maintaining ES cell identity by keeping many developmentally essential transcription factor genes poised for later expression (Bernstein, Mikkelsen *et al*. 2006). In differentiated somatic cells, these bivalent domains are largely resolved to contain either of the two marks (Bernstein, Mikkelsen *et al*. 2006).

Function

H3K27 methylation is a repressive mark that is linked to homeotic gene silencing, XCI and genomic imprinting (Ringrose & Paro 2004). Higher levels of H3K27me3 methylation at the TSS correlates with gene repression (Boyer, Plath *et al.* 2006, Lee, Jenner *et al.* 2006, Roh, Cuddapah *et al.* 2006, Barski, Cuddapah *et al.* 2007). H3K27me3 can maintain imprinting independent of DNAme in the placenta (Lewis, Mitsuya *et al.* 2004, Umlauf, Goto *et al.* 2004).

Knockdown of EZH2-PRC2, but not EZH1-PRC2 complex, results in globally reduced H3K27me2 and -me3, and increased H3K27me1 (Margueron, Li *et al.* 2008, Shen, Liu *et al.* 2008). EZH1 can still maintain

H3K27 methylation at a subset of PcG target genes in EZH2-/- mouse ES cells (Shen, Liu *et al*. 2008). In differentiated cells, EZH2 and EZH1 maintain repression in different ways. While EZH2 acts through H3K27 methylation, EZH1 acts through chromatin compaction (Margueron, Li *et al*. 2008). Knockdown effects of other PRC proteins, which can affect H3K27me3, are discussed later in this chapter (section 1.5.1).

1.3.2.2 Histone acetylation

In 1964, Allfrey and co-workers showed that both methylation and acetylation occur on histones right after their synthesis. Based on this they postulated an involvement in regulation of transcription (Allfrey, Faulkner *et al*. 1964). Particularly, acetylation on these new histones is required for their deposition into nucleosomes and is removed following deposition. Now it is well known that regions of transcribed genes are hyperacetylated, while regions of heterochromatin are hypoacetylated (Shahbazian & Grunstein 2007). The hyperacetylation correlates well with gene activation (Lee, Shibata *et al.* 2004, Pokholok, Harbison *et al.* 2005, Roh, Cuddapah *et al.* 2005). Gene activation is thought to be due to the acetyl groups neutralizing the positively charged lysine residue, both in tail and core domains of histones. Specifically, histone tail hyperacetylation reduces its interaction with core DNA (Hong, Schroth *et al*. 1993) and linker DNA, and also between surrounding nucleosomes, thereby loosening the nucleosomal core structure (Shahbazian & Grunstein 2007). This loosening of structure would either directly facilitate the loading of the RNA polymerase II (Pol II) or promote the binding of transcription factors and their associated chromatin remodeling machinery. Either event could ultimately result in transcription. In contrast, deacetylation of lysine restores its positive charge, which results in increased interaction between histone tails, DNA, and neighbouring nucleosomes. These interactions result in chromatin compaction, which can eventually suppress the gene expression (Bannister & Kouzarides 2011).

In addition to its role in gene activation, acetylation suppresses heterochromatin spreading, chromatin compaction and nucleosome assembly (Shahbazian & Grunstein 2007). Various studies have implicated histone acetylation in even much wider and more diverse functions, such as DNA repair, cell cycle progression, growth and development, and even gene silencing (Carrozza, Utley *et al*. 2003).

1.3.2.2.1 Histone acetyl transferases and deacetylases

Histones are acetylated through the post-translational transfer of an acetyl group from acetyl-CoA to the ε-amino group of lysine by enzymes known as histone acetyl transferases (HATs). Even though the fraction with HAT activity was isolated in 1979 (Cano & Pestana 1979), it was the breakthrough discovery of transcriptional co-activator GCN5 (KAT2A) as the HAT (Brownell, Zhou *et al*. 1996) that lead to a surge of identification of other HATs (Kimura, Matsubara *et al*. 2005) and HAT-containing complexes (Carrozza, Utley *et al*. 2003).

Post-translational modification of histone acetylation carried out by HATs is reversed by HDACs (Bannister & Kouzarides 2011). HDACs were initially found in 1996 (Rundlett, Carmen *et al.* 1996, Taunton, Hassig *et al.* 1996) and many more were identified by 2005 (Ekwall 2005). They are divided into four classes. While class I, II, and IV encompass zinc-dependent HDACs, Class III enzymes encompass NAD^+-dependent sirtuin family (Peserico & Simone 2011). Individual members of class I comprise HDAC1-3 and HDAC8; class II comprise HDAC4-7 and HDAC9-10; class IV comprise its sole member HDAC11; and class III comprise members of the sirtuin family, SIRT1-7 (Peserico & Simone 2011).

Both HATs and HDACs work in multisubunit complexes and their specificity is dependent on other members in the complex, encompassing special domains. These special domains include: chromodomain that binds methylated lysine residue (Nielsen, Nietlispach *et al*. 2002); TUDOR

domain that binds dimethylated arginine (Sprangers, Groves *et al*. 2003) and methylated lysine (Kim, Daniel *et al*. 2006); PHD finger that binds Zn^{2+} (Pascual, Martinez-Yamout *et al*. 2000) and methylated lysine residues (Pena, Davrazou *et al*. 2006); bromodomain that binds acetylated lysine residues (Owen, Ornaghi *et al*. 2000); and WD40 repeat that binds H3 tail (Suganuma & Workman 2010), possibly H3K4me2 (Couture, Collazo *et al*. 2006) and ubiquitin (Pashkova, Gakhar *et al*. 2010). Both class I and II HDACs are involved in repression of diverse signaling pathways (Kao, Downes *et al*. 2000). Particularly the HDAC1-containing complex is implicated in regulating the Notch pathway of signal transduction (Kao, Ordentlich *et al*. 1998). HDAC1 and HDAC2 regulate G_1-to-S progression of cell cycle usually by suppressing p21 and p57 expression, which block cell cycle progression (Yamaguchi, Cubizolles *et al*. 2010).

Understanding the dynamic regulation of acetylation is difficult. Presence of more than one HAT or HDAC in the same complex makes it difficult to know which enzyme acts on which modification (Bannister & Kouzarides 2011). Furthermore, the same HAT and HDAC can act on more than one histone lysine target (Vaquero, Scher *et al*. 2004). Both HATs and HDACs enrich at active genes and positively associate with gene transcription. Based on these observations, it was postulated that the association of HDAC with Pol II is essential to manage the acetylation levels in active genes (Wang, Zang *et al*. 2009).

1.3.2.2.2 Acetylation of H3K9

KAT9 and KAT2A HATs, belonging to same family of histone acetyltransferases, are found to be acetylating H3K9 in mammals (Wang, Mizzen *et al.* 1997, Kim, Lane *et al.* 2002). Both SIRT1 and SIRT6, class III HDACs, present in the nucleus, have been shown to be deacetylating H3K9ac (Vaquero, Scher *et al.* 2004, Michishita, McCord *et al.* 2008).

SIRT1 deacetylates both H3K9ac and H4K16ac *in vitro* and *in vivo*. Deacetylation of both H3K9 and H4K16 by overexpression of SIRT1 causes loss of H3K79 methylation and silences the reporter gene through heterochromatinization (Vaquero, Scher *et al*. 2004). Deacetylation of H3K9ac at telomeres is required for the recruitment of Werner (WRN) protein to the telomeres, which is essential for proper functioning of telomeres and preventing premature cellular senescence. Accordingly, depletion of SIRT6 results in uncharacteristic chromosome structure and increased premature senescence (Michishita, McCord *et al*. 2008). Furthermore, deacetylation of NF-κB target promoters at H3K9 by SIRT6 is involved in preventing premature aging and increasing the life-span of mouse (Kawahara, Michishita *et al*. 2009).

Function

Gene-rich regions have high levels of H3K9 acetylation. However, only hyperacetylation at promoters and gene regulatory regions correlates with gene expression (Roh, Cuddapah *et al*. 2005). H3K9ac at promoter regions promotes low nucleosome density around the TSS (Nishida, Suzuki *et al*. 2006), which in turn might facilitate Pol II transcription through chromatin (Kim, Lane *et al*. 2002). By contrast, 5′ H3 acetylation is dependent on the Pol II elongation at some genes (Rybtsova, Leimgruber *et al*. 2007). In agreement with its role in inducing open chromatin, H3K9ac, along with H3K4me3, associates with rapidly inducible genes (Roh, Cuddapah *et al*. 2006). A genome-wide high-resolution study shows, enriched H3K9ac surrounding the TSS of active genes (Wang, Zang *et al*. 2008). H3K9 and -K14 acetylation islands, clusters of histone lysine acetylation, in the intergenic and transcribed regions have been proposed to predict functional regulatory elements (Roh, Cuddapah *et al*. 2005).

1.3.2.2.3 Acetylation of H4- K5/K12/K16

Histone H4 is acetylated by several classes of HATs with considerable overlapping activities. While KAT1, -2A, -3A, -3B, -5 and -7 acetylate H4K5 and H4K12, KAT2A, -3A, -3B and -8 acetylate H4K16 (Khare, Habib *et al*. 2012). Although HATs responsible for all H4 acetylations are reported, deacetylases are only known for H4K16ac. SIRT1 and SIRT2 are reported to act as H4K16 deacetylases (Khare, Habib *et al*. 2012). On the contrary, in HoxA9 loci, SIRT1 positively regulate H4K16Ac by deacetylating KAT8, acetylation of which prevents its acetylation activity on H4K16 (Lu, Li *et al*. 2011).

Function

H4K16ac is characteristically present in euchromatin. A genome-wide high-resolution study shows H4 -K5, -K12 and- K16ac enriching at promoters and throughout transcribed regions of active genes. Furthermore, gene promoters with the highest gene transcriptional activity have both H4K5 and -K16ac (Wang, Zang *et al*. 2008). Intriguingly, mammalian cells deficient for KMT2A/B, enzymes responsible for generating H3K9me3, show invasion of H4K16ac at constitutive heterochromatic region, even though SIRT1, the enzyme responsible for deacetylating H4K16 is not affected. Strikingly, none of the other euchromatic marks invade this region where H4K16ac is present exclusively (Vaquero, Scher *et al*. 2007).

In mammals, H4K5 and -K12ac are required for incorporation of newly synthesized histones into nucleosomes. This deposition-related histone H4 acetylation is conserved through evolution (Sobel, Cook *et al*. 1995). In fibroblasts, re-stimulation of serum-starved cells induces H4 acetylations through c-Myc at several target loci, which is necessary for induction of those genes (Frank, Schroeder *et al*. 2001). Furthermore, H4K5 and -K12ac are shown to be required for normal S-phase progression (Doyon,

Cayrou *et al*. 2006). SIRT2 specifically deacetylates H4K16ac during mitosis, which is believed to be essential for chromatin condensation (Fraga, Ballestar *et al*. 2005). While hyper-acetylated H4K16 (H4K16ac) resists heterochromatin spreading by a NAD^+-dependent HDAC (Suka, Luo *et al*. 2002), non-acetylated H4K16 is required for the chromatin to form higher-order structures (Shogren-Knaak, Ishii *et al*. 2006). Accordingly, H4 acetylation is absent from X_i, which is considered one of its hallmarks (Jeppesen & Turner 1993). H4K16ac is also an important marker in cancer diagnosis. Global loss of H4K16ac and H4K20me3, with concomitant DNAme gain at CpG islands and loss at repetitive DNA sequences are all diagnostic features of cancer cells (Fraga, Ballestar *et al*. 2005).

1.4 Histone variants

Metazoans produce two types of histone variants. First, there are replication-dependent (RD) variants, whose synthesis is tightly coupled to DNA replication. Second, there are replication-independent (RI) variants, which are produced throughout the cell cycle and also in quiescence (Loyola & Almouzni 2007). While H3 and H2A have species-dependent variants, H4 and H2B are invariant (Malik & Henikoff 2003). The mammalian H3 variants are RD H3.1 and H3.2, RI H3.3, centromeric-specific centromeric protein A and testis-specific H3t (Loyola & Almouzni 2007). H2A variants are H2A.Z, the major variant, and H2A.Bdb and macroH2A, the minor variants (Campos & Reinberg 2009). Histone variants can affect transcriptional activity by modifying nucleosome structure.

1.4.1 H3 variants

H3.1, the major variant of H3, is encoded by a cluster of 10 intronless genes. By contrast, H3.2 is encoded by single gene (Koessler, Doenecke *et al*. 2003). Both H3.1 and H3.2 differ by a single amino acid and their

transcripts are regulated by stem-loop binding proteins (Banaszynski, Allis *et al*. 2010). Both their expression is coupled to S-phase and they are incorporated in RD manner. Two intron-containing genes, *H3.3A* and *H3.3B,* which encode identical proteins, encode H3.3. H3.3 differs from H3.1 by 5 amino acids. H3.3 is transcribed throughout the cell cycle and is a major H3 variant deposited into chromatin in a RI manner (Ahmad & Henikoff 2002). Aging and differentiating cells accumulate H3.3 and have reduced H3.1 (Orsi, Couble *et al*. 2009).

Loyola and co-workers (Loyola, Bonaldi *et al*. 2006) characterised the PTM patterns of human H3.1 and H3.3 in nucleosomal and non-nucleosomal fractions. While the non-nucleosomal fraction of both H3.1-H4 and H3.3-H4 dimers enriches for H4K5 and -K12 acetylations, the nucleosomal fraction enriches for different lysine methylations. Both non-nucleosomal H3.1 and H3.3 lack lysine methylation marks except for K9, but have no detectable K9me3. Non-nucleosomal H3.3, has K9me1 (17%), K9me2 (4%) and K9 and K12 diacetylation (5%). The same study also found that a subset of H3.1-containing K9me2 and diacetylated K9 and K12 resists the action of SUV39 to form K9me3, while K9me1 or unmodified K9 are amenable to SUV39 modification. These findings implicate initial marks and histone variants in influencing the final PTMs on the chromatin.

Function

Generally, H3.3 is found in regulatory elements, promoters and transcribed regions (Talbert & Henikoff 2010). Its presence in transcribed regions correlates with gene transcription and hence its loading is speculated to be reliant on Pol II-dependent displacement of the core nucleosome structure (Loyola & Almouzni 2007, Campos & Reinberg 2009, Orsi, Couble *et al.* 2009). Supporting its role as an active chromatin mark, H3.3 has two fold more acetylation compared to H3.1 (Loyola,

Bonaldi *et al*. 2006). Compared to H3.1, H3.3 is more enriched in active marks, such as K4 and K36 methylations, as well as acetylated K9, K18 and K23 (Hake, Garcia *et al.* 2006, Loyola & Almouzni 2007).

The nucleosomes containing H3.3 are unstable, while H3.3 itself undergoes rapid turnover (Campos & Reinberg 2009). This rapid turnover is linked to maintaining the accessibility of chromatin or regulatory elements to their respective binding partners to influence epigenetic inheritance (Henikoff 2008). H3.3 also contributes for inefficient reprogramming after NT. In *Xenopus* NT experiments, the epigenetic memory carried by the H3.3, probably at K4, is implicated in resisting reprogramming. H3.3 persists at myogenic gene MyoD and drive its expression at non-muscle lineages, even after 24 cell divisions in the absence of transcription (Ng & Gurdon 2008). In mammals, the same mechanism is suspected after fertilisation to carry and transmit the male-specific epigenetic information through mature sperm. Human sperm has ~15% of histones, including H3.3 (Ooi & Henikoff 2007). Mature sperm of both mouse and human contains histone variants (H3.1/H3.2), which have been shown to contribute to the paternal zygotic chromatin (van der Heijden, Ramos *et al*. 2008). H3.3 is also linked to male infertility. Homozygous H3.3 male mutants results in death of 50% transgenic mice and reduced fertility of surviving mutants (Couldrey, Carlton *et al*. 1999).

1.4.2 H2A.Z

Unlike other histone variants, H2A.Z has been conserved during evolution from lower to higher eukaryotes. By contrast, other H2A variants H2A.Bdb and macroH2A are only found in vertebrates and mammals (Campos & Reinberg 2009). H2A.Z can influence the higher-order structure through its ion-binding pocket on the surface (Suto, Clarkson *et al*. 2000). The acidic patch on H2A.Z would enhance binding with HP1α compared to H2A and the same patch would also facilitate the binding of chromatin-remodelling complexes (Talbert & Henikoff 2010). Nucleosomes-containing H3.1 and

H2A.Z are more stable than H3.3 and H2A, and as stable as H3 and H2A. By comparison, H3.3 and H2A.Z-containing nucleosomes are unstable.

Function

Nucleosomes concurrently carrying H3.3 and H2A.Z are found at highly expressed gene promoters, enhancers and coding regions (Jin & Felsenfeld 2007). In humans, +1 to -2 nucleosomes that flank active genes, enrich for H2A.Z (Campos & Reinberg 2009). At the same time, H2A.Z presence both down- and up-stream of TSS correlates well with gene transcription, whilst its presence within transcribed gene body regions moderately correlates with gene silencing in human CD4+ T cells (Barski, Cuddapah *et al*. 2007). These contradicting functions could be due to the effect of different PTMs, such as acetylation and monoubiquitylation of H2A.Z (Talbert & Henikoff 2010). In humans, acetylated H2A.Z enriches more at euchromatic regions than at heterochromatin (Hardy, Jacques *et al*. 2009). RING2 is the ubiquitinating enzyme that can preferentially monoubiquitinate H2A.Z, resulting in silencing (Creyghton, Markoulaki *et al*. 2008). H2A.Z is also found enriched at transcriptional repressor CTCF-binding insulators, as well as at enhancers (Barski, Cuddapah *et al*. 2007). Its presence on either side of the CTCF-occupied site might act to restrict the spreading of the silent marks or heterochromatin (Campos & Reinberg 2009).

Cells lacking H2A.Z show poor HP1α localisation to heterochromatin and improper chromosome segregation (Rangasamy, Greaves *et al*. 2004), even though they have H3K9me3 (Greaves, Rangasamy *et al*. 2007). Mice lacking the H2A.Z variant die shortly after implantation (Faast, Thonglairoam *et al*. 2001).

1.5 Polycomb group proteins

The complex nature of higher multicellular organisms requires maintenance of the genome and variegated gene expression patterns over several cellular replications. Homeotic genes encode major groups of proteins that determine the segmentation patterns of the body by their variegated expression. Variegated expression needs the creation and maintenance of active and inactive domains, which involves two evolutionarily conserved antagonistic groups of proteins, namely PcG and TRX. PcG proteins are transcriptional repressors that maintain the repressive state of certain key genes during development (Cao, Wang *et al*. 2002), while TRX proteins act to maintain the active state of PcG target genes (Poux, Horard *et al*. 2002). We focused on PcG proteins because their repressive functions may be particularly relevant for quiescent cells, which are generally transcriptionally repressed.

1.5.1 Polycomb repressive complexes

The PcG proteins are mainly required for suppressing homeotic genes, especially of the Hox family. In addition, they are also implicated in XCI, maintaining stem cell identity, germ cell development and cancer metastasis (Cao & Zhang 2004a). PcG proteins work in multi-protein complexes. There are two families of complexes, namely PRC2 and PRC1 (Simon & Kingston 2009). The mammalian PRC2 complex comprises four core subunits: i) EZH, a SET domain-containing H3K27 KMTase; ii) suppressor of zeste 12 (SUZ12) and iii) embryonic ectoderm development (EED), both required for stimulating EZH2, and iv) retinoblastoma-associated protein p48, which is predicted to be involved in histone binding through its WD repeats domain (Simon & Kingston 2009). The mammalian family of PRC1 forms two different complexes. The first complex consists of the classically defined PRC1 complex with core members RING2, CBX4, BMI1 and PHC. The second complex consists of core members RING1, RING2, NPSC1, BCOR and KDM2B (Simon &

Kingston 2009). Both PRC2 and PRC1 components in mammals have variants, resulting in various forms of PRC2 complexes. The best known variants are EZH1 and EZH2. EZH2 is highly expressed during embryogenesis and proliferating cells, while EZH1 is expressed in adult and non-dividing cells.

Function

In vivo EED is essential for EZH2 activity. EED-EZH2 complex action is not limited to developmentally regulated genes, as both EED-EZH2 and H3K27 are essential for imprinting of XCI of extra-embryonic female cells and embryonic cells undergoing differentiation (Kuzmichev, Jenuwein *et al*. 2004). In mammals, EED is also implicated in PRC2-independent methylation activity (Pasini, Bracken *et al.* 2004). In addition, EED may be involved in propagation of the H3K27me3 mark (Margueron, Justin *et al*. 2009). Likewise, SUZ12 is also essential for establishment of proper H3K27 methylations (Pasini, Bracken *et al*. 2004). Specifically, SUZ12 and EZH2 are required for H3K27me2 and -me3 but not -me1, while EED is required for all forms H3K27 methylations (Montgomery, Yee *et al*. 2005). The EED-EZH2 complex silences developmentally regulated genes by trimethylation of H3K27 and this methylation guides the binding of PRC1 complex (Cao, Wang *et al*. 2002).

The exact mechanism of gene suppression activity by PcG proteins is still largely unknown. Initially, it was speculated that PRC2-mediated H3K27me3 could act as a binding site for the chromodomain of PRC1 leading to ubiquitination of H2AK119 by RING2, which would impede the loading of Pol II to the chromatin (de Napoles, Mermoud *et al.* 2004, Fang, Chen *et al.* 2004). RING2 presence on X_i of both trophoblast stem (TS) and differentiating ES cells correlates with monoubiquitinated H2AK119 (H2AK119ub) on X_i (Fang, Chen *et al*. 2004). However, EED-/- ES cells that lack H3K27me3 still maintains RING2-mediated H2AK119ub,

indicating that recruitment of RING2 can be both dependent and independent of PRC2 activity (Schoeftner, Sengupta *et al*. 2006). This suggests that wide-spread PRC2-dependent targeting of PRC1 may not be universal. At times, even RING2-mediated H2AK119ub does not correlate with gene suppression (Schoeftner, Sengupta *et al*. 2006). Therefore, the mechanism of H3K27me3- and H2AK119ub-mediated gene suppression still remains to be elucidated (Bracken, Dietrich *et al.* 2006, Schoeftner, Sengupta *et al.* 2006, Simon & Kingston 2009).

Both PRC2 and PRC1 members have chromatin condensation activity independent of each other. Changes in composition of PRCs enable them to perform this task. For example, association of PRC2 complex with EZH1 instead of EZH2 could enables the complex to condense chromatinised templates *in vitro*, while having reduced KMTase activity. On the other hand, the EZH2-containing PRC2 complex does not condense chromatin, but has a high KMTase activity (Margueron, Li *et al.* 2008, Shen, Liu *et al.* 2008). Likewise, RING2 association with CBX4, BMI1 and PHC1 can enable it to compact chromatin, while association with RING1, NPSC1, BCOR and KDM2B would enable it to H2AK119 ubiquitination (Simon & Kingston 2009). In mouse, RING2 is involved in Hoxb and Hoxd loci contraction. Chromatin compaction activity of RING2 was independent of its ubiquitinating activity (Eskeland, Leeb *et al.* 2010, Bantignies & Cavalli 2011).

In loss of functional assays, EZH2 -/- mouse ES cells do not show any effect on H3K27me1. Even though there is a major reduction in H3K27me3, some genes, particularly development-related genes, still preserve this mark. As a consequence, EZH2-/- ES cells lose their capability to go through mesodermal differentiation. (Shen, Liu *et al*. 2008). During early development, the EZH2-/- mutation is lethal as mutants never complete gastrulation (O'Carroll, Erhardt *et al*. 2001). In EED-/- ES cells, all forms of H3K27 methylation are disrupted, leading into

target gene de-repression and loss of ability to properly differentiate. However, these cells remain fully pluripotent and contribute to chimeras (Chamberlain, Yee *et al.* 2008, Leeb, Pasini *et al.* 2010). EED-/- cells, although initiate XCI, fail to complete it. (Kuzmichev, Jenuwein *et al*. 2004). EED-/- embryos show disrupted anterior-posterior patterning and fail to normally gastrulate (Faust, Schumacher *et al.* 1995, Shumacher, Faust *et al.* 1996). SUZ12-/- ES cells can be generated and proliferated, but lose H3K27 methylation. However, the loss of H3K27 methylation leads to gain of H3K27 acetylation and H3K36 methylation, reducing their ability to properly differentiate. During differentiation, SUZ12-/- ES cells show characteristic de-repression of differentiation-specific genes and fail to repress ES cell-specific markers. Even though these ES cells increase H3K27me3 at specific genes, they fail to repress them, suggesting that activation cues are stronger than the repression (Pasini, Bracken *et al.* 2004, Pasini, Bracken *et al.* 2007, Jung, Pasini *et al.* 2010). Knockdown of SUZ12 in Hela cells results in cell growth defects, alteration in H3K27 methylation and up-regulation of Hox genes (Cao & Zhang 2004b). SUZ12-/- mice show severe developmental and proliferative defects and die during post-implantation stage. Specifically, those embryos lose both H3K27me2 and -me3 (Pasini, Bracken *et al.* 2004, Pasini, Bracken *et al.* 2007, Jung, Pasini *et al.* 2010). Depletion of RING2 in ES cells results in de-repression of subset of development-related genes and unsynchronized differentiation-associated pathways. They also down-regulate pluripotency markers REX-1 and SOX2, but still maintain other ES cell-specific markers, such as OCT4, NANOG and alkaline phosphatase (van der Stoop, Boutsma *et al*. 2008). RING2-/- embryos result in defects in both embryonic and extraembryonic tissues leading to gastrulation arrest. Genetically manipulated repression of the Cdkn2a (Ink4aARF) locus overcomes the gastrulation arrest effect in RING2-/- embryos. This implicates RING2 in cell cycle regulation during gastrulation (Voncken, Roelen *et al*. 2003).

1.6 Epigenetic reprogramming in germ cells

Mammalian fertilisation involves fusion of two specialised types of germ cells, sperm and oocytes. Differentiation of PGC into mature germ cells occurs in two phases of epigenetic reprogramming, which are conserved in mammals (Hyldig, Croxall *et al*. 2011). In the first phase, loss of H3K9me2 and DNAme are seen just before or at G_2-stage arrest of PGCs. The arrest continues up to the accumulation of H3K27me3. The early PGCs also accumulate H3K4me2, -me3 and H3K9Ac, probably acquiring a bivalent state that correlates with expression of *Nanog, Oct4, Sox2 and Stella* (Hemberger, Dean *et al*. 2009). In the second phase, after entry into the developing gonads, where most cells are cycling, PGCs start to gradually demethylate DNA in imprinting and other regions, which were not demethylated in first phase (Hyldig, Croxall *et al*. 2011). At this stage, the PGCs lose linker H1 and chromocenters, centres formed by clustering of many pericentric heterochromatin regions, down-regulate H3K9me3 and H3K27me3, and redistribute or down-regulate factors associated with facultative and constitutive heterochromatin. They also down-regulate a component of PRC1 like complex, CBX2 (Hemberger, Dean *et al*. 2009). Comparison of the two phases of PGC reprogramming indicates general down-regulation of most of the repression-associated epigenetic modifications. Reprogramming in these phases results in larger nuclei and lost chromocenters, reflecting a decondensed chromatin, that is amenable for further reprogramming (Hajkova, Ancelin *et al*. 2008). Following resetting of histone modifications, DNA remethylation takes place in the male germ line, creating specific patterns at differentially methylated regions of imprinting control regions (ICRs). In the female germ line, this remethylation takes place postnatally during oocyte growth, creating maternal-specific ICR patterns (Sasaki & Matsui 2008).

1.7 Epigenetic reprogramming in early embryos

Fertilisation of oocyte and sperm returns the newly formed zygote to a totipotent state. Chromatin organisation differs dramatically between the maternal and paternal gametes. While mature sperm chromatin is tightly packed by protamines and some sperm-specific histone variants (Govin, Escoffier *et al*. 2007), MII oocyte chromatin is packaged with histones.

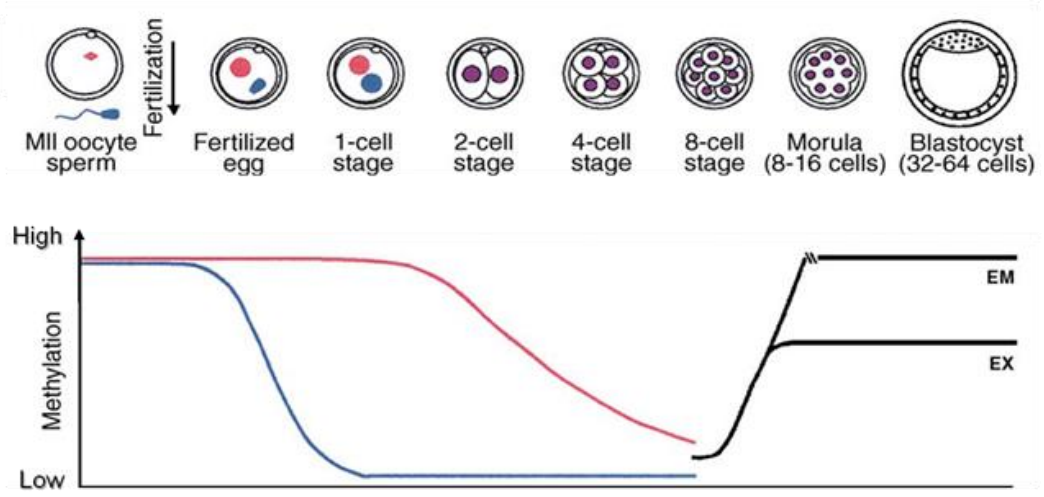

Figure 4: Dynamic reprogramming of global DNAme in bovine preimplantation embryos. (a) The bovine paternal genome (purple) undergoes active demethylation, while the maternal genome (red) is passively demethylated up to the eight-cell stage, after which de novo methylation (black line) is observed. EM, embryonic and EX, extra-embryonic lineages. Adapted from Dean, W., *et al*. (2003),

After fertilisation, the paternal genome immediately undergoes global TET3-dependent (Gu, Guo *et al*. 2011) DNA demethylation, only sparing pericentric heterochromatin and paternal imprints. The maternal DNA undergoes progressive demethylation until the eight-cell and morula stage in bovine and mouse, respectively. Thereafter, *de novo* methylation of both maternal and paternal DNA starts (Dean, Santos *et al*. 2003) (Figure 4). *De novo* methylation at the eight-cell stage coincides with the presence of DNMT1o, an oocyte-specific maintenance DNMT (Fulka, St John *et al*. 2008). In bovine, there are also reports of active demethylation and *de novo* methylation of both DNA and H3K9me3 of the paternal pronucleus to the level of the maternal pronucleus before the two-cell stage (Park, Jeong

et al. 2007). In most preimplantation embryos, DNA and H3K9 methylation is linked (Santos, Zakhartchenko *et al.* 2003, Lepikhov, Zakhartchenko *et al.* 2008). At the blastocyst stage, *de novo* methylation ensures hypermethylation of the ICM compared to the trophectoderm (TE) in some mammalian species, such as mouse and pig (Morgan, Santos *et al*. 2005). In bovine, the ICM is only slightly hypermethylated than TE (Santos, Zakhartchenko *et al*. 2003), while in human and monkey, the ICM is hypomethylated compared to the TE (Fulka, St John *et al*. 2008).

Germinal vesicle (GV)- and MII-stage oocytes can *de novo* methylate H3K9, an ability which is lost after fertilisation (Liu, Kim *et al*. 2004). Upon fertilization sperm protamines are replaced by highly acetylated maternal histones from the oocyte cytoplasm. These histones lack H3K4me1 and -me3, H3K9me2 and -me3, H3K27me2 and -me3 and H4K20me3, but carry H3K9me1 and H3K27me1. Meanwhile, the maternal genome completes meiosis and enrich for DNAme, as well as, H3K4- and H3K9 methylations, H3K27me1 and -me3, H4K20me3 and H4 acetylation (Liu, Kim *et al.* 2004, Morgan, Santos *et al.* 2005). Maintenance of this asymmetric methylation pattern after fertilisation is an active process (Liu, Kim *et al*. 2004). During pronuclear development, the paternal genome acquires H3K4me1 and -me3, H3K9me2 and H3K27me2 and -me3 (Liu, Kim *et al.* 2004, Morgan, Santos *et al.* 2005). Even though Suv39h is present from the immature oocyte up to the blastocyst stage, its function is stalled until embryonic genomic activation. H3K9 methylation gradually decreases from two-eight cell stage and increases from the morula up to the blastocyst stage (Santos, Zakhartchenko *et al*. 2003). H3K27me3 progressively decreases from bovine immature oocytes up to eight-cell stage, which coincides with absence of EED and SUZ12 in the nucleus. Thereafter, it increases from the morula to the blastocyst stage (Ross, Ragina *et al*. 2008). H3K4me3 follows a similar pattern as H3K27me3 (Wu, Li *et al*. 2011). H3K9Ac (Kubicek, Schotta *et al.* 2006a) and H4K5Ac (Monteiro, Oliveira *et al*. 2010) are dynamically regulated in early embryos,

and correlates with HDAC level (Kubicek, Schotta *et al.* 2006a). At the blastocyst stage, H3K9me3, all forms of H3K27 methylation, H4K20me3 and H3K9ac are re-established. In mouse, all these marks are up-regulated in the ICM compared to the TE. In the TE, H3K27me2 and -me3 are present only on X_i (Hemberger, Dean *et al*. 2009). By contrast, bovine blastocysts do not show any H3K -4me3 and -27me3 differences between the ICM and TE (Ross, Ragina *et al.* 2008, Wu, Li *et al.* 2011). H3K9me2 is distributed evenly between ICM and TE, and heterochromatin of both the ICM and TE is marked by H3K9me3 (Morgan, Santos *et al*. 2005).

1.8 Epigenetic reprogramming after nuclear transfer compared to *in vitro* fertilisation (IVF)

Even though the oocyte has the ability to reprogram a somatic cell, in principle, this does not result in efficient production of live animals (Wakayama 2007). This is attributed to the difficulty of reprogramming the epigenetic patterns associated with progressive donor cell differentiation. Supporting this notion, toti- and pluripotent cells, such as early blastomeres (Hiiragi & Solter 2005) and ES cells, respectively, (Rideout, Eggan *et al*. 2001) are often more amenable to reprogramming than somatic cells. It is intriguing that even though SCNT constructs down-regulate genes involved in chromatin modification compared to IVF embryos (Monteiro, Oliveira *et al*. 2010), there is little difference between SCNT and IVF-derived ES cells. This includes high similarity in DNAme, imprinted genes, as well as mRNA, microRNA and protein expression profiles (Brambrink, Hochedlinger *et al.* 2006, Wakayama 2006, Ding, Guo *et al.* 2009). This similarity is thought to be due to culture systems tailored for efficient derivation of ES cells. In contrast to the formation of live offspring, ES cell derivation appears to be rather tolerant to epigenetic abnormalities.

For successful NT cloning, the donor chromatin must be reprogrammed to the level capable of supporting further development. However, epigenetic

profile of NT embryos resembles that of the somatic donor. Moreover epigenetic reprogramming during NT is haphazard, as each NT embryo exhibits different epigenetic profiles (Kang, Koo *et al.* 2001a). There are obvious differences in the epigenetic profiles of bovine embryos produced by IVF and NT (Han, Kang *et al*. 2003). In contrast to IVF embryos, where DNA demethylation and reduction in H3K9me3 occurs in parallel up to the eight-cell stage, NT embryos exhibit hypermethylated DNA and H3K9me3 at all stages (Santos, Zakhartchenko *et al*. 2003), the pattern of which is reminiscent of donor cells (Dean, Santos *et al*. 2003). The increased DNAme can be attributed to abnormal expression of somatic DNMT1 in NT embryos (Fulka, St John *et al*. 2008). In bovine, inadequate DNA demethylation of somatic nuclei is linked to the absence of the maternal chromatin (Kang, Koo *et al.* 2001b). In bovine NT blastocysts, hypermethylation of the ICM for both H3K9 and DNA is not evident and the TE is as methylated as the ICM (Santos, Zakhartchenko *et al.* 2003, Wu, Li *et al.* 2011). NT embryos with a normal DNA and H3K9 methylation epigenotype show better blastocyst development (Santos, Zakhartchenko *et al*. 2003). High levels of H3K9 methylation in extraembryonic tissues correlates with placental abnormalities in NT animals (Kubicek, Schotta *et al.* 2006b). All these observations underline the importance of proper reprogramming of H3K9 methylation.

In bovine, H3K4me3 is hypermethylated from the pronuclear stage to the eight-cell stage in NT compared to IVF embryos. It is then transiently down-regulates at the morula and again hypermethylates at the blastocyst stage in NT (Wu, Li *et al*. 2011). In mouse IVF embryos, the ICM shows H3K27me3 staining, which is absent in SCNT blastocysts despite some TE staining for X_i (Zhang, Wang *et al*. 2009). In bovine, H3K9 is hyperacetylated in NT embryos in all stages compared to IVF embryos. H3K9 acetylation of IVF embryos reaches its minimum at four-eight cell stage and then increases with the onset of transcriptional activation at 8-16 cell stage (Santos, Zakhartchenko *et al*. 2003). At the blastocyst stage,

H3K9Ac is either less (Santos, Zakhartchenko *et al*. 2003) or not different (Wu, Li *et al*. 2011) in NT vs IVF embryos. H4K5 is also hyperacetylated until eight-cell stages in NT compared to IVF embryos (Wu, Li *et al*. 2011). The difference in H4K5Ac observed until eight-cell stages in NT compared to IVF embryos, ceases to exist from the morula to the blastocyst stage (Wu, Li *et al*. 2011). All these epigenetic differences result in various developmental abnormalities in NT embryos, foetuses and cloned offspring.

1.9 Epigenetically modified donors for nuclear transfer

After SCNT, donor cells need to undergo proper epigenetic reprogramming for successful embryonic development (Yang, Smith *et al*. 2007). The majority of embryos that do not develop normally fail to erase the epigenetic differentiation program of donor cells (Campbell, Fisher *et al*. 2007). The better success rate of ECNT over SCNT is attributed to the epigenetic state of the embryonic cells. In order to increase SCNT efficiency, modification of the epigenetic state of donor cells has been achieved by several means. Class I/II HDAC inhibitors (HDACi), such as Trichostatin A (TSA), scriptaid and sodium butyrate (NaB), as well as DNMT inhibitors, such as 5-aza-2′-deoxycytidine (5-aza-dC), have been tried extensively. In cattle, treating donor cells with TSA prior to NT increases blastocyst development (Enright, Kubota *et al*. 2003). By contrast, treating donors with 5-aza-dC either show no effect at low concentrations (Enright, Sung *et al.* 2005, Jafarpour, Hosseini *et al.* 2011) or a negative effect at higher concentrations (Enright, Kubota *et al.* 2003, Jafarpour, Hosseini *et al.* 2011). Higher doses of both TSA and NaB result in hyperacetylation and hypermethylation, and higher rates of blastocyst development (Jafarpour, Hosseini *et al*. 2011). TSA treatment of plasmids with initial low or no DNAme increases transcription of a reporter gene, while plasmids with high DNAme show little effect on reporter gene transcription (Ji, Zhang *et al*. 2003). In cattle, there is a synergetic effect

when both TSA and 5-aza-dC are used in combination. Treating both donors and embryos with both these reagents further improves blastocyst development (Ding, Wang *et al*. 2008) and cloning efficiency to weaning (Wang, Xiong *et al*. 2011). This success correlates with higher expression of *Sox2* and *Oct4* and lower expression of DNMTs at the blastocyst stage (Wang, Su *et al*. 2011).

In mouse, utilization of a hypomorphic DNMT1 allele, resulting in hypomethylated donor cells, improves both blastocyst development and ES cell-derivation (Blelloch, Wang *et al*. 2006). Some groups have explored the use of RNAi-mediated knock-down. DNMT1 siRNA-treated bovine donor cells significantly increases blastocyst development compared to control IVF (Eilertsen, Power *et al*. 2007). Knock-down results in reduced DNAme levels at the four-cell stage embryos compared to controls, but does not reduce methylation levels to that of IVF embryos (Giraldo, Lynn *et al*. 2009). Comparing knock-downs of DNMT1, DNMT2 and DNMT3a, only DNMT1 reduction significantly decreased DNAme in bovine fibroblasts (Yamanaka, Balboula *et al*. 2010). G9a, an HMTase linked to H3K9 methylation-mediated heterochromatinization and de novo DNAme, is implicated in suppression of various early embryonic genes. The use of G9a-/- ES cells as donors significantly improves blastocyst development (Epsztejn-Litman, Feldman *et al*. 2008).

1.10 Cell cycle

Continuously dividing cells move through a continuous cell cycle, which has four distinct stages: Gap 1 (G_1), DNA Synthesis (S), Gap 2 (G_2) and Mitosis. Transition from one stage to the other is governed by cyclins and their respective cyclin-dependent kinases (CDKs). Cells can exit this cell cycle and rest in a stage called quiescence (G_0). In G_0, they are neither dividing nor preparing to divide, but can re-enter the cell cycle and proliferate upon certain stimuli (Coller 2011). Quiescence as a distinct

cellular stage has been well established. G_0 cells not only down-regulate genes involved in cell proliferation, but also actively inhibit senescence, apoptosis and differentiation (Coller 2011).

Under conditions that maintain ploidy, the cell cycle stage has been postulated to influence cloning efficiency (Campbell, Loi *et al.* 1996, Wilmut, Schnieke *et al.* 1997). Wilmut *et al*. reasoned that inducing the cells into quiescence through serum-starvation was the major reason behind the first mammalian SCNT success. Later it was shown that induction of quiescence is not essential for cloning success (Cibelli, Stice *et al.* 1998, Vignon, Chesne *et al.* 1998, Kasinathan, Knott *et al.* 2001c, Wells, Laible *et al.* 2003). Treatment of donor cells with aphidicolin, a reversible inhibitor of eukaryotic nuclear DNA replication that blocks at the pre-S phase stage (Vodicka, Smetana *et al*. 2005), increases the efficiency of NT blastocyst development in mini-pig oviduct epithelial, ear skin fibroblast and cumulus cells (Zhang, Dai *et al*. 2012). Tetraploid (4n) cells at the G_2/M stage should be maximally compatible with the metaphase-arrested MII recipient. Accordingly, ES cells (Wakayama, Rodriguez *et al*. 1999), as well as transgenic (Ono, Shimozawa *et al.* 2001, Lai, Park *et al.* 2002) and non-transgenic fibroblasts (Ono, Shimozawa *et al*. 2001) successfully work as donors. Often, serum withdrawal for several days is used to induce quiescence in cells used for NT. Serum-starvation has a beneficial effect on NT efficiency compared to non-starved cycling and G_1 cells (Zakhartchenko, Durcova-Hills *et al.* 1999, Hill, Winger *et al.* 2000, Hill, Winger *et al.* 2001, Cho, Lee *et al.* 2002, Zou, Wang *et al.* 2002, Wells, Laible *et al.* 2003)

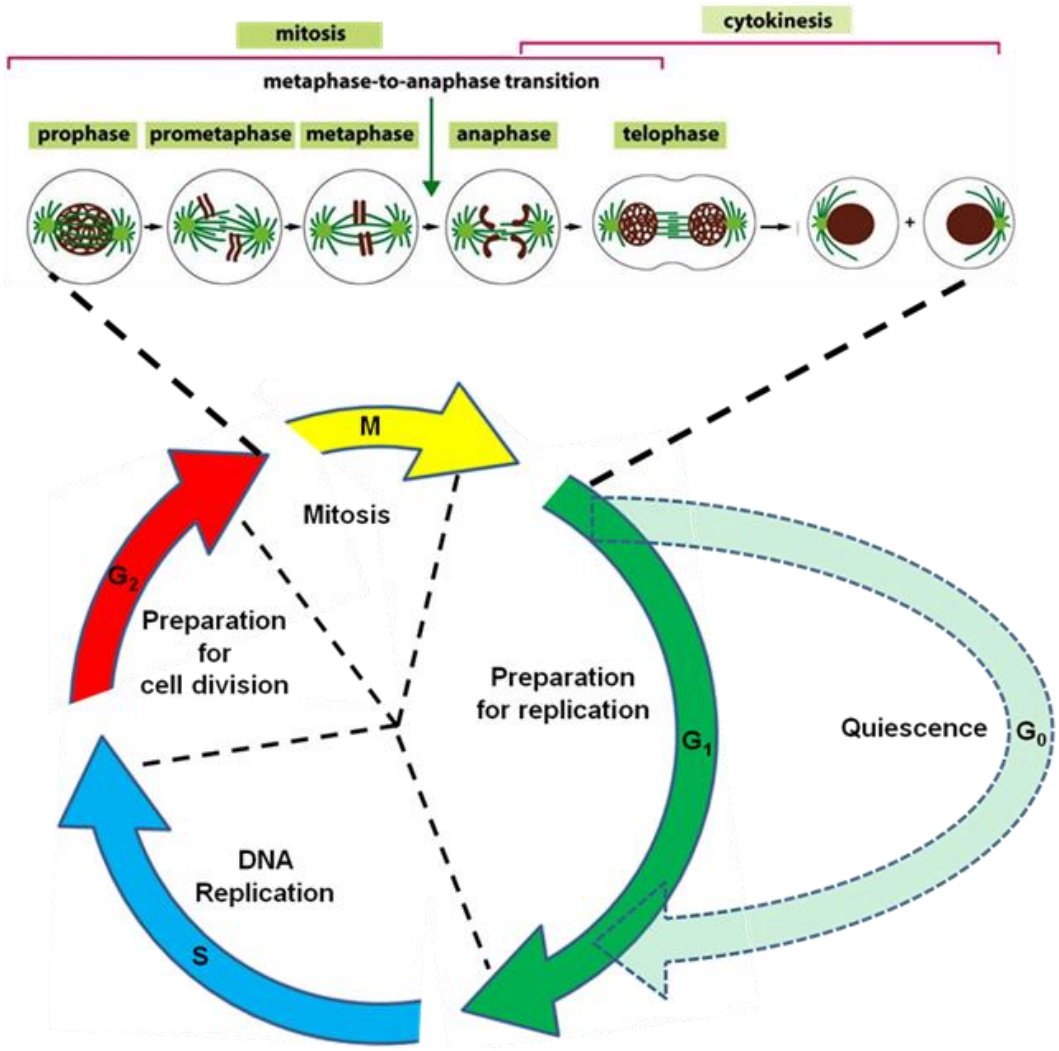

Figure 5: Cell cycle: The upper part of the figure depicts the individual stages in mitosis until cytokinesis. Cell size from prophase-anaphase is twice as that of the newly formed cells after cytokinesis. (Modified from Alberts & Johnson *et al*. 2008). Lower part of the figure depicts different stages of cell cycle (colored solid curving arrows). Under unfavorable conditions, cells can exit the cell cycle in G_1 to enter the G_0 stage (dotted curving arrow), commonly known as quiescence or resting stage. Under favorable conditions, cells can re-enter the normal cell cycle from the G_0 stage. (Modified from Coller, 2011).

Experimentally, serum-starvation, growth to confluency and inhibition of adhesion can all induce quiescence. Strikingly, cells induced into quiescence by all these three methods exhibit distinct, although overlapping, expression profiles (Coller, Sang *et al*. 2006). Few hours of serum-starvation of early G_1 (3-4 h post-mitotic) mouse 3T3 cells, push cells towards G_0. But even though the serum is withdrawn, cells that are in

late G_1 still commit to proceed through S, G_2 and M phase (Zetterberg & Larsson 1985, Larsson, Dafgard *et al.* 1986). Examples of naturally occurring G_0 cells include lymphocytes and dermal fibroblasts (Coller 2011). The quiescent lymphocytes have been shown to contain hypomethylated histone, which correlated with better NT reprogramming efficiency (Baxter, Sauer *et al*. 2004).

1.11 Summary

Cloning is an inefficient technique. Nevertheless it is useful for producing endangered species, animals with beneficial traits and transgenic animals. Over the years, there have been many unsuccessful attempts to increase the efficiency of the cloning (Campbell, Alberio *et al.* 2005, Campbell, Fisher *et al.* 2007). There are several factors that influence cloning efficiency, including the NT method, oocyte quality, donor cell status, etc. Cells from early blastomeres to terminally differentiated cells have been successfully used in cloning (Prather, Barnes *et al.* 1987, Hochedlinger & Jaenisch 2002). Following NT, the chromatin of the donor cell must be reprogrammed from a differentiated to a totipotent status through proper epigenetic modifications that include changes in DNAme and core histones. The modifications to core histones involve mainly their tail region either by acetylation, methylation, phosphorylation and/or ubiquitinisation. Considering the lower efficiency of cloning, the initial epigenetic status of the donor appears to be crucial for success. Therefore, studies have attempted to improve the initial donor cell epigenetic status.

1.12 Aim of the thesis

Methods to alter the epigenetic status of the donor cells have been successfully employed to improve the cloning efficiency (Blelloch, Wang *et al.* 2006, Wang, Xiong *et al.* 2011). Among these, inducing the donors into quiescence by serum-starvation was thought to be a major contributor to the success of the first SCNT (Wilmut, Schnieke *et al*. 1997). However this

assumption was never experimentally verified. Unpublished work at Agresearch has demonstrated that serum-starvation of donor cells more than doubles cloning efficiency to adulthood compared to mitotically-selected G_1 control donors. Therefore, we postulated that inducing donors into G_0 would alter their epigenetic status and increase their reprogrammability.

Here, we aim to identify the molecular basis for elevated reprogramming potential and induced cell plasticity in serum-starved cells. We hypothesise that serum-starvation "loosens" the epigenetic constraints imposed on the genome during differentiation, leading to changes in chromatin composition, DNA and histone methylation, as well as histone acetylation levels. We propose that artificially inducing quiescence through serum-starvation results in a more dynamic chromatin architecture that forms a structural basis for increased cloning efficiency for G_0 donors.

Specifically, my aims were:

A. Prior to NT, to test G_0 vs G_1 donors with respect to their localisation and abundance of:
   1) post-translational histone lysine methylation
   2) post-translational histone lysine acetylation
   3) PcG and chromatin-associated proteins
   4) DNAme

B. Following NT, to determine the dynamics of a subset of candidate epigenetic modifications, previously found to be different between G_0 and G_1 cells.

Chapter Two: Materials and methods

2.1 General materials and methods

2.1.1 General materials

All the materials and reagents are listed in appendix I and II.

2.1.1.1 Cell and embryo culture

Ear skin fibroblast were isolated from an adult Limousine-jersey bull (LJ801) as described previously (Oback & Wells 2003) and used for cell culture and NT studies.

2.1.2 General methods

2.1.2.1 Thawing cells

Vials-containing approximately 1 ml of LJ801, $2X10^5$-$1X10^6$ cells/ml, were removed from liquid nitrogen storage and rapidly transferred to a 37°C water bath. Vials were removed when cells were approximately 80% thawed and wiped with 70% ethanol. Cells were Immediately transferred into a tube-containing 10 ml of 37°C pre-warmed Dulbecco's Modified Eagle's medium (DMEM)/F12 + GlutaMAX™-I, supplemented with 10% v/v fetal calf serum (FCS) (DMEM/F12-10%), and centrifuged at 1000 x g for 3 min. Medium was removed carefully, the pellet was resuspended in pre-warmed DMEM/F12-10% and cells were counted using a Neubauer haemocytometer.

2.1.2.2 Cell culture

Using the pre-warmed DMEM/F12-10% culture media, cells were diluted to 10^5 cells/ml and seeded on culture dishes at a density of approximately

$1.7X10^4$ cells/cm^2. The cells were then cultured in an incubator-containing 5% CO_2 at 38.5°C.

2.1.2.3 Passaging

When cells reached 70-90% confluency, they were washed once with 37°C pre-warmed phosphate buffered saline (PBS), and then 37°C pre-warmed 0.25% trypsin-EDTA was added at 0.02 ml/cm^2 and incubated at 37°C for 2 min. After complete cell detachment from the culture dish, a fivefold excess of DMEM/F12-10% culture media was added to neutralise the trypsin. Cells were centrifuged at 1000 x g for 3 min. Medium was removed carefully, the pellet was resuspended in pre-warmed DMEM/F12-10% culture media, and cells were counted using a Neubauer haemocytometer.

2.1.2.4 Freezing

Cells were grown up to 70-90% confluency and passaged as described in section 2.1.2.3. Cells were again centrifuged for 3-5 min. During the centrifugation, the cryopreservation solution (20% DMSO in FCS) was freshly prepared. After centrifugation, medium was carefully removed and DMEM/F12-10% culture medium was added to the pellet of cells at a volume equal to 50% of total volume required. The total volume required was accordingly adjusted to give the desired density of cells. The remaining 50% volume was made up by slowly adding an equal volume of cryopreservation medium and mixed gently. Cells were then aliquoted in 1 ml volumes at required densities per cryovial and placed in a freezing box (Mr Frosty) in a -80°C freezer. After 24 h, vials were transferred into liquid nitrogen for long term storage.

2.1.2.5 Inducing quiescence (G_0) by serum-starvation

Quiescence was induced as described previously (Oback & Wells 2003). Cells were thawed and cultured for just one passage as described in sections 2.1.2.1 and 2.1.2.2, respectively. After trypsinization,

centrifugation and counting, $2.5x10^4$ cells/cm^2 were seeded for NT, immunofluorescence (IF) and biochemical assays. Cells were cultured for 6-15 h. Medium was removed, followed by washing thrice with PBS and cultured in DMEM-F12 containing 0.5% FCS (DMEM/F12–0.5%) for six days.

2.1.2.6 Isolating G_0 cells

After induction of quiescence for six days, cells were processed as described in section 2.1.2.2 but with the following minor changes. Serum-starved cells were washed once with pre-warmed PBS, incubated with pre-warmed trypsin for 4-5 min, neutralised with DMEM/F12-0.5% (10-15 fold excess of trypsin) and resuspended in H199-containing 0.5% FCS (H199-0.5%) at a density of 10^4 cells/ml.

2.1.2.7 Culturing for isolating G_1 cells

G_1 cells can be mechanically picked under a light microscope (mitotic selection) (Wells, Laible *et al*. 2003) or isolated from G_1 "mitotic shake-off" (Kasinathan, Knott *et al.* 2001b). We used a modified mitotic shake-off method to generate G_1 cells.

Passage 4 cells were thawed and cultured for one passage as described in sections 2.1.2.1 and 2.1.2.2, respectively. After trypsinization, centrifugation and counting, cells were seeded at a density of $6x10^5$ cells/100 mm culture dish and cultured for 20 h in DMEM/F12-10%, washed once with pre-warmed PBS and cultured for another 2 h in 10 ml pre-warmed DMEM/F12-10%. After 2 h, cells were scored under a microscope for presence of doublets. If doublets were starting to lift off, we proceeded with the mitotic shake-off procedure. Otherwise, we cultured them further, until doublets started to lift off, before proceeding with the mitotic shake-off.

2.1.2.8 Mitotic shake-off

5.5 ml of medium was removed and the mitotic shake-off of cells was undertaken by shaking the 100 mm culture dish on a plate shaker (IKA, MS1) at 800 rpm for 1 min, followed by a gentle tap with a finger on the sides of the plate. Medium containing the lifted cells was centrifuged at 1000 x g for 3 min in a 15 ml Falcon tube. Medium was then carefully removed and cells were gently resuspended in 500-1000 µl of H199 supplemented with 10% FCS (H199-10%).

2.1.2.9 Wide-field epifluorescence image acquisition

Slides were viewed with an Olympus BX50 microscope at either 100X, 200X, 400X or 1000X magnification. The images were first focused under phase contrast to minimize exposure to fluorescence light and bleaching. Digitized images were taken with a Spot RT-KE slider digital camera using the Spot Basic software. Exposure time and camera setting within the similar experiments were kept constant. Images were processed using the Spot Advanced software.

2.1.2.10 Confocal epifluorescence image acquisition

Slides were initially viewed at either 100X, 200X, 400X or 600X magnifications by using wide-field epifluorescence and differential interface contrast (DIC). Digital confocal images were acquired using the FluoView FV1000 software. For image acquisition, the following settings were maintained constant for all the experiments:

Image size	: 512*512
Bits/Pixel	: 12
Sampling speed	: 12.5 µs/pixel
Lens	: 60X (Oil)
Objective lens (NA)	: 1.35
Sequential mode	: Frame
Integration type	: Line (Kalman)
Integration count	: 2
Zoom	: 6 (Donor cells), 1 (Embryo)

Slice/frame thickness : 0.4 µm/slice for donor cells and 1 µm/slice for (Embryo) (As determined by optimisation function)
Pinhole : 110 µm
Laser wavelengths : 405, 488 and 543 nm

Within each experiment, settings such as PMT voltage (V), transmissivity (%), gain and offset were maintained constant for both G_0 and G_1 donors and NT embryos derived from them.

After setting all the above parameters, the upper and lower Z-limit was set by going through the entire image of each donor or embryo. The image was then acquired as a combination of different frames (stack).

The frame thickness was determined using the optimisation function and set as 400 nm for donors and 1000 nm for embryos.

2.1.3 Statistical analysis:

Antigen data were analysed using one–way ANOVA with equal variance or using t-test, either paired or unpaired, with equal or unequal variance. Data were log transformed when necessary. All bars represent either Least Significant Difference (LSD) at 5% or standard error of means (SEM). If the LSD bar extends past two data mid-points, then the difference between them is P>0.05.

2.2 Methods for chapter three

2.2.1 Characterising restimulation of quiescent cells by xCELLigence

The xCELLigence System uses special tissue culture vessels with interdigitated microelectrodes integrated on their bottom. When there are no cells on top of the E-plate microelectrodes there is no electrical impedance. When cells are grown on top of the E-plate microelectrodes, electrode impedance increases with cell number. This relative change in

electrode impedance is converted into a numerical data by the computer and displayed as dimensionless parameter called “cell index”. Thus, the cell index is directly proportional indirect measurement of cell growth.

Quiescent cell stimulation was characterised by quantifying real-time changes in cell number, viability, and morphology using an RTCA-SP xCELLigenceTM system (Roche, New Zealand) as described (Huang, Li *et al*. 2011). Passage six LJ801 cells were seeded in triplicate in 100 µl of DMEMF12-10% at $2.5x10^4$ cells/cm^2 on 96-well E-Plate. The peak cell index (CI) readings were taken every 1 h from seeding. Quiescence was induced as described in section 2.1.2.5. After six days of serum-starvation, low serum was replaced with fresh DMEMF12-10%. Both control, cells which were continuously grown in DMEMF12-10%, and restimulated cells were grown for 26 d from seeding and CI readings were recorded throughout the entire period.

2.2.2 Small scale production of G_1 cells

Cells were cultured and mitotic shake-off was performed as described (sections 2.1.2.7 and 2.1.2.8). Droplets of 30-40 µl of H199-10% culture medium-containing the mitotic cells were placed in Petri dishes and overlaid with mineral oil maintained at 38.5°C. Mitotic cells were identified by visualizing decondensing chromatin in a doublet, still connected by the thin cytoplasmic bridge of the mid-body (telophase/cytokinesis) using DIC optics. These doublets were isolated by mechanical mouth pipetting using a fine glass pipette.

2.2.2.1 Click-iT® EdU cell proliferation assay

The Click‑iT® EdU assay is a novel alternative to the antibody-based detection of the nucleoside analog bromo-deoxyuridine (BrdU). 5-ethynyl-2´-deoxyuridine (EdU) is a nucleoside analog of thymidine. When provided in the culture medium of growing cells, it can be incorporated into DNA during active DNA synthesis. The incorporated EdU can be detected

by the “click”-reaction with azide. In the presence of copper, alkyne in EdU reacts with the azide group in dye forming a stable triazole. The presence of EdU thus can be indirectly assessed using fluorescent microscopy, which serves as a proxy for DNA synthesis**.**

G_1 cells were isolated as described in section 2.2.2. For Click-iT® EdU cell proliferation assays, isolated doublets/singles were plated on heat-sterilised and 0.1% gelatin-coated coverslips placed in 4-well plates. Click-iT® EdU cell proliferation assays were then performed with slight variation to the manufacturer’s instruction as follows:

A. Isolated doublets/singles were incubated with 1 ml of H199-10% medium with or without (negative control) 10 µM EdU for 3.5 or 24 h in an incubator maintained with 5% CO_2 at 38.5°C

B. Medium was removed and washed once with pre-warmed PBS

C. Cells were fixed with 1 ml of 3.7% formaldehyde in PBS for 15 min in room temperature (RT)

D. Fixative was removed and cells were washed twice with 1 ml of 3% BSA in PBS

E. Wash solution was removed, 1 ml of 0.5% Triton® X-100 was added and incubated at RT for 20 min

F. Meanwhile, 50 µl droplets of Click-iT® reaction cocktail was placed on top of a piece of parafilm placed in a humidified chamber. The humidified chamber was covered with aluminium foil to protect the cocktail from light

G. Permeabilisation buffer was removed, washed twice with 1 ml of 3% BSA in PBS

H. Coverslips with the mitotic cells were carefully placed on droplets of 50 µl of Click-iT® reaction cocktail with the cell-containing side facing the cocktail mixture

I. Cells were incubated at RT for 30 min. Care was taken to protect the humidified chamber from light

J. Coverslips were removed from the humidified chamber and each coverslip was placed in a single well of 4-well plates with the cell-containing side facing upwards

K. Cells were washed once with 1 ml of 3% BSA in PBS and wash solution was removed

L. Cells were incubated with 0.5 ml of Hoechst 33342 (H33342) diluted to 5 µg/ml in PBS for 30 min at RT. Care was taken to protect the 4-well plates from the light

M. Repeated step K

N. Final washing was done in sterilised water

O. Each coverslip was mounted with 3 µl of DAKO fluorescent mounting medium on a clean frosted glass slide

P. Imaging and analysis was performed as described in section 2.1.2.9

2.2.2.1.1 Analysing post 3.5 and 24 h EdU incubation of singles and doublets

Following the Click-iT® EdU proliferation assay of singles and doublets incubated for 3.5 or 24 h with medium-containing 10 µM EdU, cells were observed for EdU incorporation. Images were acquired as described in section 2.1.2.9. Cells emitting green colour were scored as positive for EdU incorporation, which indicated presence of s-phase cells. Singles were also scored for doublet formation, using phase contrast and H33342 labelled DNA. Any singles forming doublets that were not positive for EdU incorporation were was considered in G_1 phase.

2.2.3 Large-scale production of G_1 cells

For producing G_1 cells on large-scale, early passage 2 cells were thawed, cultured and passaged until passage 6 as described (2.1.2.1, 2.1.2.2 and 2.1.2.3). Cells from approximately one hundred 100 mm dishes were then used for mitotic shake-off. 5.5 ml of medium was removed from each plate and mitotic shake-off was performed by shaking the 100 mm culture

dishes on plate shakers at 800 rpm for 1 min, followed by a gentle tap with a finger on the sides of the plate. Media-containing the lifted cells from 10 plates were mixed together in a 50 ml Falcon tube and centrifuged at 1000 x g for 3 min in a 15 ml Falcon tube. Medium was then carefully removed and cells were gently resuspended in 5 ml of H199-10%. 250 µl was transferred into 1.5 ml Eppendorf tubes for Click-iT® EdU cell proliferation assays. From the remaining medium, 20 µl was quickly used to fill two chambers of a Neubauer haemocytometer and allowed to settle, while the rest was plated onto a 60 mm culture dish and incubated under 5% CO_2 at 38.5°C for 3.5 h.

2.2.3.1 Analysis of cells from large-scale production

Haemocytometer cell counts were scored for the total number of cells and the distribution of cells as single (small), single (big) and doublets. The proportion of each cell type was graphed.

2.2.3.2 Determining total number of mitotic cells after wash off

After 3.5 h incubation, medium was transferred into a 15 ml Falcon tube and washed in 4°C pre-cooled PBS. PBS wash-off was also collected in the same 15 ml Falcon tube-containing the removed medium. Quickly the plates were covered with parafilm and frozen at -80°C. Removed medium plus PBS wash-off was collected in the 15 ml Falcon tube and centrifuged at 1000 x g for 3 min before solution was carefully removed. The pellet was resuspended in PBS and the washed-off cells were counted using a Neubauer haemocytometer. The number of cells counted from this wash-off was subtracted from the total number of cells plated initially on the 60 mm culture dish to determine the total number of cells remaining on the 60 mm culture dish. To calculate the total number cells, each doublet and 90% of singles were scored as two cells.

2.2.3.3 Click-iT® EdU cell proliferation assay

From 250 µl of medium-containing mitotic shake-off cells, 150 µl was used to isolate doublets and the rest was used to perform Click-iT® EdU cell proliferation assays as described in sections 2.2.2 and 2.2.2.1, respectively.

2.2.3.3.1 Analysing post 3.5 and 24 h EdU incubation of mitotic shake-off cells and doublets

The assay and analysis were performed as described in section 2.2.2.1.1 for doublets picked from mitotic shake-off and combined mitotic shake-off yield including doublets, single (small) and single (big) cells.

2.2.4 Optimising IF conditions for donors

Compositions of the solutions used are shown in Appendix I - Table 11 and the antibodies and their dilutions used are listed in Appendix II - Table 14.

2.2.4.1 Culturing no-synchronized cells for IF optimisation

After thawing or passaging the LJ801 fibroblasts, cells were seeded onto heat-sterilised coverslips placed in either 35 mm or 60 mm culture dishes and cultured in an incubator-containing 5% CO_2 at 38.5°C.

2.2.4.2 Different IF protocols used for optimisation

2.2.4.2.1 4% PFA fixation followed by permeabilisation protocol (post-TX)

A. Coverslips with randomly proliferating cells were placed in separate wells of 4-well plates

B. Cells were washed once in PBS

C. Cells were fixed in 65°C depolymerized 4% (w/v) PFA + 4% (w/v) sucrose solution in PBS for 15 min at RT

D. Cells were washed twice with PBS

E. Cells were quenched in 50 mM NH_4Cl in PBS for 10 min

F. Cells were washed once in PBS

G. Cells were permeabilized in 0.1% Triton® X-100 in PBS

H. Cells were washed once in PBS

I. Cells were blocked in 3% BSA for 1 h at RT

J. Blocked cells were incubated with appropriate concentrations of primary antibody (Appendix II - Table 14), except the negative control, which was incubated with blocking buffer (3% BSA), in humidified chambers overnight at 4°C

K. Cells were washed thrice with PBS after transferring to 4-well plates

L. Cells were simultaneously incubated with the appropriate concentration of secondary antibody (Appendix II - Table 14) and 5 µg/ml of H33342 in humidified chambers for 30 min at 37°C

M. Cells were washed thrice with PBS after again transferring to 4-well plates

Q. Cells were finally washed in sterilised water

R. Each coverslip was mounted with 3 µl of DAKO fluorescent mounting medium on a clean frosted glass slide

S. Imaging and analysis was performed as described in section 2.1.2.9

2.2.4.2.2 4% PFA fixation followed by permeabilisation protocol with an hour extra blocking (post-TX_e)

Steps A-S in section 2.2.4.2.1 were followed with an extra one hour of incubation in 2% BSA blocking solution included between steps I and J.

2.2.4.2.3 Pre-permeabilisation with Triton® X-100 protocol (pre-TX)

A. Coverslips with randomly proliferating cells were placed in separate wells of 4-well plates

B. Cells were washed once in PBS

C. Cells were prepermeabilised in 0.2% Triton® X-100 in PBS for 5 min at RT

D. Cells were washed once in PBS

E. Cells were fixed in freshly thawed and at 65°C depolymerized 4% (w/v) PFA + 4% (w/v) sucrose solution in PBS for 15 min at RT

F. Cells were washed twice with PBS

G. Cells were quenched in 50 mM NH_4Cl in PBS for 10 min

H. Cells were washed once in PBS

I. Followed the steps I to S as in section 2.2.4.2.1

2.2.4.2.4 Pre-permeabilisation with Triton® X-100 protocol and washing with 3% BSA (pre-TX_BSA)

Steps A-I in section 2.2.4.2.3 were followed with replacement of PBS washing solution with 3% BSA solution from steps E for the rest of the washing steps, except for the last wash in sterilized water.

2.2.4.2.5 Methanol fixation/permeabilisation (sim-MeOH)

A. Coverslips with randomly proliferating cells were placed in separate wells of 4-well plates

B. Cells were washed once in PBS

C. Cells were fixed and permeabilized in -20°C methanol for 6 min at -20°C

D. Cells were washed once in PBS

E. Followed the steps I to S as in section 2.2.4.2.1

2.2.4.2.6 Simultaneous permeabilisation with Triton® X-100 and fixation with 3.7% PFA protocol (sim-TX_PFA)

A. Coverslips with randomly proliferating cells were placed in separate wells of 4-well plates

B. Cells were washed once in PBS

C. Cells were simultaneously prepermeabilised with 1% Triton® X-100 and at 65°C depolymerized 3.6% (w/v) PFA + 3.6% (w/v) sucrose solution in PBS for 20 min at RT

D. Cells were washed once in PBS

E. Cells were quenched in 50 mM NH_4Cl in PBS for 10 min

F. Cells were washed once in PBS

G. Followed the steps I to S as in section 2.2.4.2.1

2.2.4.2.7 Pre-permeabilisation with Triton® X-100 followed by fixation with methanol protocol (Pre TX-MeOH)

Steps A-I in section 2.2.4.2.3 were followed with replacement of 4% PFA + 4% sucrose solution with -20°C methanol for fixing for 6 min at -20°C at step E.

2.2.4.2.8 Pre-permeabilisation with Triton® X-100 followed by fixation with methanol protocol and washing with 3% BSA (Pre TX-MeOH_BSA)

Steps in section 2.2.4.2.7 were followed with replacement of PBS wash solution with 3% BSA solution for all the washing steps from post-methanol fixation step except for last wash with sterilized water.

2.2.4.3 Coating coverslips with different substrates

Different coating substrates at different concentrations, and their ratios were used are listed in the following table. Heat sterilisation and coating was done in a laminar flow hood as follows:

Table 4: Concentrations and ratios of cell adhesion substrates

% Collagen			% Gelatin			Ratio: Collagen (2.5%): Gelatin (0.1%)		
2.5	**0.625**	**0.25**	**0.1**	**0.5**	**1**	**1:2**	**1:4**	**1:10**

A. Clean coverslips were heat-sterilised on both sides for a few seconds using a Bunsen burner flame and one coverslip was placed in each well of 4-well plates

B. Coating substrate was then applied on top of each coverslip, making sure to cover the entire surface of the coverslip and left for 15 min

C. Coating material was removed and coverslips were allowed to dry for 2-4 h

2.2.4.4 IF for G_0 and G_1 cells

G_0 cells were isolated as described in section 2.1.2.6 and plated on heat-sterilised cover slips with or without coating material. G_1 cells were isolated as described in section 2.2.2 and isolated doublets were plated on heat-sterilised coverslips with or without coating material and allowed to settle for 2-3 h. The IF protocol was performed as described in section 2.2.4.2.6.

2.2.5 Validating IF protocol for embryos

First, IVF embryos were produced by IVM, IVF and IVC as follows:

2.2.5.1 In Vitro Maturation (IVM)

In vitro matured non-activated metaphase II (MII)-arrested oocytes were derived as described previously (Oback & Wells 2003) as follows:

A. Slaughterhouse ovaries, preferably of the same breed, were collected from mature cows, placed into saline (30°C) and transported to the laboratory within 2–4 h

B. Cumulus-oocyte complexes (COCs) were collected in H199 supplemented with 925 IU/ml heparin and 20 µl/ml 20% (w/v) albumin concentrate by aspirating 3-12 mm follicles into a 15 ml Falcon tube using an 18-gauge needle and negative pressure (40-50 mm Hg). Only COCs that had an unexpanded cumulus mass with five or more layers and with homogenous ooplasm were selected for IVM

C. COCs were washed twice with H199-10%

D. COCs were then washed once in B199 with 10% (v/v) FCS (B199-10%)

E. Ten COCs in B199-10% were transferred into a 40 µl drop of IVM medium in 65 mm dishes overlaid with paraffin oil

F. Dishes were cultured in humidified 5% CO_2 at 38.5°C for 18-20 h

2.2.5.2 In Vitro Fertilisation (IVF)

After IVM for 20-22 h, in vitro matured oocytes with expanded cumulus cells were subjected to in vitro fertilization (IVF) described previously (Schurmann, Wells *et al*. 2006) as follows:

A. One hour before adding the sperm to the oocyte, a semen straw from a bull of a proven fertility was taken from liquid nitrogen and thawed in air for 5-10 min followed by thawing in a 30-35°C water bath for 30 s

B. The contents of one 0.25 ml straw-containing 1 x 10^8 spermatozoa ml^{-1} were emptied into a 5 ml Falcon tube

C. Using a sterile Pasteur pipette, the entire contents of the Falcon tube was layered upon a Percoll gradient (45%:90%) and centrifuged at 700 x g for 20 min at room temperature. Meanwhile oocytes were prepared as in steps D to G

D. Oocytes were removed from IVM drops using a 200 µl pipettor and transferred to a 35 mm Petri dish-containing HEPES buffered SOF (HSOF)

E. Cumulus cells were loosened by pipetting the COCs up and down 2-3 times. Care was taken to not to completely strip the cumulus cells but to only loosen them

F. Oocytes were washed once with HSOF and then transferred to a Petri dish-containing equilibrated 50 µl droplets of (38.5°C, 5%CO_2) IVF medium

G. IVF plates were returned to the incubator (5% CO_2 in air)

H. The motile sperm fraction was aspirated from the bottom of the tube soon after centrifugation of sperm (step C)

I. It was slowly added to the tube-containing 1 ml HSOF and mixed gently

J. Centrifuged at 200 x g for 5-10 min at RT

K. Immediately supernatant was removed and the sperm pellet was resuspended slowly in 200 µl of equilibrated (38.5°C, 5% CO_2) IVF medium

L. 10 µl of the sperm preparation was used for counting the sperm using a Neubauer haemocytometer

M. Sperm concentration was diluted to $1x10^6$ sperm ml^{-1} using the equilibrated (38.5°C, 5%CO_2) IVF medium

N. Fertilization was performed by adding 10 µl of diluted sperm to the 40 µl drop-containing oocytes prepared as in step G, under oil in a humidified modular incubation chamber (QNA International Pty Ltd., Australia) gassed with 5% CO_2, 7% O_2, and 88% N_2

O. IVF plates were then incubated for 22-24 h

2.2.5.3 In Vitro Culture (IVC)

At 22-24 h post-fertilization, in vitro culturing was performed as follows:

A. After 22-24 h post-fertilization, presumptive zygotes were washed in HSOF

B. Presumptive zygotes were then washed in early synthetic oviductal fluid (ESOF)

C. Presumptive zygotes were transferred to fresh ESOF droplets and cultured (10-15 zygotes per 20 µl droplet). All drops were overlaid with mineral oil and cultured in a humidified modular incubation chamber gassed with 5% CO_2, 7% O_2, and 88% N_2

D. On day 5, embryos were changed over to fresh drops of late synthetic oviductal fluid (LSOF) medium. All drops were overlaid with mineral oil and cultured in a humidified modular incubation chamber gassed with 5% CO_2, 7% O_2, and 88% N_2

E. Embryos were graded late on day 7 post-fertilization

F. Morphological grades 1 to 2 (B1-2) and expanded blastocysts were selected (Robertson & Nelson 1998)

2.2.5.4 IF for embryos

IVF embryos at 9, 11, 28 or 168 h post-fertilization were used for IF analysis. IF for these embryos was performed in 96 well plates using a fine glass needle to transfer them between different wells by mouth pipetting as follows:

A. Embryos were transferred into a round bottomed 96 well plate-containing 60 µl each of 65°C depolymerized 3.6% (w/v) PFA + 3.6% (w/v) sucrose solution in PBS-PVA (PBS + 0.25% PVA)
B. Embryos were incubated for simultaneous permeabilisation and fixation for 15 min at RT
C. Embryos were washed by transferring them into other wells-containing 60 µl of PBS-PVA wash solution
D. Embryos were quenched by transferring them into wells-containing 60 µl of 50 mM NH_4Cl in PBS-PVA for 10 min
E. Embryos were washed again by transferring them into other wells-containing 60 µl of PBS-PVA wash solution
F. Embryos were blocked with 3% BSA and incubated for 1 h at RT
G. Embryos were transferred into wells-containing 60 µl of appropriate concentrations of primary antibody (Appendix II - Table 14) and incubated overnight on a slowly shaking platform at 4°C
H. Embryos were washed thrice by transferring them into other wells-containing 60 µl each PBS-PVA wash solution
I. Embryos were transferred into wells-containing 60 µl of appropriate concentrations of secondary antibody (Appendix II - Table 14) and 5 µg/ml of H33342 and incubated on a slowly shaking platform for 45 min at 37°C
J. Embryos were washed thrice by transferring them into other wells-containing 60 µl of PBS-PVA wash solution

K. Finally, embryos were mounted in 3 µl of DAKO fluorescent mounting medium on a clean frosted glass slide and overlaid with a coverslip

L. Image acquisition was performed using a confocal laser scanning microscope as described in section 2.1.2.10

2.2.6 Characterising G_0 vs G_1 donors

2.2.6.1 Quantifying H33342 pixel intensities

For quantification of H33342 the following steps were followed:

A. IF for G_0 and G_1 donors was performed as described in section 2.2.4.4

B. Image acquisition was performed using confocal laser scanning microscopy as described in section 2.1.2.10

C. All images were corrected by subtracting one randomly chosen cytoplasmic area as background

D. The nuclear area was marked as the region of interest (ROI) and 'series analysis' was performed to compute nuclear area and average intensity of the entire image stack

E. Ten nuclei were randomly selected from G_0 and G_1 donors and the total amount of H33342 intensity was calculated by adding the pixel intensities from all frames

2.2.6.2 Quantifying nucleus volume

For calculating the nucleus volume, first the area of the nucleus was measured from the 'series analyses'. The height was determined by the difference between the lower and upper Z-limit. To capture the total pixel intensity the number of captured frames was automatically adjusted according to the distance between the lower and upper Z-limit. Total nuclear volume was obtained by multiplying the area of nucleus with the height.

2.2.6.3 Quantifying RNA polymerase II (Pol II) pixel intensities

For quantification of Pol II the following steps were followed:

A. Steps A-D in section 2.2.6.1 were followed

B. Within each stack, the frame with the highest average pixel intensity (FHAPI) was chosen for analysis

C. Average of HAPI was calculated from several cells and used for comparison

2.2.6.4 Comparison of chromatin condensation

To analyse the degree of chromatin condensation we used ImageJ software (NIH, 1.43u). First the background corrected FHAPIs were opened using ImageJ. Random line selection was used to pass through the image of nuclei in the H33342 channel. Using the "Analysis" tab, profiles were plotted and the results were copied in to Microsoft Excel. Using this procedure, ten random nuclei from G_0 and G_1 were analysed. Profiles from both G_0 and G_1 were plotted as a graph. To get a representative curve, the moving average of 100 pixels was calculated using the "Trendline" option in Microsoft Excel.

2.3 Methods for chapter four

2.3.1 Epigenetic characterisation of G_0 and G_1 cells

2.3.1.1 IF and confocal immunofluorescence microscopy (CIFM) to detect histone modification

A. IF for G_0 and G_1 donors was performed as described (2.2.4.4) using histone modification antibodies (Appendix II - Table 14) alone or in combination with Pol II and other antibodies

B. Image acquisition was performed using confocal laser scanning microscope as described (2.1.2.10)

C. All the images were background subtracted by using the cytoplasmic area as background

D. After scanning the H33342 staining, the nuclear area was marked as the ROI and series analysis was performed

E. The FHAPI within each stack was chosen for quantification

2.3.1.2 Quantifying histone lysine methylations by CIFM

For quantification of histone lysine methylations, the pixel intensities from FHAPI was normalised compared to corresponding pixel intensities from H33342.

2.3.1.3 Production of G_0 cells for ELISA

Cells were induced to quiescence as described (2.1.2.5) in 10-15 culture dishes (100 mm). Cells were then washed once with 4°C pre-cooled PBS and culture dishes were immediately sealed with parafilm and stored at -80°C for biochemical assays. One of the culture dishes was passaged as described in section 2.1.2.6 and the number of cells/100 mm culture dish was determined.

2.3.1.4 Production of G_1 cells for ELISA

G_1 cells were produced as described (2.2.3). The total number of cells was determined and stored at -80°C as described (2.2.3.2).

2.3.1.5 Extraction of nuclear histones

Extraction of nuclear histones for both G_0 and G_1 cells was performed using an EpiQuik™ Total Histone Extraction Kit, as described in manufacture's protocol.

A. Frozen G_0 and G_1 cells (2.3.1.3 and 2.3.1.4) were harvested by trypsinisation

B. Cells were pelleted into 1.5 ml Eppendorf tube by centrifugation at 1000 x g for 5 min at 4°C

C. Cells were resuspended in 'Pre-Lysis buffer' at 10^7 cells/ml and lysed on ice for 10 min with gentle stirring

D. Lysates were centrifuged at 10000 rpm for 5 min at 4°C

E. Supernatant was removed

F. Cells were re-suspend in lysis buffer at 200 µl/10^7 cells and incubated for 30 min on ice

G. Cells were centrifuged at 15300 x g for 5 min at 4°C and supernatant fraction was transferred into a new vial

H. 0.3 volumes of 'Balance-DTT' buffer was immediately added to the supernatant

I. Using BSA as a standard, the protein concentration was determined on a spectrophotometer at 260 nm

2.3.1.6 Analysis of histone lysine methylation by ELISA

Different histone lysine methylations were quantified using various EpiQuik™ fluorometric histone methylation quantification kits (Appendix I - Table 10) as described in the manufacture's protocol.

A. For determining a standard curve, a standard control provided by the manufacturer was diluted with 'F2 buffer' from 1-100 ng/µl at 7 points (1.5, 3, 6, 12, 25, 50 and 100 ng/µl)

B. 50 µl of 'F2 buffer' was added into each well

C. For the sample, 1 µg of the histone extract was added into the sample wells

D. 1 µl of the standard control at each of the different concentrations were added into the standard wells.

E. All the wells were mixed well and strip wells were covered with Parafilm M and incubated at RT for 1-2 h

F. Solutions from all the wells were aspirated and the wells were washed thrice with 150 µl of diluted 'F1 buffer'

G. 50 µl of diluted 'F3 solution' was added to each well and incubated at room temperature for 60 min on an orbital shaker (100 rpm)

H. 'F3 solution' was aspirated and wells were washed six times in 150 µl of diluted 'F1 buffer'

I. 50 µl of the 'fluoro-development solution' was added into the wells and incubated for 5 min in the dark at RT

J. Solution was transferred to a 96-well microplate

K. Fluorescence was measured and read on a fluorescence Synergy 2 Multi-mode plate reader at 530EX/590EM nm

L. Histone methylation % was calculated as follows:

$$\text{Histone methylation \%} = \frac{\text{RFU (treated (tested) sample – blank)}}{\text{RFU (untreated (control) sample – blank}} \times 100\%$$

RFU=Read Fluorescence Unit

For quantification, RFU was plotted versus amount of standard control and the slope was determined as the δ RFU/ng.

M. The amount of histone methylation was calculated by using the following formula:

$$\text{Amount (ng/mg protein)} = \frac{\text{RFU (sample – blank)}}{\text{Protein (µg)}^* \times \text{slope}} \times 1000$$

* Histone extract amount added into the sample well at step C.

2.3.1.7 IF and CIFM for chromatin related proteins

For IF and CIFM of different chromatin related proteins, the same procedure as described in section 2.3.1.1 was followed but with chromatin related protein antibodies as primary antibodies, except for H3.3, the procedure for which is as follows:

A. Cells were simultaneously prepermeabilised with 1% Triton® X-100 and 3.6% (w/v) PFA + 3.6% (w/v) sucrose solution in PBS for 20 min at RT

B. Cells were washed once in PBS

C. Cells were quenched in 50 mM NH_4Cl in PBS for 10 min

D. Cells were washed once in PBS

E. Cells were treated with 4 N HCl for 1 h at 37°C

F. Cells were washed thrice with PBS containing 0.05% Tween® 20 (PBST)

G. Steps I to R as in section 2.2.4.2.1 were followed

H. CIFM was performed following the steps from B to E as in section 2.3.1.1

2.3.1.8 Quantifying chromatin-related proteins by CIFM

For quantification of chromatin related-proteins the pixel intensity from FHPI was normalised compared to corresponding H33342 pixel intensity. For H3.3, as the HCL treatment interfered with DNA binding of, its pixel intensities were normalised on the nuclear area.

2.3.1.9 IF and CIFM for 5mC and 5mC/H3K9me3

5mC IF procedure was modified from as previously described (Jeon, Coppola *et al*. 2008).

A. Both G_0 and G_1 cells were fixed in methanol and acetic acid (3:1) over night at 4°C

B. Cells were treated with RNase (10 µg/ml) and Pepsin (0.1 mg/ml) for 1 h @ 37°C

C. Cells were dehydrated in 70% and 100% ethanol then air dried

D. Cells were treated with 4 N HCl for 15 min at RT

E. Cells were washed in PBS

F. Cells were blocked in PBST supplemented with 1% BSA (fatty acid-free)

G. Cells were incubated overnight up to 16 h with either 5mC alone or 5mC+H3K9me3 primary antibodies at 4°C

H. Cells were washed thrice with PBST

I. Cells were incubated simultaneously with secondary antibody and H33342 at 37°C for 1 h

J. Cells were washed thrice with PBST

K. Cells were finally washed in water

L. Cells were mounted onto a clean frosted slide in 3 µl/coverslip DAKO fluorescent mounting medium

M. CIFM was performed following the steps from B to E as in section 2.3.1.1

2.3.1.10 Quantifying 5mC by CIFM

For 5mC, the HCL treatment interfered with DNA binding of H33342, therefore, 5mC pixel intensities were normalised based on the nuclear area.

2.4 Methods for chapter five

2.4.1 Epigenetic characterisation of G_0- and G_1-derived embryos

2.4.1.1 Isolation of G_0 cells for NT assays

After inducting quiescence and isolation (2.1.2.5 and 2.1.2.6), cells were used for fusion with enucleated MII arrested oocytes (NT).

2.4.1.2 Isolation of G_1 cells for NT assays

Cells were cultured, followed by mitotic shake-off and then isolated as described (2.1.2.7, 2.1.2.8 and 2.2.2). For NT, doublets were physically separated on a micromanipulation system (Nikon Narishige, MO 188) and the resulting single cells were used for NT.

2.4.1.3 Somatic cell nuclear transfer

Somatic cell nuclear transfer was performed as described previously (Oback & Wells 2003).

2.4.1.3.1 IVM and zona-free oocyte generation

A. In vitro matured non-activated metaphase II (MII)-arrested oocytes were derived as described in section 2.2.5.1

B. After IVM for 18–20 h, the cumulus-corona was dispersed by vortexing up to 180 oocytes in 500 µl of bovine testicular hyaluronidase (1 mg/ml in H199) in a 1.5 ml tube

C. Oocytes were spun down for <3 s to recover oocytes

D. Oocytes were washed thrice with H199-PVA

E. The zona pellucida of oocytes with a first polar body was digested by 1-2 min incubation in pronase (5 mg/ml in H199). About 50 oocytes per 50 µl drop of pronase were processed. Once the zona started dissolving, oocytes were washed in H199-10% and the zona was allowed to dissolve completely

F. Oocytes were allowed to recover for >5 min to regain their spherical shape before starting enucleation

2.4.1.3.2 Zona-free oocyte enucleation

A. Zona-free oocytes were stained for 5 min in droplets of 5 µg/ml Hoechst 33342 in H199-PVA under oil and briefly washed in H199-PVA droplets. About 40 oocytes were processed at a time

B. Oocytes were transferred into a H199-10% droplet overlaid with paraffin oil in the lid of a 10 cm Petri dish on the warm microscope stage (32°C)

C. Oocytes were enucleated under constant UV-light exposure using 100X total magnification with the fluorescence lamp diaphragm closed as much as possible. As soon as the chromosomes were visible in the enucleation pipette (25–30 µm outer diameter, perpendicular break, no bevel or spike), the oocyte was moved out of the UV light

D. Oocyte and karyoplast were separated with a simple separation needle (100–150 mm outer diameter, perpendicular break, closed fire-polished tip)

2.4.1.3.3 Attachment of donor cell with zona-free oocyte

A. After isolating G_0 cells as described (2.1.2.6) cells were suspended into 40 µL drops covered with oil. G_1 cells were selected as described (2.4.1.2) in H199-10% droplets

B. With a mouth pipette about 5–10 individual cells were picked up and added to a drop of 10 µg/ml phytohemagglutinin (PHA-P) in H199-PVA, already containing 5–10 oocytes. Care was taken to minimize the carryover of H199-0.5%, since serum proteins compete with the lectin-binding sites on the oocyte and donor cell plasma membrane

C. Individual oocytes and donor cells were pushed together with the mouth pipette

D. Couplets were incubated for at least 5min, and then groups of 5–10 couplets were transferred into H199-PVA-washdrops. Couplets were kept well separated in the droplets to prevent them from sticking together. All pairs were checked for the presence of only 1 round donor cell per oocyte

2.4.1.3.4 Fusion of donor cell with zona-free oocyte

A. 10–20 couplets were briefly equilibrated in 40 µl drops of hypo-osmolar fusion buffer under oil and placed in a 35 mm dish with fusion buffer

B. 5–10 couplets were transferred in a custom-made parallel-plate fusion chamber (2 mm deep, 3 mm separation, and 35 mm long, surgical-grade titanium electrodes mounted on a glass microscope slide) connected to an ECM 200 (BTX, San Diego, CA). Electrodes with similar specifications were available from BTX (Microslide 453, 3.2 mm gap). All air bubbles were removed between electrodes

C. Couplets were automatically aligned by applying an alternating current (AC)–field (60–100 V/cm) for 5–10sec. Fusion was

performed using 2 x 10 µs direct current (DC)–pulses (1.5–2.0 kV/cm), followed by another 5–10 s AC-pulse (60–100 V/cm) at RT

D. Couplets were removed from the fusion chamber and put back into H199-PVA to score fusion success, and detached or lysed donor cells were detected

E. Fused reconstructs were washed through HSOF-10% FCS (without calcium) and transferred into drops of ESOF (Oback & Wells 2003) with 10% FCS (without calcium) until activation

2.4.1.3.5 Activation of fused reconstructs

Reconstructs were activated 3–4 h post-fusion, using a combination of ionomycin and 6-DMAP as follows:

A. Thirty minutes before activation, reconstructs were washed and held in drops of HSOF + 1 mg/ml bovine albumin

B. Activation was induced by incubating in 30 µl drops of 5 µM ionomycin in HSOF + 1 mg/ml bovine albumin for 4 min. Briefly wash in HSOF + 30 mg/ml bovine albumin before single culture in 5 µl drops of 2 mM 6-DMAP in ESOF with 10% FCS

C. After 4 h in 6-DMAP, wash reconstructs three times in HSOF and transfer into ESOF droplets for IVC

2.4.1.3.6 IVC of activated reconstructs

Reconstructed embryos were cultured in vitro for 7 days (day 0 = fusion) in biphasic ESOF/LSOF (Wells, Laible *et al*. 2003) as follows:

A. 4 x 30 µl wash drops and 30 x 5 µl culture drops of ESOF were made in 60 mm Petri dish and overlaid with 8 ml of oil. A humidified modular incubation chamber (QNA International Pty Ltd., Australia) gassed with 5% CO2, 7% O2, and 88% N2 was set up

B. Activated reconstructs were washed from HSOF through ESOF wash drops and into 5 µl single culture drops

C. On day 4 of culture (around the time of compaction), reconstructs were changed into fresh LSOF drops-containing 10 µM 2, 4-dinitrophenol (Thompson, McNaughton *et al*. 2000) to act as an uncoupler of oxidative phosphorylation. Care was taken to avoid zona-free morulae aggregation during changeover

D. Embryos were graded late on day 7 post-fusion

E. Morphological grade 1-2 (Robertson & Nelson 1998) were selected for IF

2.4.1.3.7 IF and CIFM for NT embryos

NT reconstructs within 0-10 min following NT, as well as 4, 24, 72 and 168 h post-activation were used for IF analysis. IF and confocal image acquisition of these embryos was performed as described in section 2.2.5.4.

2.4.1.3.8 Quantification of histone lysine methylation and polycomb group proteins at blastocyst stage

A. All the images from confocal microscopy were background subtracted by using the cytoplasmic area as background

B. Based on H33342 staining, five ICM nuclei and ten TE nuclei were randomly marked as the ROI and ‘series analysis’ was performed through all the channels

C. FHAPI within each stack was chosen for quantification

D. For quantification of histone lysine methylations and polycomb group proteins, the pixel intensities from FHAPI was normalised compared to corresponding H33342 pixel intensity.

Chapter Three: Donor cell isolation and immunofluorescence analysis

3.1 Serum starvation reversibly induces quiescence

For NT experiments, either quiescent (G_0) or G_1 cells were used. G_0 cells are mainly produced by either growing the culture to confluency or by serum starvation. We have used serum starvation as a method to induce quiescence. Unfavourable conditions can trigger the cells to exit the normal cell cycle and force them to either enter apoptosis or quiescence. While the former is irreversible, the latter is not. First, we determined the effect of six days of serum starvation on adult male skin fibroblasts (LJ801). To test if serum-starved cells could re-enter their normal cell cycle, we re-stimulated the serum-starved cells with 10% FCS-containing medium after six days of serum starvation (treatment) and compared them with non-starved cells continuously grown in 10% FCS-containing medium (control). Their proliferation potential was measured using the xCELLigence, a non-invasive and label-free system, which screens cellular events in real-time. Soon after seeding in 10% FCS-containing medium, both treatment and control cells entered the attachment phase and attained similar cell index (CI) values. After changing to serum starvation medium (6 h post-seeding), the CI dropped considerably. This drop in the treatment groups indicated the loss of loosely and non-attached cells. At the same time the CI increased in controls, indicating that cells were still in the attachment phase. Following their attachment and lag-phase, prior to entering into log-phase, the CI started to decline between 20-24 h. This indicated the rounding and lifting of mitotic cells before division (Figure 6 subset A). When cells round off, their cell surface area which is attached to the plate decreases, reducing the electrical impedance and CI value. After 24 h, control cells entered log-phase and continuously increased their CI up to day 4 when they reached the plateau

or stationary phase (CI=5.8). Cells maintained their CI during stationary phase from day 4-5.5. From day 5.5, they entered a decline or confluent phase, where limiting growth and survival factors lead to cell death, resulting in the decline of CI. By contrast, the CI remained constant during the time of serum starvation up to 6 days, indicating that cells were not proliferating and had entered G_0. To verify that cells can still re-enter the normal cell cycle, we re-stimulated them by changing the medium to 10% FCS-containing medium. Post 13 h re-stimulation, G_0 cells briefly reduced their CI before starting to increase, similar to the pattern observed in control cells before entering the proliferation phase (Figure 6 subset B). Increasing CI values post 17 h re-stimulation marked the entry of G_0 cells into log-phase. They continued to proliferate and reached the same plateau as control cells (CI=5.8) but took nearly 3 times longer (4 vs 11 days). This delay in reaching the plateau is possibly due to the small size of the initial cell population that entered G_0, since many cells were washed away during the change to serum starvation medium. They also exhibited a similar length of the stationary phase as controls (both 1.5 days), before entering the decline or confluent phase. Overall, after re-stimulation the treatment curve was almost identical to the control. This demonstrates that serum starvation of LJ801 induces quiescence and 6 days of serum starvation does not affect their ability to re-enter the normal cell cycle.

3.2 Mitotic shake-off does not interfere with cell cycle progression

G_1 cells can be isolated by using chemicals to inhibit cells from completing the G_1 phase or by mitotic shake-off followed by manual selection of the mitotic cells. Use of chemical inhibitors might affect the epigenetic features of the cells. Therefore, mitotic shake-off was used as a method for isolating G_1 cells.

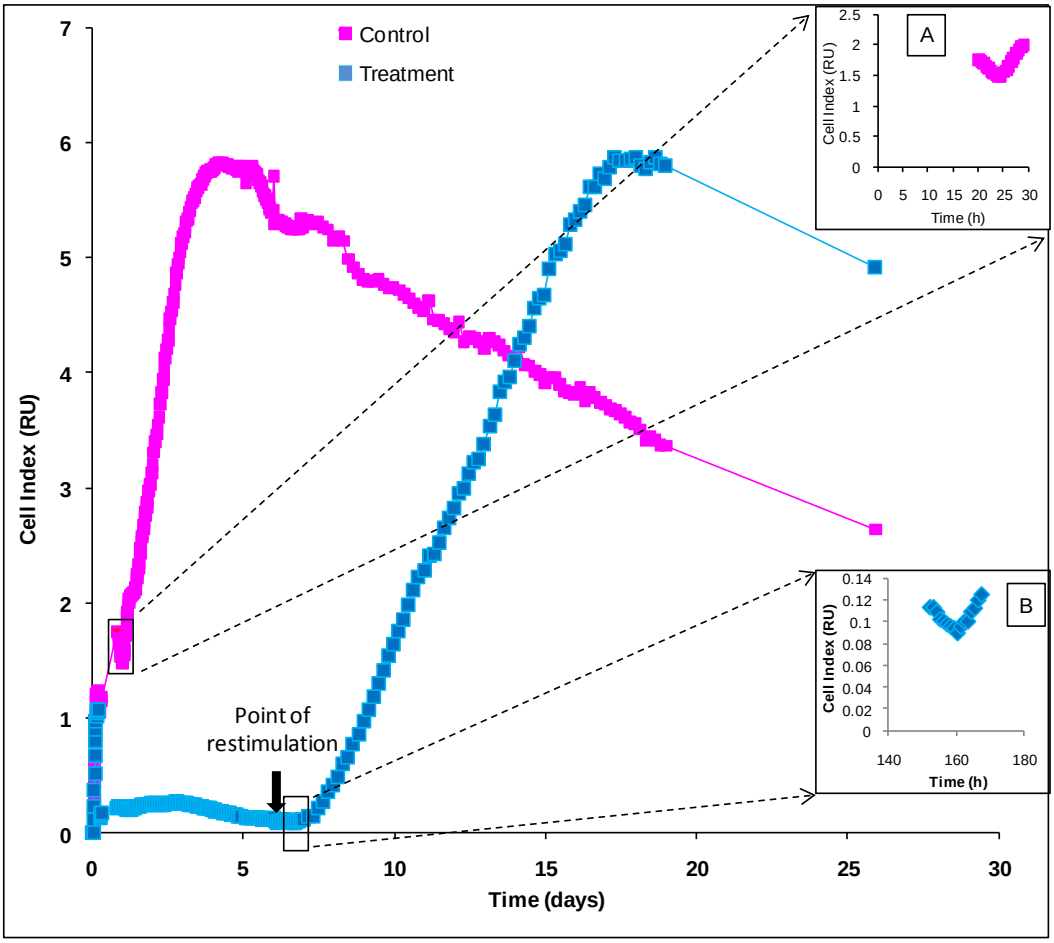

Figure 6: Cell proliferation as measured by the xCELLigence system. The cell index is derived from the relative change in electrical impedance. It varies with cell number, size, cell morphology and strength of adhesion. Data points were taken at intervals of 15 min (from 1-8 h), 30 min (8 h-2 days), 1 h (2-7 days) and 4 h (7-19 days), and the final data point was taken after 26 days. Controls were maintained in 10% FCS-containing medium throughout the culture period. Treatment cells were serum-starved for 6 days in 0.5% FCS medium, followed by changeover to 10% FCS-containing medium. Subsets A and B indicate the brief decline, followed by a rise in cell index before entering the proliferation phase, in control and treatment, respectively; RU=relative units.

3.2.1 G_1 cells from small-scale mitotic shake-off

Mitotic shake-off from a 100 mm culture dish ('small-scale production') yielded two types of cells: 1) Dumbbell-shaped cell pairs, which were still joined by a cytoplasmic bridge and are in late mitosis-early G_1 (designated as 'doublets') and 2) large round cells (designated as 'singles'). The doublets were used as G_1 control donors for NT and IF analysis. To evaluate their normal cell cycle capability, we could not use the xCELLigence system as the number of cells needed for obtaining a growth curve was higher than that could be isolated by manual selection (i.e. mouth pipetting). Therefore, we performed a Click-iT® EdU cell proliferation assay, which measures the incorporation of the nucleoside analogue 5-ethynyl-2-deoxyuridine (EdU) into newly synthesised DNA. Synthesis of DNA is used as proxy for replication. After 3.5 h of EdU incubation, doublets showed no EdU incorporation, demonstrating that they would remain prior to S-phase for at least 3.5 h following shake-off and manual selection (Figure 7A). Even singles did not incorporate EdU during 3.5 h EdU incubation, indicating absence of S-phase cells (Figure 7C). Hoechst 33342 (H33342), which binds the minor groove of double stranded DNA, staining of cells 3.5 h after EdU incubation revealed that 93% of single cells recovered after plating formed doublets, indicating cell cycle progression (Figure 7 & Figure 8). We evaluated long-term EdU incorporation for 24 h for both doublets and singles. After EdU incubation for 24 h, 94% of doublets and 87% of singles incorporated EdU, demonstrating their ability to continue with their normal cell cycle (Figure 7B & Figure 9).

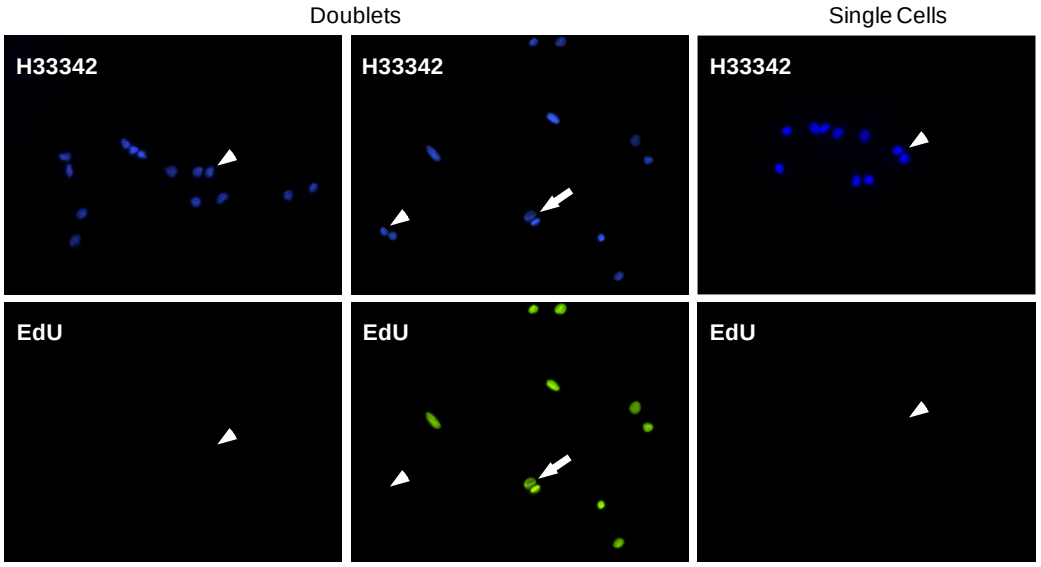

A. 3.5h post incubation with EdU **B.** 24h post incubation with EdU **C.** 3.5h post incubation with EdU

Figure 7: Click-iT® EdU cell proliferation assay of mitotic shake-off cells from small-scale production. After mitotic shake-off, EdU incubation was performed for doublets: A) for 3.5 h, and B) for 24 h, and C) single cells for 3.5 h. DNA was stained with H33342 (blue, upper row). EdU incorporation was detected as green fluorescence (lower row). Arrowheads and arrows indicate absence and presence of EdU incorporation, respectively. Arrowhead in C shows the formation of a doublet from a single cell in the upper row and absence of incorporated EdU in the lower row.

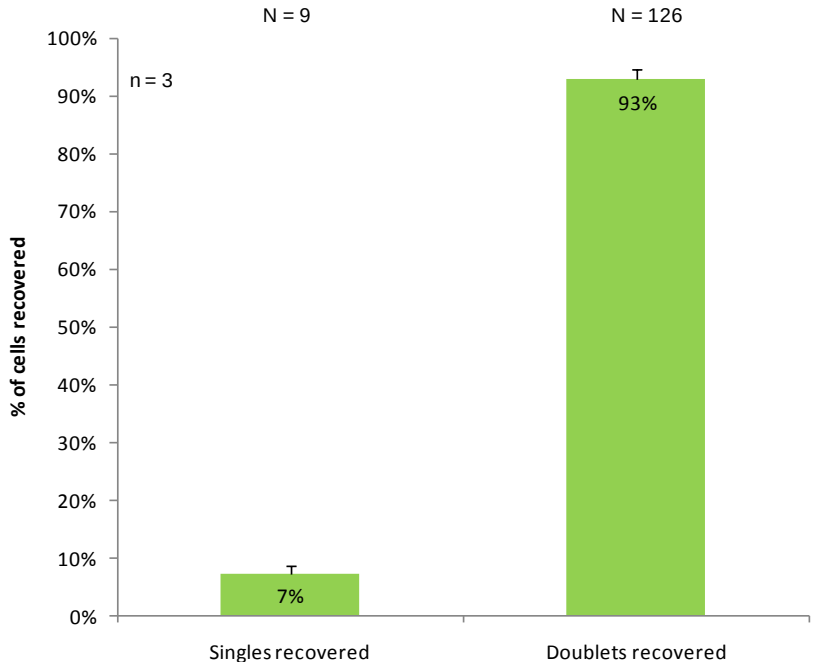

Figure 8: Proportion of doublets and singles recovered, post 3.5 h incubation of singles isolated by mitotic shake-off from small-scale production. N= number of cells recovered; n= number of replicates.

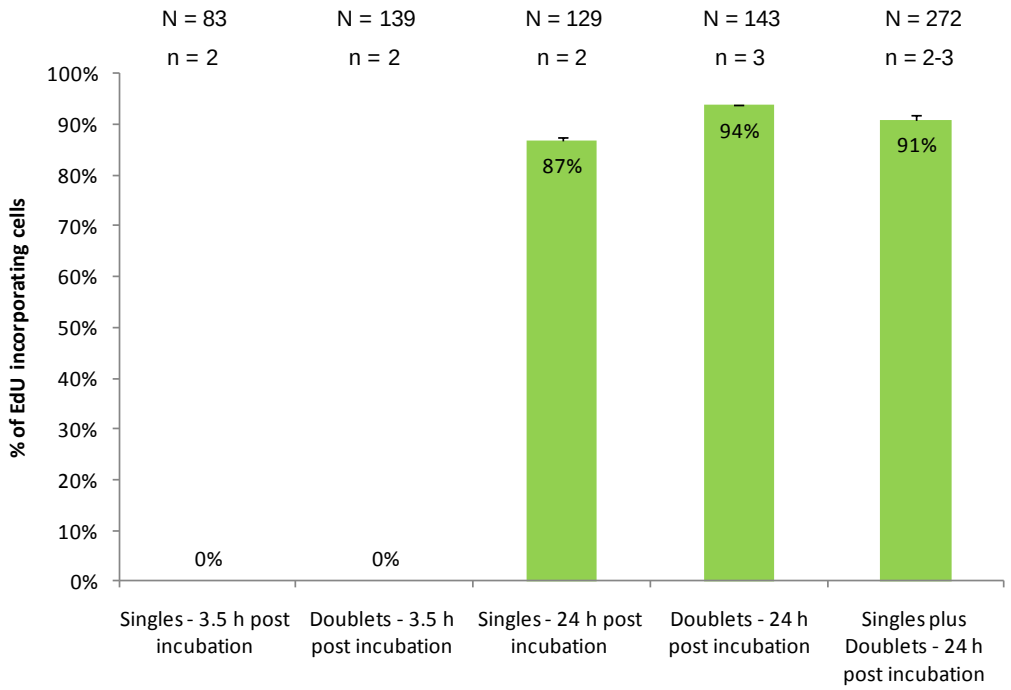

Figure 9: Proportion of EdU incorporating cells harvested by mitotic shake-off from small-scale production. Singles and doublets were isolated from mitotic shake-off, incubated with EdU for 3.5 h and 24 h, and processed according to manufacturer's protocol for detection of incorporated EdU. N= number of cells analysed; n= number of replicates.

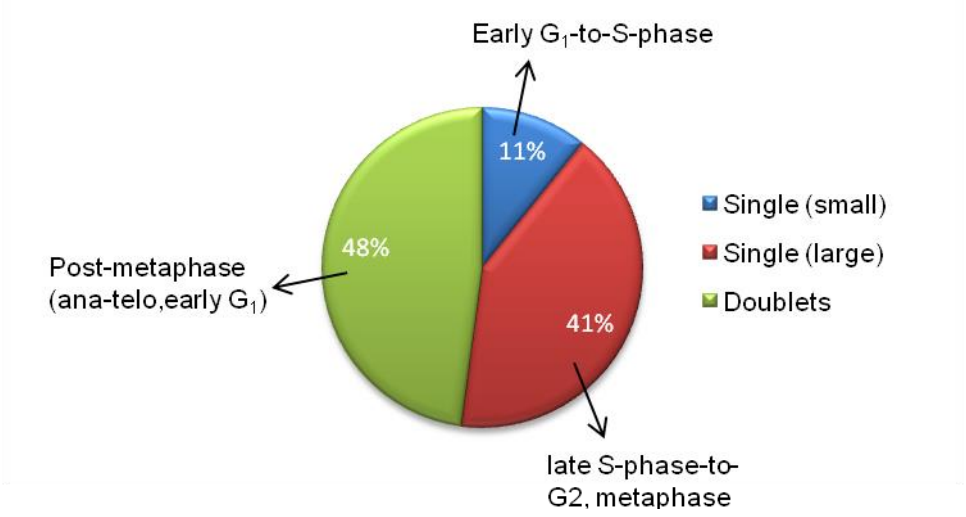

Figure 10: Proportion of different types of cells isolated by mitotic shake-off as scored and categorised based on observation under microscope. The raw yield from mitotic shake consisted of doublets and two populations of singles. See text for details.

3.2.2 G_1 cells from large-scale mitotic shake-off

The observation that single cells from the mitotic shake-off divided to produce doublets, encouraged us to use all shake-off cells for biochemical assays. Such assays require hundreds of thousands of cells which are practically difficult to obtain by mouth pipetting. To produce such large numbers of cells, we scaled up production. Given that only ~5% of cells are in mitosis at any given time ('mitotic index'), the total yield of cells produced by shake-off cannot exceed 5% of all cells plated. Therefore, we used ninety-six 100 mm culture dishes for large-scale cell production. Upon closer observation of cells obtained after large-scale mitotic shake-off under the microscope, we found two populations of differently sized singles, in addition to the predominant proportion of doublets (Figure 10). Small cells were comparable to those cells seen after separation of doublets. These are presumably in early G_1-to-S-phase. Large cells were nearly double the size in diameter of small singles and presumably in late S-phase-to-G2, metaphase. We again performed, the Click-iT® EdU cell proliferation assay to analyse the proliferation ability of large-scale produced mitotic shake-off cells.

Almost 6% of cells incorporated EdU after 3.5 h of EdU incubation (Figure 11), indicating that the large-scale production of G_1 cells was contaminated with S-phase cells. However, the proportion of small-scale vs large-scale production cells that incorporated EdU 3.5 h and 24 h after EdU incubation (0% vs 0% and 94% vs 91%, respectively), and the proportion of cells that continued through their normal cell cycle (90% vs 97%) remained comparable. These results demonstrated that large-scale production of G_1 cells did not affect their ability to continue their normal cell cycle.

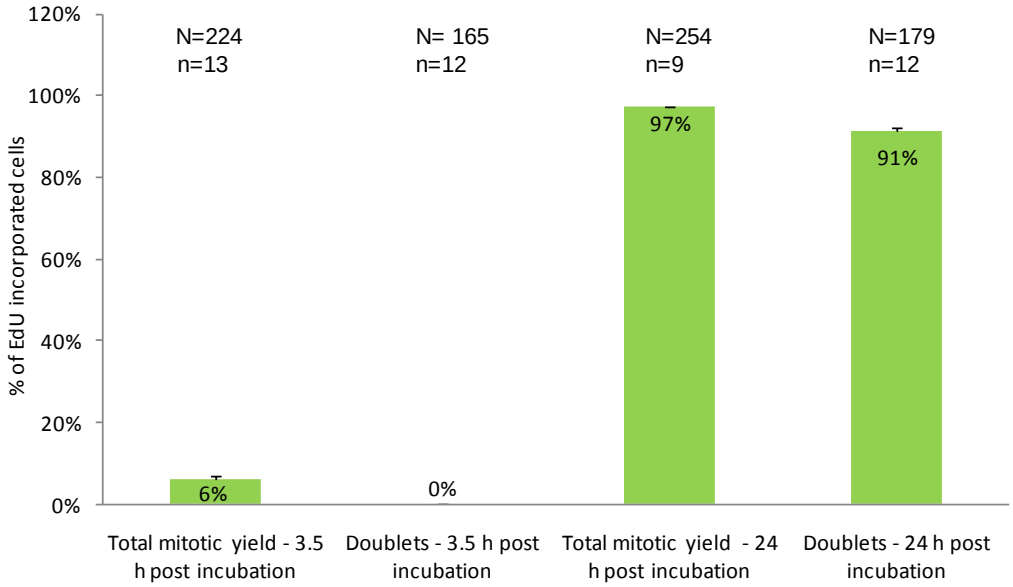

Figure 11: Proportion of EdU-incorporated cells isolated by mitotic shake-off from large-scale production. Total mitotic yield represents the yield from mitotic shake-off including doublets and two populations of singles. Doublets were again isolated from the total mitotic yield. Both doublets and total mitotic yield were incubated with EdU for 3.5 h and 24 h, and processed according to the manufacturer's protocol for detection of incorporated EdU in the cells. N= number of cells analysed; n= number of replicates.

3.3 Different IF protocols influence staining patterns in non-synchronised cells

Most of the commercially available antibodies were either developed against human or mouse antigens. There was a need to select antibodies with the highest chance of cross-reactivity with their target bovine antigens. Commercial antibodies were selected based on the highest amino acid identity between their target bovine antigen and the immunogen used to generate the antibody. All antibodies, including the ones that were kindly donated by Dr. Thomas Jenuwein, were tested on the LJ801 cell line. The intention was to use a single protocol for all antibodies. This would enable double or triple staining with the desired antibodies, allowing direct comparison of the nuclear distribution and chromosomal staining pattern, as well as quantification of protein abundance by immunofluorescence (IF). The antibodies were validated based on their expected pattern of staining. All antibodies, except those against PcG proteins, worked well with the pre-fixation followed by

permeabilisation ('post-TX') protocol for IF. Only a moderate success of this method with the PcG proteins prompted us to explore other protocols. A protocol that uses methanol as both fixation and permeabilizing agent was tried. Even though it worked for some (EZH2 and SUZ12), it did not for all PcG proteins (Figure 12). Furthermore, cells were found to have lost their morphological integrity, which could impede the comparison of distribution and localisation between different target antigens. Various alterations of the first protocol and other published protocols (Fischle, Wang *et al.* 2003, Plath, Fang *et al.* 2003) were tried. The details of all the tested and working protocols are summarised in Table 5. A modified protocol from Fischle W. *et al*. which used simultaneous permeabilisation and fixation ('sim-TX_PFA'), was found to be suitable for all antibodies (Table 5). Staining pattern comparison of different protocols, particularly for the PcG antibodies, showed that different protocols can result in entirely different staining patterns, to the extent that a nuclear antigen was absent from the nucleus and found in the cytoplasm. For example, RING2 and PHC, which are both nuclear proteins, were found to be absent in the nucleus when the methanol protocol ('sim-MeoH') was followed. When the sim-TX_PFA protocol was followed, both proteins showed their expected distribution, predominantly within the nucleus (Figure 12). The same was true when EZH2 and SUZ12 were compared for pre-TX vs sim-TX_PFA, respectively (Figure 12).

3.3.1 Validation of preferred IF protocol on bovine embryos

Validation of the sim-TX_PFA protocol on IVF embryos was done using antibodies against two different antigens, H3K9me3 and SOX2. H3K9me3 is a maternal-specific epigenetic modification, which stains mainly the female pronucleus (Hemberger, Dean *et al*. 2009). SOX2 is a transcription factor specific to the inner cell mass (ICM) and excluded from the trophectoderm (TE). Using the protocol, early zygotes (11 h post-IVF) and blastocysts were stained with H3K9me3 and SOX2, respectively.

Table 5: Different combinations of protocols tested for standardisation. Different tested protocols, each assigned with a different roman number, are listed to the left side of the table ('tested protocols'). The table lists the primary antibody (1° Ab) and corresponding 1° Ab and 2° Ab dil., as well as the working protocols. A protocol is considered as 'working' if it shows consistently the expected staining pattern for the antibody tested. The roman numbers under working protocol correspond to the protocols listed under tested protocols. The coloured text represents the simultaneous protocol. Only this protocol consistently showed the expected staining pattern for all antibodies tested. For source of antibodies refer Table 14 (Appendix I).

Tested protocols :

I. Permeabilisation with 0.2% Triton X -100 followed by 4% PFA fixation and washing with 1X PBS (pre-TX)

II. Pre-permeabilisation with 0.2% Triton X-100 followed by 4% PFA fixation and washing with 3% BSA (pre-TX_BSA)

III. Simultaneous permeabilisation with 1% Triton X-100 and fixation with 3.6% PFA (sim-TX_PFA)

IV. 4% PFA fixation followed by Triton X- 100 (post-TX)

V. 4% PFA fixation followed by Triton X- 100 with 1 h extra blocking at 4 C (post-TX_e)

VI. Pre-permeabilisation with 0.2% Triton X -100 followed by fixation with Methanol (-20 C) (pre-TX-MeOH)

VII. Pre-permeabilisation with 0.2% Triton X -100 followed by Methanol fixation and washing with 3%BSA (pre-TX-MeOH_BSA)

VIII. Methanol (-20 C) fixation/permeabilisation (sim-MeOH)

Sl. No.	1 Ab	1 Ab dil.	2 Ab dil.	Working protocols
1	H3K4me3	1 in 2000	1 in 2000*	II / **III** / V / VII
2	H3K9me1	1 in 1000	1 in 2000*	I / **III** /I V
3	H3K9me2	1 in 1000	1 in 2000*	II / **III** / IV
4	H3K9me3	1 in 1000	1 in 2000*	**III** / V
		1 in 2000	1 in 2000*	I / II / III /I V
5	4X H3K9me2	1 in 1000	1 in 2000*	I / II /**III**/ V
6	H3K27me3	1 in 1000	1 in 2000*	II / **III**
7	SUZ12	1 in 25	1 in 300**	**III**/ VIII
8	EED	1 in 100	1 in 2000*	**III**
9	EZH2	1 in 100	1 in 2000*	I / **III**
10	Ring2 (Rabbit)	1 in 100	1 in 2000*	**III**
11	Ring2 (Goat)	1 in 25	1 in 300	**III**
12	PHC1	1 in 100	1 in 300***	I / **III**
13	RNA Pol II	1 in 100	1 in 300***	I **/ III** / VIII

* Goat anti Rabbit Alexa 568
** Donkey anti Goat Rhodamine
*** Goat anti Mouse Alexa 546

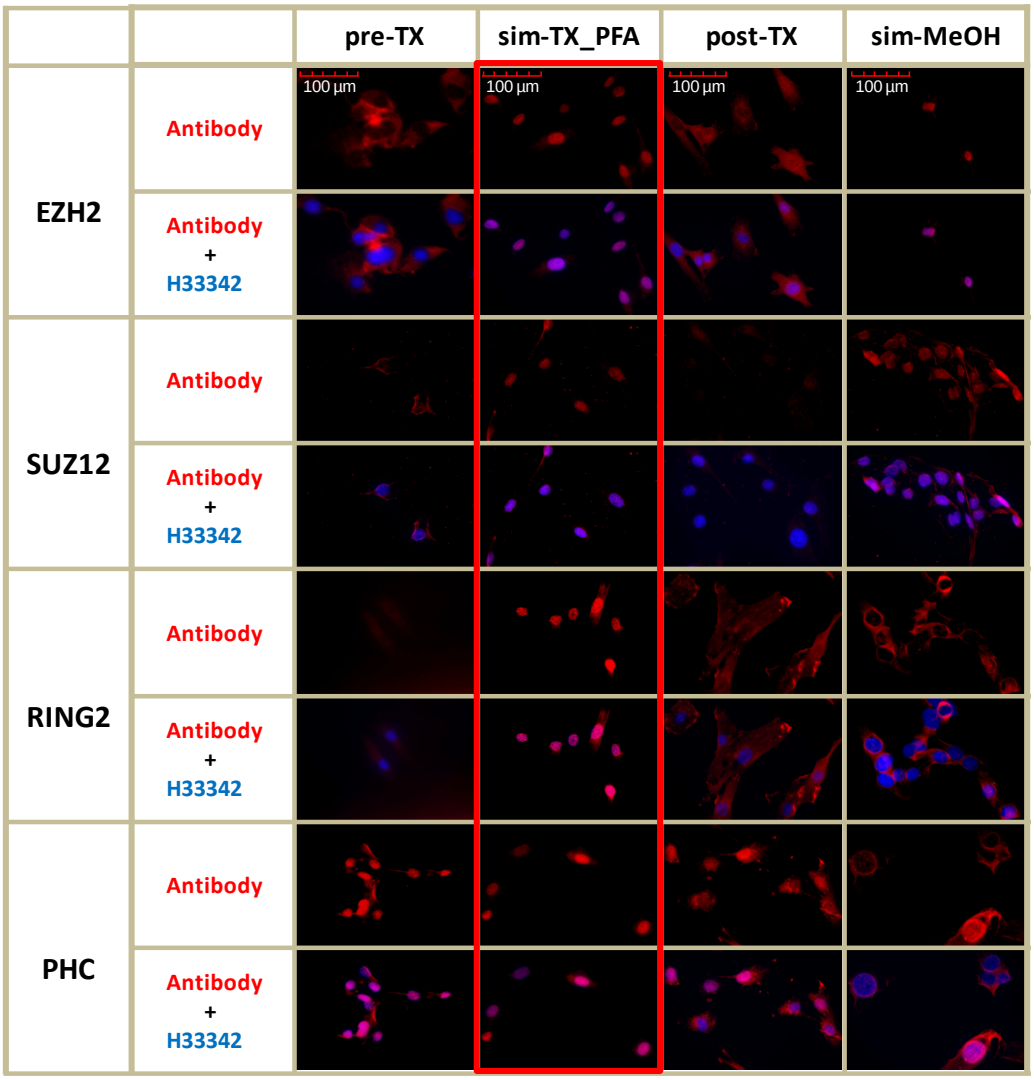

Figure 12: Comparison of PcG protein staining patterns from different IF protocols. While the sim-TX_PFA protocol (red outline) worked for all the PcG proteins tested, the other protocols gave mixed results.

Our IF protocol was able to discriminate between the male and the female pronucleus, as shown by H3K9me3 staining (Figure 13), as well as between the ICM and TE, as shown by SOX2 staining (Figure 14). The ability of SOX2 to stain mainly the ICM demonstrated that there was no accessibility problem for the antibody to penetrate the epithelial TE layer. This enabled us to quantify the differences between the ICM and TE for different antigens using confocal IF microscopy (CIFM).

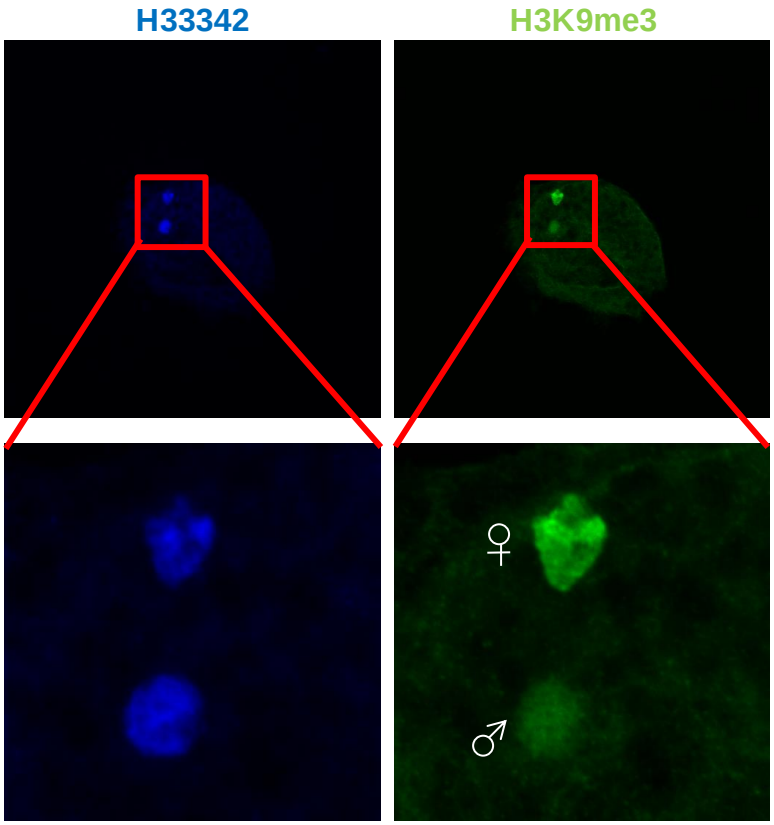

Figure 13: Differential H3K9me3 intensity pattern of the male and the female pronucleus 11 h post-IVF. The upper row shows the staining of H33342 (left) and H3K9me3 (right) in the IVF zygote. The lower row shows the enlarged portion of the male and female pronucleus. H3K9me3 is stronger in the female than the male pronucleus.

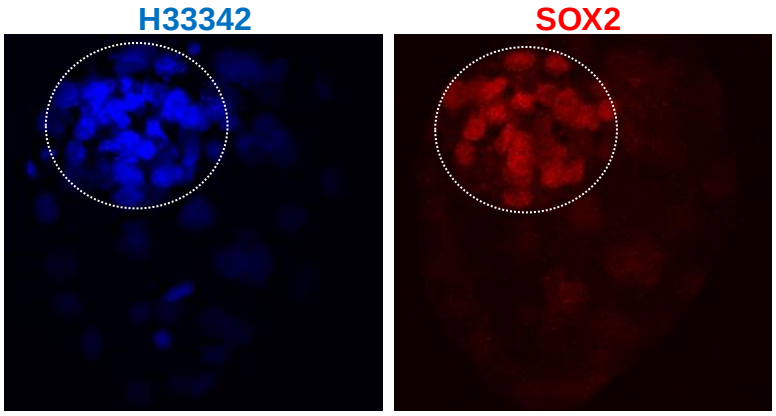

Figure 14: SOX2 distribution in Bovine IVF blastocysts. Using the sim-TX_PFA protocol, SOX2 specifically stained ICM nuclei. The white dotted circles indicate the ICM, which is identified by their small densely packed nuclei.

3.4 G_0 cells show increased substrate adhesion

The sim-TX_PFA protocol worked well with all antibodies tested and was thus chosen as protocol of choice for my experiments. However, when this protocol was tried on the experimental cell populations, G_1 cells were lost from the 0.1% gelatin-coated coverslips on which they were plated, whereas G_0 cells were efficiently retained. Different concentrations of gelatin and collagen, alone or in combination, were tried as coating substrates on the glass coverslips. A 1:2 ratio of 2.5% collagen and 0.1% gelatin best retained both G_1 and G_0 cells on the coverslips (Table 6). These results, together with the observation that serum-starved cells took longer to lift off during trypsinisation compared to non-synchronised cells, indicates increased adhesion of the G_0 vs G_1 cells.

Table 6: Effect of different substrates and their combinations on adhesion of G_0 and G_1 cells. Different percentages of gelatin, dilutions of collagen and combinations of collagen and gelatin were tested as coverslip-coating substrates. The table shows the % G_1 and G_0 cells retained on coverslips after simultaneous treatment with 3.6% PFA and 1% Triton X-100 for 20 min, followed by PBS wash. n=2.

	% Collagen			% Gelatin			Ratio:Collagen (2.5%) : Gelatin (0.1%)		
	2.5	**0.625**	**0.25**	**0.1**	**0.5**	**1**	**1:2**	**1:4**	**1:10**
G_1 (%)	10	10	13	5	3	5	81	61	17
G_0 (%)	82	56	88	92	86	88	87	91	85

3.5 G_0 cells contain similar DNA amount in a larger nuclear volume

Previous studies have used the staining intensity of DNA-binding dyes as a proxy for measuring the DNA content and used this for normalising the intensities from other antigens (McManus & Hendzel 2005). In order to use DNA content as normalising factor, we first measured the total H33342 staining intensity per cell nucleus. Integrated pixel intensity from complete confocal z-series showed no difference between G_0 vs G_1 donors (Figure 15A). This normalisation accounts for potential bias arising from

differences in ploidy, for example, in ICM vs TE cells, when G_0- vs G_1- NT blastocysts were compared. TE is known to become polyploidy during normal development (Booth, Viuff *et al*. 2003). To further validate this method, we compared the H33342-normalised Pol II pixel intensities from representative stacks of G_0 vs G_1 donors. Pol II, which is a proxy for transcriptional activity, was significantly less abundant (G_1/G_0=1.46, P=0.001) in G_0 nuclei, consistent with their reduced transcriptional activity (Figure 15B & C). The nuclear area in representative stacks was significantly higher in G_0 compared to G_1 cells (229 μm^2 vs 130 μm^2, respectively, P<0.01). The nuclear volume was also significantly greater in G_0 vs G_1 donors (2475 μm^3 vs 1474 μm^3, P<0.01, Figure 15D). This showed that G_0 chromatin was spread over a larger volume than in G_1 chromatin. There was no significant difference in the total number of frames between G_0 vs G_1 donors (11.89 vs 12.3), which corresponds to the height of nuclei. This shows that the difference observed in volume is due to a more flattened area of G_0 and both cell types contain the same amount of DNA per area. Therefore, nuclear area could also be used for normalisation. Except for H3.3 and 5mC, we normalized all CIFM data using the H33342 signal, as this was the most direct normalisation on the DNA amount present per nuclear volume analysed. We normalized H3.3 and 5mC staining on nuclear area, as the IF protocol used for these two antigens interfered with H33342 staining.

3.6 G_0 cells have more relaxed chromatin

Quiescent cells and proliferating cells have a different sub-nuclear organisation of chromosomes (Bridger, Boyle *et al*. 2000). Genome organisation changes have also been reported between interphase nuclei and cells that exited the proliferative cycle (Mehta, Amira *et al*. 2010). Specifically, serum withdrawal from cultured mammalian fibroblasts was shown to reposition all chromosomes (Mehta, Amira *et al*. 2010). How this affected chromatin condensation is not known. To analyse if serum

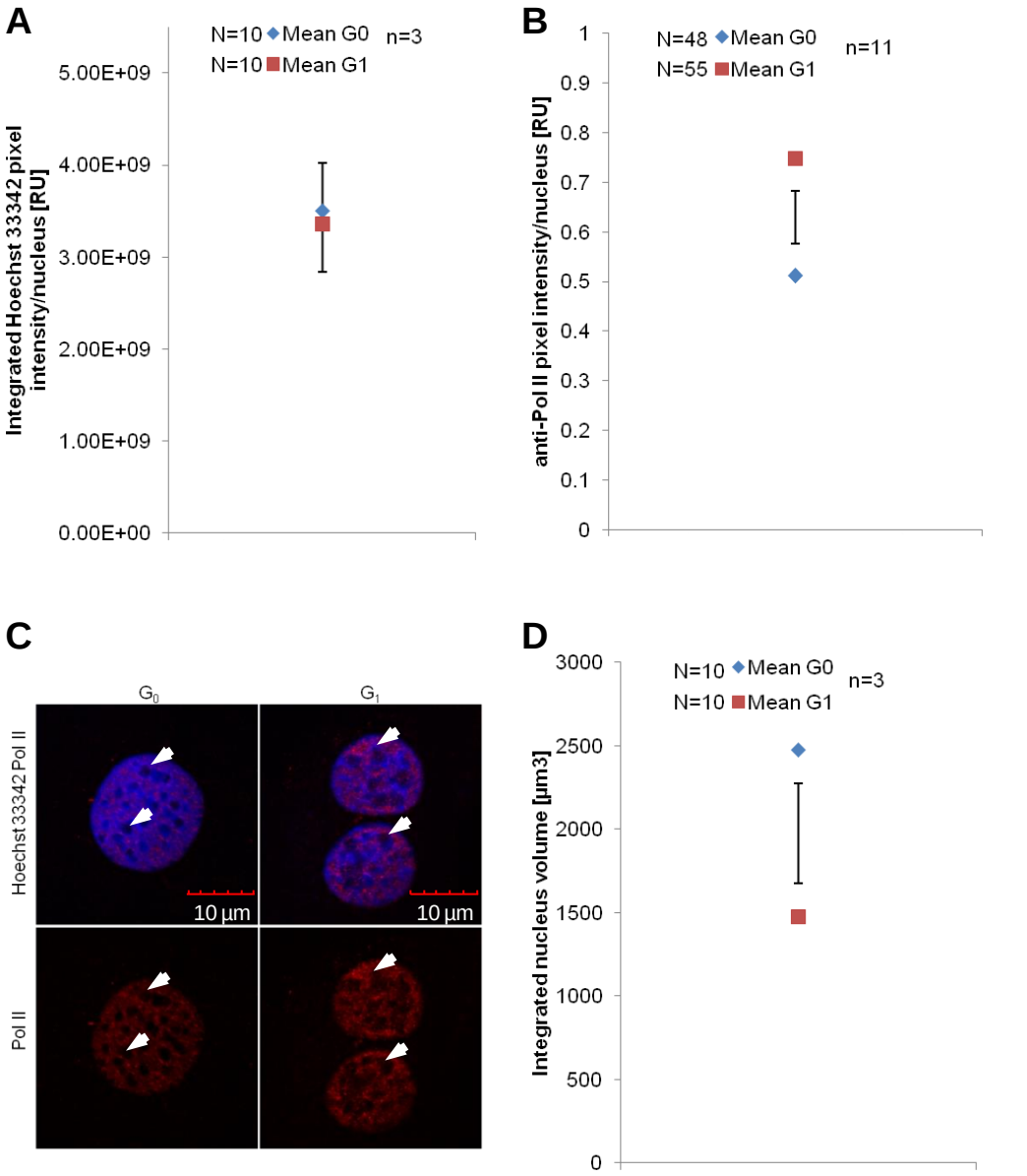

Figure 15: Characterisation of G_0 vs G_1 donor cells. A) Integrated H33342 stain as proxy for DNA content. B) Validating Pol II as proxy for transcriptional activity. Pol II intensity from representative stacks was normalised by H33342 intensity. C) Qualitative comparison of Pol II immunostaining. The red staining (lower row) indicates the loading of pol II onto the chromatin. The white arrowheads point to dark foci in both G_0 and G_1, which can be either nucleoli or regions of no DNA. G_0 had larger number dark foci than G_1 cells. D) Integrated nucleus volume. As the cells were mounted under glass slides, they assumed a flat cubical structure. Hence the nuclear volume was calculated by multiplying nuclear area with height. The bars in the graph indicate least significant difference (LSD). If the LSD bar intersects two data points, then those two points are not significantly different (A). If the LSD bar does not intersect two data points, then those data points are significantly different (B & D); RU=relative units, N= number of cells analysed, n=number of replicates.

starvation affected chromatin condensation, we compared the distribution of H33342 pixel intensities of both G_0 vs G_1 donors. Since the integrated H33342 intensity did not change between G_0 and G_1 cells, a higher H33342 pixel intensity equals more DNA per pixel. This, in turn, indicates a higher degree of DNA condensation. We measured the overall pixel intensity distribution between G_0 vs G_1 donors. The results showed that both donors have different pixel intensity distributions, with G_1 cells having a greater number of higher intensity pixels than G_0 cells (Figure 16). This suggests that G_0 cells have a more relaxed chromatin organisation. This result supports earlier reports of major heterochromatic locus decondensation in quiescent cells (Lu, Li *et al*. 2010) and a significant increase in nuclear volume accompanying loosening of chromatin during mouse germline development (Hajkova, Ancelin *et al*. 2008).

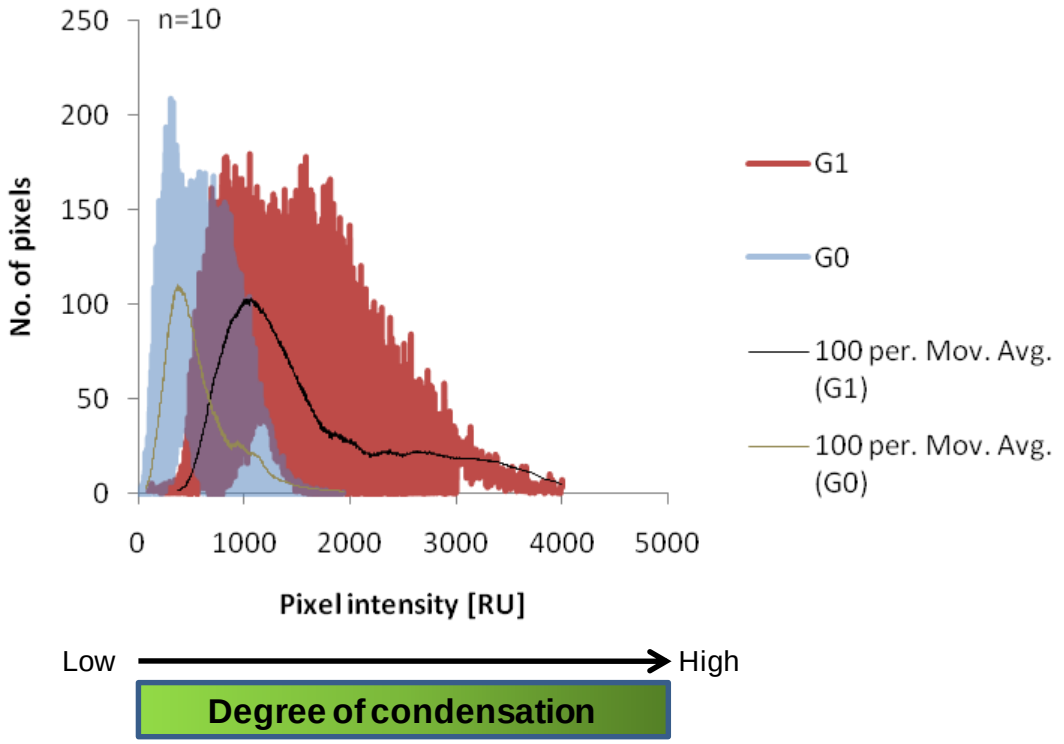

Figure 16: Pixel intensity distribution as a proxy for chromatin condensation. The trend line was calculated by a moving average of 100 pixels (100per.Mov.Avg). For computing the moving average, the 100 highest pixel intensities (1st to 100th) were averaged. Then next 100 pixel intensity were averaged (i.e. 2nd to 101st). This process was reiterated (3rd to 102nd etc.) until the last 100 pixel intensities were averaged; RU=relative units, N= number of cells analysed, n=number of replicates.

3.7 Discussion

3.7.1 Isolation of G_1 cells

Serum starvation as a method for inducing cellular quiescence is a well-established method. Our results show that LJ801 adult ear skin fibroblast can be induced into quiescence and can be re-induced into normal cell cycle progression. The fact that the growth curve mirrored the non-starved control lends credibility to this method. Isolation of G_1 cells by mitotic shake-off has been used for decades (Moser, Fallon *et al.* 1981, Kasinathan, Knott *et al.* 2001a). However, different cell lines have different cell proliferation rates and also might respond differently to shake-off. It was evident from our observation that before entering into cytokinesis, cells would increase their height and round up. Then they would form a dumbbell shape and progress through cytokinesis to form new cells. These new cells would then reduce their height and flatten out again. It was demonstrated earlier that increase in height and rounding up of cells would correspond to late anaphase and flattening of the cells would correspond to cells entering into interphase (Sanger & Sanger 1980). The flattening of cells is required to enter into S-phase but not for the progression of early to late G_1 phase (Hansen, Mooney *et al*. 1994). Cells are required to flatten post-mid G_1 phase and would remain flattened until the early anaphase by maintaining contact with the surrounding cells (Sanger & Sanger 1980). The cell rounding starts with internalisation of adhesion molecules and formation of retraction fibres (Thery & Bornens 2008). The whole idea behind the shake-off procedure is to exploit this behaviour of cells during culture. The cells which are rounded or rounding have less surface contact and would come off easily during a brief shake-off. The cells that would be dislodged easily would be the ones either in late anaphase or early G_1 phase. The results from our small-scale mitotic shake-off trials support this theoretical assumption. The result (94% doublets continuing their cell cycle progression) with shake-off doublets

after 24 h EdU incubation is in agreement with earlier result (Kasinathan, Knott *et al.* 2001a). The same study observed that nearly 60% of cells entered S-phase 2-3 h post-isolation. This contradicts our results, which showed no cells entering S-phase for up to 3.5 h post-isolation (Figure 7 & Figure 9). The difference might be due to the length of the G_1 phase. Kasinathan *et al*. used fetal fibroblasts, whereas our study used adult skin fibroblasts at passage 6. Fetal fibroblasts tend to grow more rapidly during earlier passages compared to adult fibroblasts and it is not clear which passage they have used for studying entry of doublets into S-phase. The observation that G_1 cells did not adhere well to coverslips 3.5 h post-isolation and incubation, suggests that they were slow in the flattening process. Since cell flattening is required for better adhesion and entry into S-phase, this corroborates our results that the shake-off cells did not enter S-phase post 3.5 h isolation and incubation.

The main obstacle for conducting biochemical assays was the limited number of G_1 cells that can be manually picked by mouth pipetting. To overcome this problem, we performed large-scale isolation and characterisation of all the cells originating from mitotic shake-off. Due to the characteristic rounding off and reduced surface contact of mitotic cells, one would expect a high proportion of doublets and large round single cells after mitotic shake-off. The proportions of cells obtained during our shake-off were in line with this expectation. During this large-scale isolation of G_1 cells, the observed result of nearly 6% small cells entering S-phase within 3.5 h post-plating indicates the drawback in the procedure. Doublets started to peak at a certain stage (20-24 h post-plating) and thereafter, their number would recede quickly in next 20-30 min. Due to the requirement of performing shake-off within this short period, the mitotic shake-off involved several people to shake-off plates simultaneously. During this rapid processing, there is always a chance that some cells, which have already passed the G_1-S phase restriction point and entered the mitogen-independent division phase, would come off as well. This

variation to the small-scale procedure could be introduced by different people using different shake-off technique (strength of tapping etc.). Even different types of plate shakers (equipment) could introduce variability. Nevertheless, several lines of evidence demonstrate that the large-scale method produced a high proportion of G_1 cells for biochemical assays. First, no doublets entered S-phase 3.5 h post shake-off. Second, 93% of single cells developed into doublets. Third, 97% of cells continued cell cycle progression 24 h after shake-off. Collectively, these results suggest the suitability of large-scale shake-off for generating sufficient G_1 cells for biochemical studies.

3.7.2 Optimisation of a common IF protocol

Different IF protocols resulted in varied staining outcomes, some showing a complete shift of PcG antigen localisation. Such major differences were observed only in the sim-MeoH and the pre-TX methods. Some of the epitopes are very sensitive to methanol and need acetone to permeabilise, if methanol was used as both permeabilizing and fixing agent (Abcam technical support). Furthermore, methanol was reported to be the least preserving chemical with respect to maintaining microtubule integrity (McMenamin, Reinsch *et al*. 2003), which could be attributed to its coagulating and protein-denaturing property. We also observed that methanol-treated cells lost their defined morphology. This impact on the cytoskeleton could contribute to antigen relocalisation. In case of the pre-TX method, use of Triton X-100 before fixing could result in leakage of certain nuclear antigens into the cytoplasm in the absence of a fixing agent. It is to be noted that our observed differences in the protocol mainly affected PcG antigens, which are basically localised to the nucleus. The sim-TX_PFA protocol gave a better preservation of overall cell structure, as PFA is known to preserve the proteins in their natural tertiary structure and has been reported to preserve the structure of cells and PTMs on the proteins (Bhadriraju, Elliott *et al*. 2007). It is not only a method of choice

for detecting soluble proteins like cytokines by commercial companies, but also for detecting histone PTMs (Fischle, Wang *et al*. 2003).

The sim-TX_PFA protocol clearly stained the ICM which can be a problem with other protocols. It also has the added advantage of reducing the number of steps involved in the IF protocol. This was a practical advantage for staining the limited number of SCNT embryos, reducing the chance of losing or damaging them during every step involving mouth pipetting.

3.7.3 Nuclear architecture in G_0 cells

Comparing the DNA content of both G_0 vs G_1 donors showed no difference in total DNA content between the two. Cells arrested by serum starvation and other methods have been shown to produce a uniform G_1 amount of DNA (Cooper 1998). This supports our earlier evidence that the mitotic cells used in our study post 3.5 h shake-off were in G_1. Normally, both *in vivo* and artificially induced quiescent cells were characterised by a reduced transcriptional rate and smaller cell size (Yusuf & Fruman 2003, Srivastava, Mishra *et al.* 2010). The smaller size was due to reduced cytoplasmic, not nuclear area (Tani, Morris *et al*. 2000). Very few studies have investigated the nucleus of serum-starved cells. We have specifically compared the nucleus of cells synchronised in G_0 by serum starvation vs mitotically picked cells in G_1. Since the G_1 cells used in our study reflect normal G_1 cells in culture, as they were not treated with any chemicals to synchronise them, our results reveal the true difference between serum-starved G_0 and early G_1 cells. It is to be noted that the chemicals used to synchronise the cells in G_1 stage will not stop the nucleus from growing (Maeshima, Iino *et al*. 2010) and hence they would not reflect the true G_1 cell population in culture. The observed increase in nuclear volume and area in G_0 cells could simply be due to the fact that G_1 cells represent the earliest cell cycle stage when cell volume is mimimal. What determines the cell and nuclear volume of G_0 cells is not well established and beyond the

scope of this study. For example, it is not clear at what stage of G_1 the cells enter quiescence, even though they could already make this decision in S-phase (Brooks, Bennett *et al*. 1980). It can be speculated from our results that the cells after serum withdrawal progress to a late G_1 stage, increasing their cell and nuclear size before entering quiescence. Our observed results of increased nuclear size are in close agreement with earlier published data (Moser, Fallon *et al*. 1981).

Nuclear architecture plays a critical role in modulating gene expression. Genes associated with the inner nuclear membrane lamina and peri-nucleolar chromatin tend to be silenced, while genes associated with the nuclear bodies, nuclear pore complex and nuclear speckles tend to associate with a transcriptionally active state (Zhao, Bodnar *et al*. 2009). Active genes can be moved to heterochromatin to be silenced and heritably transferred (Brown, Baxter *et al.* 1999, Grogan, Mohrs *et al.* 2001). They also can be moved away just after initiation of transcription (Josse, Mokrani-Benhelli *et al*. 2012) or to be transcribed (Francastel, Magis *et al*. 2001). In this context, the observed difference between G_0 vs G_1 chromatin distribution would suggest a differential potential for many genes to be reactivated. Even though serum-starved cells can regain their original nuclear organisation (Bridger, Boyle *et al*. 2000), their less condensed chromatin might be more amenable to NT-induced rapid chromatin remodeling in the context of an MII oocyte. Furthermore, gene-rich chromosomes, which are conducive for transcription and binding of chromatin-remodelling complexes, occupy more space in the nucleus than gene-poor chromosomes of similar size (Croft, Bridger *et al*. 1999). Such large decondensed chromatin allows better accessibility to transcription factors (Rawlings, Gatzka *et al*. 2011), supporting the notion of better reprogramming of G_0 chromatin by chromatin remodelling complexes.

Chapter Four: Epigenetic differences between G_0 and G_1 Donors

4.1 G_0 donors are globally histone lysine hypomethylated

Histone methylation is one of the key epigenetic modifications that governs heritable gene expression by conveying transcriptional memory. Hypomethylation was correlated with the ability of quiescent lymphocytes to improve *in vitro* development after NT (Baxter, Sauer *et al*. 2004). Here we sought to correlate increased *in vivo* cloning efficiency of G_0 cells with their histone methylation status. To explore this, histone lysine methylation quantification of G_0 vs G_1 control donor cells was compared using CIFM. Specifically, H3K -4me3, -9me1, -9me2, -9me3, -27me3 and pan H3/H4 methylation were compared.

4.1.1 H3K4me3

In ES cells, H3K4me3 and H3K27me3 together forms a bivalent domain on binding sites of a majority of pluripotent-associated transcription factors, such as *Nanog*, *Sox2* and *Oct4*. This keeps those target genes poised for expression during later development (Bernstein, Mikkelsen *et al*. 2006). However, when present as the only modification, H3K4me3 is generally associated with active genes. We found that while it was less abundant in G_0 donors (G_1/G_0=1.91, $P<0.05$, Figure 17), its staining pattern between the two donors remained similar (Figure 18)

4.1.2 H3K9me

H3K9me1 is found at the TSS of active genes, whereas H3K9me2 is associated with inactive genes (Barski, Cuddapah *et al*. 2007), X-inactivation and DNAme-independent imprinting (Lewis, Mitsuya *et al*.

2004). H3K9me2 also suppresses *Oct4* and *Nanog* transcription in somatic cells and its demethylation is important to reactivate these two core pluripotency genes during reprogramming (Freberg, Dahl *et al*. 2007). While H3K9me1 abundance did not differ between G_0 vs G_1 donors (G_1/G_0=0.96, P=0.92), H3K9me2 was more abundant in G_1 (G_1/G_0=1.64, P<0.05, Figure 17). Both their staining pattern was similar between G_0 vs G_1 donors (Figure 18).

H3K9me3 is mainly found in pericentric heterochromatin (Peters, O'Carroll *et al*. 2001) and also silent genes of euchromatin. Its heterochromatic foci-like staining was confirmed in interphase nuclei of LJ801 fibroblasts, where these foci excluded the Pol II staining (Figure 19). It is implicated in resisting the reprogramming of somatic nuclei to pluripotent (Fodor, Kubicek *et al.* 2006, Freberg, Dahl *et al.* 2007). In MEFs, experimentally induced H3K9me3 stably transmitted through cell divisions in the absence of strong transcriptional cues (Hathaway, Bell *et al*. 2012). Therefore, it was important to examine the abundance of this trimethyl modification. G_0 donors were significantly hypomethylated for H3K9me3 (G_1/G_0=2.39, P<0.05, Figure 17). Apart from the significant difference in quantity, qualitative differences in staining patterns were also apparent. There were mainly two types of staining patterns in G_0: 1) Dark foci with dissipating intensity in the centre (Figure 20A & Figure 20B) and 2) homogeneous staining (Figure 20C). G_1 donor nuclei, on the other hand, contained condensed dark foci (Figure 20D & Figure 20E). Furthermore, some G_0 cells showed almost no staining for H3K9me3.

4.1.3 Double staining of H3K4- and H3K9me3

H3K4me3 foci-like staining in both G_0 and G_1 resembled foci from H3K9me3 staining. H3K4me3 foci also excluded Pol II (Figure 21A & B). Therefore, we examined if there was co-existence of H3K4me3 and H3K9me3 at these foci in G_0 and G_1 donors. In G_0 cells, foci-like H3K4me3 staining coexisted with H3K9me3. However, some cells which lacked

H3K4me3 foci still showed H3K9me3 foci (Figure 21C & D). In G_1 cells, we found 100% co-existence of H3K9me3 foci with H3K4me3 (Figure 21E). At present, there are no reports of H3K4me3 foci-like staining co-occurring with H3K9me3 in any species. Occurrence appears to occur in pericentric or constitutive heterochromatin regions, as can be deduced from H3K9me3 staining. H3K4me3 antibody from different sources also showed foci-like staining excluding Pol II.

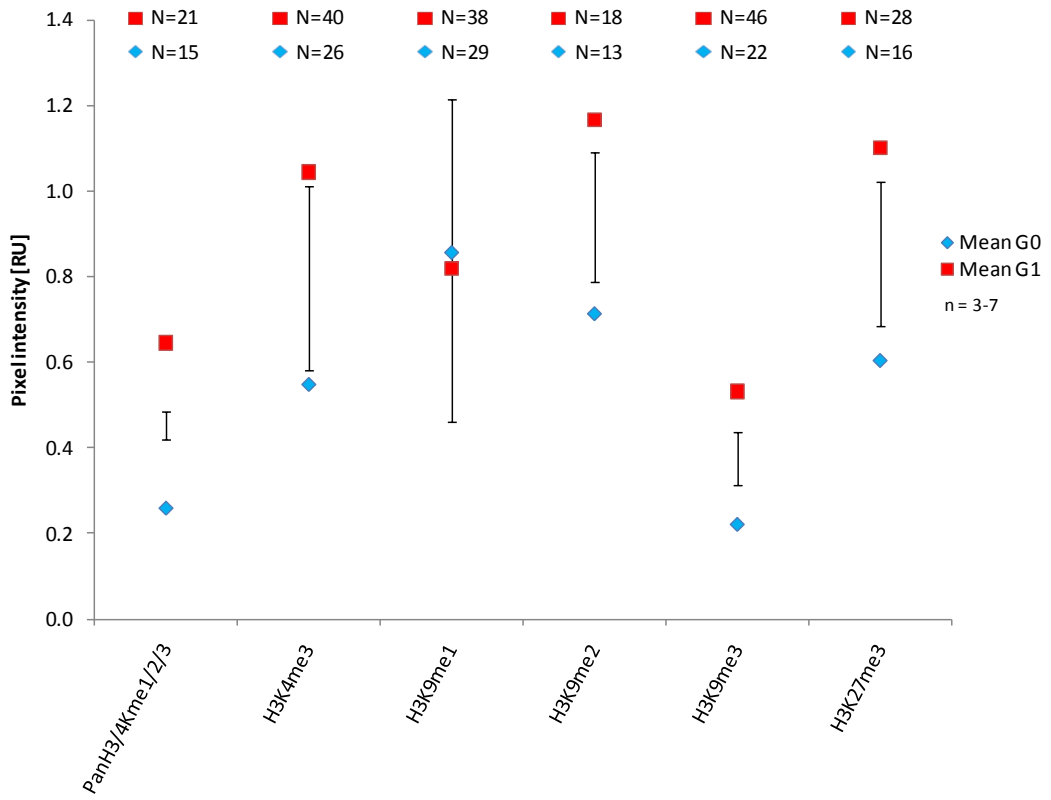

Figure 17: Abundance of histone methylations between G_0 vs G_1 donors by CIFM. The bars in the graph indicate LSD If the LSD bar intersects two data points, then those two points are not significantly different (H3K9me1). If the LSD bar does not intersect two data points, then those data points are significantly different (PanH3/4Kme1/2/3, H3K4me3, H3K9me2 and -me3, H3K27me3); N= number of cells analysed, n=number of replicates

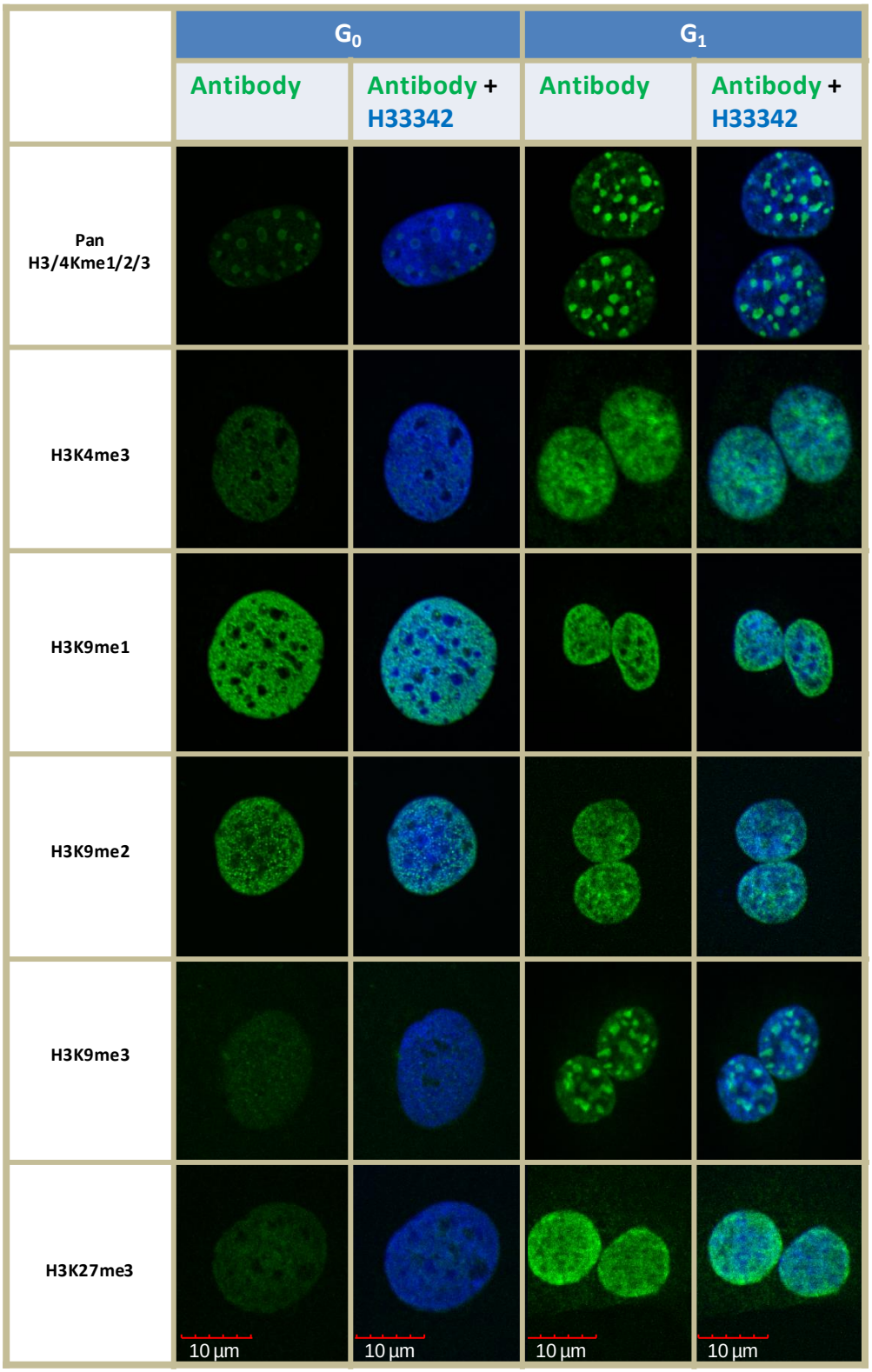

Figure 18: Qualitative comparison of different histone methylation profiles between G_0 vs G_1 donors by CIFM. The images indicate the representative single frame from a confocal stack.

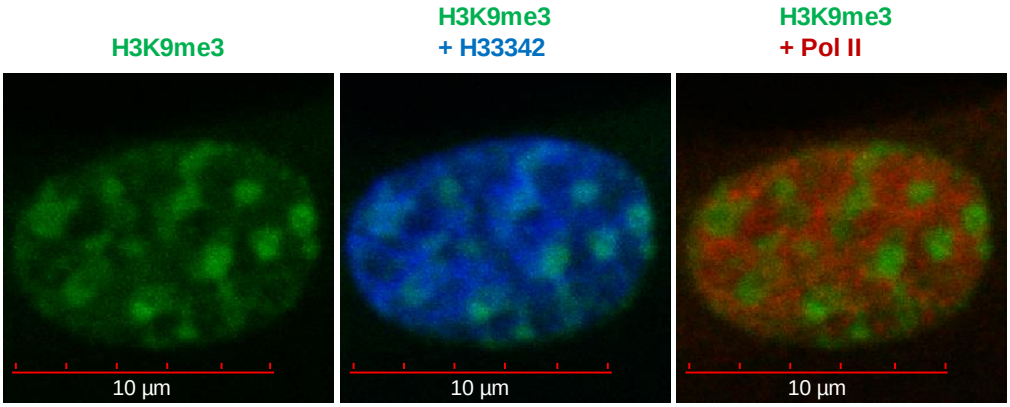

Figure 19: Heterochromatic foci-like staining of H3K9me3 in interphase nuclei of bovine LJ801 fibroblasts.

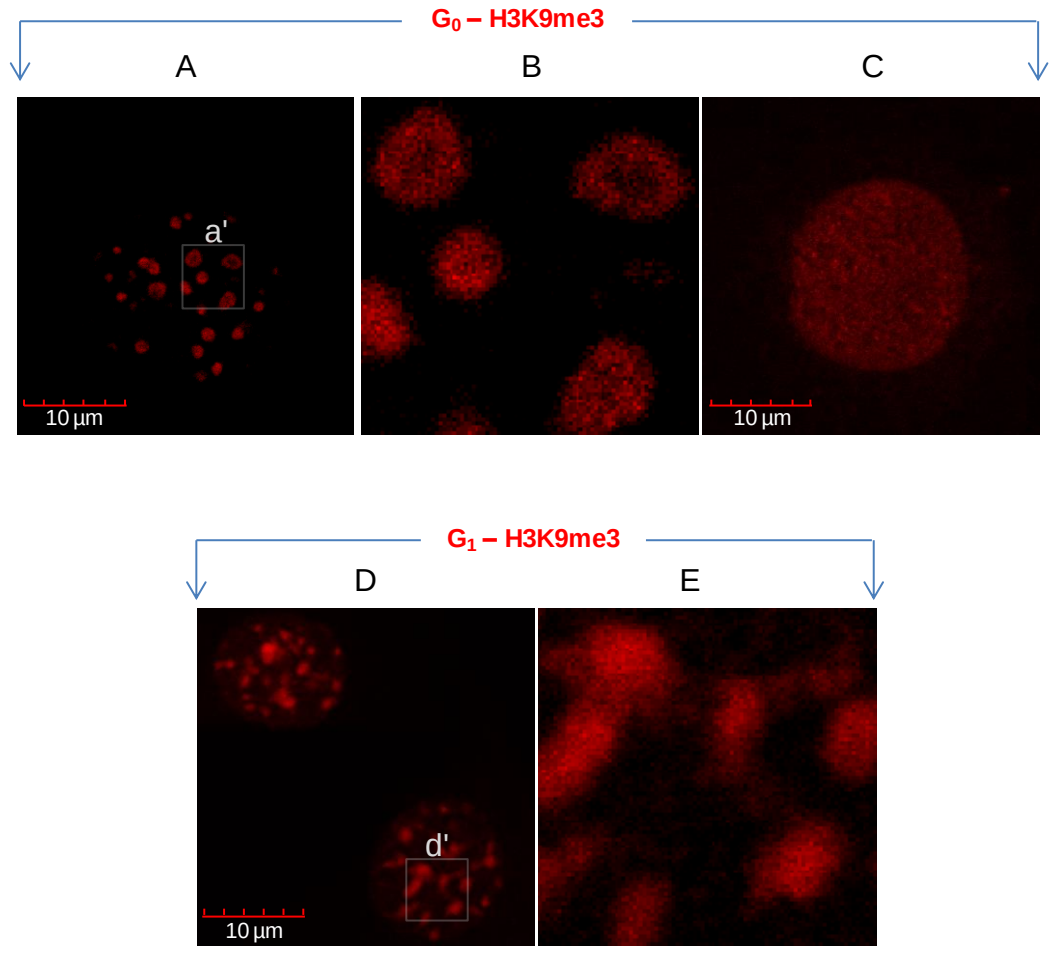

Figure 20: Different patterns of H3K9me3 methylation in serum-starved G_0* donors (A and C) compared to G_1 donors (D). A) Foci dissolving from the centre. Boxed area "a'" is shown as enlarged detail in 'B', to highlight the dissolving foci. C) Homogeneous staining. D) Strongly condensed foci. Boxed area "d'" is shown as enlarged detail in 'E', to highlight the condensed foci. (*Pixels are adjusted using look up table for better visualisation).

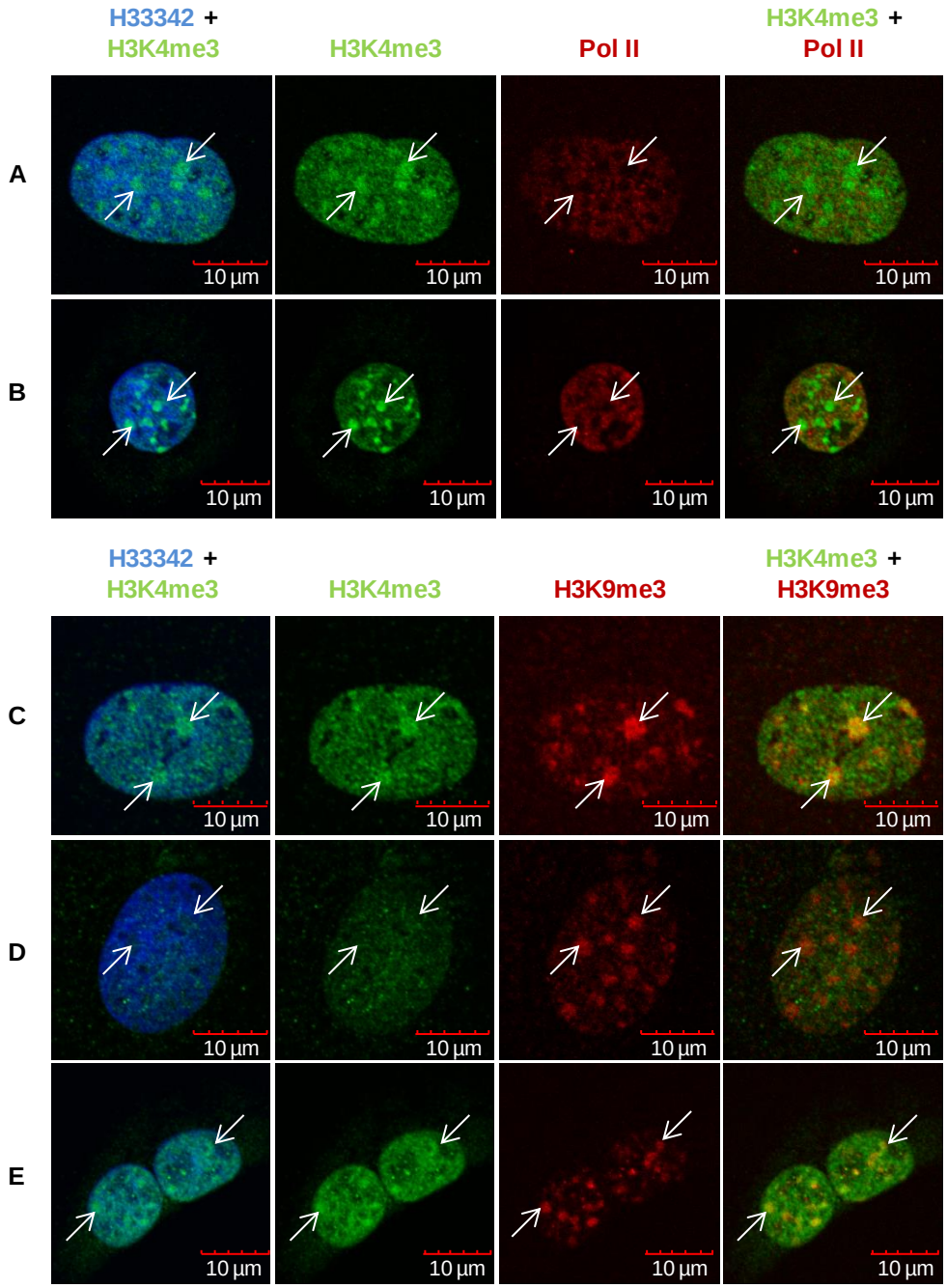

Figure 21: Comparison of foci like staining for H3K4me3 and H3K9me3 between G_0 vs G_1 donors by CIFM. A) G_0 donors exhibiting foci-like staining for H3K4me3. Arrows indicate these foci excluding staining of Pol II. B) G_1 donors exhibiting the foci-like staining for both H3K4me3. Arrows indicate co-occurrence of these foci. C) G_0 donors exhibiting foci-like staining for both H3K4me3 and H3K9me3. D) G_0 donors exhibiting absence of foci-like staining for H3K4me3 but foci pattern for H3K9me3. E) G_1 donors exhibiting foci-like staining for both H3K4me3 and H3K9me3.

4.1.4 H3K27me3

H3K27me3, which is a part of bivalent domains in ES cells, is also involved in DNA-independent genomic imprinting, X-inactivation and regulating the developmentally important *Hox* genes. We found that while the staining pattern between the two donors remained similar (Figure 18) it was less abundant in G_0 donors (G_1/G_0=1.82, P<0.01, Figure 17). Suv39-/- cells, which fail to establish H3K9me3 at pericentric regions, resort to H3K27me3 as compensatory mechanism (Peters, Kubicek *et al*. 2003). Even though quiescent cells lost most of the H3K9me3 at pericentric heterochromatin, we did not see any compensatory H3K27me3 foci.

4.1.5 Pan-histone methylation

With the exception of H3K9me1, which was unchanged, histone methylations associated with transcriptionally permissive (H3K4me3) or repressive (H3K9me2, -me3 and H3K27me3) chromatin were generally hypomethylated in G_0 donors. To confirm histone hypomethylation in G_0 donors, we used a pan H3/4K antibody that recognises H3K -4/me2/me3, -9me2/me3 (but not me1), -27me3, -36me2/me3 (me3 faintly), and -K79me2, and H4K20me3 (another pericentric heterochromatin-associated modification) (Peters, O'Carroll *et al*. 2001). We observed that this range of H3/4K methylation was reduced in G_0 cells (Figure 17), confirming the hypomethylation seen with individual epigenetic modifications. Histone methylation patterns in G_0 cells largely resembled the earlier reports on naturally quiescent B lymphocytes (Baxter, Sauer *et al*. 2004).

4.2 Biochemical evidence for global histone hypomethylation

The results of the CIFM needed to be validated using an-independent biochemical assay. Since it was difficult to get a sufficient amount of G_1 control cells for western blot analysis, we performed an epifluorescence-based ELISA assay. For ELISA experiments, we used nuclear extracts of

large-scale produced mitotic G_1 cells. ELISA results mirrored the results obtained from CIFM. Using ELISA, we found that H3K9me1 was unchanged and H3K -4me3, -9me2, -9me3 and -27me3 hypomethylated, confirming the results from CIFM (Figure 22) Even though these results were similar, there were also differences in the G_1/G_0 ratio between CIFM and ELISA. CIFM showed a greater difference between G_0 and G_1 than ELISA for H3K -4me3, -9me2, -9me3 and -27me3 (Table 7). For H3K9me1, the ELISA results confirmed the lack of significant changes previously shown by CIFM.

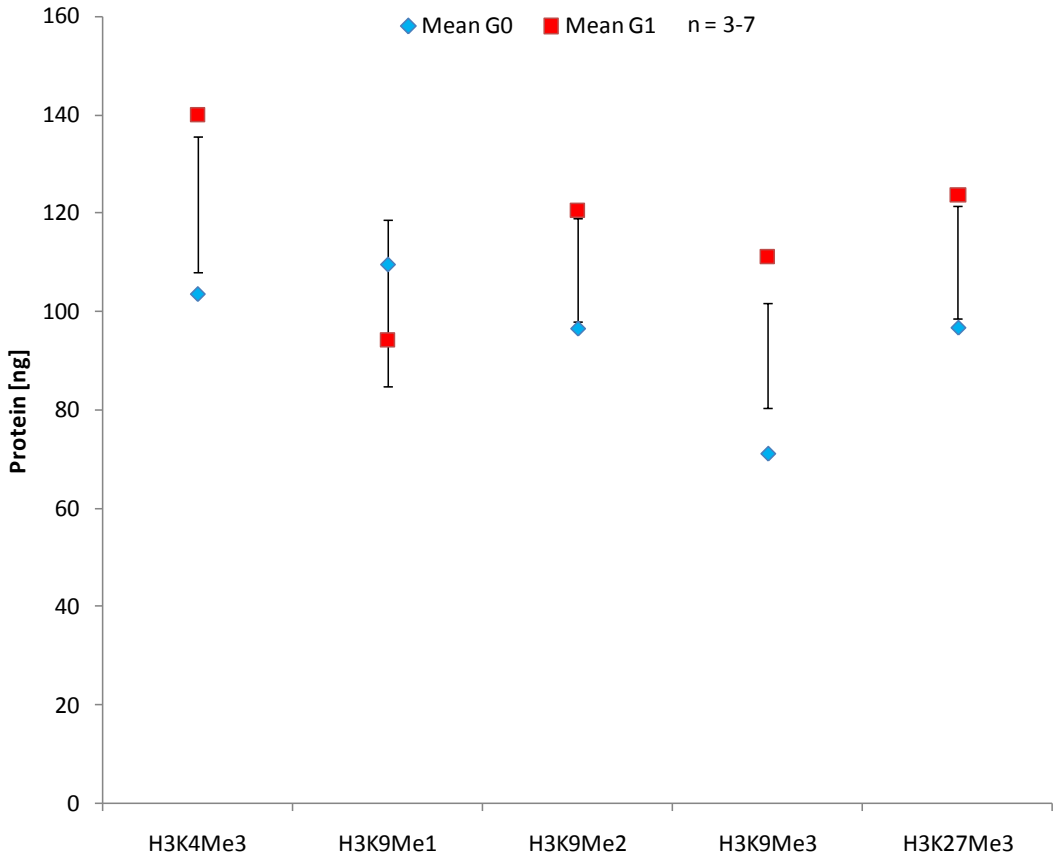

Figure 22: Abundance of different histone methylations between G_0 vs G_1 donors by ELISA. The bars in the graph indicate LSD. If the LSD bar intersects two data points, then those two points are not significantly different (H3K9me1). If the LSD bar does not intersect two data points, then those data points are significantly different (H3K4me3, H3K9me2 and -me3, H3K27me3); n=number of replicates.

Table 7: Comparison of G_1/G_0 ratio between ELISA and CIFM.

	CIFM	ELISA
H3K4Me3	1.91	1.35
H3K9Me1	0.96	0.86
H3K9Me2	1.64	1.25
H3K9Me3	2.39	1.56
H3K27Me3	1.82	1.28

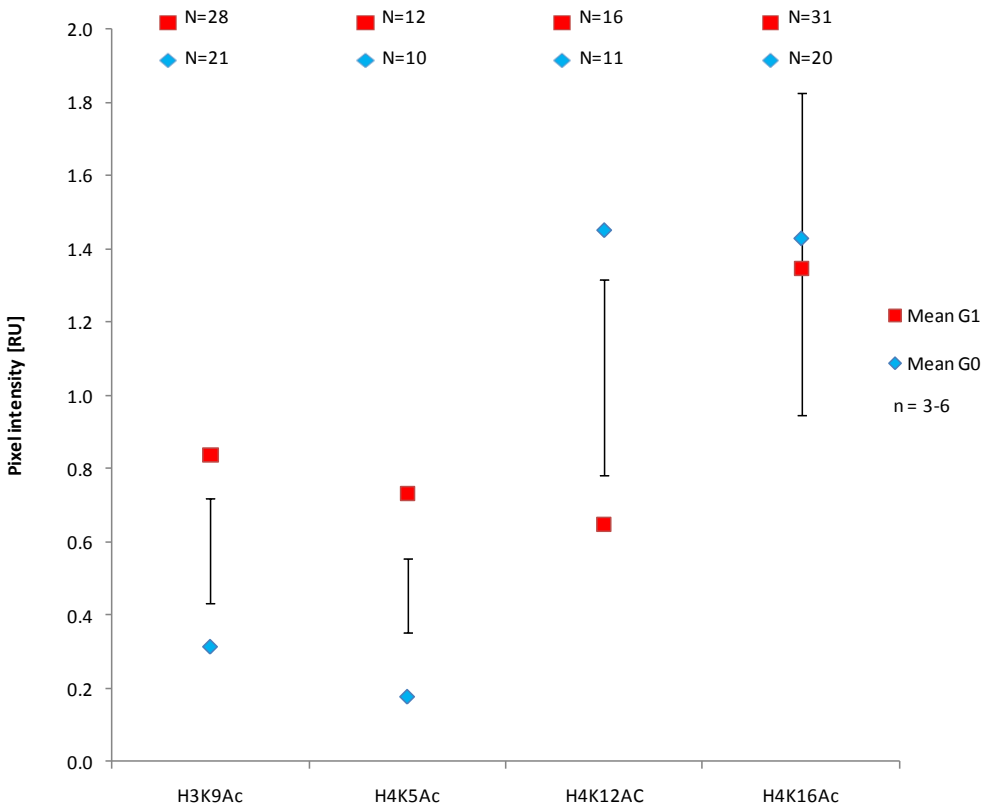

Figure 23: Abundance of different histone acetylations between G_0 vs G_1 donors by CIFM. The bars in the graph indicate LSD. If the LSD bar intersects two data points, then those two points are not significantly different (H4K16Ac). If the LSD bar does not intersect two data points, then those data points are significantly different (H3K9, H4K5 and H4K12 -Ac); RU=relative units, N= number of cells analysed, n=number of replicates.

4.3 G_0 histone acetylation levels were non-uniform

Histone acetylation is generally linked to transcription of genes and decondensed chromatin. In mammals, hyperacetylation of donors and embryos has been linked to increasing the rate of blastocyst development (Enright, Kubota *et al*. 2003). This prompted us to look into the histone acetylation profile of G_0 vs G_1 donor cells. Unlike the overall histone hypomethylation of G_0 donors, acetylation levels could not easily be generalised for G_0 vs G_1. While H3K9 and H4K5 were found to be hyperacetylated (G_1/G_0= 2.68 and 4.15, $P<0.01$ and 0.01, respectively) in G_1, H4K12 was hyperacetylated (G_1/G_0=0.45, $P<0.05$) in G_0. No significant difference (G_1/G_0=0.94, $P=0.84$) was found in the H4K16 acetylation (Figure 23). Even though H3K9 was hypomethylated, this did not lead to an increase in H3K9 acetylation. No difference in staining pattern was found for any of these modifications tested between G_0 vs G_1 (Figure 24).

4.4 Histone isoform H3.3 did not change in G_0

The overall histone hypomethylation in G_0 cells could be simply due to replacement of H3 and H4 dimers from nucleosomes with newly synthesised non-modified H3 and H4. Newly synthesised histones contain deposition-related H4K12Ac (Ma, Wu *et al*. 1998) and possibly H3K9me1 (Loyola, Bonaldi *et al*. 2006). Quiescent cells were reported to synthesise H4, and H3.3 as the only H3 variant (Wu, Tsai *et al*. 1982). However, HIRA, a chaperon responsible for H3.3 incorporation, was reported to be unchanged between quiescent and dividing cells (Polo, Theocharis *et al*. 2004). Therefore, we determined the abundance of H3.3 between G_0 vs G_1 cells. By CIFM, we found that even though there was an increase in H3.3 abundance in G_0s (G_1/G_0=0.71), it was not significant ($P=0.25$, Figure 25).

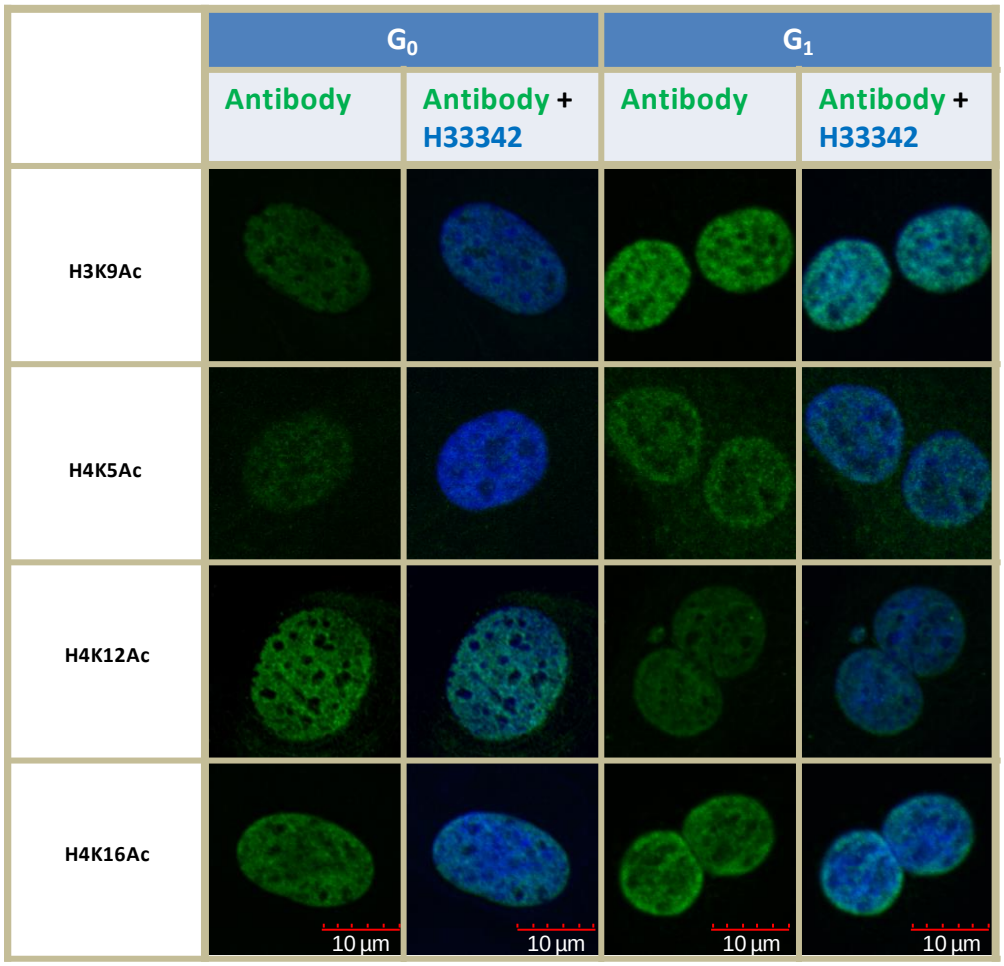

Figure 24: Qualitative comparison of different histone acetylation profiles between G_0 vs G_1 donors by CIFM.

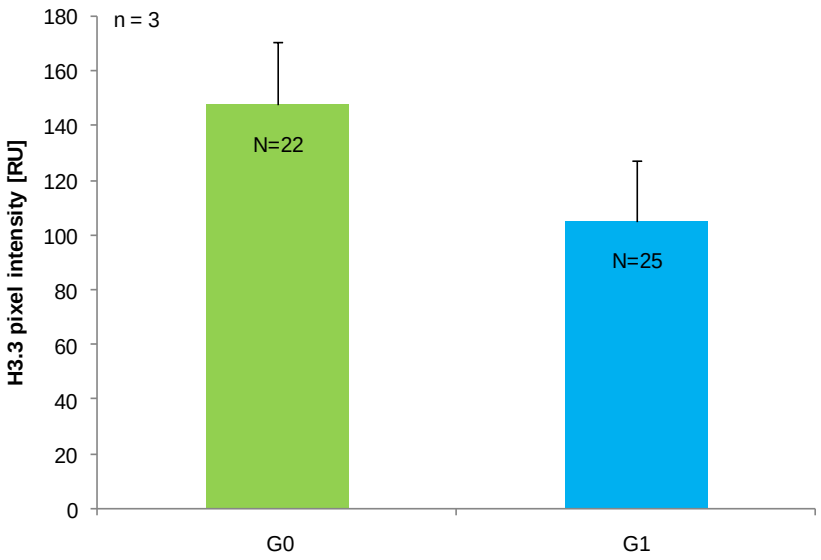

Figure 25: Quantitative comparison of H3.3 abundance between G_0 vs G_1 donors by CIFM; RU=relative units, N= number of cells analysed, n=number of replicates.

4.5 G_0 cells down-regulated most chromatin-related proteins.

Histone modification is achieved by a variety of chromatin-modifying enzymes and –associated proteins. One such group of proteins, the PcG, are responsible for maintaining several developmentally crucial genes. Differences in the expression of PRC1 and PRC2 proteins were compared using CIFM. Whilst there was no qualitative difference between their staining patterns, EED (G_1/G_0=2.54, P<0.001), SUZ12 (G_1/G_0=2.82, P<0.05), PHC1 (G_1/G_0=2.63, P<0.01) and RING2 (G_1/G_0=2.4, P<0.05) were significantly down-regulated in G_0 donors (Figure 26 & Figure 27). EZH2, an enzyme that trimethylates H3K27, did not show any differences in localisation between G_0 vs G_1 donors (Figure 26). We found that even though there was an increase in EZH2 abundance in G_1 cells (G_1/G_0=1.68), it was not significant (P=0.12, Figure 27). Likewise, HDAC1, an enzyme responsible for histone deacetylation, proliferation and embryonic development (Lagger, O'Carroll *et al*. 2002), showed no change in localisation and abundance (G_1/G_0=0.99, P=0.99) between G_0 vs G_1 donors (Figure 26 and Figure 27).

HP1α, which recognises H3K9me3 to form higher-order structure at pericentric heterochromatin, favours histone variant H2A.Z for its interaction and proper binding. Since H3K9me3 was less abundant in G_0 donors, we investigated the abundance of H2A.Z in G_0 vs G_1 donors by CIFM. H2A.Z showed no change in localisation pattern between G_0 vs G_1 donors (Figure 26). Similar to H3K9me3 hypomethylation, G_0 donors also down-regulated H2A.Z compared to G_1 (G_1/G_0=2.76, P<0.05, Figure 27).

4.6 DNA was hypomethylated in G_0 donors

DNAme is involved in genomic imprinting, X-inactivation and gene repression. There is a complex cross-talk between DNAme and histone modifications. In ES cells, H3K9me3 mediates DNAme at pericentric

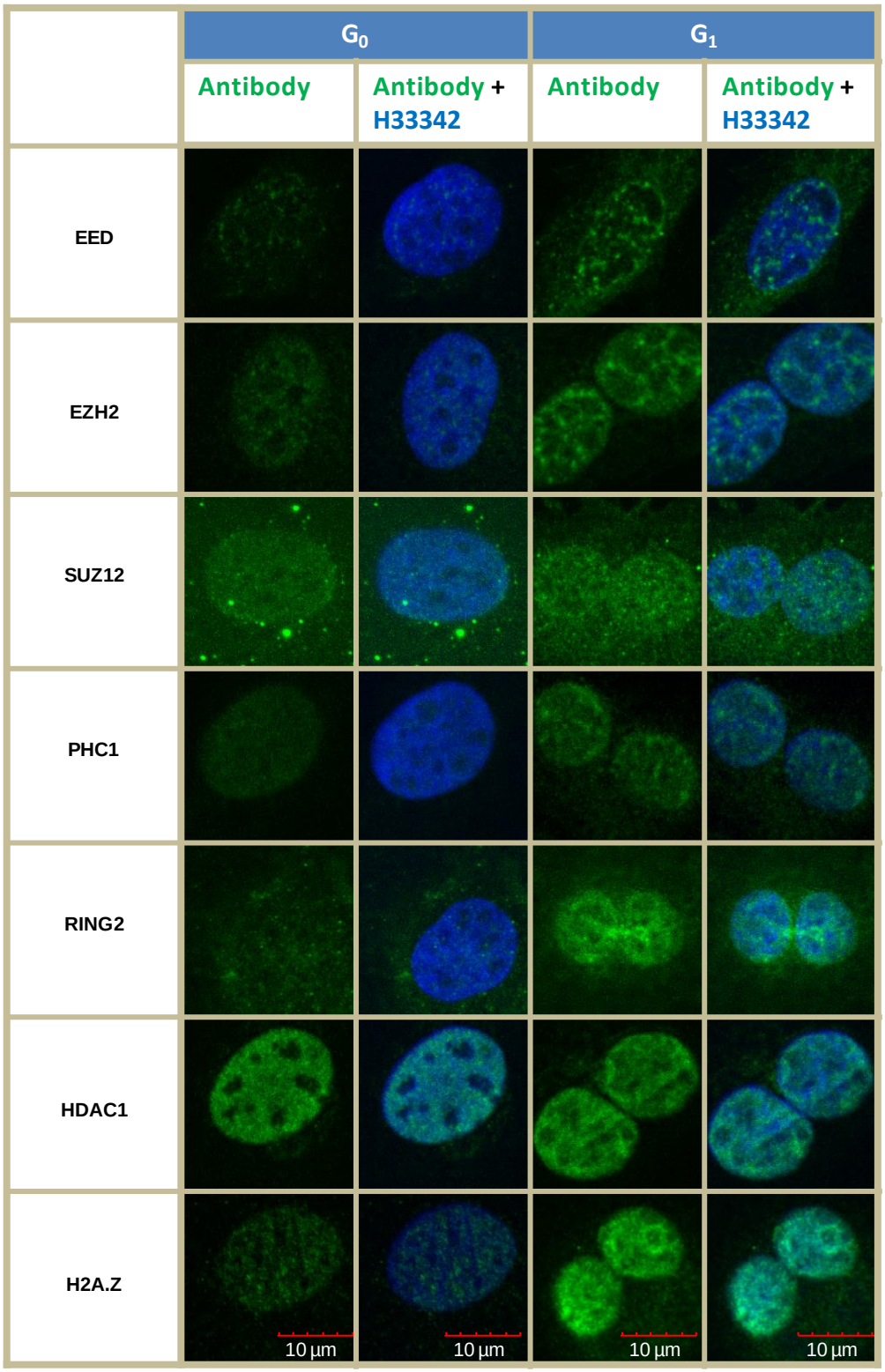

Figure 26: Qualitative comparison of different chromatin-related proteins between G_0 vs G_1 donors by CIFM.

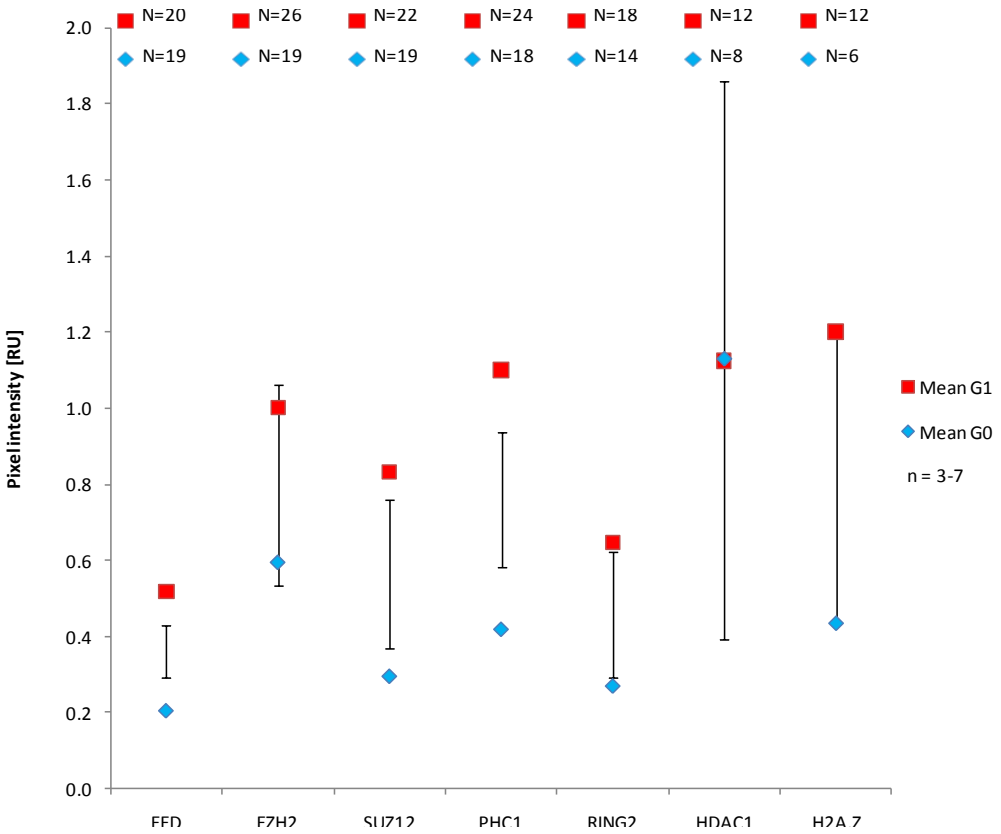

Figure 27: Abundance of different chromatin-related proteins between G_0 vs G_1 donors by CIFM. The bars in the graph indicate LSD. If the LSD bar intersects two data points, then those two points are not significantly different (EZH2 and HDAC1). If the LSD bar does not intersect two data points, then those data points are significantly different (EED, SUZ12, PHC1, RING2, H2A.Z); RU=relative units, N= number of cells analysed, n=number of replicates.

heterochromatin (Lehnertz, Ueda *et al*. 2003), while DNAme is necessary for stable perpetuation of H3K9me3 (Hathaway, Bell *et al*. 2012). Since G_0 donors were found to be H3K9me3 hypomethylated and had either no or dissolving foci at pericentric heterochromatin, we investigated whether serum starvation also affected DNAme. By using a specific antibody against 5mC, we found that 5mC had varied patterns in G_0 and a single pattern in G_1 donors, similar to H3K9me3 (Figure 28A). Simultaneous staining with H3K9me3 revealed considerable co-occurrence of these epigenetic modifications in both G_0 vs G_1 donors, particularly at the foci (Figure 28B). G_0 donors contained overall less DNAme than G_1 controls (G_1/G_0=1.64, $P<0.05$, Figure 28C).

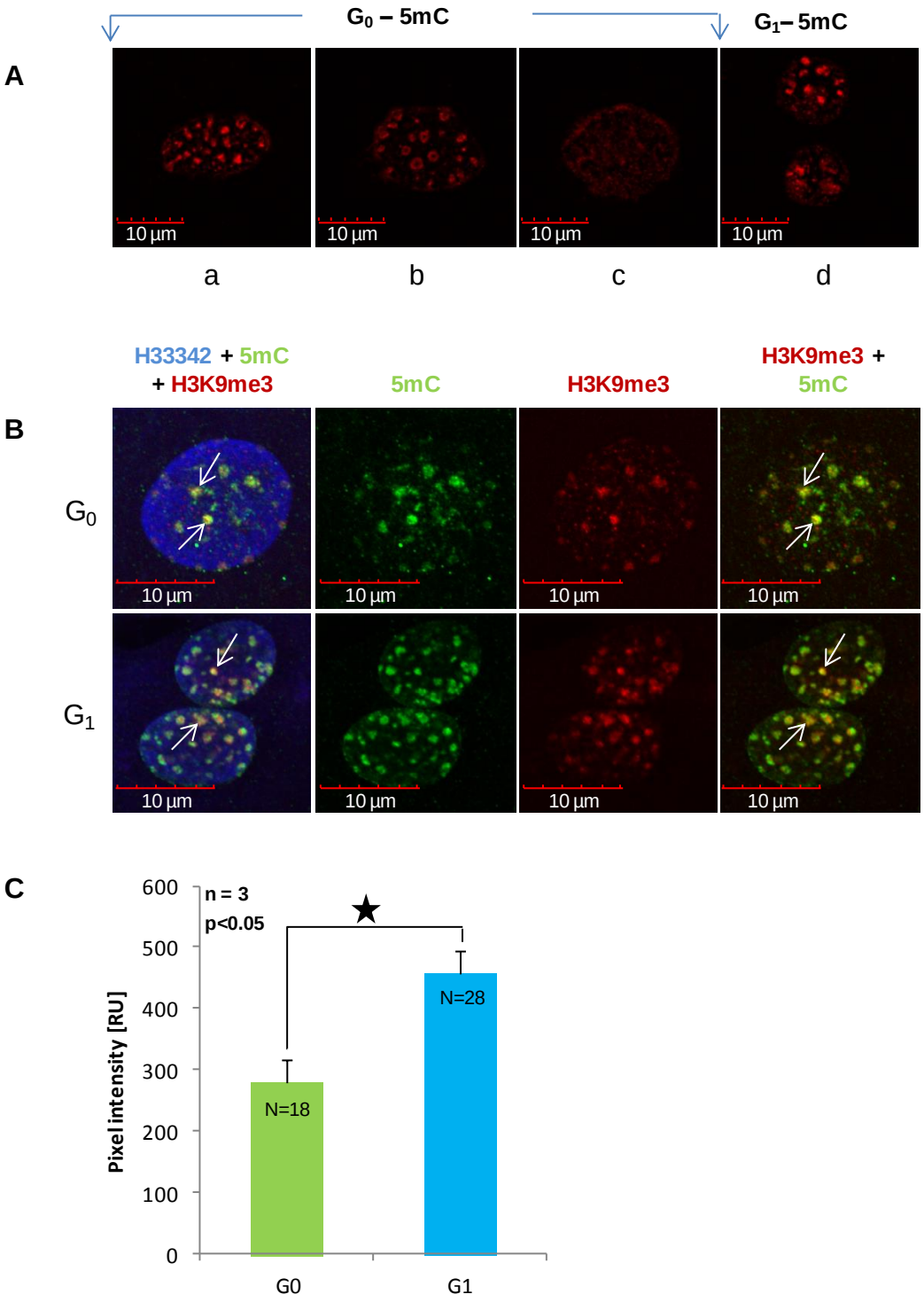

Figure 28: Characterisation of DNA methylation between G_0 vs G_1 donors. A) Different patterns of DNAme as detected by anti-5mC antibody in serum-starved G_0 (a-c) compared to G_1 donors (d). B) Both G_0 and G_1 donors exhibit the foci-like staining for both 5mC and H3K9me3. Arrows in merged images indicate co-localisation of these foci. C) Abundance of DNAme as detected by anti-5mC antibody between G_0 vs G_1 donors by CIFM. Star indicates P<0.05; RU=relative units, N= number of cells analysed, n=number of replicates.

4.7 Discussion

Both G_0 and G_1 cells have been successfully used as donors for cloning. However, G_0 donors more than doubled the cloning efficiency to term and beyond compared to early G_1 donors. We know of no other treatment that has resulted in such a dramatic increase in cattle cloning efficiency. In mouse donor histone hypomethylation correlated with *in vitro* blastocyst development (Baxter, Sauer *et al*. 2004). Therefore, in order to elucidate structural changes correlate with that increased G_0 donor reprogrammability, we investigated their epigenetic features compared to G_1 controls. By using antibodies against specific histone methylations and acetylations states, chromatin-related proteins and DNAme, we have investigated the epigenetic alterations that might contribute to the better reprogramming of G_0 donors. We found that G_0 cells were globally histone and DNA hypomethylated, down-regulated most of their chromatin-related PcG proteins and showed significant differences in acetylation abundance.

4.7.1 Histone and DNA hypomethylation in G_0

PcG enzyme EZH2 is responsible for establishing H3K27me3 and it did not vary between G_0 vs G_1 cells. In the absence of H3K9me3 at pericentric heterochromatin, H3K27me3 can act as a compensatory mechanism to mark pericentric heterochromatin (Peters, O'Carroll *et al*. 2001). Therefore, in the presence of EZH2 and down-regulation of H3K9me3, we expected hypermethylation of H3K27me3. Other studies have shown that this PcG protein works as part of multimeric domains (Schwartz & Pirrotta 2007). Therefore, down-regulation of other PcG proteins, such as EED and SUZ12 could explain the inability of the EZH2 to remethylate H3K27me3.

In the context of reprogramming, histone and DNA hypomethylation would provide several advantages to G_0 chromatin. H3K9me3 is involved in maintaining pericentric heterochromatin and permanent repression of genes in differentiating cells that resist reprogramming (Ait-Si-Ali,

Guasconi *et al.* 2004, Fodor, Kubicek *et al.* 2006). Use of H3K9me3 inhibitors increased the efficiency of iPS cell-derivation (Pasque, Jullien *et al*. 2011). An extra layer of reinforcement of the stability of heterochromatic sub-domains is achieved by DNAme (Lehnertz, Ueda *et al*. 2003). Therefore, reduction in both DNAme and H3K9me3 would help in de-repression of differentiation and pluripotency-associated genes by relaxing heterochromatin. G9a is involved in H3K9me2 methylation and directs DNAme. Its removal improves reprogramming efficiency after NT (Pasque, Jullien *et al*. 2011). Hypomethylation of H3K9me2 might help in resetting of genes in euchromatic regions, specifically pluripotency genes e.g. *NANOG, SOX2* and *OCT4*, and imprinted genes. Likewise, hypomethylation of H3K27me3 could aid in de-repression of developmentally regulated and imprinted genes. Hypomethylation of H3K4me3 would help to erase the activation cue for the transcription machinery during quiescence and reset developmentally-associated and cell-specific gene expression patterns. Together with hypo-H3K4me3, hypo-H3K27me3 might also help in resolving of bivalent domains.

4.7.2 Histone acetylation in G_0

Patterns of histone lysine acetylation were more complex than the general reduction in histone methylation in G_0 cells. Histone acetylation, commonly marking active genes, is known for its dynamic regulation. Hypomethylation of H3K9me2 and -me3 did not result in the reciprocal hyperacetylation of H3K9. Serum starvation or energy deprivation could be predicted to result in accumulation of NAD^+ (Liu, Knabb *et al*. 2009), which may activate NAD^+-dependent SIRT1, an HDAC (Noriega, Feige *et al*. 2011) that can deacetylate H3K9Ac (Khare, Habib *et al*. 2012). K9Ac is dynamically targeted to H3K4me3 bearing histones. It's rapid and continuous turnover is achieved by the combined action of HATs and HDACs, even in quiescent cells (Edmunds, Mahadevan *et al.* 2008, Lee & Mahadevan 2009). In *Dictyostelium*, lack of H3K4me3 resulted in loss of

dynamic H3K9Ac (Hsu, Chubb *et al*. 2012). These observations support concomitant H3K9Ac hypoacetylation and H3K4me3 hypomethylation in G_0 cells.

In mammals, HDAC1 is responsible for deacetylation of H4K5Ac and initiating transcriptional repression (Ma & Schultz 2008). Even though we did not observe any increase in HDAC1 abundance, there was a reduction in H4K5Ac in G_0 cells. Both HDACs and HATs appear to be part of the same multimeric groups, which allows them to dynamically target both active and silent genes (Wang, Zang *et al*. 2009). Therefore, in G_1 cells even though HDAC1 is present, HATs responsible for H4K5Ac could counteract and re-acetylate it. During serum starvation cyclic AMP goes up (Kram, Mamont *et al*. 1973). Mitochondrial acetyl CoA, a major supplier of acetyl groups for histone acetylation (Madiraju, Pande *et al*. 2009), might be limited under serum-starved condition due to its phosphorylation by AMP-activated protein kinase (AMPK) (Park, Gammon *et al*. 2002). This lack of acetyl group availability could prevent the re-acetylation of H4K5Ac in G_0 cells. There was no difference in H4K16Ac between G_0 vs G_1 cells. H4K16Ac resists chromatin condensation and is hypoacetylated during mitosis. It can be noted that G_1 cells have the lowest amount of H4K16Ac during the normal mammalian cell cycle (Vaquero, Scher *et al*. 2006) and G_0 cells maintained that basal level.

H4K12Ac was the only modification, found to be up-regulated in G_0. To explain this, we considered the following possibility. In addition to G_1 and S stages, H4 is also synthesised and incorporated into chromatin during G_0 (Wu, Perry *et al*. 1983). As H4K12Ac is a deposition-related modification on newly synthesised histones (Ma, Wu *et al*. 1998), there is also the possibility that in the S-phase preceding the G_0 entry, newly synthesised H4 is incorporated into chromatin. Lack of H4K12Ac deacetylase in G_0 could result in retention of this modification. Since the

enzyme responsible for deacetylation of H4K12Ac is unknown, its lack of abundance or activity could not be verified.

Treating donors with HDACi, such as TSA, which results in histone hyperacetylation, correlates with increased development to blastocyst and birth of live animals in mammals (Monteiro, Oliveira *et al*. 2010). G_0 donors had hyperacetylated H4K12, hypoacetylated H3K9 and H4K5 and basal levels of H4K16Ac. The beneficial effect of hyper-acetylated H4K12 in G_0 cells thus seems to be dominant over the reduced H3K9 and H4K5 acetylation. HDACi treatment results in global hyperacetylation of H3/H4, but it is not clear whether it is global hyperacetylation of histones or the hyper-acetylation of a specific subset of histones and lysines that is responsible for the beneficial effect.

4.7.3 Molecular basis for relaxed chromatin in G_0

Based on the H33342 staining distribution, we have observed a relaxed chromatin pattern in G_0 donors. This correlated with the down-regulation of H3K9me3 and DNAme, the marks of pericentric heterochromatin. There were also other factors that contributed to relaxed chromatin in G_0, probably in euchromatic regions. PRC1 is involved in chromatin compaction. Recruitment of PRC1 depends on H3K27me3 signals (Cao, Wang *et al.* 2002, Fischle, Wang *et al.* 2003). With reduced H3K27me3 in G_0 cells, PRC1-mediated chromatin compaction is less likely. During serum starvation, intracellular AdoMet levels are reduced (Fuso, Seminara *et al*. 2005). In the absence of co-factor AdoMet, the EZH1-containing PRC2 complex could condense chromatin (Margueron, Li *et al*. 2008). However, down-regulation of SUZ12 and EED would prevent such chromatin condensation. G_0 cells also down-regulated PRC1 proteins PHC1 and RING2. In particular, down-regulation of RING2 may also contribute to lack of chromatin condensation in G_0 cells, as RING2 is implicated in chromatin compaction (Eskeland, Leeb *et al*. 2010). In the same way, down-regulation of H2A.Z, which is also involved in higher-

order chromatin structure (Suto, Clarkson *et al*. 2000), would aid in relaxing G_0 chromatin. Cumulatively, all these observations correlate with the observed relaxed chromatin configuration in G_0 vs G_1 cells.

Chromatin compaction increases with lineage commitment compared to non-committed ES cells (Ahmed, Dehghani *et al*. 2010). Treatment with HDACi results in hyperacetylation, which in turn interferes with higher-order chromatin organisation. ES cells can result in higher cloning efficiency than differentiated cells but HDACi treatment does not further increase their cloning efficiency (Kishigami, Mizutani *et al*. 2006). Therefore, open chromatin might be one of hallmarks of cells with high reprogrammability. Histone and DNA hypomethylation, as well as down-regulation of RING2, would reduce heterochromatinization in G_0 cells, rendering their chromatin more accessible to chromatin-modifying complexes and increasing their reprogrammability.

Chapter Five: Differences in NT-induced epigenetic reprogramming of G_0 vs G_1 donors

Using CIFM, we next investigated how the epigenetically different G_0 vs G_1 donors would reprogram after nuclear transfer (NT) experiments. We specifically wanted to know whether this initial epigenetic differences for H3 -K4me3, -K9me1, -K9me3 and -K27me3 would be perpetuated throughout development until the blastocyst stage. H3 -K4me3 and -K27me3 were selected because these are not only markers for active and repressive chromatins, respectively, but also needed to be reset during early reprogramming, particularly at bivalent domains of developmental genes. H3K9me3 was selected as it was shown to resist reprogramming and pericentric heterochromatin, which is marked by this modification, also needs to be re-set during early development. H3K9me1 was selected as a control, since its occurrence did not change between G_0- and G_1- donors. Serum-starved and mitotically-selected G_1 control donors were electrically fused with MII-arrested oocytes to generate NT embryos. These were artificially activated and cultured up to the blastocyst stage, as described in the methods section. Up to 72 h post-activation, the intensity comparison was based on qualitative rather than quantification observation. This was due to inconsistent cytoplasmic background in NT embryos, which prevented accurate quantification. However, we performed accurate intensity quantification at the blastocyst stage.

5.1 Dynamic reprogramming of H3 methylation levels in G_0-derived cleavage-stage embryos

Within 10 min following NT, we observed that the DNA of the G_0 condensed slower than that of G_1 donors, supporting the notion of a more relaxed G_0 chromatin configuration (Figure 29). We then investigated the

dynamics of a subset of candidate histone methylation and polycomb proteins at various developmental stages up to the blastocyst. Within 10 min following NT, G_0-derived NT embryos still maintained the initial hypomethylation of H3K4me3, H3K9me3, H3K27me3 and PanH3/4 lysine methylation (Figure 30). Their staining pattern also showed qualitative differences. While in G_0-derived one cell embryos most of the histone methylation staining was outside the DNA, in G_1-derived one cell embryos it co-localised with DNA (Figure 30). However, these initial differences started to change 4 h post-activation (Figure 30). At 24 h post-activation, chromatin of G_0-derived NT embryos had acquired histone methylations levels comparable to G_1-derived NT embryos.

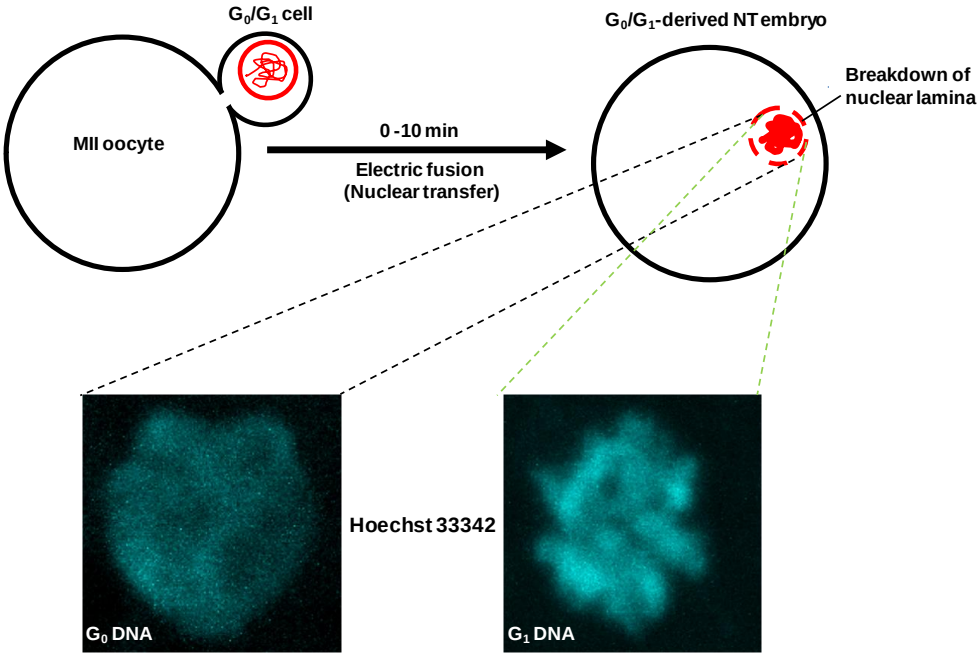

Figure 29: Chromatin configuration within 10 min of NT. A) Schematic of electrical fusion (NT) of a somatic donor with an MII oocyte and production of SCNT embryo. B) Relaxed chromatin configuration of 1 cell G_0 compared to C) condensed chromatin in G_1 as observed by H33342 staining.

H3K4me3 showed a dynamic pattern in G_0-derived NT embryos compared to the stable pattern in G_1-derived NT embryos. In G_0, H3K4me3 intensity increased from 0-10 min post-NT to 24 h post-activation before reducing again at 72 h post-activation (Figure 30, Figure 31 & Figure 32) By

comparison G_1-derived NT embryos maintained their levels until 72 h post-activation. At 72 h post-activation, there was an obvious loss of H3K4me3 in both G_0- vs G_1-derived NT embryos (Figure 30, Figure 31 & Figure 32).

H3K9me1 maintained steady levels from 4-72 h post-activation in both G_0- vs G_1-derived NT embryos with no difference in H3K9me1 intensity between them (Figure 31 & Figure 32). On the other hand, H3K9me3 methylation was up- and down-regulated in G_0-derived NT embryos. There was initial gain of this modification by 4 h post-activation (Figure 30, Figure 31 & Figure 32) and difference in little change in intensity until 24 h post-activation. By 72 h post-activation, the intensity had decreased. By contrast, G_1-derived NT embryos maintained the intensity from 0-10 min until 72 h post-activation (Figure 30, Figure 31 & Figure 32). Quantitative comparison of intensities between G_0- vs G_1-derived NT embryos at 4 and 24 h post-activation showed no difference and at 72 h post-activation showed loss of H3K9me3 in G_0-derived NT embryos (Figure 31 & Figure 32).

H3K27me3 intensity levels progressively increased until 72 h post-activation in G_0- embryos (Figure 30, Figure 31 & Figure 32), but did not change in G_1-derived NT embryos, except for some transient loss at 24 h post-activation. Comparison of intensities between G_0- vs G_1-derived NT embryos showed lower G_0 intensity levels at 0-10 min and 4 h post-activation and similar intensity levels at 24 and 72 h post-activation (Figure 30, Figure 31 & Figure 32).

5.2 EZH2 occurrence correlated with H3K27me3 in cleavage-stage NT embryos

We then compared the dynamics of PcG proteins SUZ12 and EZH2. An earlier report had described passive loss of H3K27me3 from the two-eight cell stage in bovine IVF embryos (Ross, Ragina *et al*. 2008). EZH2

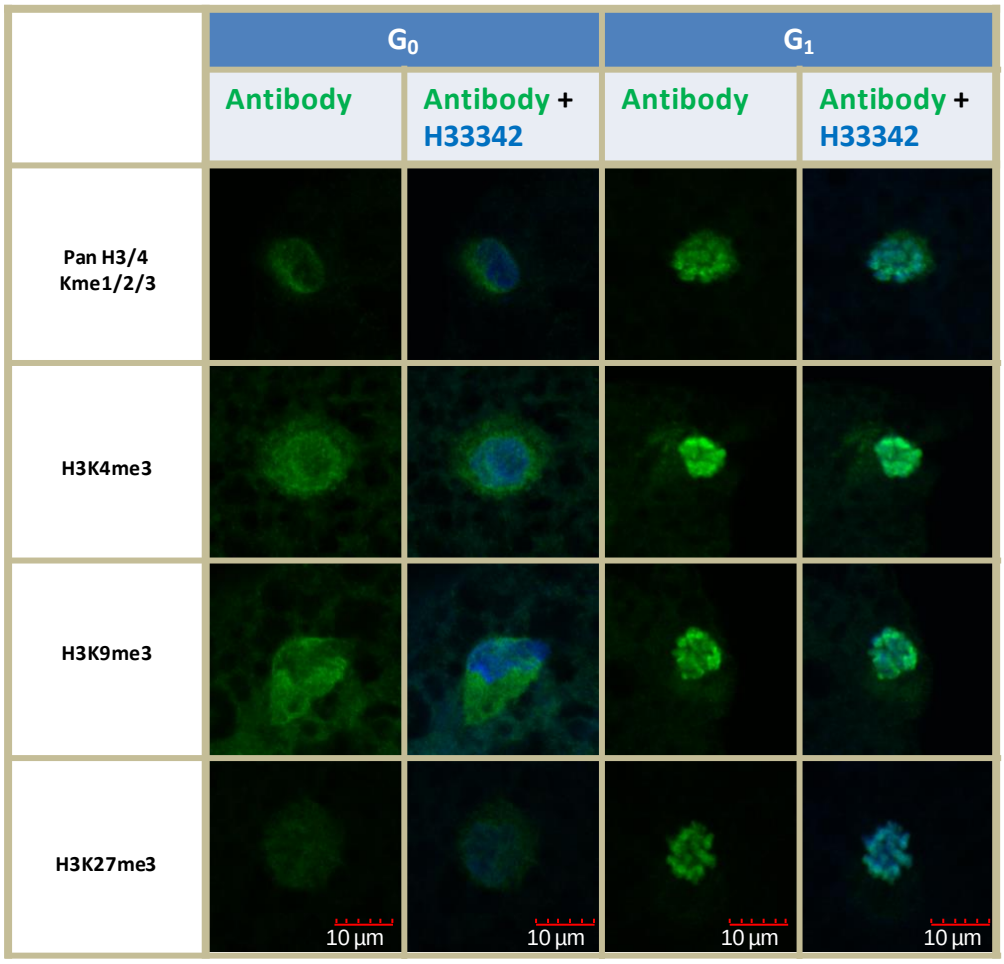

Figure 30: Characterisation of different histone methylation and degree of DNA condensation within 10 min following NT between G_0- vs G_1-derived NT embryos. G_0- and G_1-derived NT embryos showing different histone methylation levels and degree of DNA condensation.

presence correlated well with H3K27me3 in both G_0- vs G_1-derived NT embryos (Figure 31 & Figure 33). From 24 h post-activation and 72 h post-activation, SUZ12 was either absent or cytoplasmic (Figure 33). We also investigated potential changes in embryonic genome activation between G_0- vs G_1-derived NT embryos. As a proxy for onset of transcription, we tested the occurrence of Pol II on chromatin (Figure 33). We found no difference in proportions of embryos staining positive for Pol II between G_0- vs G_1-derived NT embryos (6/12 vs 6/12, 6/6 vs 6/7 and 5/6 vs 5/6 for 4 h, 24 h and 72 h post-activation, respectively).

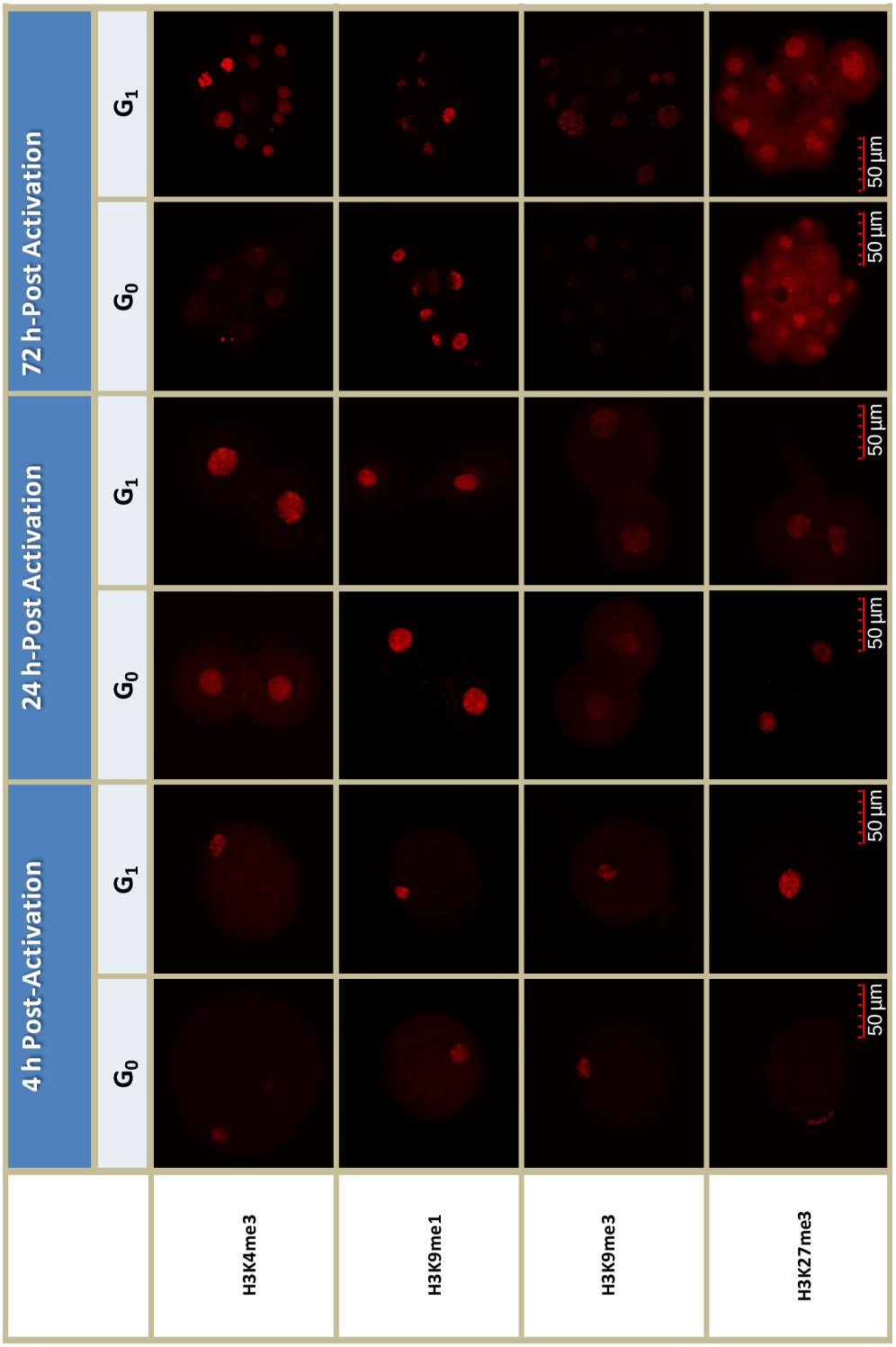

Figure 31: Histone methylation profile between G_0- and G_1-derived NT embryos from 4-72 h post-activation by CIFM.

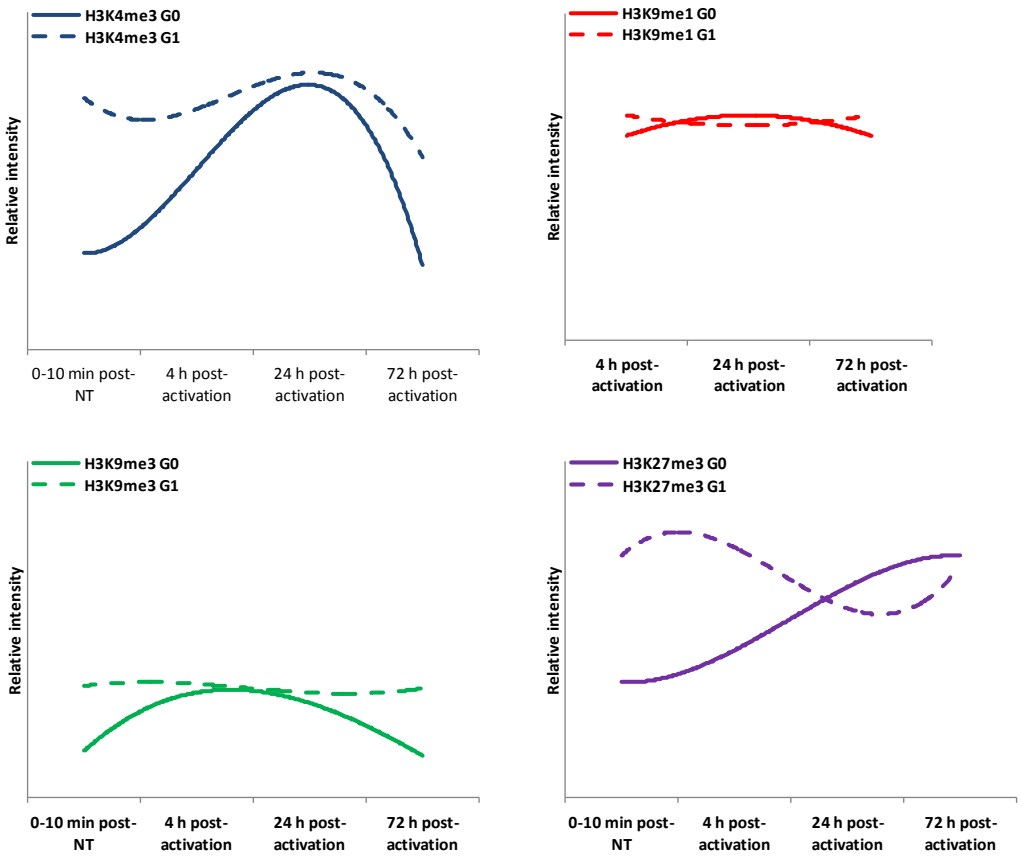

Figure 32: Developmental time-course of relative staining intensity of different histone methylations in G_0- vs G_1-derived NT embryos. Curves represent the polynomial trend line fitted for relative staining intensities observed through naked eyes. These graphs are just for qualitative illustration, as intensities were not normalised.

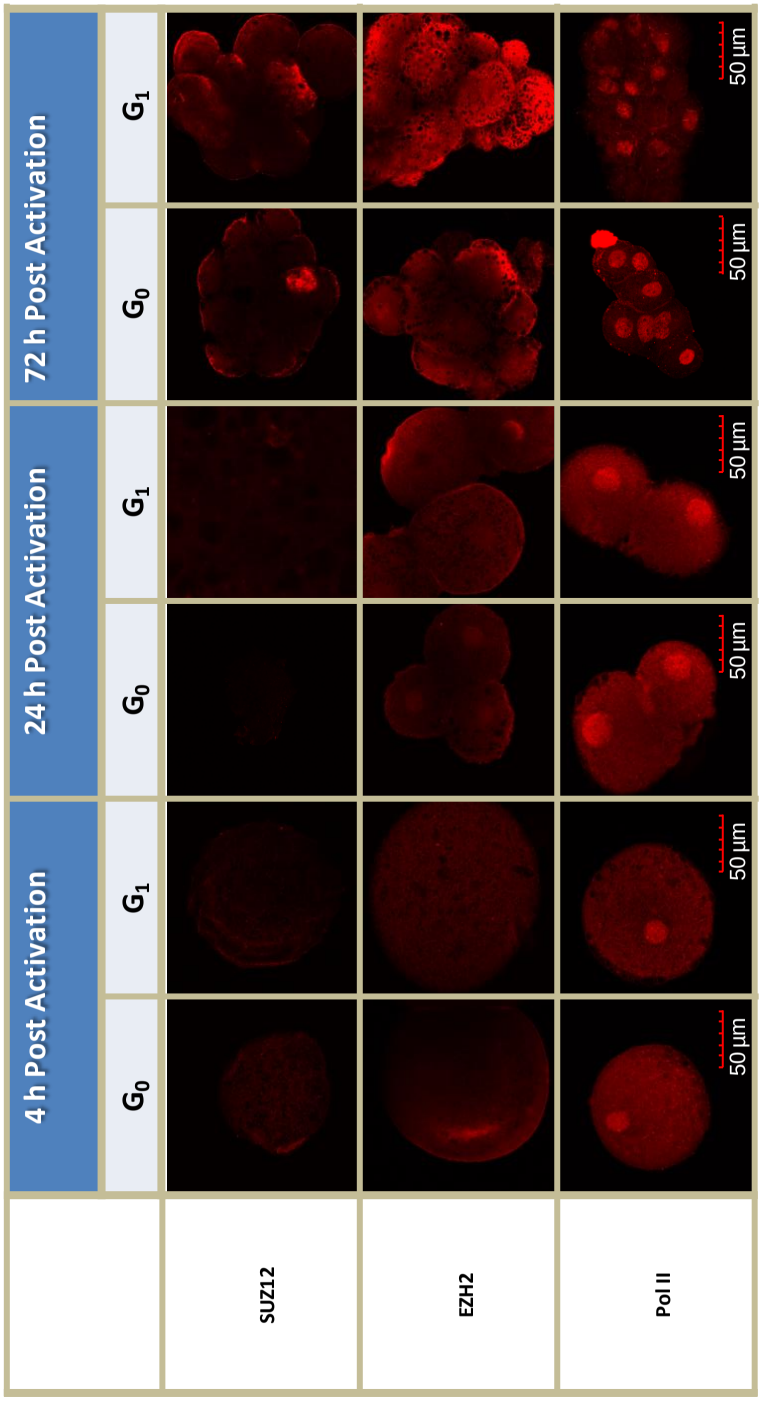

Figure 33: Comparison of chromatin-related proteins between G_0- and G_1-derived NT embryos from 4-72 h post-activation by CIFM.

5.3 G_0-derived blastocysts remained H3K9me3 hypomethylated

At the blastocyst stage, lineage separation between the ICM and TE is clearly defined. Up to 72 h post-activation, H3K -4me3, -9me3 and -27me3 were found to be varying between G_0- vs G_1-derived embryos. Therefore, we analysed the abundance of these epigenetic modifications at the blastocyst level. Only morphological grade 1-2 were selected for analysis,

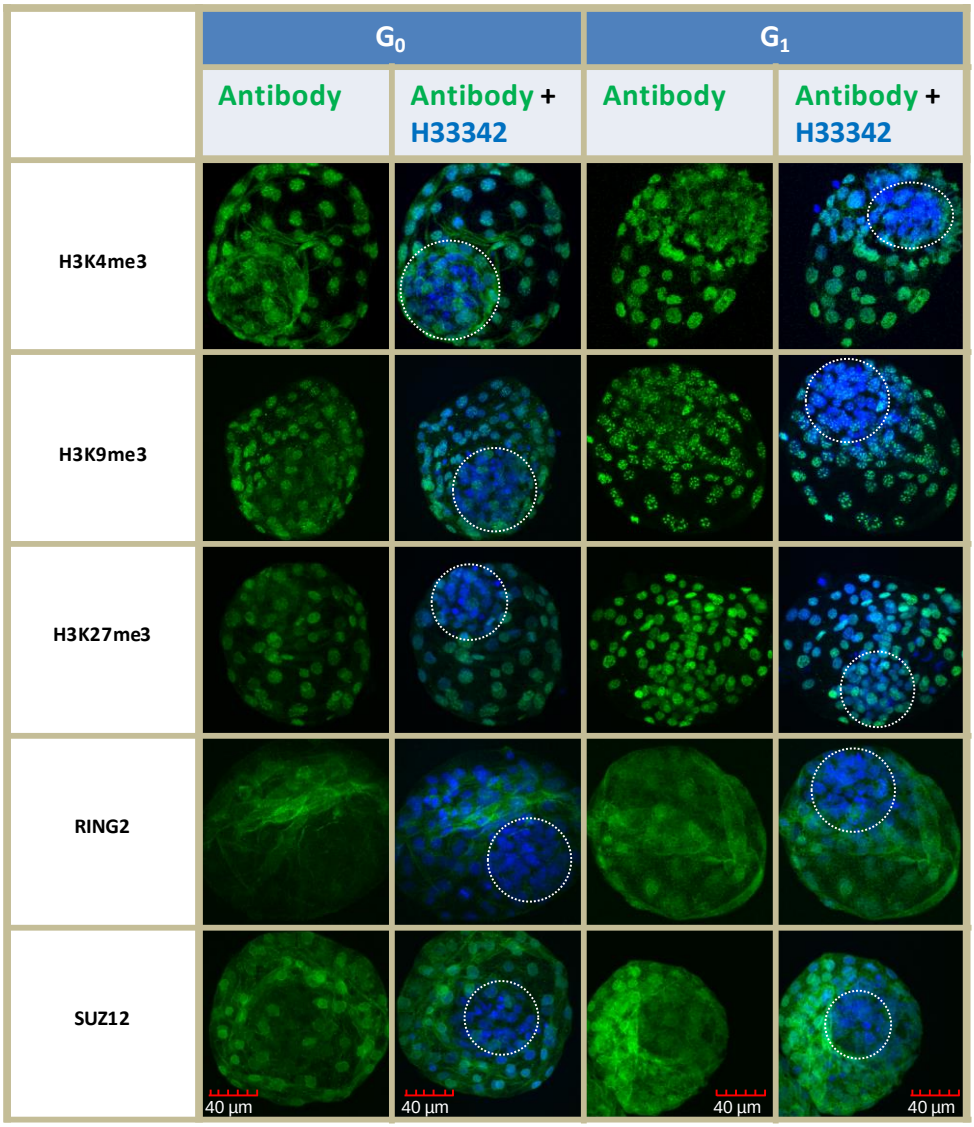

Figure 34: Qualitative comparison of histone trimethylations and PcG proteins between G_{0-} vs G_1-derived NT blastocysts by CIFM. White dotted circles in the 'antibody + H33342' column indicate ICM, which was identified by its small densely packed nuclei. The rest of the cells were considered as TE.

as these are suitable for embryo transfer into recipient cows. Except for H3K9me3 levels, G_0- vs G_1-derived NT blastocysts were epigenetically not much different from each other (Figure 34). H3K9me3 remained significantly hypomethylated (G_1/G_0=1.67) in G_0- vs G_1-derived NT blastocysts (Figure 35). H3K4me3 (G_1/G_0=1.23), which also appeared hypomethylated at 72 h post-activation, and H3K27me3 (G_1/G_0=1.32) were not significantly different at the blastocyst stage (Figure 35).

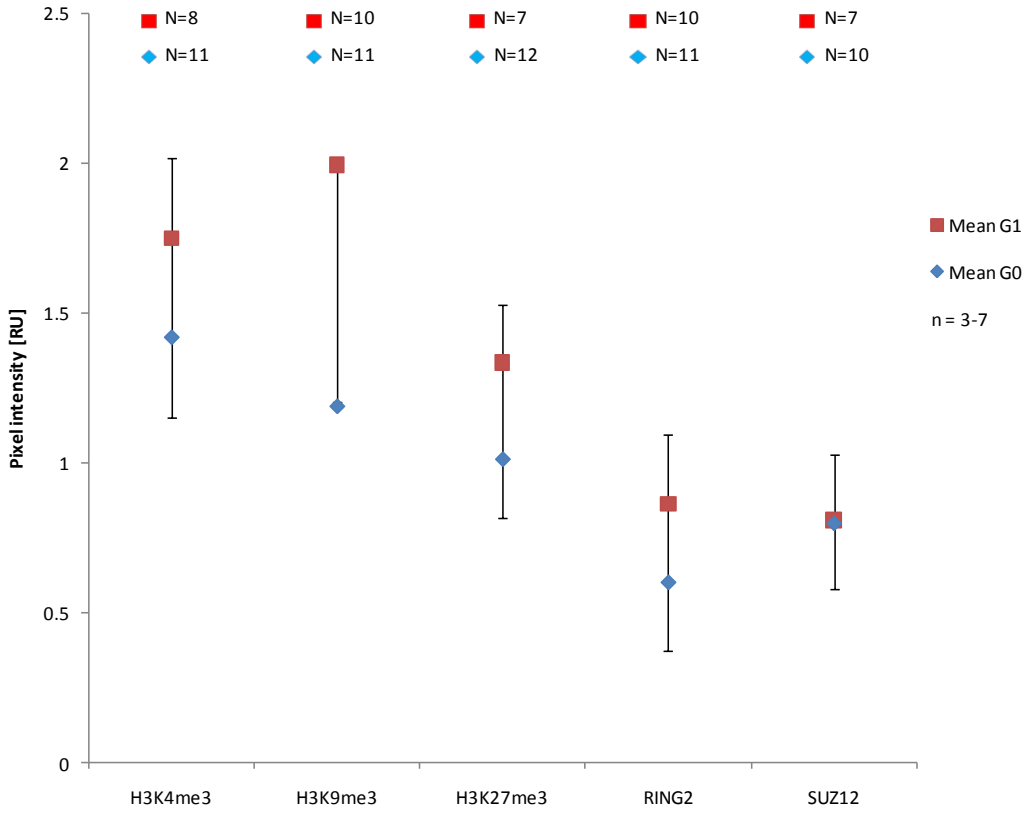

Figure 35: Abundance of histone trimethylations and PcG proteins between G_0- vs G_1-derived blastocysts by CIFM. The bars in the graph indicate LSD. If the LSD bar intersects two data points, then those two points are not significantly different (H3K4me3, H3K27me3, RING2 and SUZ12). If the LSD bar does not intersect two data points, then those data points are significantly different (H3K9me3). RU=relative units, N= number of cells analysed, n=number of replicates.

RING2 enriches at pericentric heterochromatin lacking H3K9me3 in Suv39h-deficient zygotes and also governs paternal heterochromatin-associated gene transcription (Puschendorf, Terranova *et al*. 2008). SUZ12 knockdown was shown to reduce H3K9me3 (de la Cruz, Kirmizis

et al. 2007). We therefore investigated, whether the reduction in H3K9me3 at the blastocyst stage was correlated with changes in RING2 and SUZ12 between G_0- vs G_1-derived NT blastocysts. We found no significant differences in both RING2 and SUZ12 (G_1/G_0= 1.43 and 1.01 respectively) between those two types of blastocysts (Figure 34 & Figure 35).

Comparison of ICM vs ICM and TE vs TE showed no difference for H3K -4me3 and -27me3, RING2 and SUZ12 between G_0- vs G_1-derived NT blastocysts (Figure 36). However, H3K9me3 was significantly hypomethylated both in ICM and TE (G_1/G_0= 1.7 and 1.67 respectively) of G_0-derived NT blastocysts (Figure 36).

5.4 ICMs were hypomethylated in NT blastocysts

Most mammalians exhibit epigenetic asymmetry with respect to ICM and TE in IVF blastocysts. However, in bovine blastocysts, while H3K -4me3 and -27me3 did not show any differences between ICM and TE (Ross, Ragina *et al.* 2008, Wu, Li *et al.* 2011), H3K9me3 was hypermethylated in ICM (Santos, Zakhartchenko *et al*. 2003). Therefore, we compared ICM vs TE tissues of G_0- vs G_1-derived NT blastocysts. We found that for H3K -4me3, -9me3 and -27me3, all ICMs were hypomethylated (Figure 36). Similarly, SUZ12 was significantly down-regulated in the ICM. However, there were no significant differences for RING2 between ICM vs TE, even though it was twofold increased in the TE (Figure 36).

5.5 Extensive histone re-methylation in the TE of NT blastocysts.

Often SCNT blastocysts exhibit the epigenetic features of their somatic donors. To see if there was any such correlation with G_0 vs G_1 donors, we directly compared donor intensities with ICM and TE intensities. Donor vs TE comparison showed extensive reprogramming in the TE of G_0- and G_1-derived NT blastocysts. Both blastocysts significantly up-regulated H3 -

K4me3 and -K9me3, but only G_0- blastocysts significantly up-regulated H3K27me3 in the TE. While G_1- blastocysts also up-regulated their TE H3K27me3 (~2 fold), this was not significant. Consistent with H3K27me3 regulation, SUZ12 was also significantly up-regulated in the TE of G_0-blastocysts. The twofold up-regulation of RING2 in the TE was not significant in G_0- and G_1-derived NT blastocysts. Donor vs ICM comparison showed that the difference between them was not as dramatic as the epigenetic differences between donor and TE cells. Both G_0- and G_1-derived NT blastocysts significantly up-regulated their H3K9me3 content in the ICM, while still maintaining the initial differences between them. The lack of significant difference between H3K27me3 of ICM was due to down-regulation of this modification by G_1- blastocysts. Consistent with H3K27me3 down-regulation, SUZ12 was also significantly down-regulated in G_1- blastocysts ICM.

5.6 G_0 donors resulted in better blastocyst development

G_0 donors fused significantly better with the MII arrested oocytes than their G_1 counterparts (Figure 37). In many cloning studies the rate of blastocyst development is considered a measure for gauging the developmental potential. Following fusion, G_0 donors increased the rate of development into blastocyst over G_1 donors (G_1/G_0=0.8, Figure 37).

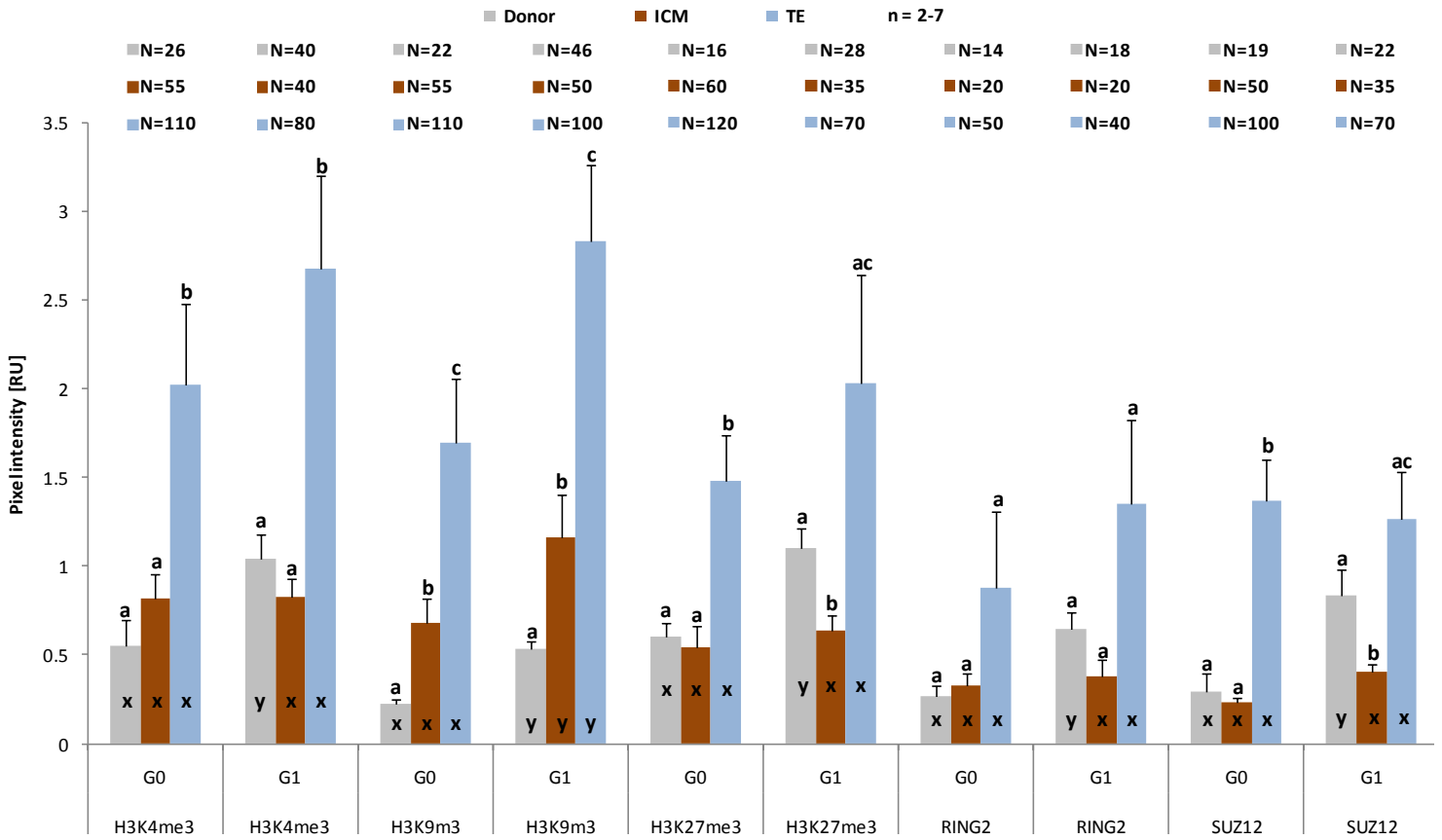

Figure 36: Comparison of abundance of histone trimethylations and PcG proteins between G_0 and G_1 donors vs G_0- and G_1-derived ICM vs TE by CIFM. Letters a, b and c: within each modification and cell cycle stage, bars with different letters differ significantly. Letters x and y: within each modification and across cell cycle stage, bars with different letters differ significantly. RU=relative units, N= number of cells analysed, n=number of replicates.

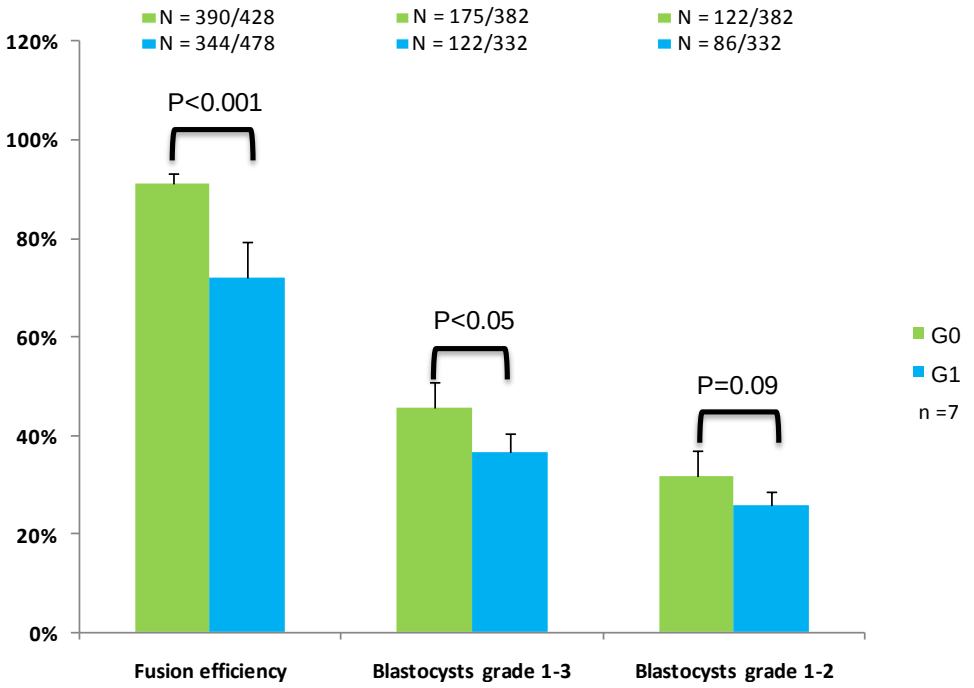

Figure 37: Comparison of fusion efficiency and blastocyst development into different grades from G_0 vs G_1 NT experiments.

5.7 Discussion

5.7.1 Epigenetic reprogramming after NT

Here we provide the first evidence for *de novo* H3K trimethylations (H3K -4me3, -9me3 and -K27me3) during the first cell cycle in bovine cloned embryos. So for it has been shown that H3K9 methylation in cloned embryos could start as early as second cell cycle (Santos & Dean 2004). Thereafter, H3K9 methylation was shown to undergo passive demethylations up to the four-eight cell stages in bovine cloned embryos. Prior to NT, G_0 donors were histone hypomethylated. This histone hypomethylation was still maintained immediately after NT. However, H3K trimethylation intensities were already up-regulated during the first S-phase, i.e. at 4 h post-activation. This increase in intensity can happen either by replacing the histones already bearing H3 methylation modifications or by *de novo* methylation. At present, it is unknown if maternal histones are incorporated into NT chromatin. However, it is well documented that maternal histones lack H3K -4me3, -9me3 and -K27me3 and are only enriched for histone acetylations (Morgan, Santos *et al*. 2005). It was also shown that non-nucleosomal histones bear only acetylation and lack any histone methylations other than H3K9me1 (Loyola, Bonaldi *et al*. 2006). Therefore, maternal histone incorporation per se would not increase H3K trimethylations. This suggests that there was *de novo* methylation concurring with the incorporation of maternal histones during S-phase, as early as 4 h post-activation. Presence of maternal chromatin can efficiently demethylate the donor genome (Kang, Koo *et al.* 2001b). In IVF embryos, it has been shown that blocking either protein synthesis or gene expression results in *de novo* H3K9 and DNA methylation at the pronuclear stage (Liu, Kim *et al*. 2004). This shows that maternal chromatin actively maintains the hypomethylated state of paternal chromatin. Consequently, removal of maternal chromatin during enucleation could favour *de novo* H3K methylation in cloned embryos.

These studies support the observed *de novo* H3K trimethylation seen during the first cell cycle in G_0-derived embryos.

Comparison of histone methylation levels in G_0- and G_1-derived embryos until 72 h post-activation showed that most histone methylation levels changed in both directions, being either up- or down-regulated. This indicates dynamic *de novo* and active or passive demethylations that continuously turn over these modifications. Both embryos gained or at least maintained H3K -9me1 and -27me3 from 4-72 h post-activation. Between G_0- vs G_1-derived blastocysts, H3K9me3 was significantly different both in the ICM and TE. In bovine IVF embryos, H3K -4me3, -9me and -27me3 declined until up to the 8-cell stage and then increased from morula to blastocyst stage (Santos, Zakhartchenko *et al.* 2003, Ross, Ragina *et al.* 2008, Wu, Li *et al.* 2011). This indicates that normal epigenetic reprogramming involves initial demethylation followed by *de novo* H3K methylation. A similar pattern was observed for two of the epigenetic modifications (H3K -4me3 and -9me3) in G_0-derived embryos, while none of the epigenetic modifications followed this pattern in G_1-derived embryos. This suggests the reprogramming of H3K -4me3 and -9me3 is more normal in early G_0-derived embryos.

Compared to IVF embryos, cloned bovine blastocysts are often reported to have either a hypermethylated ICM and TE or similar methylation levels in TE and ICM. None of the H3 trimethylations investigated showed this trend and hence our results are not consistent with the earlier reports (Santos, Zakhartchenko *et al.* 2003, Wu, Li *et al.* 2011). One possible reason for this discrepancy could be different antigen accessibility based on different IF protocols and antibodies. However, we have validated the ICM accessibility using the nuclear specific SOX2 staining. There are also differences in the cloning method and donor cell type used. It is believed that histone and DNA hypermethylation seen in the ICM is generally passed on to somatic lineages. However, this may not be universally true,

as cloned mouse blastocysts did not have any detectable H3K27me3 in their ICM and it is unlikely that the cloned mouse somatic lineages would not have any H3K27me3 (Zhang, Wang *et al*. 2009). This suggests that the ICM still reprograms later during development. Moreover, ICM histone hypomethylation is relative, and does not necessarily mean that the ICM levels were abnormal. It could also be due to abnormally high TE levels. Our comparison with donor intensity levels clearly showed that the observed ICM histone hypomethylation was due to extensive reprogramming in the TE of both G_0- and G_1-derived blastocysts. G_1-derived blastocysts appeared to require more reprogramming than G_0-derived blastocysts, as they also reprogrammed their ICM to the level of the G_0-derived blastocysts. Comparatively less reprogramming by G_0-derived embryos correlated with better rates of blastocyst development.

Chapter Six: General discussion and future prospects

Nuclear reprogramming represents a considerable challenge for basic science. Understanding the epigenetic basis for better nuclear reprogramming of differentiated somatic cells into totipotency has several applications, ranging from cloning to generation of induced pluripotent stem cells. Cloning inefficiency is mainly associated with aberrant epigenetic reprogramming of the donor nuclei, leading to failure during early development. Reprogramming efficiency is influenced by species and donor cell type. Levels of donor epigenetic modification, such as histone methylation and acetylation, may be a helpful guide to predict the cloning efficiency in mouse (Rybouchkin, Kato *et al.* 2006, Bui, Wakayama *et al.* 2008). Since the birth of Dolly, the first mammalian SCNT clone, it has been postulated that inducing G_0 in donors would be beneficial for cloning. However, evidence for this hypothesis has been lacking. At Agresearch, we have shown that serum-starved G_0 donors more than doubled cloning efficiency into adulthood compared to mitotically-selected G_1 control cells. If and how serum starvation would affect the epigenetic status of the donor cells and blastocysts derived from them is unknown. Here we investigated the epigenetic basis for improved cloning efficiency in G_0 cells to better understand the epigenetic features underlying increased reprogrammability.

By the combined use of CIFM and specific antibodies against DNAme, histone methylation and acetylation, we provide the evidence that serum starvation of adult ear skin fibroblasts results in hypomethylated DNA and histones, concurrent with the down-regulation of chromatin-related proteins and dynamic changes in histone acetylations. We also provide evidence that most of these donor cell differences have disappeared by

the blastocyst stage. However, H3K9me3 remains hypomethylated both in the ICM and TE. Therefore, H3K9me3 hypomethylation provides an epigenetic correlate for increased donor cell reprogrammability and cloning efficiency. In addition, we also observed that serum starvation results in increased cell adhesion, cell and nuclear volume and relaxed chromatin.

Histone and DNA hypomethylation

Except for H3K9me1, we found that G_0 donors were globally DNA and histone hypomethylated. This overall histone hypomethylation, irrespective of whether the lysine modification is involved in transcriptional repression or activation, was perplexing. Since G_0 cells reduce their transcriptional activity 3-5 times (Choder 1991), one would expect the repressive modifications, such as H3K27me3, H3K9me2 and -me3 and DNAme to increase. To explain the concerted demethylation of a range of modifications with diverse functions, we propose a cell cycle-dependent scenario. During the cell cycle, histones are incorporated into the newly synthesised DNA during S-phase. These new histones are largely unmethylated (Loyola, Bonaldi *et al*. 2006). We postulate that this transient state is permanently fixed in serum-starved cells entering quiescence. Cells enter G_0 from the G_1 phase, when mitogen is withdrawn before a specific time point. Specifically, it was shown that serum-starved cells in G_1ps (pre-S-phase; more than 3-4 h after mitosis) will not stop entering S-phase. Only cells serum-starved in G_1pm (post-mitotic; less than 3-4 h after mitosis) will enter G_0 (Zetterberg & Larsson 1985). The G_1pm period is constant across cell lines (Foster, Yellen *et al*. 2010). In steady-state, the majority of proliferating cultured cells will be in post G_1pm/S-phase, since this phase occupies the larger proportion of the total cell cycle length. Therefore, these cells will continue to divide when starvation medium is added to the culture. We propose that serum-starved S-phase cells acquire hemi methylated DNA and unmethylated histones, but do not

further methylate them in preparation for G_0. This would result in halving of these modifications in daughter cells following cytokinesis. The observed G_1/G_0 ratios (1.6-2.4) for DNA and histone modifications, except H3K9me1, would support this hypothesis. In non-starved control G_1 cells abundance of all H3K9 methylations peak at metaphase (McManus, Biron *et al*. 2006), suggesting that these modifications are largely acquired post S-phase. *De novo* DNA methylation is acquired during S-phase using the hemi-methylated strand as a template (Bird 2002). DNAme also reduced during S-phase while the newly synthesised DNA strand is initially unmethylated.

The above hypothesis accounts for most of the histone modifications but does not explain H3K9me1 and histone acetylations. Monomethylation is acquired at or immediately after incorporation into the nucleosome (Scharf, Barth *et al*. 2009) and is a prerequisite for acquiring di- and tri-methylations (Schotta, Lachner *et al.* 2004b, Scharf, Meier *et al.* 2009). The lack of H3K9me1 difference can be explained by the ability of cells to monomethylate at the time of incorporation. H3K9me1 primes H3 for subsequent acquisition of di- and tri-methylation, which is a slow process and some modifications might take one whole cell cycle, while acetylations are rapidly acquired (Scharf, Barth *et al*. 2009). The non-uniform histone acetylations could be attributed to their rapid incorporation during S-phase and their dynamic regulation (Scharf, Barth *et al*. 2009).

Relaxed chromatin architecture

In quiescent B lymphocytes, chromatin was found to be DNase-resistant, indicating a high degree of condensation, as well as histone hypomethylated (Baxter, Sauer *et al*. 2004). By contrast, we found that artificially induced G_0 cells had a relaxed chromatin configuration. This difference might be due to the difference in the way they reached G_0. After being produced in the thymus, terminally differentiated B lymphocytes

migrate to secondary lymphoid tissues and, in the absence of any strong stimulation of its B-cell antigen receptor by antigen, they enter quiescence. This quiescence is thus due to differentiation. By contrast, we artificially induced G_0 by serum starvation. Here cells enter G_0 due to lack of growth and surviving factors.

Reduction in H3K9 methylation was shown to result in release of heterochromatin from nuclear periphery and de-repression (Towbin, Gonzalez-Aguilera *et al*. 2012). HP1α mediated heterochromatinization and repression involves H3K9me3, a hallmark of pericentric heterochromatin. RING2 is known to condense chromatin (Eskeland, Leeb *et al*. 2010). G_0 cells down-regulated H3K9me2 and -me3, RING2, as well as DNAme, another hallmark of pericentric heterochromatin. Down-regulation of these could aid in formation of relaxed chromatin. Furthermore, in addition to its role in reducing transcription, down-regulation of H2A.Z in G_0 cells could also play a role in relaxing chromatin. At constitutive heterochromatic regions, lack of H2A.Z disrupts the interaction of HP1α with the heterochromatic foci and pericentric heterochromatin, even in the presence of H3K9me3 (Rangasamy, Greaves *et al*. 2004). Therefore, down-regulation of H2A.Z and H3K9me3 could affect the HP1α-mediated heterochromatinization in G_0 cells. In addition to its role in constitutive heterochromatic regions, H2A.Z may also play a role in the formation of facultative heterochromatin. H2A.Z is preferred by RING2 (Creyghton, Markoulaki *et al*. 2008). Therefore, it is possible that down-regulation of H2A.Z contributed to RING2-mediated facultative heterochromatinization in G_0. To sum up, relaxed chromatin configuration in serum-starved G_0 cells correlated well with down-regulation of H3K9me3, DNAme, RING2 and H2A.Z.

Reduced transcription

In G_0 cells, down-regulation of repressive chromatin modification is seemingly at odds with a transcriptionally less active environment. However, even relatively low levels of these modifications may be enough to maintain active and silent chromatin domains in G_0 (Baxter, Sauer *et al*. 2004). Others have shown that temporary silencing of genes, such as in G_0, did not involve H3K9me3-mediated pericentric heterochromatin compartmentalisation (Guasconi, Pritchard *et al*. 2010). This was also found to be true in quiescent primary B lymphocytes, where additional repressive epigenetic modifications, such as H3K9me2 and H3K27me3, were also reduced (Brown, Baxter *et al.* 1999, Baxter, Sauer *et al.* 2004). This suggests that cells may have less permanent mechanisms, other than histone and DNA methylation, to keep their genes repressed. One such mechanism could be histone acetylation. H4 acetylation follows a sequential pattern in mammalian somatic and ES cells; H4K16Ac is followed by H4K8 and -K12Ac and ultimately H4K5Ac. Therefore, hyper-H4K5Ac represents hyper-H4, which correlates with transcriptional activation (Ma & Schultz 2008). For H3, H3K9Ac dynamically targets H3K4me3, which correlates with gene expression (Hazzalin & Mahadevan 2005) and this process is conserved during evolution (Crump, Hazzalin *et al*. 2011). Therefore, low levels of H4K5Ac and H3K9Ac could achieve general transcriptional repression in G_0 donors.

Another mechanism could be the regulation of proteins related to transcription. In support of this, we found that G_0 cells down-regulated RNA Pol II. Earlier it was found that serum starvation reduced POLR2I, a gene that encodes one of the three subunits of Pol II, at least twofold (Coller, Sang *et al*. 2006). This could explain why G_0 cells had reduced transcription despite having open and transcriptionally permissive chromatin. Furthermore, G_0 cells up-regulated transcriptional repressors such as MXI1, ATBF1 and BCL6 (Liu, Adler *et al*. 2007). Some of these

act through modifying chromatin. For example, BCL6 repression involves recruitment of class I and class II HDACs (Lemercier, Brocard *et al*. 2002). Histone acetylation is continuously turned over by HATs and HDACs. Mitochondrial acetyl CoA, a major supplier of acetyl groups for histone acetylation (Madiraju, Pande *et al*. 2009), might be limited under serum-starved condition due to its phosphorylation by AMP-activated protein kinase (AMPK) (Park, Gammon *et al*. 2002). Lack of acetyl groups, could lead to only deacetylation by HDACs. Therefore, it is plausible that in the absence of DNA and histone repressive methylation, cells could still act by down-regulating their histone acetylations and transcriptional activators, as well as up-regulating the transcriptional repressors.

Cell adhesion

The increased adhesion of G_0 cells is supported by earlier transcription profiling studies (Coller, Sang *et al.* 2006, Liu, Adler *et al.* 2007), where serum starvation was found to up-regulate the expression of adhesion related molecules such as laminin-C1 (*LAMC1*), tenascin C (*TNC*), and collagen-3A1 (*COL3A1*). LAMC1 is a laminin, which belongs to a family of extracellular matrix (ECM) glycoproteins. Laminins are the major non-collagenous component of basement membranes and have been implicated in a wide variety of biological processes, including cell adhesion. TNC is a founding member of the tenascin family. It is a large ECM oligomeric glycoprotein localised to some adult and many embryonic tissues (Erickson & Bourdon 1989, Erickson 1993). The protein is prominent during growth and development of embryonic tissues. Even though its role in binding activity is controversial, it was shown that plastic coated with TNC in a particular way was bound by mammalian cells (Erickson 1993). The binding of fibroblasts is mediated by their cell surface proteoglycans. Type III collagen is a fibrillar forming collagen expressed from early embryos to throughout embryogenesis. In adults, it is a major component of the ECM. It is essential for collagen I fibrillogenesis and

homozygous mutants dye due to rupture of major blood vessels (Liu, Wu *et al*. 1997). COL3A is bound by variety of collagen binding receptors, such as integrins, glycoproteins, etc. Up-regulation of these three proteins (LAMC1, TNC, and COL3A1) may aid cellular adhesion and anchorage of G_0 cells.

Conclusion

Treatment with class I and II HDACis, such as TSA and scriptaid, was shown to increase cloning efficiency in mouse. TSA treatment results in histone hyperacetylation, nuclear decondensation (Bui, Wakayama *et al*. 2010), and increased expression of c-*Myc*, *Nanog* and *Sox2* (Monteiro, Oliveira *et al*. 2010). Overall, TSA treatment appears to induce relaxed chromatin and increased expression of pluripotency-associated factors in the NT embryo. Serum-starved G_0 cells had relaxed chromatin. They also down-regulated pericentric heterochromatin marks, DNAme and H3K9me3, which could release many differentiation-related genes from heterochromatin-association and remove epigenetic constraints on pluripotency factors, such as OCT4 and NANOG. Therefore, inducing quiescence could serve similar functions as HDACi-treatment, namely relaxing the chromatin and releasing the epigenetic constraints.

Globally hypomethylated and partially hypoacetylated histone B lymphocytes resulted in better blastocyst development (Baxter, Sauer *et al*. 2004). However, it could be specifically hypo-H3K9me3, not global hypomethylation per se that is important for increasing cloning efficiency. In pig, H3K9me3 shows resistance to reprogramming by NT, even though phosphorylation and acetylation could be reprogrammed (Bui, Van Thuan *et al*. 2006). Inhibition of KMT1A, an H3K9me3 KMT, improved iPSC derivation efficiency (Onder, Kara *et al*. 2012). In a recent study at Agresearch, KDM4B-inducible ES cells were used for NT cloning (Anthony J. *et al*. submitted). It was shown that KDM4B induction resulted in a 63%

loss of H3K9me3. When these KDMB induced ES cells were used for mouse cloning, they significantly improved blastocyst development. Donor hypo- H3K9me3 and H3K9Ac correlated with increased expression of the pluripotency factor OCT4 in cloned mouse blastocyst (Bui, Wakayama *et al*. 2008). Furthermore, the hypo-H3K9me3 levels persisted up to blastocyst stage, which correlated with increased cloning efficiency to term. These results support our finding in bovine, where hypo-H3K9me3 in G_0 donors resulted in hypomethylated H3K9me3 at the blastocyst stage, increasing blastocyst development and cloning efficiency.

Future prospects

Use of G_0 donors more than doubled cloning efficiency to about 10%. However, even this improved efficiency still compares unfavourably to other assisted reproductive technologies, such as IVF, which operates over 30% efficiency. Therefore, there is still room for further improvement. One way to improve cloning efficiency could be by targeting other epigenetic modifications that did not reprogram well after NT. For instance, we have seen that H3K27me3 did not show any passive demethylation in both G_0- and G_1-derived embryos, whereas IVF embryos did (Ross, Ragina *et al*. 2008). Therefore, inhibiting H3K27me3 remethylation or selectively reducing H3K27me3 by ectopic overexpression of KDM6B could be a way to further improve cloning efficiency. Inhibiting H3K27me3 remethylation could also be combined with serum starving the donors. It is often found that female inactive X-chromosome (X_i) is hard to reprogram and presents an obstacle during SCNT (Bao, Miyoshi *et al*. 2005). X_i is marked by H3K9me2, H3K27me3, DNAme and RING2-mediated H2AK119 ubiquitination. G_0 donors down-regulated H3K9me2, H3K27me3, DNAme and RING2. Therefore, it would be interesting to see if serum starvation affects X-chromosome inactivation and if this would further improve cloning efficiency compared to male G_0 donors.

We have shown that inducing G_0 by serum starvation results in relaxed chromatin and global DNA and histone hypomethylation. This provides a structural correlate for increased cloning efficiency. Therefore, it is reasonable to postulate that G_0 presents a chromatin that is more amenable to be reprogrammed into totipotency. It would be worthwhile to investigate whether G_0 cells could improve reprogramming into pluripotency. This could result in improved derivation of iPSCs. Complimentary to SCNT, iPSC derivation is a functional assay for cell reprogrammability. Generation of patient specific iPSCs has implications and potential to medical science. Even though these could be possibly generated from any somatic cells, the efficiency is very low. As with NT, this could also be due to the resistance by differentiated chromatin to get reprogrammed. During iPSC generation process by Yamanaka factors (*c-Myc, Oct4, Sox2 and Klf4*), c-MYC binds early in the reprogramming process. The rest, which co-occupy a large number of promoters, bind only later during reprogramming (Skene & Henikoff 2012). This delayed binding, which appears to be due to repressive chromatin status of somatic nuclei at their binding sites, is thought to be a major roadblock during iPSC reprogramming. Therefore, G_0 cells, which have down-regulated their repressive modifications could aid better iPSC reprogramming. Studies have used HDAC and DNMT inhibitors to enhance the efficiency up to 100 fold (Huangfu, Maehr *et al*. 2008). Likewise, other studies have used histone methylase inhibition for improving generation of iPSCs efficiency (Onder, Kara *et al*. 2012). Therefore, it would be interesting to see if use of G_0 cells alone or in combination with pharmacological treatments, such as exposure to HDACi valproic acid (VPA), would improve iPSC derivation.

The improved reprogramming ability of G_0 cells could be due to releasing of differentiation-associated genes from heterochromatin. Therefore, it would be interesting to examine if serum starvation induces repositioning of any particular genes, such as genes related to pluripotency, from

facultative or pericentric heterochromatin. Furthermore, examination by chromatin immunoprecipitation (ChIP)-on-Chip could reveal a specific epigenetic signature at individual genes during serum starvation that could aid the cell to become totipotent. During serum starvation most of the genes are repressed. By looking at the individual gene level, one could examine how these marks behave during serum-deprived scenario, where cells try to be as economical as possible. This would illustrate how important are these modifications for gene regulation or are they just an extra layer for chromatin compartmentalisation to govern the transcription.

It would also be interesting to investigate other aspects of the G_0 donors that may have contributed to their better reprogrammability. For instance, H3.3 accumulation at rDNA, major satellite repeats and regulatory regions of the pluripotency gene *Oct4* was shown to be a necessary step during reprogramming by the oocyte (Jullien, Astrand *et al*. 2012). Since H3.3 is thought to be incorporated during serum-starved G_0 phase, it would be interesting to see if this happens at rDNA, major satellite repeats and regulatory regions of the pluripotency gene *OCT4*, which could further explain the amenability of serum-starved cells to be better reprogrammed. One could also test the microRNA profile of G_0 cells. It is known that pluripotent cells, such as ES cells, express high levels of ESC-specific cell cycle regulating (ESCC) miRNAs such as miR-290 cluster, while somatic cells have high levels of Let-7 (Melton, Judson *et al*. 2010). De-differentiation of somatic cells during iPSC generation was supported by either inhibiting Let-7 or introduction of ESCC miRNAs (Judson, Babiarz *et al.* 2009, Melton, Judson *et al.* 2010). Therefore, it would be interesting to see if there was any change in profiles of these microRNAs in G_0 cells.

There is no consensus on how histone epigenetic modifications are faithfully perpetuated through the cell cycle. Recently, it was shown in rapidly dividing *Drosophila* embryo cells that during replication cells either remove the old modifications or replace modified H3 during replication.

These modifications were later re-established by HMTases that remain associated with the replicating DNA (Petruk, Sedkov *et al*. 2012). Specifically, this was shown for H3K27me3 and H3K4me3. It is possible that the growing embryo needs to reset its epigenetic status over many chromatin domains. Losing epigenetic modifications entirely and re-establishing them later might have evolved as a beneficial strategy in this biological context. It is to be noted that these two modifications form bivalent domains in early development and need to be resolved as cells differentiate. It is not known if the mechanism suggested by Petruk *et al.* also applies to differentiated somatic cells and other species. An alternative model predicts that during DNA replication, there would be an equal but random distribution of parental histones, bearing epigenetic marks, onto the daughter strands. The parental modifications would then serve as a template for re-establishing the modified domain (Zhu & Reinberg 2011). Our results favour this latter, more conventional model. In accordance with this model, we observed an approximate two fold reduction in histone methylation levels. We did not observe cells that lacked H3K4me3 or H3K27me in unsynchronised cultures, which contained mostly cells in S-phase. This is in contrast with the observation by Petruk *et al*. that S-phase cells largely lacked these modifications. Therefore, it would be interesting to follow-up on exactly when serum-starved cells loose their epigenetic modifications, particularly DNA and histone methylations. The model by Zhu *et al* and our predicted hypothesis that cells undergoing DNA replication in serum starved medium would acquire hemi methylated DNA and unmethylated histones, but do not further methylate them in preparation for G_0 could be tested by EdU pulse labelling experiments. For example, one could first incubate mitotic doublets with EdU in serum-containing medium for 3 h, followed by serum starvation in EdU-containing medium for variable periods of time. This would allow cells to replicate and divide once. The initial 3 h incubation in serum is necessary to commit the cells to enter the mitogen-independent

pre-DNA synthesis phase. The control cells would continue to grow in serum-containing medium with EdU. Then cells are stained for the simultaneous abundance of pan H3/H4 methylation and EdU. Cells that continued S-phase would incorporate increasing amount of EdU and can be distinguished from cell that do not enter S-phase. If the EdU positive cells halved their methylation levels under serum starvation compared to non-starved cells, it would suggest serum starvation instructed them to stop modifying their histone methylation. Since EdU incorporation is directly proportional to the amount of synthesised DNA and time in S-phase, this would further define the time points of re-methylation during S-phase.

Thus the findings that serum-starved G_0 cells have a specific chromatin signature that correlates with improved cloning efficiency could be potentially used beyond its immediate applications of improving cloning efficiency in cattle. The findings could be extended to assist the direct reprogramming by pluripotent factors during iPSCs generation with potential benefits for stem cell-based therapy and therapeutic cloning. For basic research, they could help to elucidate the mechanisms by which the cells faithfully perpetuate their epigenetic signature.

Appendices

Appendix I: List of chemicals, reagents, enzymes, kits, solutions and antibodies.

Table 8: General chemicals and reagents used

Chemicals/Reagents	Manufacturer
2-mercaptoethanol	Sigma
Acetone	JT Baker
Acrylamide	Bio Rad
Agarose	Ray lab
Ammonium chloride (NH_4Cl)	Sigma
Ammonium persulfate	Bio Rad
Bovine Serum albumin (BSA) (Fatty acid-free)	Sigma
Bromophenol blue	Bio Rad
Collagen type I (from rat tail)	Sigma
Comassie brilliant blue R-250 crystals	Bio Rad
DAKO fluorescent medium	DAKO
DAPI	Sigma
Dimethyl sulfoxide (DMSO)	Sigma
Disodium- Ethylenediaminetetraacetic Acid (EDTA)	Sigma
Dithiothreitol (DTT)	Invitrogen (USA)
Ethanol	Fisher chemicals
Gelatin	Sigma
Glacial acetic acid	JT Baker
Glycerol	JT baker

Glycine	JT Baker
H33342	Sigma
Hydrochloric acid (HCl)	J T Baker (USA)
KCl	Sigma
KH_2PO_4	Sigma
Methanol (Analytic grade)	Fisher chemicals
$MgSO_4.7H_2O$	Sigma
N, N, N', N'- Tetraethylethylenediamine (TEMED)	Sigma (USA)
N-2-ethane-sulphonic acid (HEPES)	Invitrogen (USA)
NaCl	JT baker
NaOH 1 M	JT Baker
Paraformaldehyde (PFA)	Sigma
Phenol Red	Sigma
Phosphate buffered saline (PBS) tablets	MP Biomedicals
Polyvinyl Alcohol (PVA)	Sigma
Ponceau Stain	Sigma
SeeBlue plus2 prestained protein ladder	Invitrogen
Sodium bicarbonate ($NaHCO_3$)	Sigma (USA)
Sodium chloride (NaCl)	Sigma (USA)
Sodium dodecyl sulfate (SDS)	Bio Rad,
Sodium hydroxide (NaOH)	BDH (UK)
Sucrose	Sigma
Sulphuric acid	JT Baker
Tris (ultra-pure)	JT baker
Triton X-100	Sigma
Tween 20	Bio Rad

Table 9: Enzymes

Enzyme	Manufacturer
Hyaluronidase	Sigma
Pepsin	BM (Germany)
Pronase	Sigma
Proteinase K	Invitrogen
RNase	Roche

Table 10: Kits

Kits	Manufacturer
BCA protein assay kit	Thermo Fisher Scientific Inc (USA)
Click-iT® EdU imaging kits	Invitrogen
EpiQuik™ Global Di-methyl Histone H3-K9 Quantification kit (fluorometric)	Epigentek
EpiQuik™ Global Mono-methyl Histone H3-K9 Quantification kit (fluorometric)	Epigentek
EpiQuik™ Global Tri-methyl Histone H3-K27 Quantification kit (fluorometric)	Epigentek
EpiQuik™ Global Tri-methyl Histone H3-K4 Quantification kit (fluorometric)	Epigentek
EpiQuik™ Global Tri-methyl Histone H3-K9 Quantification kit (fluorometric)	Epigentek
EpiQuik™ total histone extraction kit	Epigentek

Table 11: Solutions used for IF

Solution	Composition
10% Triton X	10% w/v diluted in PBS
3% BSA wash	3% w/v Fatty acid free BSA dissolved in PBS
4% PFA	4% paraformaldehyde, 4% sucrose, few drops of phenol red and few drops of NAOH to adjust pH to 7-7.5 and dissolved at 56°C
4 N HCl	4 N v/v HCl in MilliQ H_2O
Blocking buffer	3% w/v Fatty acid free BSA dissolved in PBS
H33342	Stock made as 1 mg/ml in MilliQ H_2O
NH_4Cl	50 mM working solution
PBS-PVA	0.25% PVA in PBS
PBST	0.05% Tween 20 in PBS

Table 12: Chemicals and reagents used in tissue and embryo culture

Chemicals	Stock	Manufacturer
0.025% trypsin EDTA		Invitrogen
17-b-estradiol		Sigma
2-, 4-dinitrophenol		sigma
6-Dimethylaminopurine (6-DMAP)	500 mM	Sigma
Albumin Bovine	20% Stock solution made in MilliQ H2O	Sigma
BM essential amino acids	50X	Sigma
$CaCl_2$. $2H_2O$	0.94 g dissolved in 5 ml ddH_2O to make a stock of 1000X	Sigma
Cysteamine		Sigma

D- Mannitol		Sigma
D-Glucose		Sigma
Dimethyl sulfoxide (DMSO) cell culture grade		Sigma
DMEM/F12 + GlutaMax™-I		Gibco
D-Penicillamine		Sigma
Fetal calf serum (FCS)		Gibco (USA)
Follicle- stimulating hormone (FSH)		Ovagen; ImmunoChemicals Products (ICP)
Gelatin	1 g gelatin dissolved and made to 100 ml final volume in % MilliQ H_2O	Sigma
GlutaMAX™	200 mM solution	Invitrogen
Heparin sodium salt		Sigma
Hypotaurine		Sigma
Ionomycin calcium salt	5 mM	Sigma
Kanamycin monosulfate		Sigma
M199		Life Technologies
MEM Non-essential amino acids	100X	Sigma
Mineral oil for culture of embryos and oocytes		Sigma
Na-Pyruvate	0.15 g dissolved in 5 ml MilliQ H_2O to make a stock of 1000X	Sigma
Ovine luteinizing hormone (LH)		ICP
Sodium Lactate		Sigma

Table 13: Tissue and embryo culture media composition

Media/solutions	Composition
B199	M199 with 25 mM NaHCO3, 0.2 mM Pyruvate and 0.086 mM kanamycin monosulfate
Cryopreservation medium	20% DMSO in FCS
Early SOF (ESOF)	1.71 mM CaCl2:2H20, 25 mM NaHCO3, 107.7 mM NaCl, 3.32 mM sodium lactate, 7.15 mM KCl, 0.30 mM KH2PO4, 0.15 mM D-Glucose, 0.33 mM pyruvate, 0.04 mM kanamycin monosulfate, and 0.081 g/L non-essential amino acids, 8 mg/ml fatty acid free bovine albumin and 1 mM GlutaMAX™
Fibroblast medium	DMEM/F12 + GlutaMAX™-I supplemented with 10% FCS
H199	M199 with 15 mM HEPES, 5 mMNaHCO3 and 0.086 mM kanamycin monosulfate
H199-PVA	H199 with 0.1 mg/ml cold soluble PVA
HSOF	Hepes-buffered synthetic oviduct fluid (SOF) with 1.71 mM CaCl2.2H2O, 5 mM NaHCO3, 107.7 mM NaCl, 3.32 mM sodium lactate, 7.15 mM KCl, 20 mM Hepes, 0.3 mM KH2PO4, 0.069 mM kanamycin monosulfate, 0.33 mM pyruvate and 3 mg/ml fatty acid free bovine serum albumin
Hypoosmolar fusion buffer	165 mM mannitol, 500 µM Hepes, 50 µM CaCl2, 100 µM MgCl2, 0.05% bovine albumin pH 7.3
IVF media	25 mM $NaHCO_3$, 107.7 mM NaCl, sodium lactate, 7.15 mM KCl, 3.32 mM 0.3 mM KH_2PO_4, 0.04 mM kanamycin monosulfate, 1.71 mM $CaCl_2.2H_2O$, 0.33 mM pyruvate, 8 mg/ml fatty acid free bovine albumin, supplemented with 0.2 mM Penicillamine, 0.1 mM hypotaurine and 0.001 mM heparin
IVM media	B199 with 10%FCS, 1 µg/ml ovine LH, 10 µg/ml ovine FSH, 1 µg/ml 17-b-estradiol and 0.1 mM cysteamine
Late SOF (LSOF)	1.71 mM CaCl2:2H20, 0.49 mM MgCl2:6H2O 25 mM

	NaHCO3, 107.7 mM NaCl, 3.32 mM sodium lactate, 7.15 mM KCl, 0.30 mM KH2PO4, 1 mM DNP (2-, 4-dinitrophenol), 1.5 mM D-Glucose, 0.33 mM pyruvate, 0.04 mM kanamycin monosulfate, and 0.081 g/L non-essential amino acids, 0.22 g/L BM essential amino acids, 8 mg/ml fatty acid free bovine albumin and 1 mM GlutaMAX™
M199	Medium 199-containing Earle's salts and L-glutamine
Oocyte aspiration medium	H199 + 925 IU/ml heparin 20 µl/ml 20% Albumin
Serum starvation medium	DMEM/F12 + GlutaMAX™-I supplemented with 0.5% FCS

Table 14: Primary and secondary antibodies used and their dilutions

Antibody	Dilutions	Manufacturer or Source
Donkey anti goat AF 488	1:2000	Invitrogen, NZ
Donkey anti goat AF 568	1:2000	Invitrogen, NZ
Donkey anti goat Rhodamine	1:300	Millipore
Donkey anti mouse AF 488	1:2000	Invitrogen, NZ
Donkey anti mouse AF 568	1:2000	Invitrogen, NZ
Donkey anti rabbit AF 488	1:2000	Invitrogen, NZ
Donkey anti rabbit Cy2	1:200	Jackson ImmunoResearch Laboratories
Donkey anti sheep AF 488	1:2000	Molecular Probes
Goat anti mouse Alexa Fluor (AF) 546	1:300 1:2000	Invitrogen, NZ
Goat anti rabbit AF 488	1:2000	Invitrogen, NZ
Goat anti rabbit AF 568	1:2000	Invitrogen, NZ
Goat anti RING2	1:25	Abcam (Ab14751)
Goat anti SOX2	1:30	R&D Systems (AF2018)

Goat anti SUZ12	1:25	Santa Cruz Biotechnology (sc-46264)
Mouse anti 5-MC	1:200	Abcam (Ab10805)
Mouse anti H3K4me3	1:500	Abcam (Ab1012)
Mouse anti H3K9me3	1:20	Millipore (Cat.# 05-1242)
Mouse anti PHC1	1:100	Abnova (Catalog ID # H00001911-M05)
Rabbit anti EED	1:100	Abcam (Ab4469)
Rabbit anti EZH2	1:100	Abcam (Ab3748)
Rabbit anti H3.3	1:500	Abcam (Ab62642)
Rabbit anti H3K27me3	1:1000	Dr. Thomas Jenuwein (Max Planck Institute, Freiberg, Germany)
Rabbit anti H3K27me3	1:500	Millipore (Cat.# 07-449)
Rabbit anti H3K4me3	1:2000	Abcam (Ab8580)
Rabbit anti H3K9Ac	1:250	Millipore (Cat.# 04-1003)
Rabbit anti H3K9me1	1:1000	Dr. Thomas Jenuwein (Max Planck Institute, Freiberg, Germany)
Rabbit anti H3K9me2	1:1000	Dr. Thomas Jenuwein (Max Planck Institute, Freiberg, Germany)
Rabbit anti H3K9me3	1:1000	Dr. Thomas Jenuwein (Max Planck Institute, Freiberg, Germany)
Rabbit anti H4K12Ac	1:500	Millipore (Cat.# 06-1352)
Rabbit anti H4K16Ac	1:250	Millipore (Cat.# 07-329)
Rabbit anti H4K5Ac	1:100	Upstate (Catalog # 06-7593)
Rabbit anti HDAC1	1:100	Millipore (Cat.# 06-720)
Rabbit anti pan-H3/4Kme1/2/3	1:1000	Dr. Thomas Jenuwein (Max Planck Institute, Freiburg, Germany)
Rabbit anti Pol II CTD	1:1000	Abcam (Ab817)
Sheep anti H2A.Z	1:200	Dr. David Tremethick (ANU College of Medicine, Canberra ACT, Australia)

Appendix II: List of equipment and software applications

Table 15: Equipment and software

Equipment/software	Manufacturer	Local supplier
Agarose gel casting mould and combs	Bio Rad	Bio Rad, NZ
BTX electrocell manipulator	BTX	BTX Instrument Division, USA
BTX optimizer	BTX	BTX Instrument Division, USA
Cell culture incubator	Forma scientific	Thermo Fisher Scientific, NZ
Gen5 data analysis software	BioTek	Millennium Sciences, NZ
Gilmont® micrometer syringe	Cole-Parmer Instruments, IL	Cole-Parmer, NZ
GS800 scanner	Bio Rad	Bio Rad, NZ
Horizontal micropipette puller (P-87)	Sutter Instrument Company	SDR Clinical Technology, Australia
Humidified modular incubation chamber	QNA International	QNA International, Australia
ImageJ software (1.43u)	National Institutes of Health (NIH)	National Institutes of Health, USA
Leica application suit software	Leica	Bio-Strategy, NZ
Leica DFC290 camera	Leica	Bio-Strategy, NZ
Leica DM1L inverted phase contrast microscope	Leica	Bio-Strategy, NZ
Mini protean tetra SDS gel casting system	Bio Rad	Bio Rad, NZ
MO-188 hydraulic hanging joystick micromanipulators	Nikon Narishige	Nikon, USA

MP-9 microforge	Narishige	Leica Microsystems, Australia
MS1 minishaker	IKA®	Global science, NZ
Nano-Drop 1000 Spectrophotometer	Thermo Scientific	Bio-Strategy, NZ
Nikon SMZ-2B stereomicroscope	Nikon	Nikon, USA
Nikon SMZ800 stereomicroscope	Nikon	Nikon, USA
Nikon TMS	Nikon	Nikon, USA
Nikon TMS inverted phase contrast microscope	Nikon	Nikon, USA
Nikon Transformer	Nikon	Nikon, USA
Olympus BX50 microscope	Olympus	Olympus, NZ
Olympus FV-1000 confocal scanning	Olympus	Olympus, NZ
Olympus IX70 Inverted Fluorescence Microscope	Olympus	Olympus, NZ
Olympus IX81 inverted microscope	Olympus	Olympus, NZ
PowerPac basic supply	Bio Rad	Bio Rad, NZ
Quantity One software	Bio Rad	Bio Rad, NZ
Spectrafuge mini C1301	Lab net international	Total lab systems, NZ
Spot Basic and Advanced software	Diagnostics Instruments Inc	Diagnostics Instruments Inc., MI, USA
SPOT RT-KE slider	Diagnostics Instruments Inc	Diagnostics Instruments Inc., MI, USA
Synergy 2 Multi-mode plate reader	BioTek	Millennium Sciences, Pvt. Ltd, NZ
Transfer cassette and tank	Bio Rad	Bio Rad, NZ
xCELLigence RTCA-SP	ACEA Biosciences	Roche, NZ

References

Agger K., Cloos P. A., Christensen J., Pasini D., Rose S., Rappsilber J., Issaeva I., Canaani E., Salcini A. E. & Helin K. (2007). *UTX and JMJD3 are histone H3K27 demethylases involved in HOX gene regulation and development*. Nature, 449, 731-734.

Ahmad K. & Henikoff S. (2002). *The histone variant H3.3 marks active chromatin by replication-independent nucleosome assembly*. Mol Cell, 9, 1191-1200.

Ahmed K., Dehghani H., Rugg-Gunn P., Fussner E., Rossant J. & Bazett-Jones D. P. (2010). *Global chromatin architecture reflects pluripotency and lineage commitment in the early mouse embryo*. PLoS One, 5, e10531.

Ait-Si-Ali S., Guasconi V., Fritsch L., Yahi H., Sekhri R., Naguibneva I., Robin P., Cabon F., Polesskaya A. & Harel-Bellan A. (2004). *A Suv39h-dependent mechanism for silencing S-phase genes in differentiating but not in cycling cells*. EMBO J, 23, 605-615.

Allfrey V. G., Faulkner R. & Mirsky A. E. (1964). *Acetylation and Methylation of Histones and Their Possible Role in the Regulation of Rna Synthesis*. Proc Natl Acad Sci U S A, 51, 786-794.

Arat S., Rzucidlo S. J., Gibbons J., Miyoshi K. & Stice S. L. (2001). *Production of transgenic bovine embryos by transfer of transfected granulosa cells into enucleated oocytes*. Mol Reprod Dev, 60, 20-26.

Baba A., Ohtake F., Okuno Y., Yokota K., Okada M., Imai Y., Ni M., Meyer C. A., Igarashi K., Kanno J., *et al.* (2011). *PKA-dependent regulation of the histone lysine demethylase complex PHF2-ARID5B*. Nat Cell Biol, 13, 668-675.

Banaszynski L. A., Allis C. D. & Lewis P. W. (2010). *Histone variants in metazoan development*. Dev Cell, 19, 662-674.

Bannister A. J. & Kouzarides T. (2011). *Regulation of chromatin by histone modifications*. Cell Res, 21, 381-395.

Bannister A. J., Schneider R. & Kouzarides T. (2002). *Histone methylation: dynamic or static?* Cell, 109, 801-806.

Bannister A. J., Zegerman P., Partridge J. F., Miska E. A., Thomas J. O., Allshire R. C. & Kouzarides T. (2001). *Selective recognition of methylated lysine 9 on histone H3 by the HP1 chromo domain*. Nature, 410, 120-124.

Bantignies F. & Cavalli G. (2011). *Polycomb group proteins: repression in 3D*. Trends Genet, 27, 454-464.

Bao S., Miyoshi N., Okamoto I., Jenuwein T., Heard E. & Azim Surani M. (2005). *Initiation of epigenetic reprogramming of the X chromosome in somatic nuclei transplanted to a mouse oocyte*. EMBO Rep, 6, 748-754.

Barski A., Cuddapah S., Cui K., Roh T. Y., Schones D. E., Wang Z., Wei G., Chepelev I. & Zhao K. (2007). *High-resolution profiling of histone methylations in the human genome*. Cell, 129, 823-837.

Baxter J., Sauer S., Peters A., John R., Williams R., Caparros M. L., Arney K., Otte A., Jenuwein T., Merkenschlager M., *et al.* (2004). *Histone hypomethylation is an indicator of epigenetic plasticity in quiescent lymphocytes*. EMBO J, 23, 4462-4472.

Bernstein B. E., Kamal M., Lindblad-Toh K., Bekiranov S., Bailey D. K., Huebert D. J., McMahon S., Karlsson E. K., Kulbokas E. J., 3rd, Gingeras T. R., *et al.* (2005). *Genomic maps and comparative analysis of histone modifications in human and mouse*. Cell, 120, 169-181.

Bernstein B. E., Mikkelsen T. S., Xie X., Kamal M., Huebert D. J., Cuff J., Fry B., Meissner A., Wernig M., Plath K., *et al.* (2006). *A bivalent chromatin structure marks key developmental genes in embryonic stem cells*. Cell, 125, 315-326.

Bestor T. H. (2000). *The DNA methyltransferases of mammals*. Hum Mol Genet, 9, 2395-2402.

Bhadriraju K., Elliott J. T., Nguyen M. & Plant A. L. (2007). *Quantifying myosin light chain phosphorylation in single adherent cells with automated fluorescence microscopy*. BMC Cell Biol, 8, 43.

Bird A. (2002). *DNA methylation patterns and epigenetic memory*. Genes Dev, 16, 6-21.

Bird A. P. & Wolffe A. P. (1999). *Methylation-induced repression--belts, braces, and chromatin*. Cell, 99, 451-454.

Blelloch R., Wang Z., Meissner A., Pollard S., Smith A. & Jaenisch R. (2006). *Reprogramming efficiency following somatic cell nuclear transfer is influenced by the differentiation and methylation state of the donor nucleus*. Stem Cells, 24, 2007-2013.

Booth P. J., Viuff D., Tan S., Holm P., Greve T. & Callesen H. (2003). *Numerical chromosome errors in day 7 somatic nuclear transfer bovine blastocysts*. Biol Reprod, 68, 922-928.

Boyer L. A., Plath K., Zeitlinger J., Brambrink T., Medeiros L. A., Lee T. I., Levine S. S., Wernig M., Tajonar A., Ray M. K., *et al.* (2006). *Polycomb complexes repress developmental regulators in murine embryonic stem cells*. Nature, 441, 349-353.

Bracken A. P., Dietrich N., Pasini D., Hansen K. H. & Helin K. (2006). *Genome-wide mapping of Polycomb target genes unravels their roles in cell fate transitions*. Genes Dev, 20, 1123-1136.

Brambrink T., Hochedlinger K., Bell G. & Jaenisch R. (2006). *ES cells derived from cloned and fertilized blastocysts are transcriptionally and functionally indistinguishable*. Proc Natl Acad Sci U S A, 103, 933-938.

Bridger J. M., Boyle S., Kill I. R. & Bickmore W. A. (2000). *Re-modelling of nuclear architecture in quiescent and senescent human fibroblasts*. Curr Biol, 10, 149-152.

Briggs S. D., Bryk M., Strahl B. D., Cheung W. L., Davie J. K., Dent S. Y., Winston F. & Allis C. D. (2001). *Histone H3 lysine 4 methylation is mediated by Set1 and required for cell growth and rDNA silencing in Saccharomyces cerevisiae*. Genes Dev, 15, 3286-3295.

Brinkman A. B., Roelofsen T., Pennings S. W., Martens J. H., Jenuwein T. & Stunnenberg H. G. (2006). *Histone modification patterns associated with the human X chromosome*. EMBO Rep, 7, 628-634.

Brooks R. F., Bennett D. C. & Smith J. A. (1980). *Mammalian cell cycles need two random transitions*. Cell, 19, 493-504.

Brown K. E., Baxter J., Graf D., Merkenschlager M. & Fisher A. G. (1999). *Dynamic repositioning of genes in the nucleus of lymphocytes preparing for cell division*. Mol Cell, 3, 207-217.

Brownell J. E., Zhou J., Ranalli T., Kobayashi R., Edmondson D. G., Roth S. Y. & Allis C. D. (1996). *Tetrahymena histone acetyltransferase A: a homolog to yeast Gcn5p linking histone acetylation to gene activation*. Cell, 84, 843-851.

Bui H. T., Van Thuan N., Wakayama T. & Miyano T. (2006). *Chromatin remodeling in somatic cells injected into mature pig oocytes*. Reproduction, 131, 1037-1049.

Bui H. T., Wakayama S., Kishigami S., Kim J. H., Van Thuan N. & Wakayama T. (2008). *The cytoplasm of mouse germinal vesicle stage oocytes can*

enhance somatic cell nuclear reprogramming. Development, 135, 3935-3945.

Bui H. T., Wakayama S., Kishigami S., Park K. K., Kim J. H., Thuan N. V. & Wakayama T. (2010). *Effect of trichostatin A on chromatin remodeling, histone modifications, DNA replication, and transcriptional activity in cloned mouse embryos*. Biol Reprod, 83, 454-463.

Byvoet P., Shepherd G. R., Hardin J. M. & Noland B. J. (1972). *The distribution and turnover of labeled methyl groups in histone fractions of cultured mammalian cells*. Arch Biochem Biophys, 148, 558-567.

Campbell K. H., Alberio R., Choi I., Fisher P., Kelly R. D., Lee J. H. & Maalouf W. (2005). *Cloning: eight years after Dolly*. Reprod Domest Anim, 40, 256-268.

Campbell K. H., Fisher P., Chen W. C., Choi I., Kelly R. D., Lee J. H. & Xhu J. (2007). *Somatic cell nuclear transfer: Past, present and future perspectives*. Theriogenology, 68 Suppl 1, S214-231.

Campbell K. H., Loi P., Otaegui P. J. & Wilmut I. (1996). *Cell cycle co-ordination in embryo cloning by nuclear transfer*. Rev Reprod, 1, 40-46.

Campos E. I. & Reinberg D. (2009). *Histones: annotating chromatin*. Annu Rev Genet, 43, 559-599.

Cano A. & Pestana A. (1979). *Purification and properties of a histone acetyltransferase from Artemia salina, highly efficient with H1 histone*. Eur J Biochem, 97, 65-72.

Cao R., Wang L., Wang H., Xia L., Erdjument-Bromage H., Tempst P., Jones R. S. & Zhang Y. (2002). *Role of histone H3 lysine 27 methylation in Polycomb-group silencing*. Science, 298, 1039-1043.

Cao R. & Zhang Y. (2004a). *The functions of E(Z)/EZH2-mediated methylation of lysine 27 in histone H3*. Curr Opin Genet Dev, 14, 155-164.

Cao R. & Zhang Y. (2004b). *SUZ12 is required for both the histone methyltransferase activity and the silencing function of the EED-EZH2 complex*. Mol Cell, 15, 57-67.

Carrozza M. J., Utley R. T., Workman J. L. & Cote J. (2003). *The diverse functions of histone acetyltransferase complexes*. Trends Genet, 19, 321-329.

Chamberlain S. J., Yee D. & Magnuson T. (2008). *Polycomb repressive complex 2 is dispensable for maintenance of embryonic stem cell pluripotency*. Stem Cells, 26, 1496-1505.

Chang G., Liu S., Wang F., Zhang Y., Kou Z., Chen D. & Gao S. (2009). *Differential methylation status of imprinted genes in nuclear transfer derived ES (NT-ES) cells*. Genomics, 93, 112-119.

Chen T. & Li E. (2004). *Structure and function of eukaryotic DNA methyltransferases*. Curr Top Dev Biol, 60, 55-89.

Chen Z. X. & Riggs A. D. (2011). *DNA methylation and demethylation in mammals*. J Biol Chem, 286, 18347-18353.

Cheong H. T., Takahashi Y. & Kanagawa H. (1993). *Birth of mice after transplantation of early cell-cycle-stage embryonic nuclei into enucleated oocytes*. Biol Reprod, 48, 958-963.

Cho J. K., Lee B. C., Park J. I., Lim J. M., Shin S. J., Kim K. Y., Lee B. D. & Hwang W. S. (2002). *Development of bovine oocytes reconstructed with different donor somatic cells with or without serum starvation*. Theriogenology, 57, 1819-1828.

Choder M. (1991). *A general topoisomerase I-dependent transcriptional repression in the stationary phase in yeast*. Genes Dev, 5, 2315-2326.

Christensen J., Agger K., Cloos P. A., Pasini D., Rose S., Sennels L., Rappsilber J., Hansen K. H., Salcini A. E. & Helin K. (2007). *RBP2 belongs to a family of demethylases, specific for tri-and dimethylated lysine 4 on histone 3*. Cell, 128, 1063-1076.

Cibelli J. B., Stice S. L., Golueke P. J., Kane J. J., Jerry J., Blackwell C., Ponce de Leon F. A. & Robl J. M. (1998). *Cloned transgenic calves produced from nonquiescent fetal fibroblasts*. Science, 280, 1256-1258.

Clark S. J., Harrison J. & Frommer M. (1995). *CpNpG methylation in mammalian cells*. Nat Genet, 10, 20-27.

Coller H. A. (2011). *Cell biology. The essence of quiescence*. Science, 334, 1074-1075.

Coller H. A., Sang L. & Roberts J. M. (2006). *A new description of cellular quiescence*. PLoS Biol, 4, e83.

Cooper S. (1998). *Mammalian cells are not synchronized in G1-phase by starvation or inhibition: considerations of the fundamental concept of G1-phase synchronization*. Cell Prolif, 31, 9-16.

Couldrey C., Carlton M. B., Nolan P. M., Colledge W. H. & Evans M. J. (1999). *A retroviral gene trap insertion into the histone 3.3A gene causes partial neonatal lethality, stunted growth, neuromuscular deficits and male sub-fertility in transgenic mice*. Hum Mol Genet, 8, 2489-2495.

Couture J. F., Collazo E. & Trievel R. C. (2006). *Molecular recognition of histone H3 by the WD40 protein WDR5*. Nat Struct Mol Biol, 13, 698-703.

Creyghton M. P., Markoulaki S., Levine S. S., Hanna J., Lodato M. A., Sha K., Young R. A., Jaenisch R. & Boyer L. A. (2008). *H2AZ is enriched at polycomb complex target genes in ES cells and is necessary for lineage commitment*. Cell, 135, 649-661.

Croft J. A., Bridger J. M., Boyle S., Perry P., Teague P. & Bickmore W. A. (1999). *Differences in the localization and morphology of chromosomes in the human nucleus*. J Cell Biol, 145, 1119-1131.

Crump N. T., Hazzalin C. A., Bowers E. M., Alani R. M., Cole P. A. & Mahadevan L. C. (2011). *Dynamic acetylation of all lysine-4 trimethylated histone H3 is evolutionarily conserved and mediated by p300/CBP*. Proc Natl Acad Sci U S A, 108, 7814-7819.

Daujat S., Weiss T., Mohn F., Lange U. C., Ziegler-Birling C., Zeissler U., Lappe M., Schubeler D., Torres-Padilla M. E. & Schneider R. (2009). *H3K64 trimethylation marks heterochromatin and is dynamically remodeled during developmental reprogramming*. Nat Struct Mol Biol, 16, 777-781.

Davey C. A., Sargent D. F., Luger K., Maeder A. W. & Richmond T. J. (2002). *Solvent mediated interactions in the structure of the nucleosome core particle at 1.9 a resolution*. J Mol Biol, 319, 1097-1113.

de la Cruz C. C., Kirmizis A., Simon M. D., Isono K., Koseki H. & Panning B. (2007). *The polycomb group protein SUZ12 regulates histone H3 lysine 9 methylation and HP1 alpha distribution*. Chromosome Res, 15, 299-314.

de Napoles M., Mermoud J. E., Wakao R., Tang Y. A., Endoh M., Appanah R., Nesterova T. B., Silva J., Otte A. P., Vidal M., *et al.* (2004). *Polycomb group proteins Ring1A/B link ubiquitylation of histone H2A to heritable gene silencing and X inactivation*. Dev Cell, 7, 663-676.

Dean W., Santos F. & Reik W. (2003). *Epigenetic reprogramming in early mammalian development and following somatic nuclear transfer*. Semin Cell Dev Biol, 14, 93-100.

Dean W., Santos F., Stojkovic M., Zakhartchenko V., Walter J., Wolf E. & Reik W. (2001). *Conservation of methylation reprogramming in mammalian development: aberrant reprogramming in cloned embryos*. Proc Natl Acad Sci U S A, 98, 13734-13738.

Delaval K. & Feil R. (2004). *Epigenetic regulation of mammalian genomic imprinting*. Curr Opin Genet Dev, 14, 188-195.

Demers C., Chaturvedi C. P., Ranish J. A., Juban G., Lai P., Morle F., Aebersold R., Dilworth F. J., Groudine M. & Brand M. (2007). *Activator-mediated recruitment of the MLL2 methyltransferase complex to the beta-globin locus*. Mol Cell, 27, 573-584.

Ding J., Guo Y., Liu S., Yan Y., Chang G., Kou Z., Zhang Y., Jiang Y., He F., Gao S., *et al.* (2009). *Embryonic stem cells derived from somatic cloned and fertilized blastocysts are post-transcriptionally indistinguishable: a MicroRNA and protein profile comparison*. Proteomics, 9, 2711-2721.

Ding X., Wang Y., Zhang D., Guo Z. & Zhang Y. (2008). *Increased pre-implantation development of cloned bovine embryos treated with 5-aza-2'-deoxycytidine and trichostatin A*. Theriogenology, 70, 622-630.

Dong K. B., Maksakova I. A., Mohn F., Leung D., Appanah R., Lee S., Yang H. W., Lam L. L., Mager D. L., Schubeler D., *et al.* (2008). *DNA methylation in ES cells requires the lysine methyltransferase G9a but not its catalytic activity*. EMBO J, 27, 2691-2701.

Dou Y., Milne T. A., Tackett A. J., Smith E. R., Fukuda A., Wysocka J., Allis C. D., Chait B. T., Hess J. L. & Roeder R. G. (2005). *Physical association and coordinate function of the H3 K4 methyltransferase MLL1 and the H4 K16 acetyltransferase MOF*. Cell, 121, 873-885.

Doyon Y., Cayrou C., Ullah M., Landry A. J., Cote V., Selleck W., Lane W. S., Tan S., Yang X. J. & Cote J. (2006). *ING tumor suppressor proteins are critical regulators of chromatin acetylation required for genome expression and perpetuation*. Mol Cell, 21, 51-64.

Edmunds J. W., Mahadevan L. C. & Clayton A. L. (2008). *Dynamic histone H3 methylation during gene induction: HYPB/Setd2 mediates all H3K36 trimethylation*. EMBO J, 27, 406-420.

Eggan K., Akutsu H., Loring J., Jackson-Grusby L., Klemm M., Rideout W. M., 3rd, Yanagimachi R. & Jaenisch R. (2001). *Hybrid vigor, fetal overgrowth, and viability of mice derived by nuclear cloning and tetraploid embryo complementation*. Proc Natl Acad Sci U S A, 98, 6209-6214.

Eilertsen K. J., Power R. A., Harkins L. L. & Misica P. (2007). *Targeting cellular memory to reprogram the epigenome, restore potential, and improve somatic cell nuclear transfer*. Anim Reprod Sci, 98, 129-146.

Ekwall K. (2005). *Genome-wide analysis of HDAC function*. Trends Genet, 21, 608-615.

Enright B. P., Kubota C., Yang X. & Tian X. C. (2003). *Epigenetic characteristics and development of embryos cloned from donor cells*

treated by trichostatin A or 5-aza-2'-deoxycytidine. Biol Reprod, 69, 896-901.

Enright B. P., Sung L. Y., Chang C. C., Yang X. & Tian X. C. (2005). *Methylation and acetylation characteristics of cloned bovine embryos from donor cells treated with 5-aza-2'-deoxycytidine*. Biol Reprod, 72, 944-948.

Enright B. P., Taneja M., Schreiber D., Riesen J., Tian X. C., Fortune J. E. & Yang X. (2002). *Reproductive characteristics of cloned heifers derived from adult somatic cells*. Biol Reprod, 66, 291-296.

Epsztejn-Litman S., Feldman N., Abu-Remaileh M., Shufaro Y., Gerson A., Ueda J., Deplus R., Fuks F., Shinkai Y., Cedar H., *et al.* (2008). *De novo DNA methylation promoted by G9a prevents reprogramming of embryonically silenced genes*. Nat Struct Mol Biol, 15, 1176-1183.

Erickson H. P. (1993). *Tenascin-C, tenascin-R and tenascin-X: a family of talented proteins in search of functions*. Curr Opin Cell Biol, 5, 869-876.

Erickson H. P. & Bourdon M. A. (1989). *Tenascin: an extracellular matrix protein prominent in specialized embryonic tissues and tumors*. Annu Rev Cell Biol, 5, 71-92.

Eskeland R., Leeb M., Grimes G. R., Kress C., Boyle S., Sproul D., Gilbert N., Fan Y., Skoultchi A. I., Wutz A., *et al.* (2010). *Ring1B compacts chromatin structure and represses gene expression independent of histone ubiquitination*. Mol Cell, 38, 452-464.

Faast R., Thonglairoam V., Schulz T. C., Beall J., Wells J. R., Taylor H., Matthaei K., Rathjen P. D., Tremethick D. J. & Lyons I. (2001). *Histone variant H2A.Z is required for early mammalian development*. Curr Biol, 11, 1183-1187.

Falandry C., Fourel G., Galy V., Ristriani T., Horard B., Bensimon E., Salles G., Gilson E. & Magdinier F. (2010). *CLLD8/KMT1F is a lysine methyltransferase that is important for chromosome segregation*. J Biol Chem, 285, 20234-20241.

Fan J. Y., Rangasamy D., Luger K. & Tremethick D. J. (2004). *H2A.Z alters the nucleosome surface to promote HP1alpha-mediated chromatin fiber folding*. Mol Cell, 16, 655-661.

Fang J., Chen T., Chadwick B., Li E. & Zhang Y. (2004). *Ring1b-mediated H2A ubiquitination associates with inactive X chromosomes and is involved in initiation of X inactivation*. J Biol Chem, 279, 52812-52815.

Fang R., Barbera A. J., Xu Y., Rutenberg M., Leonor T., Bi Q., Lan F., Mei P., Yuan G. C., Lian C., *et al.* (2010). *Human LSD2/KDM1b/AOF1 regulates gene transcription by modulating intragenic H3K4me2 methylation*. Mol Cell, 39, 222-233.

Faust C., Schumacher A., Holdener B. & Magnuson T. (1995). *The eed mutation disrupts anterior mesoderm production in mice*. Development, 121, 273-285.

Fischle W., Wang Y., Jacobs S. A., Kim Y., Allis C. D. & Khorasanizadeh S. (2003). *Molecular basis for the discrimination of repressive methyl-lysine marks in histone H3 by Polycomb and HP1 chromodomains*. Genes Dev, 17, 1870-1881.

Fodor B. D., Kubicek S., Yonezawa M., O'Sullivan R. J., Sengupta R., Perez-Burgos L., Opravil S., Mechtler K., Schotta G. & Jenuwein T. (2006). *Jmjd2b antagonizes H3K9 trimethylation at pericentric heterochromatin in mammalian cells*. Genes Dev, 20, 1557-1562.

Foster D. A., Yellen P., Xu L. & Saqcena M. (2010). *Regulation of G1 Cell Cycle Progression: Distinguishing the Restriction Point from a Nutrient-Sensing Cell Growth Checkpoint(s)*. Genes Cancer, 1, 1124-1131.

Fraga M. F., Ballestar E., Villar-Garea A., Boix-Chornet M., Espada J., Schotta G., Bonaldi T., Haydon C., Ropero S., Petrie K., *et al.* (2005). *Loss of acetylation at Lys16 and trimethylation at Lys20 of histone H4 is a common hallmark of human cancer*. Nat Genet, 37, 391-400.

Francastel C., Magis W. & Groudine M. (2001). *Nuclear relocation of a transactivator subunit precedes target gene activation*. Proc Natl Acad Sci U S A, 98, 12120-12125.

Frank S. R., Schroeder M., Fernandez P., Taubert S. & Amati B. (2001). *Binding of c-Myc to chromatin mediates mitogen-induced acetylation of histone H4 and gene activation*. Genes Dev, 15, 2069-2082.

Freberg C. T., Dahl J. A., Timoskainen S. & Collas P. (2007). *Epigenetic reprogramming of OCT4 and NANOG regulatory regions by embryonal carcinoma cell extract*. Mol Biol Cell, 18, 1543-1553.

Frescas D., Guardavaccaro D., Bassermann F., Koyama-Nasu R. & Pagano M. (2007). *JHDM1B/FBXL10 is a nucleolar protein that represses transcription of ribosomal RNA genes*. Nature, 450, 309-313.

Fujiki R., Chikanishi T., Hashiba W., Ito H., Takada I., Roeder R. G., Kitagawa H. & Kato S. (2009). *GlcNAcylation of a histone methyltransferase in retinoic-acid-induced granulopoiesis*. Nature, 459, 455-459.

Fuks F., Hurd P. J., Wolf D., Nan X., Bird A. P. & Kouzarides T. (2003). *The methyl-CpG-binding protein MeCP2 links DNA methylation to histone methylation*. J Biol Chem, 278, 4035-4040.

Fulka H., St John J. C., Fulka J. & Hozak P. (2008). *Chromatin in early mammalian embryos: achieving the pluripotent state*. Differentiation, 76, 3-14.

Fuso A., Seminara L., Cavallaro R. A., D'Anselmi F. & Scarpa S. (2005). *S-adenosylmethionine/homocysteine cycle alterations modify DNA methylation status with consequent deregulation of PS1 and BACE and beta-amyloid production*. Mol Cell Neurosci, 28, 195-204.

Gao S., Chung Y. G., Williams J. W., Riley J., Moley K. & Latham K. E. (2003). *Somatic cell-like features of cloned mouse embryos prepared with cultured myoblast nuclei*. Biol Reprod, 69, 48-56.

Giraldo A. M., Lynn J. W., Purpera M. N., Vaught T. D., Ayares D. L., Godke R. A. & Bondioli K. R. (2009). *Inhibition of DNA methyltransferase 1 expression in bovine fibroblast cells used for nuclear transfer*. Reprod Fertil Dev, 21, 785-795.

Goo Y. H., Sohn Y. C., Kim D. H., Kim S. W., Kang M. J., Jung D. J., Kwak E., Barlev N. A., Berger S. L., Chow V. T., *et al.* (2003). *Activating signal cointegrator 2 belongs to a novel steady-state complex that contains a subset of trithorax group proteins*. Mol Cell Biol, 23, 140-149.

Govin J., Escoffier E., Rousseaux S., Kuhn L., Ferro M., Thevenon J., Catena R., Davidson I., Garin J., Khochbin S., *et al.* (2007). *Pericentric heterochromatin reprogramming by new histone variants during mouse spermiogenesis*. J Cell Biol, 176, 283-294.

Gowher H. & Jeltsch A. (2001). *Enzymatic properties of recombinant Dnmt3a DNA methyltransferase from mouse: the enzyme modifies DNA in a non-processive manner and also methylates non-CpG [correction of non-CpA] sites*. J Mol Biol, 309, 1201-1208.

Greaves I. K., Rangasamy D., Ridgway P. & Tremethick D. J. (2007). *H2A.Z contributes to the unique 3D structure of the centromere*. Proc Natl Acad Sci U S A, 104, 525-530.

Grogan J. L., Mohrs M., Harmon B., Lacy D. A., Sedat J. W. & Locksley R. M. (2001). *Early transcription and silencing of cytokine genes underlie polarization of T helper cell subsets*. Immunity, 14, 205-215.

Gu T. P., Guo F., Yang H., Wu H. P., Xu G. F., Liu W., Xie Z. G., Shi L., He X., Jin S. G., *et al.* (2011). *The role of Tet3 DNA dioxygenase in epigenetic reprogramming by oocytes*. Nature, 477, 606-610.

Guasconi V., Pritchard L. L., Fritsch L., Mesner L. D., Francastel C., Harel-Bellan A. & Ait-Si-Ali S. (2010). *Preferential association of irreversibly silenced E2F-target genes with pericentromeric heterochromatin in differentiated muscle cells*. Epigenetics, 5, 704-709.

Guo J. U., Su Y., Zhong C., Ming G. L. & Song H. (2011). *Hydroxylation of 5-methylcytosine by TET1 promotes active DNA demethylation in the adult brain*. Cell, 145, 423-434.

Hajkova P., Ancelin K., Waldmann T., Lacoste N., Lange U. C., Cesari F., Lee C., Almouzni G., Schneider R. & Surani M. A. (2008). *Chromatin dynamics during epigenetic reprogramming in the mouse germ line*. Nature, 452, 877-881.

Hake S. B., Garcia B. A., Duncan E. M., Kauer M., Dellaire G., Shabanowitz J., Bazett-Jones D. P., Allis C. D. & Hunt D. F. (2006). *Expression patterns and post-translational modifications associated with mammalian histone H3 variants*. J Biol Chem, 281, 559-568.

Hamamoto R., Furukawa Y., Morita M., Iimura Y., Silva F. P., Li M., Yagyu R. & Nakamura Y. (2004). *SMYD3 encodes a histone methyltransferase involved in the proliferation of cancer cells*. Nat Cell Biol, 6, 731-740.

Han S. & Brunet A. (2012). *Histone methylation makes its mark on longevity*. Trends Cell Biol, 22, 42-49.

Han Y. M., Kang Y. K., Koo D. B. & Lee K. K. (2003). *Nuclear reprogramming of cloned embryos produced in vitro*. Theriogenology, 59, 33-44.

Hansen L. K., Mooney D. J., Vacanti J. P. & Ingber D. E. (1994). *Integrin binding and cell spreading on extracellular matrix act at different points in the cell cycle to promote hepatocyte growth*. Mol Biol Cell, 5, 967-975.

Hardy S., Jacques P. E., Gevry N., Forest A., Fortin M. E., Laflamme L., Gaudreau L. & Robert F. (2009). *The euchromatic and heterochromatic landscapes are shaped by antagonizing effects of transcription on H2A.Z deposition*. PLoS Genet, 5, e1000687.

Hata K., Okano M., Lei H. & Li E. (2002). *Dnmt3L cooperates with the Dnmt3 family of de novo DNA methyltransferases to establish maternal imprints in mice*. Development, 129, 1983-1993.

Hathaway N. A., Bell O., Hodges C., Miller E. L., Neel D. S. & Crabtree G. R. (2012). *Dynamics and memory of heterochromatin in living cells*. Cell, 149, 1447-1460.

Hayashi K., Yoshida K. & Matsui Y. (2005). *A histone H3 methyltransferase controls epigenetic events required for meiotic prophase*. Nature, 438, 374-378.

Hazzalin C. A. & Mahadevan L. C. (2005). *Dynamic acetylation of all lysine 4-methylated histone H3 in the mouse nucleus: analysis at c-fos and c-jun*. PLoS Biol, 3, e393.

He Y. F., Li B. Z., Li Z., Liu P., Wang Y., Tang Q., Ding J., Jia Y., Chen Z., Li L., *et al.* (2011). *Tet-mediated formation of 5-carboxylcytosine and its excision by TDG in mammalian DNA*. Science, 333, 1303-1307.

Heard E. (2004). *Recent advances in X-chromosome inactivation*. Curr Opin Cell Biol, 16, 247-255.

Heintzman N. D., Stuart R. K., Hon G., Fu Y., Ching C. W., Hawkins R. D., Barrera L. O., Van Calcar S., Qu C., Ching K. A., *et al.* (2007). *Distinct and predictive chromatin signatures of transcriptional promoters and enhancers in the human genome*. Nat Genet, 39, 311-318.

Hemberger M., Dean W. & Reik W. (2009). *Epigenetic dynamics of stem cells and cell lineage commitment: digging Waddington's canal*. Nat Rev Mol Cell Biol, 10, 526-537.

Henikoff S. (2008). *Nucleosome destabilization in the epigenetic regulation of gene expression*. Nat Rev Genet, 9, 15-26.

Heyman Y., Chavatte-Palmer P., LeBourhis D., Camous S., Vignon X. & Renard J. P. (2002). *Frequency and occurrence of late-gestation losses from cattle cloned embryos*. Biol Reprod, 66, 6-13.

Hiiragi T. & Solter D. (2005). *Reprogramming is essential in nuclear transfer*. Mol Reprod Dev, 70, 417-421.

Hill J. R., Winger Q. A., Burghardt R. C. & Westhusin M. E. (2001). *Bovine nuclear transfer embryo development using cells derived from a cloned fetus*. Anim Reprod Sci, 67, 17-26.

Hill J. R., Winger Q. A., Long C. R., Looney C. R., Thompson J. A. & Westhusin M. E. (2000). *Development rates of male bovine nuclear transfer embryos derived from adult and fetal cells*. Biol Reprod, 62, 1135-1140.

Hochedlinger K. & Jaenisch R. (2002). *Monoclonal mice generated by nuclear transfer from mature B and T donor cells*. Nature, 415, 1035-1038.

Hong L., Schroth G. P., Matthews H. R., Yau P. & Bradbury E. M. (1993). *Studies of the DNA binding properties of histone H4 amino terminus.*

Thermal denaturation studies reveal that acetylation markedly reduces the binding constant of the H4 "tail" to DNA. J Biol Chem, 268, 305-314.

Hsu D. W., Chubb J. R., Muramoto T., Pears C. J. & Mahadevan L. C. (2012). *Dynamic acetylation of lysine-4-trimethylated histone H3 and H3 variant biology in a simple multicellular eukaryote*. Nucleic Acids Res, 40, 7247-7256.

Huang B., Li T., Alonso-Gonzalez L., Gorre R., Keatley S., Green A., Turner P., Kallingappa P. K., Verma V. & Oback B. (2011). *A virus-free poly-promoter vector induces pluripotency in quiescent bovine cells under chemically defined conditions of dual kinase inhibition*. PLoS One, 6, e24501.

Huangfu D., Maehr R., Guo W., Eijkelenboom A., Snitow M., Chen A. E. & Melton D. A. (2008). *Induction of pluripotent stem cells by defined factors is greatly improved by small-molecule compounds*. Nat Biotechnol, 26, 795-797.

Hyldig S. M., Croxall N., Contreras D. A., Thomsen P. D. & Alberio R. (2011). *Epigenetic reprogramming in the porcine germ line*. BMC Dev Biol, 11, 11.

Ito S., Shen L., Dai Q., Wu S. C., Collins L. B., Swenberg J. A., He C. & Zhang Y. (2011). *Tet proteins can convert 5-methylcytosine to 5-formylcytosine and 5-carboxylcytosine*. Science, 333, 1300-1303.

Iwase S., Lan F., Bayliss P., de la Torre-Ubieta L., Huarte M., Qi H. H., Whetstine J. R., Bonni A., Roberts T. M. & Shi Y. (2007). *The X-linked mental retardation gene SMCX/JARID1C defines a family of histone H3 lysine 4 demethylases*. Cell, 128, 1077-1088.

Izzo A. & Schneider R. (2010). *Chatting histone modifications in mammals*. Brief Funct Genomics, 9, 429-443.

Jackson J. P., Lindroth A. M., Cao X. & Jacobsen S. E. (2002). *Control of CpNpG DNA methylation by the KRYPTONITE histone H3 methyltransferase*. Nature, 416, 556-560.

Jaenisch R., Eggan K., Humpherys D., Rideout W. & Hochedlinger K. (2002). *Nuclear cloning, stem cells, and genomic reprogramming*. Cloning Stem Cells, 4, 389-396.

Jafarpour F., Hosseini S. M., Hajian M., Forouzanfar M., Ostadhosseini S., Abedi P., Gholami S., Ghaedi K., Gourabi H., Shahverdi A. H., *et al.* (2011). *Somatic cell-induced hyperacetylation, but not hypomethylation, positively and reversibly affects the efficiency of in vitro cloned blastocyst production in cattle*. Cell Reprogram, 13, 483-493.

Jenuwein T. & Allis C. D. (2001). *Translating the histone code*. Science, 293, 1074-1080.

Jeon B. G., Coppola G., Perrault S. D., Rho G. J., Betts D. H. & King W. A. (2008). *S-adenosylhomocysteine treatment of adult female fibroblasts alters X-chromosome inactivation and improves in vitro embryo development after somatic cell nuclear transfer*. Reproduction, 135, 815-828.

Jeppesen P. & Turner B. M. (1993). *The inactive X chromosome in female mammals is distinguished by a lack of histone H4 acetylation, a cytogenetic marker for gene expression*. Cell, 74, 281-289.

Ji Y., Zhang J., Lee A. I., Cedar H. & Bergman Y. (2003). *A multistep mechanism for the activation of rearrangement in the immune system*. Proc Natl Acad Sci U S A, 100, 7557-7562.

Jiang C. L., Jin S. G. & Pfeifer G. P. (2004). *MBD3L1 is a transcriptional repressor that interacts with methyl-CpG-binding protein 2 (MBD2) and components of the NuRD complex*. J Biol Chem, 279, 52456-52464.

Jin C. & Felsenfeld G. (2007). *Nucleosome stability mediated by histone variants H3.3 and H2A.Z*. Genes Dev, 21, 1519-1529.

Josse T., Mokrani-Benhelli H., Benferhat R., Shestakova E., Mansuroglu Z., Kakanakou H., Billecocq A., Bouloy M. & Bonnefoy E. (2012). *Association of the interferon-beta gene with pericentromeric heterochromatin is dynamically regulated during virus infection through a YY1-dependent mechanism*. Nucleic Acids Res, 40, 4396-4411.

Judson R. L., Babiarz J. E., Venere M. & Blelloch R. (2009). *Embryonic stem cell-specific microRNAs promote induced pluripotency*. Nat Biotechnol, 27, 459-461.

Jullien J., Astrand C., Szenker E., Garrett N., Almouzni G. & Gurdon J. (2012). *HIRA dependent H3.3 deposition is required for transcriptional reprogramming following nuclear transfer to Xenopus oocytes*. Epigenetics Chromatin, 5, 17.

Jung H. R., Pasini D., Helin K. & Jensen O. N. (2010). *Quantitative mass spectrometry of histones H3.2 and H3.3 in Suz12-deficient mouse embryonic stem cells reveals distinct, dynamic post-translational modifications at Lys-27 and Lys-36*. Mol Cell Proteomics, 9, 838-850.

Kaneda M., Okano M., Hata K., Sado T., Tsujimoto N., Li E. & Sasaki H. (2004). *Essential role for de novo DNA methyltransferase Dnmt3a in paternal and maternal imprinting*. Nature, 429, 900-903.

Kang H. B., Choi Y., Lee J. M., Choi K. C., Kim H. C., Yoo J. Y., Lee Y. H. & Yoon H. G. (2009). *The histone methyltransferase, NSD2, enhances androgen receptor-mediated transcription*. FEBS Lett, 583, 1880-1886.

Kang Y. K., Koo D. B., Park J. S., Choi Y. H., Chung A. S., Lee K. K. & Han Y. M. (2001a). *Aberrant methylation of donor genome in cloned bovine embryos*. Nat Genet, 28, 173-177.

Kang Y. K., Koo D. B., Park J. S., Choi Y. H., Lee K. K. & Han Y. M. (2001b). *Influence of oocyte nuclei on demethylation of donor genome in cloned bovine embryos*. FEBS Lett, 499, 55-58.

Kao H. Y., Downes M., Ordentlich P. & Evans R. M. (2000). *Isolation of a novel histone deacetylase reveals that class I and class II deacetylases promote SMRT-mediated repression*. Genes Dev, 14, 55-66.

Kao H. Y., Ordentlich P., Koyano-Nakagawa N., Tang Z., Downes M., Kintner C. R., Evans R. M. & Kadesch T. (1998). *A histone deacetylase corepressor complex regulates the Notch signal transduction pathway*. Genes Dev, 12, 2269-2277.

Kasinathan P., Knott J. G., Moreira P. N., Burnside A. S., Jerry D. J. & Robl J. M. (2001a). *Effect of fibroblast donor cell age and cell cycle on development of bovine nuclear transfer embryos in vitro*. Biol Reprod, 64, 1487-1493.

Kasinathan P., Knott J. G., Moreira P. N., Burnside A. S., Joseph Jerry D. & Robl J. M. (2001b). *Effect of Fibroblast Donor Cell Age and Cell Cycle on Development of Bovine Nuclear Transfer Embryos In Vitro*. Biology of Reproduction, 64, 1487-1493.

Kasinathan P., Knott J. G., Wang Z., Jerry D. J. & Robl J. M. (2001c). *Production of calves from G1 fibroblasts*. Nat Biotechnol, 19, 1176-1178.

Kato Y., Tani T., Sotomaru Y., Kurokawa K., Kato J., Doguchi H., Yasue H. & Tsunoda Y. (1998). *Eight calves cloned from somatic cells of a single adult*. Science, 282, 2095-2098.

Kato Y., Tani T. & Tsunoda Y. (2000). *Cloning of calves from various somatic cell types of male and female adult, newborn and fetal cows*. J Reprod Fertil, 120, 231-237.

Kawahara T. L., Michishita E., Adler A. S., Damian M., Berber E., Lin M., McCord R. A., Ongaigui K. C., Boxer L. D., Chang H. Y., *et al.* (2009). *SIRT6 links histone H3 lysine 9 deacetylation to NF-kappaB-dependent gene expression and organismal life span*. Cell, 136, 62-74.

Kelly S. J. (1977). *Studies of the developmental potential of 4- and 8-cell stage mouse blastomeres*. J Exp Zool, 200, 365-376.

Khare S. P., Habib F., Sharma R., Gadewal N., Gupta S. & Galande S. (2012). *HIstome--a relational knowledgebase of human histone proteins and histone modifying enzymes*. Nucleic Acids Res, 40, D337-342.

Kim J., Daniel J., Espejo A., Lake A., Krishna M., Xia L., Zhang Y. & Bedford M. T. (2006). *Tudor, MBT and chromo domains gauge the degree of lysine methylation*. EMBO Rep, 7, 397-403.

Kim J. H., Lane W. S. & Reinberg D. (2002). *Human Elongator facilitates RNA polymerase II transcription through chromatin*. Proc Natl Acad Sci U S A, 99, 1241-1246.

Kim K. C., Geng L. & Huang S. (2003). *Inactivation of a histone methyltransferase by mutations in human cancers*. Cancer Res, 63, 7619-7623.

Kim S. M., Kee H. J., Eom G. H., Choe N. W., Kim J. Y., Kim Y. S., Kim S. K., Kook H. & Seo S. B. (2006). *Characterization of a novel WHSC1-associated SET domain protein with H3K4 and H3K27 methyltransferase activity*. Biochem Biophys Res Commun, 345, 318-323.

Kimura A., Matsubara K. & Horikoshi M. (2005). *A decade of histone acetylation: marking eukaryotic chromosomes with specific codes*. J Biochem, 138, 647-662.

Kinney S. M., Chin H. G., Vaisvila R., Bitinaite J., Zheng Y., Esteve P. O., Feng S., Stroud H., Jacobsen S. E. & Pradhan S. (2011). *Tissue-specific distribution and dynamic changes of 5-hydroxymethylcytosine in mammalian genomes*. J Biol Chem, 286, 24685-24693.

Kishi M., Itagaki Y., Takakura R., Imamura M., Sudo T., Yoshinari M., Tanimoto M., Yasue H. & Kashima N. (2000). *Nuclear transfer in cattle using colostrum-derived mammary gland epithelial cells and ear-derived fibroblast cells*. Theriogenology, 54, 675-684.

Kishigami S., Mizutani E., Ohta H., Hikichi T., Thuan N. V., Wakayama S., Bui H. T. & Wakayama T. (2006). *Significant improvement of mouse cloning technique by treatment with trichostatin A after somatic nuclear transfer*. Biochem Biophys Res Commun, 340, 183-189.

Koessler H., Doenecke D. & Albig W. (2003). *Aberrant expression pattern of replication-dependent histone h3 subtype genes in human tumor cell lines*. DNA Cell Biol, 22, 233-241.

Kram R., Mamont P. & Tomkins G. M. (1973). *Pleiotypic control by adenosine 3':5'-cyclic monophosphate: a model for growth control in animal cells*. Proc Natl Acad Sci U S A, 70, 1432-1436.

Kriaucionis S. & Heintz N. (2009). *The nuclear DNA base 5-hydroxymethylcytosine is present in Purkinje neurons and the brain*. Science, 324, 929-930.

Krogan N. J., Kim M., Tong A., Golshani A., Cagney G., Canadien V., Richards D. P., Beattie B. K., Emili A., Boone C., *et al.* (2003). *Methylation of histone H3 by Set2 in Saccharomyces cerevisiae is linked to transcriptional elongation by RNA polymerase II*. Mol Cell Biol, 23, 4207-4218.

Kubicek S. & Jenuwein T. (2004). *A crack in histone lysine methylation*. Cell, 119, 903-906.

Kubicek S., Schotta G., Lachner M., Sengupta R., Kohlmaier A., Perez-Burgos L., Linderson Y., Martens J. H., O'Sullivan R. J., Fodor B. D., *et al.* (2006a). *The role of histone modifications in epigenetic transitions during normal and perturbed development*. Ernst Schering Res Found Workshop, 1-27.

Kubicek S., Schotta G., Lachner M., Sengupta R., Kohlmaier A., Perez-Burgos L., Linderson Y., Martens J. H. A., O'Sullivan R. J., Fodor B. D., *et al.* (2006b). *The role of histone modifications in epigenetic transitions during normal and perturbed development*. Ernst Schering Research Foundation Workshop, 1-27.

Kubota C., Yamakuchi H., Todoroki J., Mizoshita K., Tabara N., Barber M. & Yang X. (2000). *Six cloned calves produced from adult fibroblast cells after long-term culture*. Proc Natl Acad Sci U S A, 97, 990-995.

Kuzmichev A., Jenuwein T., Tempst P. & Reinberg D. (2004). *Different EZH2-containing complexes target methylation of histone H1 or nucleosomal histone H3*. Mol Cell, 14, 183-193.

Lachner M., Sengupta R., Schotta G. & Jenuwein T. (2004). *Trilogies of histone lysine methylation as epigenetic landmarks of the eukaryotic genome*. Cold Spring Harb Symp Quant Biol, 69, 209-218.

Lagger G., O'Carroll D., Rembold M., Khier H., Tischler J., Weitzer G., Schuettengruber B., Hauser C., Brunmeir R., Jenuwein T., *et al.* (2002). *Essential function of histone deacetylase 1 in proliferation control and CDK inhibitor repression*. EMBO J, 21, 2672-2681.

Lai L., Park K. W., Cheong H. T., Kuhholzer B., Samuel M., Bonk A., Im G. S., Rieke A., Day B. N., Murphy C. N., *et al.* (2002). *Transgenic pig expressing the enhanced green fluorescent protein produced by nuclear transfer using colchicine-treated fibroblasts as donor cells*. Mol Reprod Dev, 62, 300-306.

Lan F., Bayliss P. E., Rinn J. L., Whetstine J. R., Wang J. K., Chen S., Iwase S., Alpatov R., Issaeva I., Canaani E., *et al.* (2007). *A histone H3 lysine 27 demethylase regulates animal posterior development*. Nature, 449, 689-694.

Larsson O., Dafgard E., Engstrom W. & Zetterberg A. (1986). *Immediate effects of serum depletion on dissociation between growth in size and cell division in proliferating 3T3 cells*. J Cell Physiol, 127, 267-273.

Lee B. M. & Mahadevan L. C. (2009). *Stability of histone modifications across mammalian genomes: implications for 'epigenetic' marking*. J Cell Biochem, 108, 22-34.

Lee C. K., Shibata Y., Rao B., Strahl B. D. & Lieb J. D. (2004). *Evidence for nucleosome depletion at active regulatory regions genome-wide*. Nat Genet, 36, 900-905.

Lee S., Lee D. K., Dou Y., Lee J., Lee B., Kwak E., Kong Y. Y., Lee S. K., Roeder R. G. & Lee J. W. (2006). *Coactivator as a target gene specificity determinant for histone H3 lysine 4 methyltransferases*. Proc Natl Acad Sci U S A, 103, 15392-15397.

Lee T. I., Jenner R. G., Boyer L. A., Guenther M. G., Levine S. S., Kumar R. M., Chevalier B., Johnstone S. E., Cole M. F., Isono K., *et al.* (2006). *Control of developmental regulators by Polycomb in human embryonic stem cells*. Cell, 125, 301-313.

Leeb M., Pasini D., Novatchkova M., Jaritz M., Helin K. & Wutz A. (2010). *Polycomb complexes act redundantly to repress genomic repeats and genes*. Genes Dev, 24, 265-276.

Lehnertz B., Ueda Y., Derijck A. A., Braunschweig U., Perez-Burgos L., Kubicek S., Chen T., Li E., Jenuwein T. & Peters A. H. (2003). *Suv39h-mediated histone H3 lysine 9 methylation directs DNA methylation to major satellite repeats at pericentric heterochromatin*. Curr Biol, 13, 1192-1200.

Lemercier C., Brocard M. P., Puvion-Dutilleul F., Kao H. Y., Albagli O. & Khochbin S. (2002). *Class II histone deacetylases are directly recruited by BCL6 transcriptional repressor*. J Biol Chem, 277, 22045-22052.

Lepikhov K., Zakhartchenko V., Hao R., Yang F., Wrenzycki C., Niemann H., Wolf E. & Walter J. (2008). *Evidence for conserved DNA and histone H3 methylation reprogramming in mouse, bovine and rabbit zygotes*. Epigenetics Chromatin, 1, 8.

Lewis A., Mitsuya K., Umlauf D., Smith P., Dean W., Walter J., Higgins M., Feil R. & Reik W. (2004). *Imprinting on distal chromosome 7 in the placenta*

involves repressive histone methylation independent of DNA methylation. Nat Genet, 36, 1291-1295.

Li E., Beard C. & Jaenisch R. (1993). *Role for DNA methylation in genomic imprinting*. Nature, 366, 362-365.

Lister R., Pelizzola M., Dowen R. H., Hawkins R. D., Hon G., Tonti-Filippini J., Nery J. R., Lee L., Ye Z., Ngo Q. M., *et al.* (2009). *Human DNA methylomes at base resolution show widespread epigenomic differences*. Nature, 462, 315-322.

Liu H., Adler A. S., Segal E. & Chang H. Y. (2007). *A transcriptional program mediating entry into cellular quiescence*. PLoS Genet, 3, e91.

Liu H., Kim J. M. & Aoki F. (2004). *Regulation of histone H3 lysine 9 methylation in oocytes and early pre-implantation embryos*. Development, 131, 2269-2280.

Liu H., Knabb J. R., Spike B. T. & Macleod K. F. (2009). *Elevated poly-(ADP-ribose)-polymerase activity sensitizes retinoblastoma-deficient cells to DNA damage-induced necrosis*. Mol Cancer Res, 7, 1099-1109.

Liu W., Tanasa B., Tyurina O. V., Zhou T. Y., Gassmann R., Liu W. T., Ohgi K. A., Benner C., Garcia-Bassets I., Aggarwal A. K., *et al.* (2010). *PHF8 mediates histone H4 lysine 20 demethylation events involved in cell cycle progression*. Nature, 466, 508-512.

Liu X., Wu H., Byrne M., Krane S. & Jaenisch R. (1997). *Type III collagen is crucial for collagen I fibrillogenesis and for normal cardiovascular development*. Proc Natl Acad Sci U S A, 94, 1852-1856.

Loyola A. & Almouzni G. (2007). *Marking histone H3 variants: how, when and why?* Trends Biochem Sci, 32, 425-433.

Loyola A., Bonaldi T., Roche D., Imhof A. & Almouzni G. (2006). *PTMs on H3 variants before chromatin assembly potentiate their final epigenetic state*. Mol Cell, 24, 309-316.

Loyola A., Tagami H., Bonaldi T., Roche D., Quivy J. P., Imhof A., Nakatani Y., Dent S. Y. & Almouzni G. (2009). *The HP1alpha-CAF1-SetDB1-containing complex provides H3K9me1 for Suv39-mediated K9me3 in pericentric heterochromatin*. EMBO Rep, 10, 769-775.

Lu J., Li F., Murphy C. S., Davidson M. W. & Gilbert D. M. (2010). *G2 phase chromatin lacks determinants of replication timing*. J Cell Biol, 189, 967-980.

Lu L., Li L., Lv X., Wu X. S., Liu D. P. & Liang C. C. (2011). *Modulations of hMOF autoacetylation by SIRT1 regulate hMOF recruitment and activities on the chromatin*. Cell Res, 21, 1182-1195.

Luger K., Mader A. W., Richmond R. K., Sargent D. F. & Richmond T. J. (1997). *Crystal structure of the nucleosome core particle at 2.8 A resolution*. Nature, 389, 251-260.

Ma P. & Schultz R. M. (2008). *Histone deacetylase 1 (HDAC1) regulates histone acetylation, development, and gene expression in preimplantation mouse embryos*. Dev Biol, 319, 110-120.

Ma X. J., Wu J., Altheim B. A., Schultz M. C. & Grunstein M. (1998). *Deposition-related sites K5/K12 in histone H4 are not required for nucleosome deposition in yeast*. Proc Natl Acad Sci U S A, 95, 6693-6698.

Madiraju P., Pande S. V., Prentki M. & Madiraju S. R. (2009). *Mitochondrial acetylcarnitine provides acetyl groups for nuclear histone acetylation*. Epigenetics, 4, 399-403.

Maeshima K., Iino H., Hihara S., Funakoshi T., Watanabe A., Nishimura M., Nakatomi R., Yahata K., Imamoto F., Hashikawa T., *et al.* (2010). *Nuclear pore formation but not nuclear growth is governed by cyclin-dependent kinases (Cdks) during interphase*. Nat Struct Mol Biol, 17, 1065-1071.

Malik H. S. & Henikoff S. (2003). *Phylogenomics of the nucleosome*. Nat Struct Biol, 10, 882-891.

Margueron R., Justin N., Ohno K., Sharpe M. L., Son J., Drury W. J., 3rd, Voigt P., Martin S. R., Taylor W. R., De Marco V., *et al.* (2009). *Role of the polycomb protein EED in the propagation of repressive histone marks*. Nature, 461, 762-767.

Margueron R., Li G., Sarma K., Blais A., Zavadil J., Woodcock C. L., Dynlacht B. D. & Reinberg D. (2008). *Ezh1 and Ezh2 maintain repressive chromatin through different mechanisms*. Mol Cell, 32, 503-518.

Martin C. & Zhang Y. (2005). *The diverse functions of histone lysine methylation*. Nat Rev Mol Cell Biol, 6, 838-849.

Maunakea A. K., Nagarajan R. P., Bilenky M., Ballinger T. J., D'Souza C., Fouse S. D., Johnson B. E., Hong C., Nielsen C., Zhao Y., *et al.* (2010). *Conserved role of intragenic DNA methylation in regulating alternative promoters*. Nature, 466, 253-257.

McManus K. J., Biron V. L., Heit R., Underhill D. A. & Hendzel M. J. (2006). *Dynamic changes in histone H3 lysine 9 methylations: identification of a*

mitosis-specific function for dynamic methylation in chromosome congression and segregation. J Biol Chem, 281, 8888-8897.

McManus K. J. & Hendzel M. J. (2005). *Using quantitative imaging microscopy to define the target substrate specificities of histone post-translational-modifying enzymes*. Methods, 36, 351-361.

McMenamin S., Reinsch S. & Conway G. (2003). *Direct comparison of common fixation methods for preservation of microtubules in zebrafish embryos*. Biotechniques, 34, 468-470, 472.

Mehta I. S., Amira M., Harvey A. J. & Bridger J. M. (2010). *Rapid chromosome territory relocation by nuclear motor activity in response to serum removal in primary human fibroblasts*. Genome Biol, 11, R5.

Melton C., Judson R. L. & Blelloch R. (2010). *Opposing microRNA families regulate self-renewal in mouse embryonic stem cells*. Nature, 463, 621-626.

Metzger E., Wissmann M., Yin N., Muller J. M., Schneider R., Peters A. H., Gunther T., Buettner R. & Schule R. (2005). *LSD1 demethylates repressive histone marks to promote androgen-receptor-dependent transcription*. Nature, 437, 436-439.

Michishita E., McCord R. A., Berber E., Kioi M., Padilla-Nash H., Damian M., Cheung P., Kusumoto R., Kawahara T. L., Barrett J. C., *et al.* (2008). *SIRT6 is a histone H3 lysine 9 deacetylase that modulates telomeric chromatin*. Nature, 452, 492-496.

Miller T., Krogan N. J., Dover J., Erdjument-Bromage H., Tempst P., Johnston M., Greenblatt J. F. & Shilatifard A. (2001). *COMPASS: a complex of proteins associated with a trithorax-related SET domain protein*. Proc Natl Acad Sci U S A, 98, 12902-12907.

Monteiro F. M., Oliveira C. S., Oliveira L. Z., Saraiva N. Z., Mercadante M. E., Lopes F. L., Arnold D. R. & Garcia J. M. (2010). *Chromatin modifying agents in the in vitro production of bovine embryos*. Vet Med Int, 2011.

Montgomery N. D., Yee D., Chen A., Kalantry S., Chamberlain S. J., Otte A. P. & Magnuson T. (2005). *The murine polycomb group protein Eed is required for global histone H3 lysine-27 methylation*. Curr Biol, 15, 942-947.

Morgan H. D., Santos F., Green K., Dean W. & Reik W. (2005). *Epigenetic reprogramming in mammals*. Hum Mol Genet, 14 Spec No 1, R47-58.

Mosammaparast N. & Shi Y. (2010). *Reversal of histone methylation: biochemical and molecular mechanisms of histone demethylases*. Annu Rev Biochem, 79, 155-179.

Moser G. C., Fallon R. J. & Meiss H. K. (1981). *Fluorimetric measurements and chromatin condensation patterns of nuclei from 3T3 cells throughout G1*. J Cell Physiol, 106, 293-301.

Murayama A., Ohmori K., Fujimura A., Minami H., Yasuzawa-Tanaka K., Kuroda T., Oie S., Daitoku H., Okuwaki M., Nagata K., *et al.* (2008). *Epigenetic control of rDNA loci in response to intracellular energy status*. Cell, 133, 627-639.

Nakayama J., Rice J. C., Strahl B. D., Allis C. D. & Grewal S. I. (2001). *Role of histone H3 lysine 9 methylation in epigenetic control of heterochromatin assembly*. Science, 292, 110-113.

Ng H. H., Jeppesen P. & Bird A. (2000). *Active repression of methylated genes by the chromosomal protein MBD1*. Mol Cell Biol, 20, 1394-1406.

Ng R. K. & Gurdon J. B. (2008). *Epigenetic memory of an active gene state depends on histone H3.3 incorporation into chromatin in the absence of transcription*. Nat Cell Biol, 10, 102-109.

Nielsen P. R., Nietlispach D., Mott H. R., Callaghan J., Bannister A., Kouzarides T., Murzin A. G., Murzina N. V. & Laue E. D. (2002). *Structure of the HP1 chromodomain bound to histone H3 methylated at lysine 9*. Nature, 416, 103-107.

Nielsen S. J., Schneider R., Bauer U. M., Bannister A. J., Morrison A., O'Carroll D., Firestein R., Cleary M., Jenuwein T., Herrera R. E., *et al.* (2001). *Rb targets histone H3 methylation and HP1 to promoters*. Nature, 412, 561-565.

Nishida H., Suzuki T., Kondo S., Miura H., Fujimura Y. & Hayashizaki Y. (2006). *Histone H3 acetylated at lysine 9 in promoter is associated with low nucleosome density in the vicinity of transcription start site in human cell*. Chromosome Res, 14, 203-211.

Nishioka K., Chuikov S., Sarma K., Erdjument-Bromage H., Allis C. D., Tempst P. & Reinberg D. (2002). *Set9, a novel histone H3 methyltransferase that facilitates transcription by precluding histone tail modifications required for heterochromatin formation*. Genes Dev, 16, 479-489.

Noriega L. G., Feige J. N., Canto C., Yamamoto H., Yu J., Herman M. A., Mataki C., Kahn B. B. & Auwerx J. (2011). *CREB and ChREBP oppositely regulate SIRT1 expression in response to energy availability*. EMBO Rep, 12, 1069-1076.

O'Carroll D., Erhardt S., Pagani M., Barton S. C., Surani M. A. & Jenuwein T. (2001). *The polycomb-group gene Ezh2 is required for early mouse development*. Mol Cell Biol, 21, 4330-4336.

O'Carroll D., Scherthan H., Peters A. H., Opravil S., Haynes A. R., Laible G., Rea S., Schmid M., Lebersorger A., Jerratsch M., *et al.* (2000). *Isolation and characterization of Suv39h2, a second histone H3 methyltransferase gene that displays testis-specific expression*. Mol Cell Biol, 20, 9423-9433.

Oback B. (2009). *Cloning from stem cells: different lineages, different species, same story*. Reprod Fertil Dev, 21, 83-94.

Oback B. (2010). *Cloning: stem cells of different developmental potency*. Encyclopedia of Biotechnology in Agriculture and Food, pp. 167–170. .

Oback B. & Wells D. (2002). *Donor cells for nuclear cloning: many are called, but few are chosen*. Cloning Stem Cells, 4, 147-168.

Oback B. & Wells D. N. (2003). *Cloning cattle*. Cloning Stem Cells, 5, 243-256.

Oback B. & Wells D. N. (2007). *Cloning cattle: the methods in the madness*. Adv Exp Med Biol, 591, 30-57.

Ogawa H., Ishiguro K., Gaubatz S., Livingston D. M. & Nakatani Y. (2002). *A complex with chromatin modifiers that occupies E2F- and Myc-responsive genes in G0 cells*. Science, 296, 1132-1136.

Okano M., Bell D. W., Haber D. A. & Li E. (1999). *DNA methyltransferases Dnmt3a and Dnmt3b are essential for de novo methylation and mammalian development*. Cell, 99, 247-257.

Onder T. T., Kara N., Cherry A., Sinha A. U., Zhu N., Bernt K. M., Cahan P., Mancarci O. B., Unternaehrer J., Gupta P. B., *et al.* (2012). *Chromatin-modifying enzymes as modulators of reprogramming*. Nature.

Ono Y., Shimozawa N., Ito M. & Kono T. (2001). *Cloned mice from fetal fibroblast cells arrested at metaphase by a serial nuclear transfer*. Biol Reprod, 64, 44-50.

Ooi S. L. & Henikoff S. (2007). *Germline histone dynamics and epigenetics*. Curr Opin Cell Biol, 19, 257-265.

Orsi G. A., Couble P. & Loppin B. (2009). *Epigenetic and replacement roles of histone variant H3.3 in reproduction and development*. Int J Dev Biol, 53, 231-243.

Owen D. J., Ornaghi P., Yang J. C., Lowe N., Evans P. R., Ballario P., Neuhaus D., Filetici P. & Travers A. A. (2000). *The structural basis for the recognition of acetylated histone H4 by the bromodomain of histone acetyltransferase gcn5p*. EMBO J, 19, 6141-6149.

Park J. S., Jeong Y. S., Shin S. T., Lee K. K. & Kang Y. K. (2007). *Dynamic DNA methylation reprogramming: active demethylation and immediate remethylation in the male pronucleus of bovine zygotes*. Dev Dyn, 236, 2523-2533.

Park S. H., Gammon S. R., Knippers J. D., Paulsen S. R., Rubink D. S. & Winder W. W. (2002). *Phosphorylation-activity relationships of AMPK and acetyl-CoA carboxylase in muscle*. J Appl Physiol, 92, 2475-2482.

Pascual J., Martinez-Yamout M., Dyson H. J. & Wright P. E. (2000). *Structure of the PHD zinc finger from human Williams-Beuren syndrome transcription factor*. J Mol Biol, 304, 723-729.

Pashkova N., Gakhar L., Winistorfer S. C., Yu L., Ramaswamy S. & Piper R. C. (2010). *WD40 repeat propellers define a ubiquitin-binding domain that regulates turnover of F box proteins*. Mol Cell, 40, 433-443.

Pasini D., Bracken A. P., Hansen J. B., Capillo M. & Helin K. (2007). *The polycomb group protein Suz12 is required for embryonic stem cell differentiation*. Mol Cell Biol, 27, 3769-3779.

Pasini D., Bracken A. P., Jensen M. R., Lazzerini Denchi E. & Helin K. (2004). *Suz12 is essential for mouse development and for EZH2 histone methyltransferase activity*. EMBO J, 23, 4061-4071.

Pasque V., Jullien J., Miyamoto K., Halley-Stott R. P. & Gurdon J. B. (2011). *Epigenetic factors influencing resistance to nuclear reprogramming*. Trends Genet, 27, 516-525.

Patel A., Dharmarajan V., Vought V. E. & Cosgrove M. S. (2009). *On the mechanism of multiple lysine methylation by the human mixed lineage leukemia protein-1 (MLL1) core complex*. J Biol Chem, 284, 24242-24256.

Pena P. V., Davrazou F., Shi X., Walter K. L., Verkhusha V. V., Gozani O., Zhao R. & Kutateladze T. G. (2006). *Molecular mechanism of histone H3K4me3 recognition by plant homeodomain of ING2*. Nature, 442, 100-103.

Penn N. W., Suwalski R., O'Riley C., Bojanowski K. & Yura R. (1972). *The presence of 5-hydroxymethylcytosine in animal deoxyribonucleic acid*. Biochem J, 126, 781-790.

Peserico A. & Simone C. (2011). *Physical and functional HAT/HDAC interplay regulates protein acetylation balance*. J Biomed Biotechnol, 2011, 371832.

Peters A. H., Kubicek S., Mechtler K., O'Sullivan R. J., Derijck A. A., Perez-Burgos L., Kohlmaier A., Opravil S., Tachibana M., Shinkai Y., *et al.* (2003). *Partitioning and plasticity of repressive histone methylation states in mammalian chromatin*. Mol Cell, 12, 1577-1589.

Peters A. H., O'Carroll D., Scherthan H., Mechtler K., Sauer S., Schofer C., Weipoltshammer K., Pagani M., Lachner M., Kohlmaier A., *et al.* (2001). *Loss of the Suv39h histone methyltransferases impairs mammalian heterochromatin and genome stability*. Cell, 107, 323-337.

Peters A. H. & Schubeler D. (2005). *Methylation of histones: playing memory with DNA*. Curr Opin Cell Biol, 17, 230-238.

Petruk S., Sedkov Y., Johnston D. M., Hodgson J. W., Black K. L., Kovermann S. K., Beck S., Canaani E., Brock H. W. & Mazo A. (2012). *TrxG and PcG proteins but not methylated histones remain associated with DNA through replication*. Cell, 150, 922-933.

Plath K., Fang J., Mlynarczyk-Evans S. K., Cao R., Worringer K. A., Wang H., de la Cruz C. C., Otte A. P., Panning B. & Zhang Y. (2003). *Role of histone H3 lysine 27 methylation in X inactivation*. Science, 300, 131-135.

Pokholok D. K., Harbison C. T., Levine S., Cole M., Hannett N. M., Lee T. I., Bell G. W., Walker K., Rolfe P. A., Herbolsheimer E., *et al.* (2005). *Genome-wide map of nucleosome acetylation and methylation in yeast*. Cell, 122, 517-527.

Polo S. E., Theocharis S. E., Klijanienko J., Savignoni A., Asselain B., Vielh P. & Almouzni G. (2004). *Chromatin assembly factor-1, a marker of clinical value to distinguish quiescent from proliferating cells*. Cancer Res, 64, 2371-2381.

Poux S., Horard B., Sigrist C. J. & Pirrotta V. (2002). *The Drosophila trithorax protein is a coactivator required to prevent re-establishment of polycomb silencing*. Development, 129, 2483-2493.

Powell A. M., Talbot N. C., Wells K. D., Kerr D. E., Pursel V. G. & Wall R. J. (2004). *Cell donor influences success of producing cattle by somatic cell nuclear transfer*. Biol Reprod, 71, 210-216.

Pradhan S., Bacolla A., Wells R. D. & Roberts R. J. (1999). *Recombinant human DNA (cytosine-5) methyltransferase. I. Expression, purification, and comparison of de novo and maintenance methylation*. J Biol Chem, 274, 33002-33010.

Prather R. S., Barnes F. L., Sims M. M., Robl J. M., Eyestone W. H. & First N. L. (1987). *Nuclear transplantation in the bovine embryo: assessment of donor nuclei and recipient oocyte*. Biol Reprod, 37, 859-866.

Probst A. V., Dunleavy E. & Almouzni G. (2009). *Epigenetic inheritance during the cell cycle*. Nat Rev Mol Cell Biol, 10, 192-206.

Puschendorf M., Terranova R., Boutsma E., Mao X., Isono K., Brykczynska U., Kolb C., Otte A. P., Koseki H., Orkin S. H., *et al.* (2008). *PRC1 and Suv39h specify parental asymmetry at constitutive heterochromatin in early mouse embryos*. Nat Genet, 40, 411-420.

Rada-Iglesias A., Bajpai R., Swigut T., Brugmann S. A., Flynn R. A. & Wysocka J. (2011). *A unique chromatin signature uncovers early developmental enhancers in humans*. Nature, 470, 279-283.

Rangasamy D., Greaves I. & Tremethick D. J. (2004). *RNA interference demonstrates a novel role for H2A.Z in chromosome segregation*. Nat Struct Mol Biol, 11, 650-655.

Rawlings J. S., Gatzka M., Thomas P. G. & Ihle J. N. (2011). *Chromatin condensation via the condensin II complex is required for peripheral T-cell quiescence*. EMBO J, 30, 263-276.

Rea S., Eisenhaber F., O'Carroll D., Strahl B. D., Sun Z. W., Schmid M., Opravil S., Mechtler K., Ponting C. P., Allis C. D., *et al.* (2000). *Regulation of chromatin structure by site-specific histone H3 methyltransferases*. Nature, 406, 593-599.

Reik W., Dean W. & Walter J. (2001). *Epigenetic reprogramming in mammalian development*. Science, 293, 1089-1093.

Rideout W. M., 3rd, Eggan K. & Jaenisch R. (2001). *Nuclear cloning and epigenetic reprogramming of the genome*. Science, 293, 1093-1098.

Rideout W. M., 3rd, Wakayama T., Wutz A., Eggan K., Jackson-Grusby L., Dausman J., Yanagimachi R. & Jaenisch R. (2000). *Generation of mice from wild-type and targeted ES cells by nuclear cloning*. Nat Genet, 24, 109-110.

Ringrose L. & Paro R. (2004). *Epigenetic regulation of cellular memory by the Polycomb and Trithorax group proteins*. Annu Rev Genet, 38, 413-443.

Robertson I. & Nelson R. 1998. Certification and identification of the embryo. In *Manual of the International Embryo Transfer Society*, pp. 103-134.

Roh S., Shim H., Hwang W. S. & Yoon J. T. (2000). *In vitro development of green fluorescent protein (GFP) transgenic bovine embryos after nuclear transfer using different cell cycles and passages of fetal fibroblasts*. Reprod Fertil Dev, 12, 1-6.

Roh T. Y., Cuddapah S., Cui K. & Zhao K. (2006). *The genomic landscape of histone modifications in human T cells*. Proc Natl Acad Sci U S A, 103, 15782-15787.

Roh T. Y., Cuddapah S. & Zhao K. (2005). *Active chromatin domains are defined by acetylation islands revealed by genome-wide mapping*. Genes Dev, 19, 542-552.

Ross P. J., Ragina N. P., Rodriguez R. M., Iager A. E., Siripattarapravat K., Lopez-Corrales N. & Cibelli J. B. (2008). *Polycomb gene expression and histone H3 lysine 27 trimethylation changes during bovine preimplantation development*. Reproduction, 136, 777-785.

Rundlett S. E., Carmen A. A., Kobayashi R., Bavykin S., Turner B. M. & Grunstein M. (1996). *HDA1 and RPD3 are members of distinct yeast histone deacetylase complexes that regulate silencing and transcription*. Proc Natl Acad Sci U S A, 93, 14503-14508.

Ruthenburg A. J., Allis C. D. & Wysocka J. (2007). *Methylation of lysine 4 on histone H3: intricacy of writing and reading a single epigenetic mark*. Mol Cell, 25, 15-30.

Rybouchkin A., Kato Y. & Tsunoda Y. (2006). *Role of histone acetylation in reprogramming of somatic nuclei following nuclear transfer*. Biol Reprod, 74, 1083-1089.

Rybtsova N., Leimgruber E., Seguin-Estevez Q., Dunand-Sauthier I., Krawczyk M. & Reith W. (2007). *Transcription-coupled deposition of histone modifications during MHC class II gene activation*. Nucleic Acids Res, 35, 3431-3441.

Sanger J. W. & Sanger J. M. (1980). *Surface and shape changes during cell division*. Cell Tissue Res, 209, 177-186.

Santos-Rosa H., Schneider R., Bannister A. J., Sherriff J., Bernstein B. E., Emre N. C., Schreiber S. L., Mellor J. & Kouzarides T. (2002). *Active genes are tri-methylated at K4 of histone H3*. Nature, 419, 407-411.

Santos F. & Dean W. (2004). *Epigenetic reprogramming during early development in mammals*. Reproduction, 127, 643-651.

Santos F., Peters A. H., Otte A. P., Reik W. & Dean W. (2005). *Dynamic chromatin modifications characterise the first cell cycle in mouse embryos*. Dev Biol, 280, 225-236.

Santos F., Zakhartchenko V., Stojkovic M., Peters A., Jenuwein T., Wolf E., Reik W. & Dean W. (2003). *Epigenetic marking correlates with developmental*

potential in cloned bovine preimplantation embryos. Curr Biol, 13, 1116-1121.

Sasaki H. & Matsui Y. (2008). *Epigenetic events in mammalian germ-cell development: reprogramming and beyond*. Nat Rev Genet, 9, 129-140.

Scharf A. N., Barth T. K. & Imhof A. (2009). *Establishment of histone modifications after chromatin assembly*. Nucleic Acids Res, 37, 5032-5040.

Scharf A. N., Meier K., Seitz V., Kremmer E., Brehm A. & Imhof A. (2009). *Monomethylation of lysine 20 on histone H4 facilitates chromatin maturation*. Mol Cell Biol, 29, 57-67.

Schoeftner S., Sengupta A. K., Kubicek S., Mechtler K., Spahn L., Koseki H., Jenuwein T. & Wutz A. (2006). *Recruitment of PRC1 function at the initiation of X inactivation independent of PRC2 and silencing*. EMBO J, 25, 3110-3122.

Schotta G., Lachner M., Peters A. H. & Jenuwein T. (2004a). *The indexing potential of histone lysine methylation*. Novartis Found Symp, 259, 22-37; discussion 37-47, 163-169.

Schotta G., Lachner M., Sarma K., Ebert A., Sengupta R., Reuter G., Reinberg D. & Jenuwein T. (2004b). *A silencing pathway to induce H3-K9 and H4-K20 trimethylation at constitutive heterochromatin*. Genes Dev, 18, 1251-1262.

Schubeler D., MacAlpine D. M., Scalzo D., Wirbelauer C., Kooperberg C., van Leeuwen F., Gottschling D. E., O'Neill L. P., Turner B. M., Delrow J., *et al.* (2004). *The histone modification pattern of active genes revealed through genome-wide chromatin analysis of a higher eukaryote*. Genes Dev, 18, 1263-1271.

Schuettengruber B., Martinez A. M., Iovino N. & Cavalli G. (2011). *Trithorax group proteins: switching genes on and keeping them active*. Nat Rev Mol Cell Biol, 12, 799-814.

Schurmann A., Wells D. N. & Oback B. (2006). *Early zygotes are suitable recipients for bovine somatic nuclear transfer and result in cloned offspring*. Reproduction, 132, 839-848.

Schwartz Y. B. & Pirrotta V. (2007). *Polycomb silencing mechanisms and the management of genomic programmes*. Nat Rev Genet, 8, 9-22.

Shahbazian M. D. & Grunstein M. (2007). *Functions of site-specific histone acetylation and deacetylation*. Annu Rev Biochem, 76, 75-100.

Shen X., Liu Y., Hsu Y. J., Fujiwara Y., Kim J., Mao X., Yuan G. C. & Orkin S. H. (2008). *EZH1 mediates methylation on histone H3 lysine 27 and complements EZH2 in maintaining stem cell identity and executing pluripotency*. Mol Cell, 32, 491-502.

Shi Y., Lan F., Matson C., Mulligan P., Whetstine J. R., Cole P. A. & Casero R. A. (2004). *Histone demethylation mediated by the nuclear amine oxidase homolog LSD1*. Cell, 119, 941-953.

Shilatifard A. (2006). *Chromatin modifications by methylation and ubiquitination: implications in the regulation of gene expression*. Annu Rev Biochem, 75, 243-269.

Shogren-Knaak M., Ishii H., Sun J. M., Pazin M. J., Davie J. R. & Peterson C. L. (2006). *Histone H4-K16 acetylation controls chromatin structure and protein interactions*. Science, 311, 844-847.

Shumacher A., Faust C. & Magnuson T. (1996). *Positional cloning of a global regulator of anterior-posterior patterning in mice*. Nature, 383, 250-253.

Simon J. A. & Kingston R. E. (2009). *Mechanisms of polycomb gene silencing: knowns and unknowns*. Nat Rev Mol Cell Biol, 10, 697-708.

Sims J. K., Houston S. I., Magazinnik T. & Rice J. C. (2006). *A trans-tail histone code defined by monomethylated H4 Lys-20 and H3 Lys-9 demarcates distinct regions of silent chromatin*. J Biol Chem, 281, 12760-12766.

Sims R. J., 3rd, Millhouse S., Chen C. F., Lewis B. A., Erdjument-Bromage H., Tempst P., Manley J. L. & Reinberg D. (2007). *Recognition of trimethylated histone H3 lysine 4 facilitates the recruitment of transcription postinitiation factors and pre-mRNA splicing*. Mol Cell, 28, 665-676.

Sinha K. M., Yasuda H., Coombes M. M., Dent S. Y. & de Crombrugghe B. (2010). *Regulation of the osteoblast-specific transcription factor Osterix by NO66, a Jumonji family histone demethylase*. EMBO J, 29, 68-79.

Skene P. J. & Henikoff S. (2012). *Chromatin roadblocks to reprogramming 50 years on*. BMC Biol, 10, 83.

Sobel R. E., Cook R. G., Perry C. A., Annunziato A. T. & Allis C. D. (1995). *Conservation of deposition-related acetylation sites in newly synthesized histones H3 and H4*. Proc Natl Acad Sci U S A, 92, 1237-1241.

Sprangers R., Groves M. R., Sinning I. & Sattler M. (2003). *High-resolution X-ray and NMR structures of the SMN Tudor domain: conformational variation in the binding site for symmetrically dimethylated arginine residues*. J Mol Biol, 327, 507-520.

Squazzo S. L., O'Geen H., Komashko V. M., Krig S. R., Jin V. X., Jang S. W., Margueron R., Reinberg D., Green R. & Farnham P. J. (2006). *Suz12 binds to silenced regions of the genome in a cell-type-specific manner*. Genome Res, 16, 890-900.

Srivastava S., Mishra R. K. & Dhawan J. (2010). *Regulation of cellular chromatin state: insights from quiescence and differentiation*. Organogenesis, 6, 37-47.

Stroud H., Feng S., Morey Kinney S., Pradhan S. & Jacobsen S. E. (2011). *5-Hydroxymethylcytosine is associated with enhancers and gene bodies in human embryonic stem cells*. Genome Biol, 12, R54.

Su R. C., Brown K. E., Saaber S., Fisher A. G., Merkenschlager M. & Smale S. T. (2004). *Dynamic assembly of silent chromatin during thymocyte maturation*. Nat Genet, 36, 502-506.

Suganuma T. & Workman J. L. (2010). *WD40 repeats arrange histone tails for spreading of silencing*. J Mol Cell Biol, 2, 81-83.

Suka N., Luo K. & Grunstein M. (2002). *Sir2p and Sas2p opposingly regulate acetylation of yeast histone H4 lysine16 and spreading of heterochromatin*. Nat Genet, 32, 378-383.

Suto R. K., Clarkson M. J., Tremethick D. J. & Luger K. (2000). *Crystal structure of a nucleosome core particle containing the variant histone H2A.Z*. Nat Struct Biol, 7, 1121-1124.

Tachibana M., Matsumura Y., Fukuda M., Kimura H. & Shinkai Y. (2008). *G9a/GLP complexes independently mediate H3K9 and DNA methylation to silence transcription*. EMBO J, 27, 2681-2690.

Tachibana M., Sugimoto K., Fukushima T. & Shinkai Y. (2001). *Set domain-containing protein, G9a, is a novel lysine-preferring mammalian histone methyltransferase with hyperactivity and specific selectivity to lysines 9 and 27 of histone H3*. J Biol Chem, 276, 25309-25317.

Tachibana M., Sugimoto K., Nozaki M., Ueda J., Ohta T., Ohki M., Fukuda M., Takeda N., Niida H., Kato H., *et al.* (2002). *G9a histone methyltransferase plays a dominant role in euchromatic histone H3 lysine 9 methylation and is essential for early embryogenesis*. Genes Dev, 16, 1779-1791.

Tachibana M., Ueda J., Fukuda M., Takeda N., Ohta T., Iwanari H., Sakihama T., Kodama T., Hamakubo T. & Shinkai Y. (2005). *Histone methyltransferases G9a and GLP form heteromeric complexes and are both crucial for methylation of euchromatin at H3-K9*. Genes Dev, 19, 815-826.

Tahiliani M., Koh K. P., Shen Y., Pastor W. A., Bandukwala H., Brudno Y., Agarwal S., Iyer L. M., Liu D. R., Aravind L., *et al.* (2009). *Conversion of 5-methylcytosine to 5-hydroxymethylcytosine in mammalian DNA by MLL partner TET1*. Science, 324, 930-935.

Takahashi K. & Yamanaka S. (2006). *Induction of pluripotent stem cells from mouse embryonic and adult fibroblast cultures by defined factors*. Cell, 126, 663-676.

Talbert P. B. & Henikoff S. (2010). *Histone variants--ancient wrap artists of the epigenome*. Nat Rev Mol Cell Biol, 11, 264-275.

Tamaru H. & Selker E. U. (2001). *A histone H3 methyltransferase controls DNA methylation in Neurospora crassa*. Nature, 414, 277-283.

Tani H., Morris R. J. & Kaur P. (2000). *Enrichment for murine keratinocyte stem cells based on cell surface phenotype*. Proc Natl Acad Sci U S A, 97, 10960-10965.

Taunton J., Hassig C. A. & Schreiber S. L. (1996). *A mammalian histone deacetylase related to the yeast transcriptional regulator Rpd3p*. Science, 272, 408-411.

Thery M. & Bornens M. (2008). *Get round and stiff for mitosis*. HFSP J, 2, 65-71.

Thiru A., Nietlispach D., Mott H. R., Okuwaki M., Lyon D., Nielsen P. R., Hirshberg M., Verreault A., Murzina N. V. & Laue E. D. (2004). *Structural basis of HP1/PXVXL motif peptide interactions and HP1 localisation to heterochromatin*. EMBO J, 23, 489-499.

Thomas G., Lange H. W. & Hempel K. (1972). *[Relative stability of lysine-bound methyl groups in arginie-rich histones and their subfrations in Ehrlich ascites tumor cells in vitro]*. Hoppe Seylers Z Physiol Chem, 353, 1423-1428.

Thompson J. G., McNaughton C., Gasparrini B., McGowan L. T. & Tervit H. R. (2000). *Effect of inhibitors and uncouplers of oxidative phosphorylation during compaction and blastulation of bovine embryos cultured in vitro*. J Reprod Fertil, 118, 47-55.

Torres-Padilla M. E., Parfitt D. E., Kouzarides T. & Zernicka-Goetz M. (2007). *Histone arginine methylation regulates pluripotency in the early mouse embryo*. Nature, 445, 214-218.

Towbin B. D., Gonzalez-Aguilera C., Sack R., Gaidatzis D., Kalck V., Meister P., Askjaer P. & Gasser S. M. (2012). *Step-wise methylation of histone H3K9 positions heterochromatin at the nuclear periphery*. Cell, 150, 934-947.

Tsukada Y., Ishitani T. & Nakayama K. I. (2010). *KDM7 is a dual demethylase for histone H3 Lys 9 and Lys 27 and functions in brain development*. Genes Dev, 24, 432-437.

Umlauf D., Goto Y., Cao R., Cerqueira F., Wagschal A., Zhang Y. & Feil R. (2004). *Imprinting along the Kcnq1 domain on mouse chromosome 7 involves repressive histone methylation and recruitment of Polycomb group complexes*. Nat Genet, 36, 1296-1300.

Vakoc C. R., Mandat S. A., Olenchock B. A. & Blobel G. A. (2005). *Histone H3 lysine 9 methylation and HP1gamma are associated with transcription elongation through mammalian chromatin*. Mol Cell, 19, 381-391.

van der Heijden G. W., Dieker J. W., Derijck A. A., Muller S., Berden J. H., Braat D. D., van der Vlag J. & de Boer P. (2005). *Asymmetry in histone H3 variants and lysine methylation between paternal and maternal chromatin of the early mouse zygote*. Mech Dev, 122, 1008-1022.

van der Heijden G. W., Ramos L., Baart E. B., van den Berg I. M., Derijck A. A., van der Vlag J., Martini E. & de Boer P. (2008). *Sperm-derived histones contribute to zygotic chromatin in humans*. BMC Dev Biol, 8, 34.

van der Stoop P., Boutsma E. A., Hulsman D., Noback S., Heimerikx M., Kerkhoven R. M., Voncken J. W., Wessels L. F. & van Lohuizen M. (2008). *Ubiquitin E3 ligase Ring1b/Rnf2 of polycomb repressive complex 1 contributes to stable maintenance of mouse embryonic stem cells*. PLoS One, 3, e2235.

Van Holde K. E. (1988). *Chromatin. Series in Molecular Biology*. J Mol Recognit, 2, 530.

Vaquero A., Scher M., Erdjument-Bromage H., Tempst P., Serrano L. & Reinberg D. (2007). *SIRT1 regulates the histone methyl-transferase SUV39H1 during heterochromatin formation*. Nature, 450, 440-444.

Vaquero A., Scher M., Lee D., Erdjument-Bromage H., Tempst P. & Reinberg D. (2004). *Human SirT1 interacts with histone H1 and promotes formation of facultative heterochromatin*. Mol Cell, 16, 93-105.

Vaquero A., Scher M. B., Lee D. H., Sutton A., Cheng H. L., Alt F. W., Serrano L., Sternglanz R. & Reinberg D. (2006). *SirT2 is a histone deacetylase with preference for histone H4 Lys 16 during mitosis*. Genes Dev, 20, 1256-1261.

Vignon X., Chesne P., Le Bourhis D., Flechon J. E., Heyman Y. & Renard J. P. (1998). *Developmental potential of bovine embryos reconstructed from enucleated matured oocytes fused with cultured somatic cells*. C R Acad Sci III, 321, 735-745.

Vodicka P., Smetana K., Jr., Dvorankova B., Emerick T., Xu Y. Z., Ourednik J., Ourednik V. & Motlik J. (2005). *The miniature pig as an animal model in biomedical research*. Ann N Y Acad Sci, 1049, 161-171.

Voncken J. W., Roelen B. A., Roefs M., de Vries S., Verhoeven E., Marino S., Deschamps J. & van Lohuizen M. (2003). *Rnf2 (Ring1b) deficiency causes gastrulation arrest and cell cycle inhibition*. Proc Natl Acad Sci U S A, 100, 2468-2473.

Wakayama T. (2006). *Establishment of nuclear transfer embryonic stem cell lines from adult somatic cells by nuclear transfer and its application*. Ernst Schering Res Found Workshop, 111-123.

Wakayama T. (2007). *Production of cloned mice and ES cells from adult somatic cells by nuclear transfer: how to improve cloning efficiency?* J Reprod Dev, 53, 13-26.

Wakayama T., Rodriguez I., Perry A. C., Yanagimachi R. & Mombaerts P. (1999). *Mice cloned from embryonic stem cells*. Proc Natl Acad Sci U S A, 96, 14984-14989.

Wakayama T. & Yanagimachi R. (1999). *Cloning of male mice from adult tail-tip cells*. Nat Genet, 22, 127-128.

Wang H., An W., Cao R., Xia L., Erdjument-Bromage H., Chatton B., Tempst P., Roeder R. G. & Zhang Y. (2003). *mAM facilitates conversion by ESET of dimethyl to trimethyl lysine 9 of histone H3 to cause transcriptional repression*. Mol Cell, 12, 475-487.

Wang L., Mizzen C., Ying C., Candau R., Barlev N., Brownell J., Allis C. D. & Berger S. L. (1997). *Histone acetyltransferase activity is conserved between yeast and human GCN5 and is required for complementation of growth and transcriptional activation*. Mol Cell Biol, 17, 519-527.

Wang P., Lin C., Smith E. R., Guo H., Sanderson B. W., Wu M., Gogol M., Alexander T., Seidel C., Wiedemann L. M., *et al.* (2009). *Global analysis of H3K4 methylation defines MLL family member targets and points to a role for MLL1-mediated H3K4 methylation in the regulation of transcriptional initiation by RNA polymerase II*. Mol Cell Biol, 29, 6074-6085.

Wang Y., Su J., Wang L., Xu W., Quan F., Liu J. & Zhang Y. (2011). *The effects of 5-aza-2'- deoxycytidine and trichostatin A on gene expression and DNA methylation status in cloned bovine blastocysts*. Cell Reprogram, 13, 297-306.

Wang Y. S., Xiong X. R., An Z. X., Wang L. J., Liu J., Quan F. S., Hua S. & Zhang Y. (2011). *Production of cloned calves by combination treatment of*

both donor cells and early cloned embryos with 5-aza-2/-deoxycytidine and trichostatin A. Theriogenology, 75, 819-825.

Wang Z., Zang C., Cui K., Schones D. E., Barski A., Peng W. & Zhao K. (2009). *Genome-wide mapping of HATs and HDACs reveals distinct functions in active and inactive genes*. Cell, 138, 1019-1031.

Wang Z., Zang C., Rosenfeld J. A., Schones D. E., Barski A., Cuddapah S., Cui K., Roh T. Y., Peng W., Zhang M. Q., *et al.* (2008). *Combinatorial patterns of histone acetylations and methylations in the human genome*. Nat Genet, 40, 897-903.

Wells D. N., Laible G., Tucker F. C., Miller A. L., Oliver J. E., Xiang T., Forsyth J. T., Berg M. C., Cockrem K., L'Huillier P. J., *et al.* (2003). *Coordination between donor cell type and cell cycle stage improves nuclear cloning efficiency in cattle*. Theriogenology, 59, 45-59.

Wells D. N., Misica P. M. & Tervit H. R. (1999). *Production of cloned calves following nuclear transfer with cultured adult mural granulosa cells*. Biol Reprod, 60, 996-1005.

Wen H., Li J., Song T., Lu M., Kan P. Y., Lee M. G., Sha B. & Shi X. (2010). *Recognition of histone H3K4 trimethylation by the plant homeodomain of PHF2 modulates histone demethylation*. J Biol Chem, 285, 9322-9326.

Whetstine J. R., Nottke A., Lan F., Huarte M., Smolikov S., Chen Z., Spooner E., Li E., Zhang G., Colaiacovo M., *et al.* (2006). *Reversal of histone lysine trimethylation by the JMJD2 family of histone demethylases*. Cell, 125, 467-481.

Wilmut I., Schnieke A. E., McWhir J., Kind A. J. & Campbell K. H. (1997). *Viable offspring derived from fetal and adult mammalian cells*. Nature, 385, 810-813.

Wu H., Chen X., Xiong J., Li Y., Li H., Ding X., Liu S., Chen S., Gao S. & Zhu B. (2011). *Histone methyltransferase G9a contributes to H3K27 methylation in vivo*. Cell Res, 21, 365-367.

Wu H., D'Alessio A. C., Ito S., Wang Z., Cui K., Zhao K., Sun Y. E. & Zhang Y. (2011). *Genome-wide analysis of 5-hydroxymethylcytosine distribution reveals its dual function in transcriptional regulation in mouse embryonic stem cells*. Genes Dev, 25, 679-684.

Wu M., Wang P. F., Lee J. S., Martin-Brown S., Florens L., Washburn M. & Shilatifard A. (2008). *Molecular regulation of H3K4 trimethylation by Wdr82, a component of human Set1/COMPASS*. Mol Cell Biol, 28, 7337-7344.

Wu R. S., Perry L. J. & Bonner W. M. (1983). *Fate of newly synthesized histones in G1 and G0 cells*. FEBS Lett, 162, 161-166.

Wu R. S., Tsai S. & Bonner W. M. (1982). *Patterns of histone variant synthesis can distinguish G0 from G1 cells*. Cell, 31, 367-374.

Wu S. & Rice J. C. (2011). *A new regulator of the cell cycle: the PR-Set7 histone methyltransferase*. Cell Cycle, 10, 68-72.

Wu X., Li Y., Xue L., Wang L., Yue Y., Li K., Bou S., Li G. P. & Yu H. (2011). *Multiple histone site epigenetic modifications in nuclear transfer and in vitro fertilized bovine embryos*. Zygote, 19, 31-45.

Yamaguchi T., Cubizolles F., Zhang Y., Reichert N., Kohler H., Seiser C. & Matthias P. (2010). *Histone deacetylases 1 and 2 act in concert to promote the G1-to-S progression*. Genes Dev, 24, 455-469.

Yamanaka K., Balboula A. Z., Sakatani M. & Takahashi M. (2010). *Gene silencing of DNA methyltransferases by RNA interference in bovine fibroblast cells*. J Reprod Dev, 56, 60-67.

Yamane K., Tateishi K., Klose R. J., Fang J., Fabrizio L. A., Erdjument-Bromage H., Taylor-Papadimitriou J., Tempst P. & Zhang Y. (2007). *PLU-1 is an H3K4 demethylase involved in transcriptional repression and breast cancer cell proliferation*. Mol Cell, 25, 801-812.

Yamane K., Toumazou C., Tsukada Y., Erdjument-Bromage H., Tempst P., Wong J. & Zhang Y. (2006). *JHDM2A, a JmjC-containing H3K9 demethylase, facilitates transcription activation by androgen receptor*. Cell, 125, 483-495.

Yang X., Smith S. L., Tian X. C., Lewin H. A., Renard J. P. & Wakayama T. (2007). *Nuclear reprogramming of cloned embryos and its implications for therapeutic cloning*. Nat Genet, 39, 295-302.

Yuan W., Xu M., Huang C., Liu N., Chen S. & Zhu B. (2011). *H3K36 methylation antagonizes PRC2-mediated H3K27 methylation*. J Biol Chem, 286, 7983-7989.

Yusuf I. & Fruman D. A. (2003). *Regulation of quiescence in lymphocytes*. Trends Immunol, 24, 380-386.

Zakhartchenko V., Durcova-Hills G., Stojkovic M., Schernthaner W., Prelle K., Steinborn R., Muller M., Brem G. & Wolf E. (1999). *Effects of serum starvation and re-cloning on the efficiency of nuclear transfer using bovine fetal fibroblasts*. J Reprod Fertil, 115, 325-331.

Zetterberg A. & Larsson O. (1985). *Kinetic analysis of regulatory events in G1 leading to proliferation or quiescence of Swiss 3T3 cells*. Proc Natl Acad Sci U S A, 82, 5365-5369.

Zhang M., Wang F., Kou Z., Zhang Y. & Gao S. (2009). *Defective chromatin structure in somatic cell cloned mouse embryos*. J Biol Chem, 284, 24981-24987.

Zhang T. Y., Dai J. J., Wu C. F., Gu X. L., Liu L., Wu Z. Q., Xie Y. N., Wu B., Chen H. L., Li Y., *et al.* (2012). *Positive effects of treatment of donor cells with aphidicolin on the preimplantation development of somatic cell nuclear transfer embryos in Chinese Bama mini-pig (Sus Scrofa).* Anim Sci J, 83, 103-110.

Zhang Y. & Reinberg D. (2001). *Transcription regulation by histone methylation: interplay between different covalent modifications of the core histone tails*. Genes Dev, 15, 2343-2360.

Zhao R., Bodnar M. S. & Spector D. L. (2009). *Nuclear neighborhoods and gene expression*. Curr Opin Genet Dev, 19, 172-179.

Zhu B. & Reinberg D. (2011). *Epigenetic inheritance: uncontested?* Cell Res, 21, 435-441.

Zhu Z., Wang Y., Li X., Xu L., Wang X., Sun T., Dong X., Chen L., Mao H., Yu Y., *et al.* (2010). *PHF8 is a histone H3K9me2 demethylase regulating rRNA synthesis*. Cell Res, 20, 794-801.

Zou X., Wang Y., Cheng Y., Yang Y., Ju H., Tang H., Shen Y., Mu Z., Xu S. & Du M. (2002). *Generation of cloned goats (Capra hircus) from transfected foetal fibroblast cells, the effect of donor cell cycle*. Mol Reprod Dev, 61, 164-172.